การประเมินผลความสามารถของหลุมผลิตแบบใช้ท่อผลิตร่วมด้วยข้อมูลการผลิต

นาย ทวน อานห์ เหงียน

ลิขสิทธิ์ของจุฬาลงกรณ์มหาวิทยาลัย

# PERFORMANCE EVALUATION OF COMMINGLED WELLS
# WITH PRODUCTION DATA
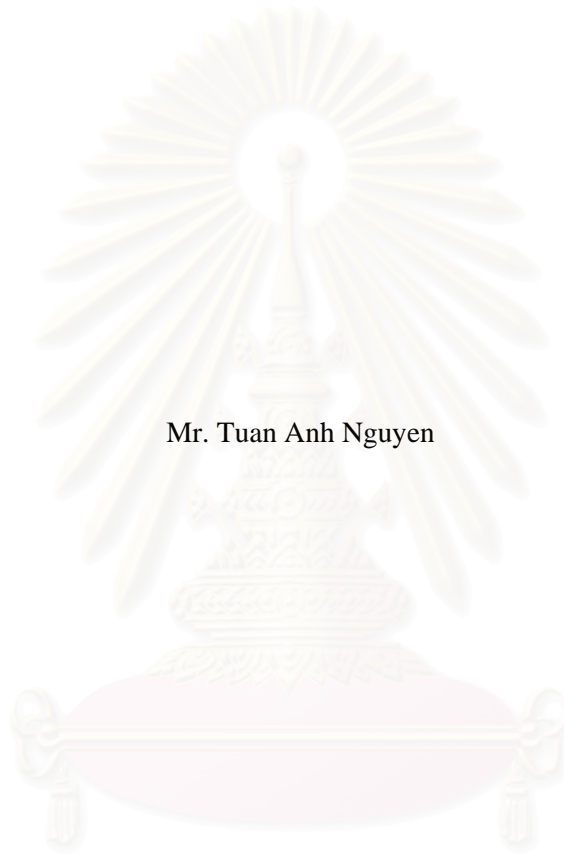
Mr. Tuan Anh Nguyen

A Thesis Submitted in Partially Fulfillment of the Requirements
for the Degree of Master of Engineering program in Petroleum Engineering
Department of Mining and Petroleum Engineering
Faculty of Engineering
Chulalongkorn University
Academic Year 2006

Thesis Title          PERFORMACE EVALUATION OF COMMINGLED
WELLS WITH PRODUCTION DATA

By                 Tuan Anh Nguyen

Field of Study      Petroleum Engineering

Thesis Advisor     Suwat Athichanagorn, Ph.D.

Thesis Co-advisor  Dyung Tien Vo, Ph.D.

---

Accepted by the Faculty of Engineering, Chulalongkorn University in
Partial Fulfillment of the Requirements for the Master's Degree.

.....................................Dean of the Faculty of Engineering

(Professor Direk Lavansiri, Ph.D.)

THESIS COMMITTEE

........................................ Chairman

(Associate Professor Sarithdej Pathanasethpong)

........................................ Thesis Advisor

(Assistant Professor Suwat Athichanagorn, Ph.D.)

........................................ Thesis Co-advisor

(Dyung Tien Vo, Ph.D.)

........................................ Member

(Jirawat Chewaroungroaj, Ph.D.)

ทวน อานห์ เหงียน:    การประเมินผลความสามารถของหลุมผลิตจากแหล่งกักเก็บร่วมด้วย
ข้อมูลการผลิต (PERFORMANCE EVALUATION OF COMMINIGLED
WELLS WITH PRODUCTION DATA) อ. ที่ปรึกษา: ผศ.ดร.สุวัฒน์ อธิชนากร อ. ที่
ปรึกษาร่วม: ดร.ดยัง เทียน โว 199 หน้า ISBN 974-14-3390-5

จุดประสงค์ในรายงานฉบับนี้เกิดจากความต้องการเทคนิคแบบง่ายที่จะวิเคราะห์ข้อมูลการ
ผลิตของหลุมน้ำมันและก๊าซที่ผลิตจากแหล่งกักเก็บร่วมกันเพื่อที่จะประมาณปริมาณน้ำมันที่
สามารถผลิตได้จากแหล่งกักเก็บ  เมื่อการผลิตของหลุมเข้าสู่ภาวะสมดุลย์อย่างเทียมอัตราการผลิตที่
ทำให้เป็นมาตรฐาน   จะสามารถให้ค่าประมาณเบื้องต้นของปริมาณการผลิตสะสมสูงสุด  ของทั้ง
แหล่งกักเก็บเดี่ยวและแหล่งกักเก็บหลายชั้น  อัตราการไหลของชั้นการผลิตที่มีความสามารถในการ
ผลิตต่างกันสามารถถูกค้นพบเชิงคุณภาพได้

สำหรับแหล่งกักเก็บน้ำมันและก๊าซ   เมื่ออัตราการผลิตที่ทำให้เป็นมาตรฐานรวมกับการดุลย์
มวลสารอย่างพลวัตร        สามารถถูกใช้เป็นเครื่องมือในการวินิจฉัยเพื่อช่วยวิศวกรแหล่งกักเก็บ
ประเมินผลและจัดการสมรรถนะของหลุมอย่างมีประสิทธิผล      นอกจากข้อได้เปรียบที่อ้างถึงแล้ว
การรวมแผนภาพ  ของอัตราการผลิตที่ถูกทำให้เป็นมาตรฐานและการดุลย์มวลสารเชิงพลวัตร ช่วย
ให้การพยากรณ์ปริมาณสำรองไฮโดรคาร์บอนที่สามารถผลิตได้หลังจากที่การผลิตอยู่ในภาวะที่การ
ไหลของไฮโดรคาร์บอนเคลื่อนที่จากขอบเขตของแหล่งกักเก็บ

แผนภูมิอัตราการผลิตที่ทำให้เป็นมาตรฐานเป็นการลากเส้นระหว่างอัตราการผลิตที่ทำให้
เป็นมาตรฐานกับปริมาณการผลิตสะสม    โดยที่ข้อมูลการผลิตบนพื้นผิวเป็นสิ่งจำเป็นในการสร้าง
แผนภูมินี้

ภาควิชา วิศวกรรมเหมืองแร่และปิโตรเลียม          ลายมือชื่อนิสิต..................................
สาขาวิชา วิศวกรรมปิโตรเลียม                        ลายมือชื่ออาจารย์ที่ปรึกษา ......................
ปีการศึกษา 2549                                  ลายมือชื่ออาจารย์ที่ปรึกษาร่วม ..................

TUAN ANH NGUYEN: PERFORMANCE EVALUATION OF COMMINGLED WELLS WITH PRODUCTION DATA. THESIS ADVISOR: SUWAT ATHICHANAGORN, Ph. D., THESIS CO-ADVISOR: DYUNG TIEN VO, Ph. D., 199 pp, ISBN 974-14-3390-5

The objective of this work is to build a simple technique to analyze production data of oil wells producing from commingled reservoirs, in order to estimate the amount of movable oil in place. When a well producing in pseudo-steady-state period, rate normalization enables early estimation of ultimate recovery on both single and multi-layer reservoirs. Contribution of layers with different productivity can be qualitatively recognized.

For oil and gas reservoirs, when combined with dynamic material balance chart, the rate normalization technique serves as a diagnostic tool to help reservoir practitioners evaluate and manage well performance more effectively. Combination of the two plots (rate normalization and flowing material balance) visually allows for the forecast of producible reserve after all boundaries have been felt.

Rate normalization graph is a plot between normalized rate and cumulative production. Surface production data are necessary for constructing the graph.

Department: Mining and Petroleum Engineering     Student's Signature:...................

Field of Study: ... Petroleum Engineering.........     Advisor's Signature:...................

Academic Year: ..................... 2006..................     Co-Advisor's Signature:...................

# ACKNOWLEDGEMENTS

I would like to express my sincerest gratitude and appreciation to:

# CONTENTS

# CONTENTS

# CONTENTS

**CHAPTER**                                                                 **Page**

# LIST OF TABLES

# LIST OF TABLES

**TABLE**                                                                                          **Page**

# LIST OF FIGURES

# LIST OF FIGURES

**LIST OF FIGURES**

# LIST OF FIGURES

# LIST OF FIGURES

# NOMENCLATURE

<u>Field Variables</u>

*Formation and Fluid Parameters*

| | | |
|---|---|---|
| $A$ | = | drainage or injection area, ft$^2$ |
| $B$ | = | formation volume factor, RB/STB |
| $B_o$ | = | oil formation volume factor, RB/STB |
| $B_g$ | = | gas formation volume factor, RB/MCF |
| $C$ | = | wellbore storage coefficient, RB/psia or cc/atm |
| $h$ | = | formation thickness, ft |
| $k$ | = | absolute permeability, md or cm$^2$ |
| $k_1$ | = | absolute permeability of layer one, md |
| $k_2$ | = | absolute permeability of layer two, md |
| $k_j$ | = | absolute permeability of layer j, md |
| $(kh)_t$ | = | Total permeability –thickness product, mdft |
| $k_e$ | = | effective permeability, md |
| $k_g$ | = | effective permeability to gas, md |
| $k_o$ | = | effective permeability to oil, md |
| $k_w$ | = | effective permeability to water, md |
| $k_{rg}$ | = | relative gas permeability, fraction |
| $k_{ro}$ | = | relative oil permeability, fraction |
| $k_{rw}$ | = | relative water permeability, fraction |
| $\bar{k}$ | = | average permeability, md |
| $L$ | = | length, any units system |
| $H$ | = | vertical length, any units system |
| $\mu$ | = | fluid viscosity, cp |
| $\mu_g$ | = | gas viscosity, cp |
| $\mu_o$ | = | oil viscosity, cp |
| $N$ | = | original oil-in-place, STB |
| $N_p$ | = | cumulative oil production, STB |
| $\phi$ | = | porosity, percent or fraction |
| $r_e$ | = | reservoir drainage radius, ft |

$R_p$      = producing gas-oil ratio, scf/STB

$R_s$      = solution gas-oil ratio, scf/STB

$r_w$      = wellbore radius, ft

$r_{wa}$      = apparent wellbore radius (includes formation damage or stimulation), ft

$\rho_b$      = saturated bulk density, g/cc

$S$      = the Laplace transform parameter

$S_g$      = gas saturation, fraction

$S_{gr}$      = residual gas saturation, fraction

$S_{gv}$      = surface area per unit grain volume, $1/10^{-6}$ m

$S_o$      = oil saturation, fraction

$S_{or}$      = residual oil saturation, fraction

$S_{nwp}$      = non-wetting phase saturation, fraction

$S_w$      = water saturation, fraction

$S_{wi}$      = irreducible water saturation, fraction

$STB$      = stock tank barrel, 5.6148 $ft^3$

$T$      = temperature, $^o$F

$u$      = Laplace transform parameter, 1/t

$d$      = tubing diameter, inch

$e$      = tubing roughness, inch.

*Pressure/Rate/Time Parameters*

$b$      = Fetkovich/Arps decline curve exponent

$b_{pss}$      = constant for the liquid flow equation as defined in Eq. 3-25

$r_{eD}$      = dimensionless drainage radius

$c_g$      = gas compressibility, $psi^{-1}$

$c_o$      = oil compressibility, $psi^{-1}$

$c_{rock}$      = formation compressibility, $psi^{-1}$

$c_t$      = total system compressibility, $psi^{-1}$

$c_{ti}$      = initial total system compressibility, $psi^{-1}$

$c_w$      = water compressibility, $psi^{-1}$

$D$      = decline rate, % per year.

$K$      = constant as defined by Eq. 2-21

| | | |
|---|---|---|
| $m$ | = | constant in the pseudosteady-state equation for liquid flow, as defined by Eq. 3-24, psi/STB |
| $p$ | = | pressure, psia |
| $\bar{p}$ | = | average reservoir pressure, psia |
| $\Delta p$ | = | $p_i - p_{wf}$, total reservoir pressure drop, psi |
| $p_i$ | = | initial reservoir pressure, psia |
| $p_{tf}$ | = | flowing surface tubing pressure, psig |
| $p_{wf}$ | = | flowing bottomhole pressure, psia |
| $p_{ws}$ | = | shut-in bottomhole pressure, psia |
| $q$ | = | production rate, STB/day |
| $q_g$ | = | gas rate, scf/day |
| $q_t$ | = | total gas rate, scf/day |
| $q_o$ | = | oil flow rate, STB/day |
| $q_{sf}$ | = | surface flow rate, STB/day |
| $J$ | = | well productivity defined by Eq. 3-36, STB/psi/day |
| $J_1$ | = | ordinary Bessel function, first kind, first order |
| $J_0$ | = | ordinary Bessel function, first kind, zero order |
| $f_m$ | = | Moody friction factor defined by Eq. 3-39 & 3-40 |
| $Q$ | = | cumulative production, STB |
| $Q_p$ | = | cumulative production at any time defined by Eq. 2-25, STB |
| $Q_{Dd}$ | = | dimensionless cumulative production defined by Eq. 2-37 to 2-39, STB |
| $Q_m$ | = | modified cumulative production defined by Eq. 2-49, STB |
| $(q/\Delta p)$ | = | pressure drop normalized rate function, STB/D/psi |
| $(q/\Delta p)_i$ | = | pressure drop normalized rate integral function, STB/D/psi |
| $(q/\Delta p)_{id}$ | = | pressure drop normalized rate integral-derivative function, STB/D/psi |
| $t$ | = | time, days or hours |
| $\bar{t}$ | = | material balance time defined by $\bar{t} = \dfrac{N_p}{q_o}$, days |
| $t_c$ | = | $Q/q$, material balance time, days |
| $t_{ca}$ | = | material balance time for gas defined by Eq.2-42, days |
| $t_{pss}$ | = | time for the onset of pseudosteady-state, days |
| $s$ | = | skin |

| | | |
|---|---|---|
| $s_{pss}$ | = | equivalent skin during pseudo steady state flow |
| $\overline{\eta}$ | = | constant defined by Eq. 3-33 |
| $C_A$ | = | reservoir shape factor |
| $\gamma_g$ | = | gas specific gravity |
| $\gamma_o$ | = | oil specific gravity |
| $\gamma_{wg}$ | = | gas-water mixture specific gravity |
| $M_o$ | = | oil molecular weight |

Dimensionless Variables

| | | |
|---|---|---|
| $p_{wD}$ | = | dimensionless pressure in the wellbore |
| $p_{wD}'$ | = | logarithmic derivative of dimensionless pressure in the wellbore |
| $q_D$ | = | dimensionless rate |
| $r_D$ | = | dimensionless radius |
| $R_D$ | = | $r/r_w$, dimensionless radial distance. |
| $r_{eD}$ | = | dimensionless drainage radius |
| $t_D$ | = | dimensionless time |
| $t_{Dd}$ | = | dimensionless time defined in Arps type curve |
| $(t_{DA})_{pss}$ | = | dimensionless time at pseudo steady state $(=t_D r^2_w/A)$ |
| $C_D$ | = | dimensionless wellbore storage coefficient |
| $p_{wsD}$ | = | total dimensionless wellbore pressure with skin effects |
| $p_{wCD}$ | = | total dimensionless wellbore pressure with wellbore storage and skin effects |
| $\overline{p}_{wD}$ | = | total dimensionless wellbore pressure in the Laplace domain |
| $\overline{p}_{wsD}$ | = | total dimensionless wellbore pressure with skin effects in the Laplace domain |
| $\overline{p}_{wCD}$ | = | total dimensionless wellbore pressure with wellbore storage/skin effects in the Laplace domain |
| $\overline{q}_D$ | = | dimensionless rate in the Laplace domain |
| $\overline{q}_{sD}$ | = | dimensionless rate with skin effects in the Laplace domain |
| $\overline{q}_{CD}$ | = | dimensionless rate with wellbore storage and skin effects in the Laplace domain |

Material Balance Decline Type Curve Analysis

$N_{pDd}$ = dimensionless decline cumulative production function

$p_D$ = $\dfrac{kh}{141.2\,qB\mu}\Delta p$ dimensionless pressure function for the constant flow rate case

$q_D$ = $141.2\dfrac{B\mu}{kh\,(p_i-p_{wf})}q$ dimensionless rate function for the constant flow rate case

$t_D$ = $0.00633\dfrac{kt}{\phi\mu c_t r_w^2}$ dimensionless time based on wellbore radius

$t_{DA}$ = $0.00633\dfrac{kt}{\phi\mu c_t A}$ dimensionless time based on drainage area

$t_{Dd}$ = $\dfrac{2\pi}{b_{Dpss}}t_{DA}=0.00633\dfrac{kt}{\phi\mu c_t A}$, (t=days), dimensionless decline time as defined by Fetkovich.

Pressure Transient Analysis

$p_{wD}$ = $\dfrac{kh}{141.2\,qB\mu}\Delta p$, dimensionless wellbore pressure function for constant injection rate case, including wellbore storage and skin effects

$p_{wD}{}'$ = $t_D\dfrac{dp_{wD}}{dt_D}=\dfrac{dp_{wD}}{d(\ln t_D)}$, logarithmic derivative of dimensionless wellbore pressure function for the constant flow rate case, including wellbore storage and skin effects

$p_{wDi}$ = $\dfrac{1}{t_D}\displaystyle\int_0^{t_D}p_{wD}(\tau)d\tau$, dimensionless wellbore pressure integral function, including wellbore storage and skin effects

$p_{wDi}{}'$ = $t_D\dfrac{dp_{wDi}}{dt_D}=\dfrac{dp_{wDi}}{d(\ln t_D)}$, logarithmic derivative of dimensionless wellbore pressure integral function, including wellbore storage and skin effects

$t_D$ = $0.0002637\dfrac{k}{\phi\mu c_t r_w^2}t$, (t=hours) dimensionless time based on the wellbore radius

Special Functions

$I_0(x)$ = modified Bessel function of the 1st kind, zero order

$I_1(x)$ = modified Bessel function of the 1st kind, 1st order

$K_0(x)$ = modified Bessel function of the 2nd kind, zero order

$K_1(x)$ = modified Bessel function of the 2nd kind, 1st order

Special Subscripts

$i$ = integral function or initial value

$id$ = integral derivative

$inf$ = infinite-acting reservoir

$o$ = oil

$g$ = gas

$pss$ = pseudosteady-state

$w$ = water

$id$ = integral-derivative function

Operators/Constants:

M = thousand

MM = million

$e$ = exponential operator

exp = exponential operator

$\gamma$ = Euler's Constant = 0.577216

$\pi$ = circumference to diameter ratio = 3.14159265

Functions

$Y(t)$ = transient solution in well-pressure equation

$Z_j(t)$ = transient solution in rate equation for $j$th layer

$Y_0$ = ordinary Bessel function, second kind, zero order

$Y_1$ = ordinary Bessel function, second kind, first order

# CHAPTER 1

# INTRODUCTION

Estimating reserve and predicting production from reservoirs has been a challenge for reservoir practitioners. Many methods have been developed in the past several decades. One frequently used basic technique is decline curve analysis for estimating recoverable reserve. Most of the existing decline curves analysis techniques are based on the empirical Arps equation[1]: exponential, hyperbolic, and harmonic equations. Decline curve analysis is based on the fundamental assumption that past operating conditions will remain unchanged. The following is a list of inherent assumptions implied when performing rate-time decline curve analysis:

- The well is produced at or near capacity
- The well drainage area remains constant
- The well is produced under constant bottom-hole pressure.

In reality, it is difficult to foresee which declining trend the reservoir will follow, which lead to potential error of each approach. For example, the exponential decline curve tends to underestimate reserve and production rates; the harmonic decline curve has a tendency to over predict reservoir performance[2]. In some cases, production decline data do not follow any model but cross over the entire set of curve[3].

Fetkovich[4] combined the transient rate and the pseudo steady state decline curve in a single graph. He also related the empirical equations of Arps[1] to the single phase flow solution and attempted to provide theoretical basis for the Arps equations. This was realized by developing the connection between the material balance and the flow rate equation based on his previous work[5, 6].

Many derivations[7, 8] were based on the assumption of single phase oil flow in close boundary systems. These solutions were only suitable for under-saturated (single phase) oil flow. However, in reality, there are many oil wells produce under

condition where reservoir pressure is below the bubble point (production below the saturation pressure). Therefore, two phase flow instead of single phase flow are often the norm. In this case, Lefkovits *et al.*[9] derived the exponential decline for gravity drainage reservoir with a free surface by neglecting capillary pressure. Fetkovich *et al.*[10] included gas oil relative permeability effects on oil production for solution gas drive through pressure ratio term. This assumes the oil relative permeability is a function of fluid saturation which depends on fluid/rock properties.

Reserve estimate from multi-layer reservoirs has been the centre of study by many engineers and scientists. Wattenbarger and El-banbi[11], [12] combined the gas material balance equation with the stabilized flow equation to analyze commingled reservoirs producing either at constant or variable bottom hole pressure and took into account non-Darcy flow into their "Layered Stabilized Flow Model" (LSFM), by history-matching with production data, OGIP, Darcy flow and non-Darcy flow coefficients, and flow rate of each individual layer was determined. LSFM can tolerate numerous transient periods caused by variations in producing conditions. These commingled reservoirs are layered reservoirs linking only through the wellbore. These reservoirs do not experience cross flow within their reservoir boundaries. The LSFM method was further improved by Arevalo-Villagran[13] by combining the material balance gas equation with the real gas boundary dominated flow equation for each layer of the multiple layers commingled system. This method is extended to allow modeling of re-completion and differential pressure in the layers.

Gulf of Thailand geological formation characteristics are dominantly faulty with sands and shale inter-bedded, formed from the fluvial depositional environment. Hydrocarbon is distributed from depths as shallow as 4000' True Vertical Depth (TVD) to as deep as 11,000' TVD. Although gas is accounted for 80% of hydrocarbon underground, its stacked pays and compartmentalized reservoir nature lead most producing companies towards mono-bore completion in their operations. From initial production until pseudo-steady state flow period, the duration of zonal effects can change significantly between zones due to dynamic flow between reservoirs communicated through the wellbore. Assessment of zonal properties and reserve estimate from commingled production are complicated due to the dynamic contribution between zones at different times. Depending on the number of zones

being commingled often driven by the business need, challenges for reservoir surveillance and reserve assessment for commingled production thus often deal with the practicality of data collection and the ambiguity of data evaluation.

On the basis of these recent established works on commingled pressure transient theory and advanced decline curve technique, this study combines and extends the theory and application of both techniques to examining field tests for gas and oil commingling producers in the Gulf of Thailand. This work should help establish a solid basis for the common commingling practice in the region and also add to the literature which is currently limited with field test examples for the problem of interest. The study combines pressure transient theory with advanced decline curve analysis technique for single-layer system and extends its application to commingled systems with focus on rate normalization.

The study is divided into two phases:

Phase One

- Use commercial software to build single layer and two-layer gas reservoirs with variable Darcy flow coefficients. Production data, generated from the above models, will be used in rate normalization analysis to estimate ultimate recovery of the reservoirs. Zonal contribution of each layer in two-layer reservoir system is studied by varying reservoir properties of each layer and analyzing production data. Plotting $P/Z$ versus cumulative production to estimate original gas in place (OGIP) and compare with the actual OGIP.

- Build a model for single layer oil reservoir and apply the rate normalization technique to verify its application for the liquid case.

- Further extend the model to two-layer reservoirs with variable Inflow Performance Relationship (IPR) of the two layers. Use rate normalization and cumulative production to estimate ultimate recovery of the oil reservoir as well

as understand contribution of each layer throughout the life of the reservoir system.

Phase Two

- Apply rate normalization method on actual production data obtain from single and multiple layered oil and gas wells.

- Analyze case history to determine the usefulness of rate normalization when combining with conventional $P/Z$ curve to monitor and make a necessary decision to manage and improve performance of oil and gas reservoirs.

# CHAPTER 2

# LITERATURE REVIEW

A large number of reservoirs have been found where producing formation is composed of two or more layers of different physical characteristics, such as permeability and porosity, and where also the thickness of the layers differs. Extensive studies have been done to understand the behavior of commingled reservoirs. A number of papers have been written on the development of alternative approaches in analyzing production performance and estimating layered properties, reservoir drainage area, and hydrocarbon in place of commingled oil and gas reservoir systems. Behavior of multi layered reservoir without crossflow and overview of decline and type curves will be discussed in the following sections.

## 2.1 General Definition of Layered Reservoirs

Before proceeding further, it is appropriate to define a few terms used extensively throughout this report. Layered reservoirs can be classified into two groups:

## 2.1.1 Layered Reservoirs with Crossflow

**Figure 2.1** shows a crossflow reservoir, which consists of four continuous layers that are communicating at the contact planes. These layers are not entirely separated by impervious layers; therefore, interlayer crossflow could occur during the production life of the reservoir. The crossflow would be directed from the layer of low permeability to the layer of higher permeability, as shown in the figure. If $k_1$ is greater than $k_2$, then the pressure transient would travel faster in the layer of permeability $k_1$ than in the layer of permeability $k_2$. The duration of the crossflow period depends on the storage of each layer. If the storage of the layer of permeability $k_1$ is negligible when compared to the storage of the layer of permeability $k_2$, then crossflow will continue throughout the life of the well. If the opposite occurs, then the duration of the crossflow period will be short. Pressure transient testing in such

reservoirs has the same behavior as that of a homogeneous system. The following relationship can be applied for such systems.

Permeability-thickness product

$$(kh)_t = \sum_{j=1}^{n} (kh)_j \tag{2.1}$$

Porosity-compressibility product

$$(\phi c_t h)_t = \sum_{j=1}^{n} (\phi c_t h)_j \tag{2.2}$$

The total number of layers is $n$. The individual layer permeability may be approximated from

$$k_j = \left(\frac{q_j}{q}\right)\left[\frac{(kh)_t}{h_j}\right], \quad j = 1, 2, ...., n \tag{2.3}$$
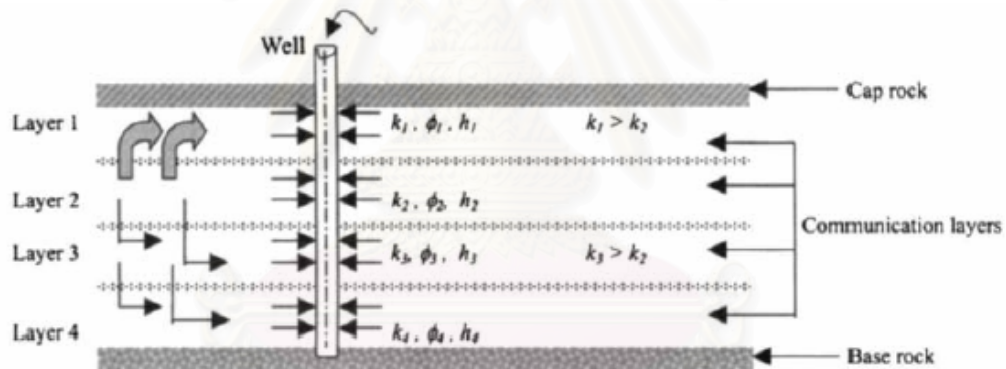


**Figure 2.1**:    Four-layer crossflow reservoir[14].

## 2.1.2 Layered Reservoirs Without Crossflow

This type of reservoir consists of two or more layers separated by impervious layers. The fluid is carried to the surface through a common wellbore. Each layer has different properties as shown in **Figure 2.2**.

**Figure 2.3** shows a graph of dimensionless pressure, $p_D$, versus dimensionless time, $t_D$ for a two-layer reservoir with permeability ration $k_1/k_2$ of 1, 2, 10 and 100. All four curves are for $r_e/r_w$ of 2000. Production is commingled at the well, so layers

communicate only through the wellbore. From well testing perspective, early-time pressure drawdown behavior in such a system yield a straight line on the semilog plot as shown in **Figure 2.3**. Boundary effect causes the upward bending in **Figure 2.3**. After a long production time, pseudo-steady-state conditions exist and pressure behavior will be linear with time. For two-layer reservoir systems, pseudo steady state begins approximately at[15]

$$\left(t_{DA}\right)_{pss} = 23.5\left(\frac{k_1}{k_2}\right), \quad k_1 > k_2 \tag{2.4}$$
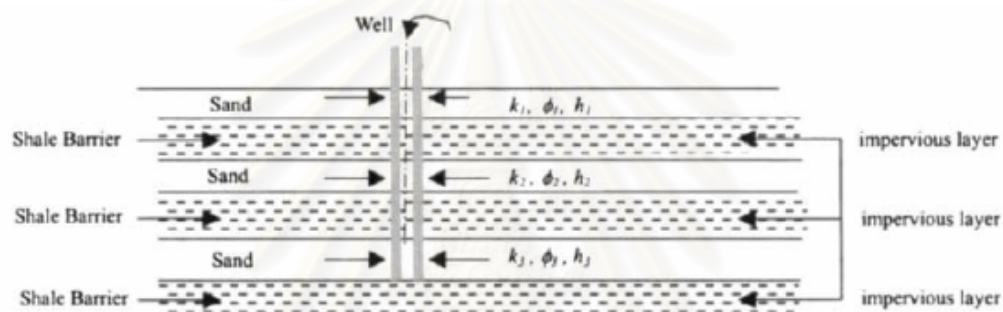


**Figure 2.2**:    Three-layer crossflow reservoir[14].

The time at the beginning of pseudo steady state also depends on

- Relationship between $\phi$, $h$, and total compressibility in the various layers
- Reservoir shape
- Number of layers
- Well location
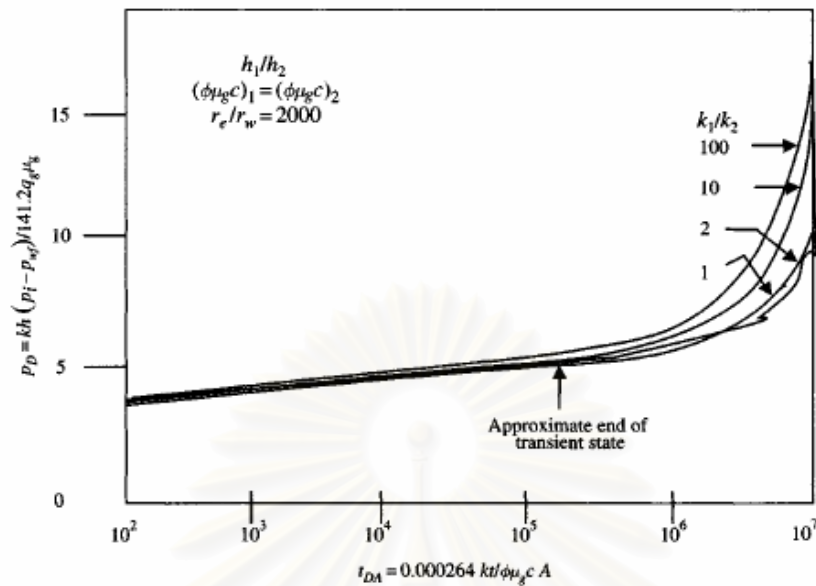
**Figure 2.3**: Muskat straight line intercepts for two-layer reservoirs without crossflow (after Ramey and Miller, JPT, Jan 1972)[16].

## 2.2 Behavior of Commingled Reservoirs

Many papers have been published on modeling single-layer gas reservoir system. Most of the work show how a gas system can be modeled as a liquid system using appropriate transforms. The two most generally used transforms are pseudo-pressure[17] and pseudo-time[18]. Fraim and Wattenbarger[19] and Ding *et al.*[20] showed that, during the boundary dominated flow period, gas properties evaluated at the average reservoir pressure should be used to evaluate pseudo-time.

Multi layers without crossflow (no crossflow) system where each layer has the same initial pressure has been investigated by several authors. Rigorous solutions describing pressure and flow-rate behavior of such bounded system were developed by Lefkovits *et al.*[21] The paper also contains report result of Horner[44] giving the solution for the infinite-acting period. Papadopulos[45] investigated unbounded two-layer aquifers with unequal initial pressures and gave both exact solutions as contour integrals and asymptotic approximations for pressure and flow-rate behavior.

The following section will review pressure and rate responses of layered reservoir through Leftkovits *et al.*[21] solution (Laplace domain and approximation real domain formulation), Tariq and Ramey[22] solution (dimensionless reformulation of the Lefkovits *et al.* solution), Spath *et al.*[23] (approach based on superposition of layer pressures), and Blasingame *et al.*[24] (approximate $p_{wCD}(t_D)$ solutions — wellbore storage/skin effects).

### 2.2.1 Lefkovits, Hazebroek, Allen, and Matthews Solution

The first rigorous study of pressure behavior for layered reservoir systems was developed by Lefkovits, Hazebroek, Allen, and Matthews in 1961. Their work served as the basis for much of the work that followed. Their reservoir model is assumed to be homogenous and isotropic, and the reservoir pore space is assumed to be filled with a fluid of small and constant compressibility. The reservoir consists of *n* number of layers with distinct layer properties including permeability, *k*, thickness, *h*, porosity, $\phi$, viscosity, $\mu$, total compressibility, $c_t$, wellbore and outer radii, $r_w$ and $r_e$, and skin, *s*, Lefkovits *et al.*[21] formulated the following Laplace domain solution for pressure drop and layer flow rates.

$$\Delta \overline{p}_w(u) \;=\; \frac{q}{2\pi u^{3/2}} \frac{1}{\displaystyle\sum_{j=1}^{n} \beta_j \alpha_j \frac{\psi_{1j}(u)}{\psi_j(u)}} \tag{2.5}$$

And

$$\frac{\overline{q}_j}{q}(u) \;=\; \beta_j \alpha_j \frac{\psi_{1j}(u)}{\psi_j(u)} \frac{1}{u \displaystyle\sum_{j=1}^{n} \beta_j \alpha_j \frac{\psi_{1j}(u)}{\psi_j(u)}} \tag{2.6}$$

where the following "shorthand" variables are used:

$$\psi_{0j}(u) \;=\; K_0(\alpha_j \sqrt{u})\, I_1(\gamma_j \sqrt{u}) + I_0(\alpha_j \sqrt{u})\, K_1(\gamma_j \sqrt{u})$$

$$\psi_{1j}(u) \;=\; K_1(\alpha_j \sqrt{u})\, I_1(\gamma_j \sqrt{u}) - I_1(\alpha_j \sqrt{u})\, K_1(\gamma_j \sqrt{u})$$

$$\psi_j(u) = \alpha_j s_j \sqrt{u}\,\psi_{1j}(u) + \psi_{0j}(u)$$

and the following parameters are defined:

$u$ = Laplace transform parameter

$q$ = total flow rate, cc/sec

$s_j$ = skin factor for layer $j$ (dimensionless)

The following "grouped" variables are used to simply this formulation

$$\beta_j = \frac{k_j h_j}{\mu_j} \qquad \alpha_j = \frac{r_{wj}}{\sqrt{\eta_j}} \qquad \gamma_j = \frac{r_{ej}}{\sqrt{\eta_j}} \qquad \eta_j = \frac{k_j}{\phi_j \mu_j c_j}$$

Lefkovits *et al.*[21] also proposed the approximate real domain solutions for pressure drop and layer flow rates where these results are valid for all but very small times:

$$p_i\text{-}p_{wf}(t) = \frac{q}{2\pi}\left[\frac{2t}{\sum\limits_{j=1}^{n}\phi_j h_j r_e^2 c_t} + \frac{1}{\sum\limits_{j=1}^{n}\phi_j h_j}\sum\limits_{j=1}^{n}(\phi_j^2 h_j \mu / k_j)\,(\ln[r_e/r_w]-3/4)\right] + Y(t) \qquad (2.7)$$

and

$$q_j(t) = q\,\frac{\phi_j h_j}{\sum\limits_{j=1}^{n}\phi_j h_j} + Z_j(t) \qquad (2.8)$$

where

$$Y(t) = -\frac{\pi}{4}q\sum\limits_{k=1}^{\infty}\frac{\exp(-x_k^2 t)}{\sum\limits_{j=1}^{n}\frac{1-J_1^2(\gamma_j x_k)}{\left[\frac{2}{\pi}J_1(\gamma_j x_k)\ln\left[\frac{\gamma}{2}\alpha_j x_k\right]-Y_1(\gamma_j x_k)\right]^2}} \qquad (2.9)$$

and

$$Z_j(t) = \pi \beta_j \sum_{k=1}^{\infty} \frac{\dfrac{\dfrac{2}{\pi} J_1(\gamma_j x_k)\ln\left[\dfrac{\gamma}{2}\alpha_j x_k\right] - Y_1(\gamma_j x_k)}{J_1(\gamma_j x_k)}\exp(-x_k^2 t)}{\displaystyle\sum_{j=1}^{n}\beta_j \dfrac{1 - J_1^2(\gamma_j x_k)}{\left[\dfrac{2}{\pi} J_1(\gamma_j x_k)\ln\left[\dfrac{\gamma}{2}\alpha_j x_k\right] - Y_1(\gamma_j x_k)\right]^2}} \qquad (2.10)$$

The $x_k$ are the non-vanishing roots of Equation 2.10a

$$\sum_{j=1}^{n}\beta_j\alpha_j \frac{K_1\left(\alpha_j S\right)I_1\left(\gamma_j S\right) - I_1\left(\alpha_j S\right)K_1\left(\gamma_j S\right)}{K_0\left(\alpha_j S\right)I_1\left(\gamma_j S\right) + I_0\left(\alpha_j S\right)K_1\left(\gamma_j S\right)} = 0 \qquad (2.10a)$$

The derivation of Equations 2.7 and 2.8 is quite detailed, and these solutions (Equations 2.7 and 2.8) provide accurate approximations only for large times (*i.e.*, as $Y(t)$ and $Z_j(t)$ approach zero with increasing times). These solutions were validated by numerical inversion results obtained using Spath *et al.*[23] formulation.

**Figure 2.4** presents the dimensionless wellbore pressure versus dimensionless time behavior for two different cases of a two-layer reservoir system. The properties of the reservoirs systems are:

Case 1:                Case 2:

$k_1/k_2$ = 10/1      $k_1/k_2$ = 1.25/1

$h_1/h_2$ = 1/1      $h_1/h_2$ = 1/1

$\phi_1/\phi_2$ = 1/1      $\phi_1/\phi_2$ = 1/1

$s_1 = s_2$ = 0      $s_1 = s_2$ = 0

$r_{eD1} = r_{eD2}$= 2000      $r_{eD1} = r_{eD2}$= 2000

**Figure 2.5** shows the production rate from the more permeable layer (layer 1) for the two cases described above. The Lefkovits *et al.*[21] data shown in **Figures 2.4** and **2.5** were digitized from ref. 21.

The other validations of the Lefkovits *et al.*[21] solution with the numerical inversion results are given in **Figures 2.6** to **2.10**. **Figure 2.6** shows dimensionless wellbore pressure versus dimensionless time for the following reservoir properties:

$k_1/k_2 = 4/1$, $h_1/h_2 = 1/20$, $\phi_1/\phi_2 = 2/1$, and $s_1 = s_2 = 0$. **Figure 2.7** shows the production rate from the more permeable layer (layer 1) for this case. **Figure 2.8** presents dimensionless wellbore pressure versus dimensionless time for the following reservoir properties: $k_1/k_2 = 10/1$, $h_1/h_2 = 10/1$, $\phi_1/\phi_2 = 1/1$, and $r_{eD1} = r_{eD2} = 2000$. **Figure 2.9** shows the production rate from the more permeable layer (layer 1) for this case. In each graph, curve "$a$" refers to the case where no skin was present in either layer (*i.e.*, $s_1 = 0$ and $s_2 = 0$), curve "$b$" refers to the case where the skin effects were taken to be $s_1 = 10$ and $s_2 = 1$, and curve "$c$" refers to the case where the skin effects were taken to be $s_1 = 1$ and $s_2 = 10$.
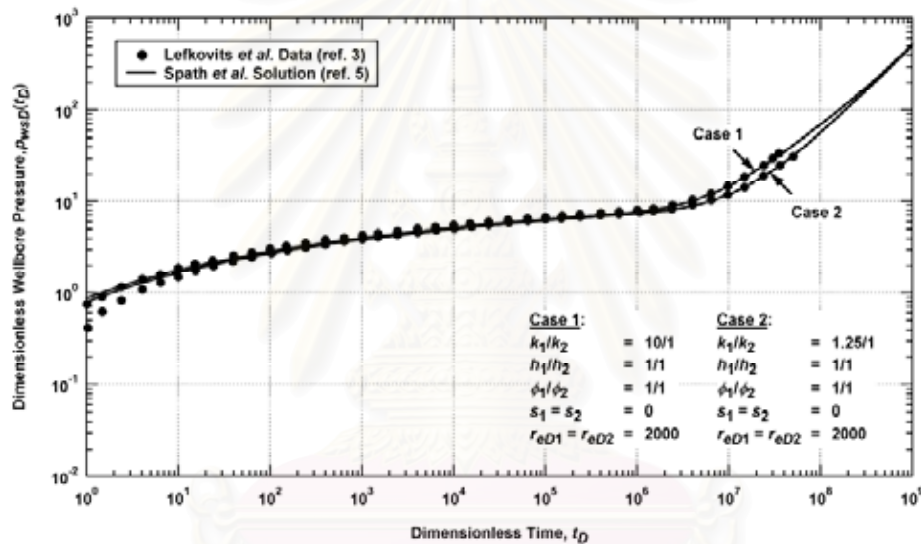


**Figure. 2.4**:     Lefkovits *et al.*[21] data and the numerical inversion results obtained using Spath *et al.*[23] formulation ($p_{wsD}(t_D)$ versus $t_D$ for two examples two-layer reservoir cases).
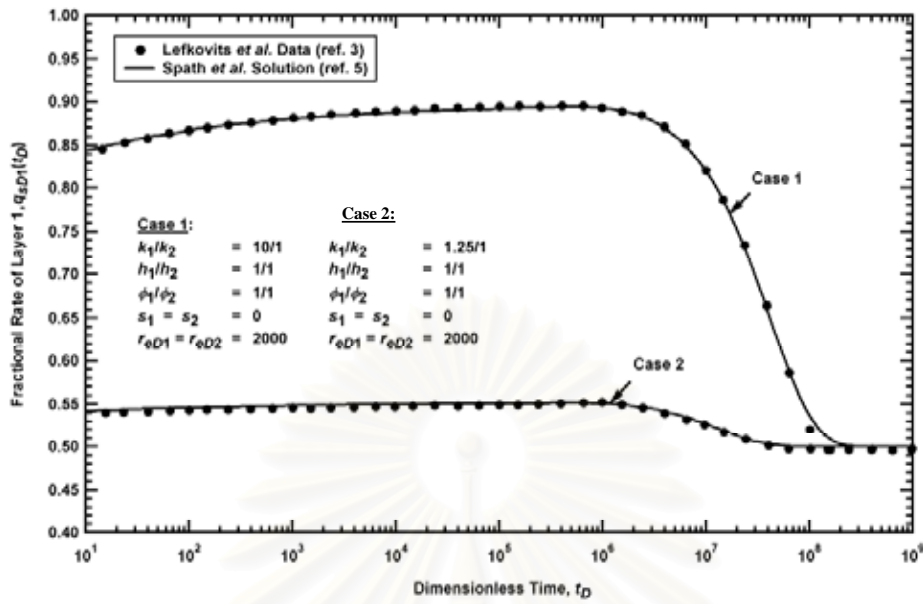
**Figure 2.5**:     Lefkovits *et al.*[21] data and the numerical inversion results obtained using Spath *et al.*[23] formulation ($q_{sD1}(t_D)$ versus $t_D$ for two examples two-layer reservoir cases).
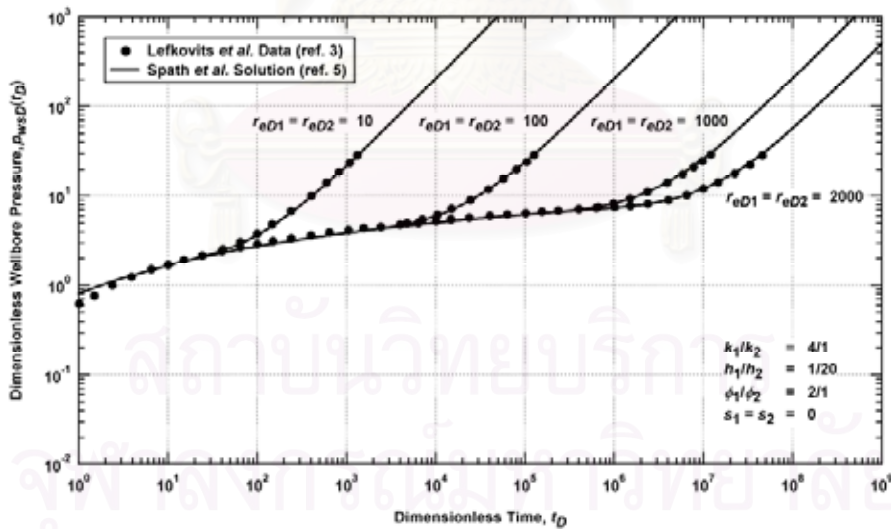


**Figure 2.6**:     Lefkovits *et al.*[21] data and the numerical inversion results obtained using Spath *et al.*[23] formulation ($p_{wsD}(t_D)$ versus $t_D$ for the case of a two-layer reservoir) for several $r_{eD}$ values.
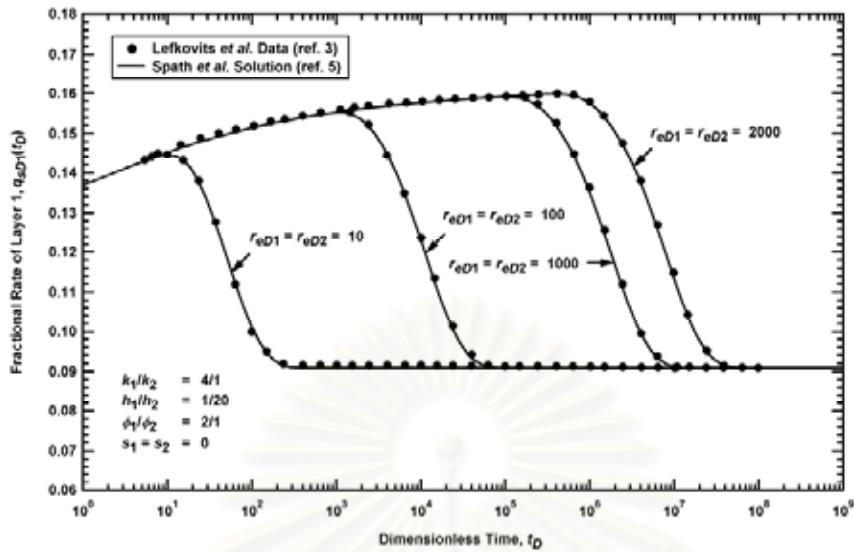
**Figure 2.7**: Lefkovits *et al.*[21] data and the numerical inversion results obtained using Spath *et al.*[23] formulation ($q_{sD1}(t_D)$ versus $t_D$ for the case of a two-layer reservoir) for several $r_{eD}$ values.
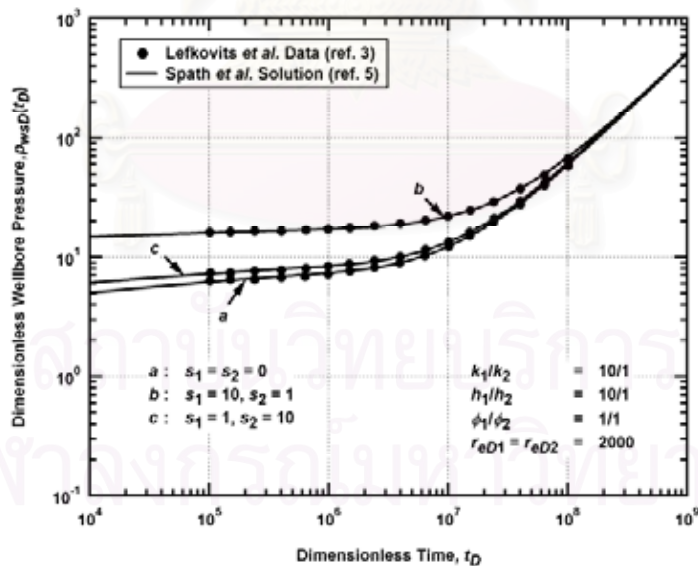


**Figure 2.8**: Lefkovits *et al.*[21] data and the numerical inversion results obtained using Spath *et al.*[23] formulation ($p_{wsD}(t_D)$ versus $t_D$ for the case of a two-layer reservoir) with skin.
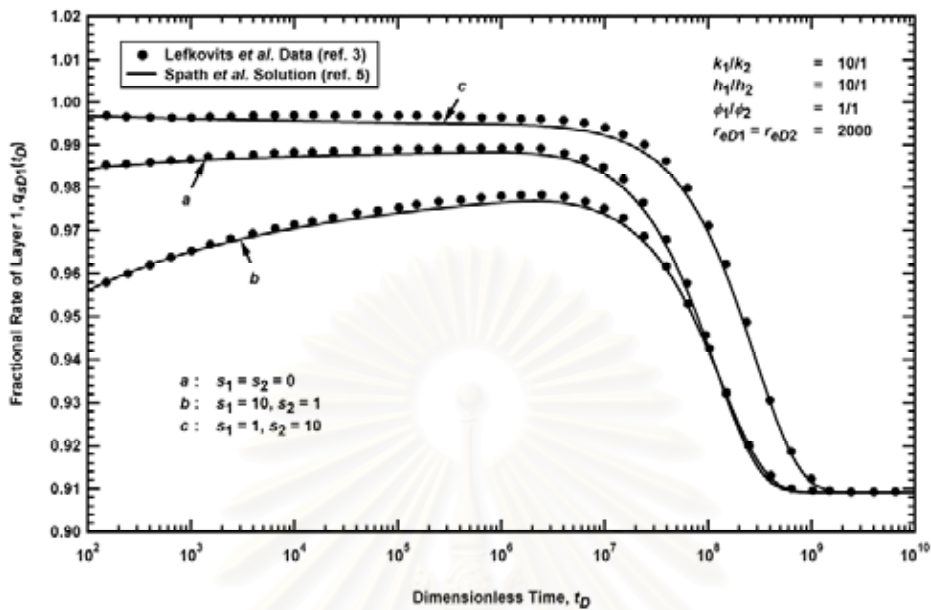
**Figure 2.9**    Lefkovits *et al.*[21] data and the numerical inversion results obtained using Spath *et al.*[23] formulation ($q_{sD1}(t_D)$ versus $t_D$ for the case of a two-layer reservoir) with skin.

**Figure 2.10** presents dimensionless wellbore pressure versus dimensionless time of a three-layer reservoir system. Lefkovits *et al.*[21] data shown on this plot were digitized from ref. 21. **Figure 2.10** also shows the numerical inversion results, obtained by using Spath *et al.*[23] formulation. This reservoir system has the following layer properties:

$k_1/k_2/k_3$  = 0.01/0.1/1

$h_1/h_2/h_3$  = 0.1/0.5/1

$\phi_1/\phi_2/\phi_3$  = 1/1/1

$s_1 = s_2 = s_3 =$  0

### 2.2.2 Tariq and Ramey Solution

Tariq and Ramey[22] (1978) reformulated the problem of a bounded (circular) multilayer reservoir system produced at a constant rate to include the "skin effect" in each layer as well as a total "wellbore storage" model (wellbore storage is not allocated on a layer basis). The resulting partial differential equations were transformed into the Laplace domain, and a dimensionless solution in the Laplace domain was obtained. The solution in the real domain was obtained using numerical inversion of the transformed solution (using the technique proposed by Stehfest[25]).
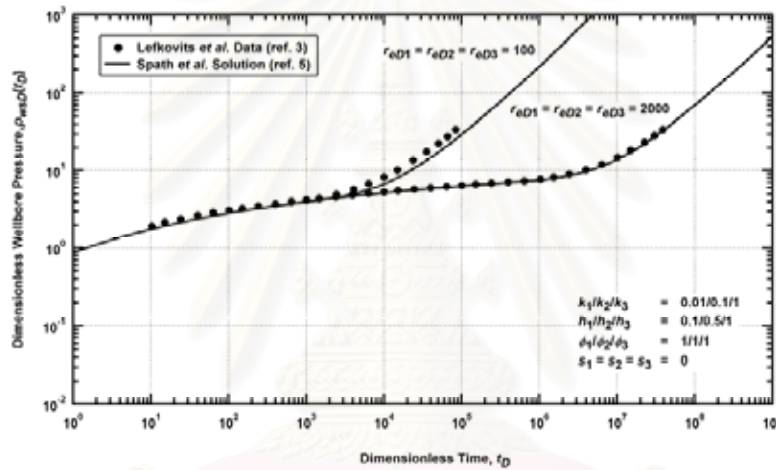


**Figure 2.10:**    Lefkovits *et al.*[21] data and the numerical inversion results obtained using Spath *et al.*[23] formulation ($p_{wsD}(t_D)$) versus $t_D$ for the case of a three-layer reservoir).

The Laplace domain solution for the pressure drop in a producing well proposed by Tariq and Ramey[22] with skin and wellbore storage effects is given by:

$$\Delta \overline{p}_w(u) = \frac{q}{2\pi u^{3/2}} \frac{1}{\dfrac{C\sqrt{u}}{2\pi} + \displaystyle\sum_{j=1}^{n} \dfrac{\beta_j \alpha_j \psi_{1j}(u)}{K_1(\gamma_j \sqrt{u})\delta_I + I_1(\gamma_j \sqrt{u})\delta_K}} \tag{2.11}$$

where the following parameters are defined:

   $u$   = Laplace transform parameter

$q$ = flow rate, cc/sec

$C$ = wellbore storage coefficient, cc/atm

$s_j$ = skin factor for layer $j$ (dimensionless)

and the following "shorthand" variables are used:

$$\delta_I \quad = \quad I_0(\alpha_j \sqrt{u}) - \alpha_j s_j \sqrt{u}\, I_1(\alpha_j \sqrt{u})$$

$$\delta_K \quad = \quad K_0(\alpha_j \sqrt{u}) + \alpha_j s_j \sqrt{u}\, K_1(\alpha_j \sqrt{u})$$

$$\psi_{0j}(u) \quad = \quad K_0(\alpha_j \sqrt{u})\, I_1(\gamma_j \sqrt{u}) + I_0(\alpha_j \sqrt{u})\, K_1(\gamma_j \sqrt{u})$$

$$\psi_{1j}(u) \quad = \quad K_1(\alpha_j \sqrt{u})\, I_1(\gamma_j \sqrt{u}) - I_1(\alpha_j \sqrt{u})\, K_1(\gamma_j \sqrt{u})$$

The following "grouped" variables are used to simplify the formulation

$$\beta_j = \frac{h_j k_j}{\mu_j} \qquad \alpha_j = \frac{r_{wj}}{\sqrt{\eta_j}} \qquad \gamma_j = \frac{r_{ej}}{\sqrt{\eta_j}} \qquad \eta_j = \frac{k_j}{\phi_j \mu_j c_{tj}}$$

Tariq and Ramey[22] gave the following formulation for the ratio of the producing rate of the $j^{th}$ layer with respect to the total production rate (Laplace domain result):

$$\frac{\bar{q}_j}{q}(u) \quad = \quad \frac{\dfrac{\beta_j \alpha_j\, \psi_{1j}(u)}{u\,[K_1(\gamma_j \sqrt{u})\,\delta_I + I_1(\gamma_j \sqrt{u})\,\delta_K]}}{\dfrac{C\sqrt{u}}{2\pi} + \displaystyle\sum_{j=1}^{n} \dfrac{\beta_j \alpha_j\, \psi_{1j}(u)}{K_1(\gamma_j \sqrt{u})\,\delta_I + I_1(\gamma_j \sqrt{u})\,\delta_K}} \tag{2.12}$$

The Tariq and Ramey solution were also validated with numerical inversion results obtained using the Spath et al.[23] formulation. **Figure 2.11** presents the dimensionless wellbore pressure and pressure derivative functions versus dimensionless time for a two-layer reservoir system using several values of dimensionless drainage radius. The properties of the reservoir system are:

$k_1/k_2$ = 10/1

$h_1/h_2$ = 1/1

$\phi_1/\phi_2$ = 1/1

$s_1 = s_2 = 0$

$$r_{eD1} = r_{eD2} = 500, 2000, 5000, 10000$$

The "Tariq and Ramey" data shown in **Figure 2.11** were obtained by numerical inversion of Equation 2.11 ($C$=0). **Figure 2.12** presents the production rate of the more permeable layer (layer 1) for the reservoir system described above, these solutions were obtained by numerical inversion of Equation 2.12 ($C$=0). One can note an exceptional agreement in the solutions plotted on **Figures 2.11** and **2.12** — but one also recognize that the Tariq and Ramey and the Spath *et al.*[23] formulations are mathematically equivalent (though given in different forms).

Another two-layer reservoir case is presented in **Figures 2.13** and **2.14**. The properties of this reservoir system are $h_1/h_2 = 1/1$, $\phi_1/\phi_2 = 1/1$, $s_1 = s_2 = 0$, and $r_{eD1}/r_{eD2} = 2000/50$.
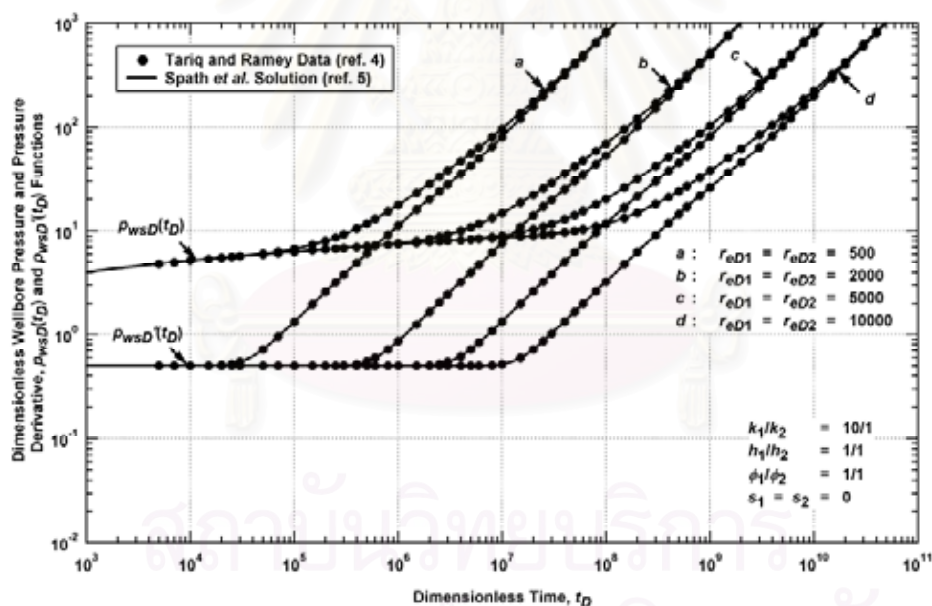


**Figure 2.11:** Tariq and Ramey solution compared to the Spath *et al.*[23] results for the cylindrical source solution, $p_{wsD}(t_D)$ and $p_{wsD}'(t_D)$ versus $t_D$ (two-layer reservoir case).
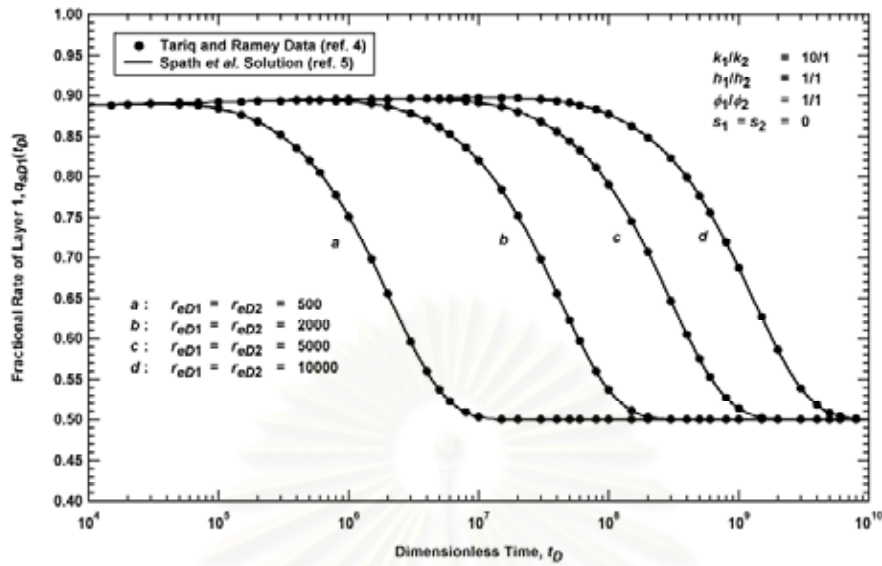
**Figure 2.12**: Tariq and Ramey solution compared to the Spath *et al.*[(23)] results for the cylindrical source solution, $q_{sD1}(t_D)$ versus $t_D$ (two-layer reservoir case).
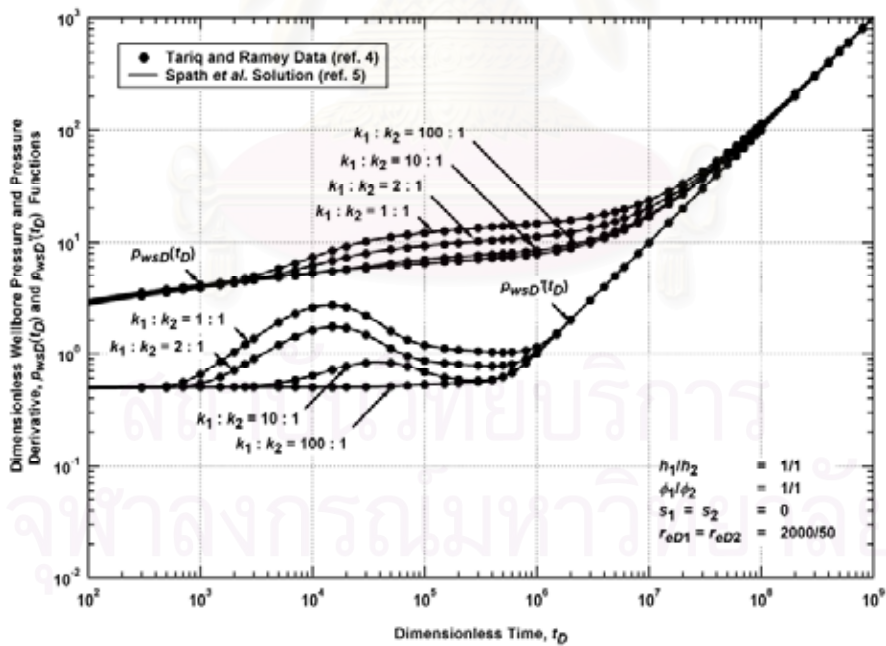


**Figure 2.13**: Tariq and Ramey solution compared to the Spath *et al.*[(23)] results for the cylindrical source solution, $p_{wsD}(t_D)$ and $p_{wsD}{}'(t_D)$ versus $t_D$ (two-layer reser-voir case) for different ratios of $k_1/k_2$.
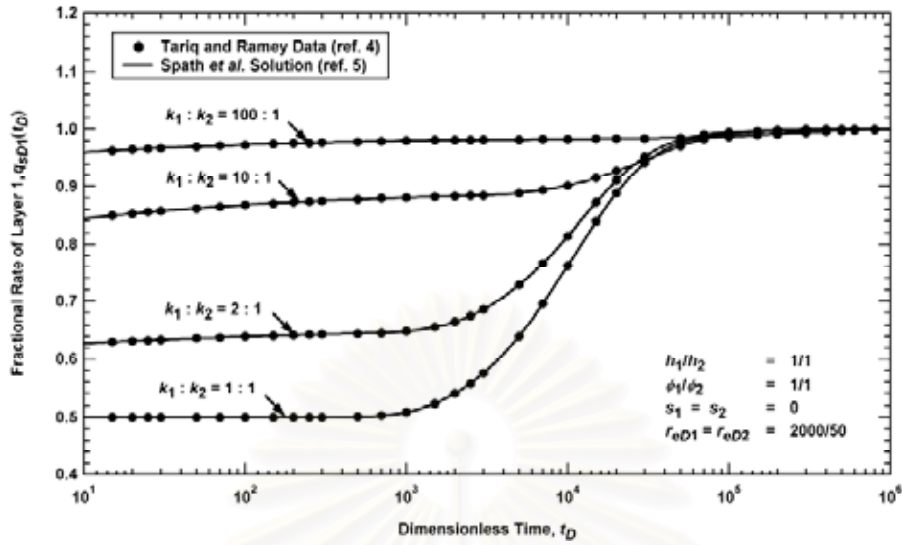
**Figure 2.14**:    Tariq and Ramey solution compared to the Spath *et al.*[23] results for the cylindrical source solution, $q_{sD1}(t_D)$ versus $t_D$ (two-layer reservoir case) for different ratios of $k_1/k_2$.

## 2.2.3 Spath, Ozkan, and Raghavan Solution

Spath, Ozkan, and Raghavan[23] (1990) proposed a stable and robust algorithm to compute pressure and rate responses from wells that produce from commingled reservoirs. This solution approach takes advantage of a unique feature of commingled reservoir production for the constant wellbore pressure solution. This approach yields a viable method for determining the well responses for constant or variable-rate production. Spath *et al.*[23] proposed the following formulation for the dimensionless pressure response for a commingled reservoir:

$$\overline{p}_{wsD}(u) = \frac{1}{\sum_{j=1}^{n} \dfrac{k_j h_j}{kh} \dfrac{1}{\overline{p}_{wDj}(u)}} \qquad (2.13)$$

Note that Equation 2.13 is based on the constant rate dimensionless pressure solution for each layer.

The Spath *et al.*[23] formulation for individual layer rate responses can be obtained by applying Duhamel's theorem to each layer. This gives the following flow rate function

$$\bar{q}_{sDj}(u) \;\; = \frac{k_j h_j}{\overline{k h}} \frac{\bar{p}_{wsD}(u)}{u\,\bar{p}_{wDj}(u)} \tag{2.14}$$

where $\bar{q}_{sDj}(u)$ is simply the $q_j/q$ ratio in the Laplace domain form.

**Table 2.1** presents a comparison of the $p_{wsD}(t_D)$ solutions for the case of a two-layer reservoir system (with skin effects included for each layer) computed using Tariq and Ramey approach (ref. 22), Spath *et al.* formulation (refs. 23 and 26), and the rigorous Laplace domain solution inverted using *Mathematica*.[27]

In terms of applications for these types of solutions, Johnston and Lee[28] in 1991 applied the Spath *et al.*[23] algorithm for the analysis of well test data from wells in a low permeability gas reservoir. This study was particularly useful in that it provided illustrative behavior from multilayer reservoir systems.

## 2.2.4  Blasingame, Johnston, Lee, and Raghavan Solution

Another issue that has not been directly addressed is the incorporation of wellbore storage effects in explicit (yet approximate) solutions. Towards this end, Blasingame, Johnston, Lee, and Raghavan[6] proposed explicit (discrete data) methods to compute the effects of wellbore storage and wellbore phase redistribution distortion and provided three approximate formulations. In particular, the base $p_{wsD}(t_D)$ function (with no wellbore storage) is approximated using piecewise continuous functional approximations.

**Table 2.1** – Comparison of various $p_{wsD}(t_D)$ solutions for a two-layer reservoir system

($k_1 / k_2 = 10$, $r_{eD1} = r_{eD2} = 2000$)

| $t_D$ | $p_{wsD}(t_D)$ for $s_1 = +7$, $s_2 = +3$ | | | $p_{wsD}(t_D)$ for $s_1 = +3$, $s_2 = +7$ | | |
|---|---|---|---|---|---|---|
| | Tariq and Ramey | Spath *et al.* | Numerical Inversion (*Mathematica*) | Tariq and Ramey | Spath *et al.* | Numerical Inversion (*Mathematica*) |
| $2.5 \times 10^2$ | 9.6321 | 9.6300 | 9.6323 | 6.7880 | 6.7890 | 6.6552 |
| $5.0 \times 10^2$ | 9.9958 | 9.9960 | 9.9946 | 7.0012 | 7.0017 | 7.0019 |
| $1.0 \times 10^3$ | 10.3570 | 10.3573 | 10.3570 | 7.3495 | 7.3499 | 7.3496 |
| $5.0 \times 10^3$ | 11.1958 | 11.1959 | 11.1957 | 8.1571 | 8.1571 | 8.1581 |
| $1.0 \times 10^4$ | 11.5550 | 11.5554 | 11.5553 | 8.5064 | 8.5065 | 8.5065 |
| $5.0 \times 10^4$ | 12.3874 | 12.3874 | 12.3866 | 9.3150 | 9.3151 | 9.3152 |
| $1.0 \times 10^5$ | 12.7430 | 12.7432 | 12.7432 | 9.6634 | 9.6634 | 9.6634 |
| $5.0 \times 10^5$ | 13.5782 | 13.5784 | 13.5774 | 10.4816 | 10.4816 | 10.4819 |
| $1.0 \times 10^6$ | 14.0441 | 14.0442 | 14.0438 | 10.9601 | 10.9601 | 10.9597 |
| $5.0 \times 10^6$ | 17.2022 | 17.2020 | 17.1922 | 14.4277 | 14.4275 | 14.4271 |
| $1.0 \times 10^7$ | 20.9530 | 20.9512 | 20.9521 | 18.6420 | 18.6407 | 18.6418 |
| $5.0 \times 10^7$ | 48.1501 | 48.1542 | 48.0628 | 49.1720 | 49.1709 | 49.1543 |
| $1.0 \times 10^8$ | 77.4070 | 77.4000 | 77.4029 | 81.7970 | 81.7898 | 81.7728 |
| $5.0 \times 10^8$ | 281.5500 | 281.5532 | 280.8949 | 290.7860 | 290.7814 | 290.7373 |

These approximations are substituted into the rigorous Laplace domain formulation, manipulated into algebraically convenient forms, then inverted to yield approximate solutions, $p_{wCD}(t_D)$, where these solutions include wellbore storage and skin effects.

The piecewise approximations used by Blasingame *et al.*[24] are:

- Constant $p_{wsD}(t_D)$ case: $p_{wsD}(t_D) = $ constant
- Linear $p_{wsD}(t_D)$ case: $p_{wsD}(t_D) = a + b\, t_D$
- Quadratic $p_{wsD}(t_D)$ case: $p_{wsD}(t_D) = a_0 + a_1\, t_D + a_2\, t_D^2$.

Of the three relations, the "linear $p_{wsD}(t_D)$" case appears to give the most accurate results. In general, the computations are quite accurate compared to results obtained using Laplace transform inversion of the Laplace space solutions.

## 2.3 Decline Curves and Type Curves

Decline curve analysis method, in a variety of forms, has been used in petroleum industry for more than fifty years to analyze production data and forecast reserves. Decline curves represent production from the reservoir under "boundary dominated flow" conditions. This means that during the early life of a well, while it is in "transient flow" and the reservoir boundaries have not been reached, decline curves should not be expected to be applicable. Typically, during transient flow, the decline rate is high, but it stabilizes once boundary dominated flow is reached. For most wells, this happens within the first few months of production. However, for low permeability wells (tight gas wells, in particular) transient flow conditions can last several years, and strictly speaking, should not be analyzed by decline curve methods until after they have reached stabilization. Type curve analysis methods, on the other hand, have become popular, during the last thirty years, to analyze pressure transient test (build up and drawn-down) data. Type curves approach extends the Arps[1] type curve into transient flow region and combines Apr's originally empirical decline curve equations to generate a set of curves that can be used to predict production and estimate reserve throughout the life of a well.

## 2.3.1 Decline Curves

Decline curve analysis is not grounded in fundamental theory but is based on empirical observations of production decline. Three types of decline curves have been identified, namely, exponential, hyperbolic, and harmonic. There are some theoretical equivalents to these decline curves (for example, it can be demonstrated that under certain circumstances, such as constant well back-pressure, equations of fluid flow through porous media under "boundary dominated flow" conditions are equivalent to "exponential" decline). However, by and large, decline curve analysis is

fundamentally an empirical process based on historical observations of well performance. Because of its empirical nature, decline curve analysis is applied, as is deemed appropriate for any particular situation, on single fluid streams or multiple fluid streams. For example, in some instances, the oil rate may exhibit an exponential decline, while in other situations it is the total liquids (oil + water) that exhibits the exponential trend. Thus, in some instances the analysis is conducted on one fluid, sometimes on another, sometimes on the total fluids, sometimes on the ratio (for example Water-Oil-Ratio (*WOR*) or even (*WOR* + 1)). Since there is no overwhelming justification for any single variable to follow a particular trend, the practical approach to decline curve analysis is to choose the variable (gas, oil, oil + water, *WOR*, *WGR* etc..) that results in a recognizable trend and to use that decline curve to forecast future performance.

### 2.3.1.1 Exponential Decline

All decline curve theory starts from the definition of the instantaneous or current decline rate, *D*, as follows:

$$D = -\frac{\Delta q / q}{\Delta t} = \frac{\Delta q}{\Delta t} / q \qquad (2.15)$$

*D*, the decline rate, is "the fractional change in rate per unit time", frequently expressed in "% per year". **Figure 2.15** gives an example of an exponential decline curve, *D* = Slope/Rate.

Exponential decline occurs when the decline rate, *D*, is constant. If *D* varies, the decline is considered to be either hyperbolic or harmonic; in which case, an exponent "*b*" is incorporated into the equation of the decline curve to account for the changing decline rate. For exponential decline, integrating Equation 2.15 yields:

$$\ln\left(\frac{q}{q_i}\right) = -D * t \qquad (2.16)$$

or

$$\frac{q}{q_i} = \frac{1}{e^{Dt}} \ , \text{ or } \ln\left(\frac{q}{q_i}\right) = -\frac{D*t}{2.303} \tag{2.17}$$

where $D$ is decline rate and is constant

Equation 2.17 illustrates that a plot of log-rate versus time will yield a straight line of slope $D/2.303$.
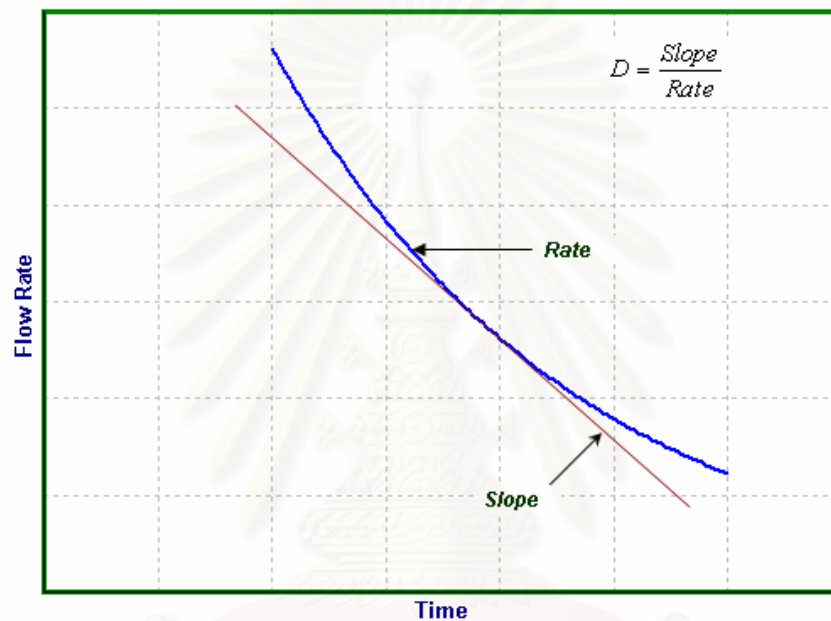


**Figure 2.15**:    Exponential decline curve, decline rate $D$ is constant.

Cumulative production is obtained by integrating the rate-time relationship.  It can be shown that the flow rate is related to the cumulative production by:

$$q = q_i - D * N_p \tag{2.18}$$

which shows that a plot of rate versus cumulative production ($N_p$) will be a straight line of slope $D$.  Extrapolation of this straight line to any specified abandonment rate (including zero) gives the recoverable reserves.

Cumulative production between times $t_1$ and $t_2$ can be obtained from

$$N_p = \frac{q_1 - q_2}{D} \qquad (2.19)$$

or, in terms of time

$$N_p = \frac{q_1}{D}\left(1 - e^{\left(\frac{(t_2 - t_1)}{D}\right)}\right) \qquad (2.20)$$

## 2.3.1.2 Hyperbolic Decline

With hyperbolic decline, the decline rate, $D$, is not constant (in contrast to exponential decline, when $D$ is constant). Empirically, it has been found that for some production profiles, $D$ is proportional to the production rate raised to the power $b$, where $b$ is between zero and 1. A value of $b = 0$ corresponds to exponential decline. A value of $b = 1$ is called harmonic decline.

For hyperbolic decline, $D$ varies with the rate according to:

$$D = K * q^b \qquad (2.21)$$

where $K$ is a constant equal to $D_i / (q_i^b)$, and $b$ is a constant with a value between 0 and 1. (It can be shown that the decline rate $D$ at any time, $t$, is related to $D_i$ and $b$ by:

$$D = \frac{D_i}{(1 + bD_i t)} \qquad (2.22)$$

When $b = 0$, $D$ becomes a constant, independent of the flow rate, $q$, and the hyperbolic decline becomes identical with exponential decline. When $b = 1$, the hyperbolic decline becomes harmonic decline.

Combining the equations above and integrating gives the hyperbolic decline equation:

$$q = \frac{q_i}{\left(1 + bD_i t\right)^{\frac{1}{b}}} \qquad (2.23)$$

where, $q_i$ and $D_i$ are the initial flow rate and the initial decline, respectively, corresponding to the time, $t = 0$.

There is no simple way of re-casting this equation to obtain a straight line. Hence, when analyzing production data using hyperbolic decline, a non-linear regression must be performed to find the values of the constants $b$, $D_i$ and $q_i$ that best fit the data.

In order to obtain the flow rate at any future time, the cumulative production up to that time, or the total recoverable reserves, the production decline curve must be extrapolated using the hyperbolic decline Equation 2.22. Having obtained the constants $b$, $D_i$ and $q_i$ from a curve fit of the production data, the flow rate at any time, $t$, is given by:

$$q = \frac{q_i}{\left(1 + bD_i t\right)^{\frac{1}{b}}} \qquad (2.24)$$

The cumulative production, $Q$, at any time, $t$, is obtained is from:

$$Q_p = \frac{q_i}{(1-b)D_i}\left[1 - \left(\left(1 + bD_i t\right)^{1-\frac{1}{b}}\right)\right] \qquad (2.25)$$

or in term of $q$ from:

$$\Delta Q_p = \frac{q_i^{\,b}}{(1-b)D_i}\left(q_i^{\,1-b} - q_2^{\,1-b}\right) = \frac{q_i}{(1-b)D_i}\left[1 - \left(\frac{q}{q_i}\right)^{1-b}\right] \qquad (2.26)$$

Thus, at an abandonment rate, $q_2 = 0$, the total recoverable oil can be read from an extrapolation of the graph based on the hyperbolic decline equation, or it can be calculated from:

$$Q_{p-\max} = \frac{q_i}{D_i(1-b)} \qquad (2.27)$$

## 2.3.1.3 Harmonic Decline

Harmonic decline is a special case of hyperbolic decline, with $b = 1$, i.e. the decline rate, $D$, is proportional to $q$. This means that the decline rate, $D$, goes to zero when $q$ approaches zero. This type of performance is expected when very effective recovery mechanisms such as gravity drainage are active. Another example of harmonic decline is the production of high viscosity oil driven by encroaching edge-water. Due to unfavorable mobility ratio, early water breakthrough occurs and the bulk of the oil production will be obtained at high water cuts. If the total fluid rate is kept constant, then the increasing amount of water in the total fluid will cause the oil production to decline. This decline in oil rate may follow a harmonic decline. From Equation 2.22, with $b = 1$ the hyperbolic formula can be shortened to

$$q = \frac{q_i}{(1 + D_i t)} \qquad (2.28)$$

The cumulative production between $t_1$ and $t_2$ corresponding to the two flow rates, $q_1$ and $q_2$, can be calculated from

$$\Delta Q_p = \frac{q_i}{D_i} \ln\left(\frac{q_i}{q_2}\right) \qquad (2.29)$$

or in term of time, from

$$\Delta Q_p = \frac{q_i}{D_i} \ln(1 + D_i t) \qquad (2.30)$$

The ultimate production (at zero flow-rate) cannot be determined. From the above equations, it can be seen that the way to obtain a straight line for harmonic decline is to plot log-rate versus cumulative production.

The constants $D_i$ and $q_i$ can be determined by regression, or from a plot of log-rate versus cumulative production. The flow rate at any future time, the cumulative production until that time, and recoverable reserves at a specified abandonment rate can be found either from extrapolation of the curves or from the equations above.

A summary of production decline curves through value of b can be written as follows:

When *b* equals 1, the curve is said to be Harmonic.
When $0 < b < 1$, the curve is said to be Hyperbolic.
When *b*=0, this form of the equation becomes indeterminate, but it can be shown that it is equivalent to Exponential decline.

**Figure 2.16** shows plots of Exponential, Hyperbolic, and Harmonic decline curves.
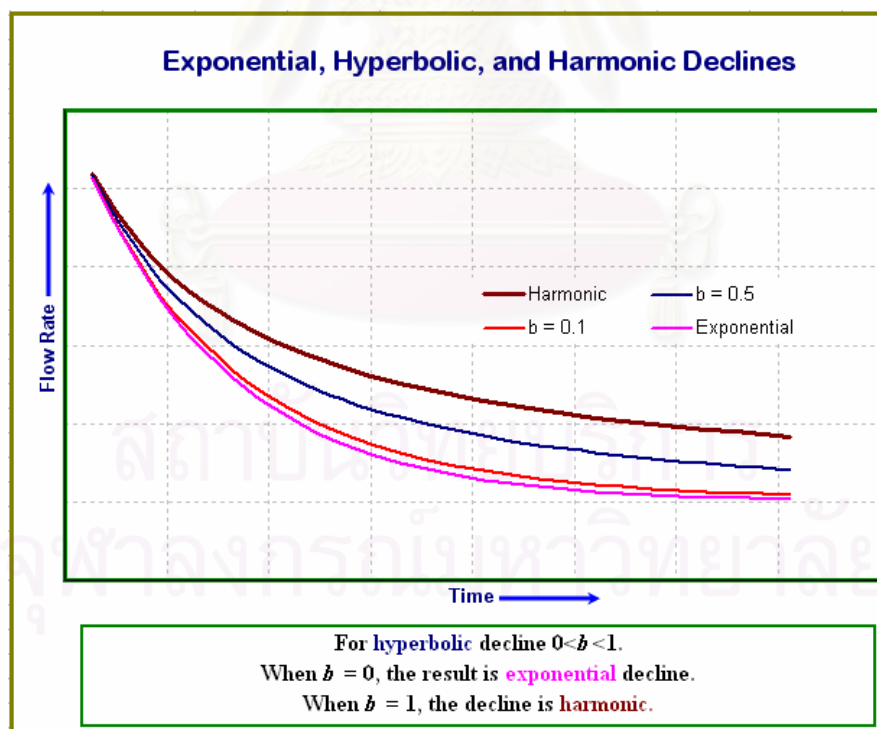


**Figure 2.16**:    Summary of production decline curves.

The following table summarizes rate, time, and cumulative production relationship in Arps[1] conventional decline curves.

**Table 2.2**: Conventional Arps decline curves.

| Decline Type | Hyperbolic | Exponential | Harmonic |
|---|---|---|---|
| Rate–Time | $q(t) = q_i/(1 + bD_i t)^{1/b}$ | $q(t) = q_i/e^{D_i t}$ | $q(t) = q_i/(1 + D_i t)$ |
| Time to q(t) | $t = \{[q_i/q(t)]^b - 1\}/bD_i$ | $t = \ln[q_i - q(t)]/D_i$ | $t = \{[q_i/q(t)] - 1\}/D_i$ |
| Cumulative–Time | $Q_p = [q_i/(1-b)D_i]\left[1 - (1 + bD_i t)^{(b\ 1/b)}\right]$ | $Q_p = (q_i/D_i)(1 - e^{D_i t})$ | $Q_p = (q_i/D_i)\left[\ln(1 + D_i t)\right]$ |
| Rate–Cumulative | $Q_p = [q_i b/(1-b)D_i]\left[q_i^{(1-b)} - q(t)^{(1-b)}\right]$ | $Q_p = [q_i - q(t)]/Q_{D_i}$ | $Q_p = (q_i/D_i)\ln[q_i/q(t)]$ |
| From Rate–Cum. $D_i$ at q(t)=0 | $D_i = [1/(1-b)](q_i/Q_{puo})$ | $D_i = q_i/Q_{puo}$ | $D_i$ is not definable; ($Q_{puo}$ is infinite). |
| $D_i$(oil) | $D_i = [(2n + 1)/2](q_i/N_{puo})$<br>$N_{puo} = N \times (RF)$ where $RF = f(K_g/K_o)$ | $n = 0.5;\ D_i = (q_i/N_{puo})$ | Not derivable |
| $D_i$(gas) | $D_i = 2n(q_i/G)$ | $n = 0.5;\ D_i = (q_i/G)$ | Not derivable |
| b(oil) where $p_{wf} \approx 0$<br>b(gas) where $p_{wf} \approx 0$ | $G = G_i \times (RF)$ where $RF = \left[1 - (p_{wf}/\bar{p}_R)\right]$<br>$b = (2n - 1)/(2n + 1)$ where $n$ is between 0.5 and 1<br>$b = (2n - 1)/2n$ where $n$ is between 0.5 and 1 | | |

## 2.3.2 Decline Type Curves

The following section reviews typical type curves which are widely used to estimate reserves and reservoir properties.

## 2.3.2.1 Fetkovich Decline Type Curve

Fetkovich[4] presented a new set of type curves that extends the Arps type curves into the transient flow region. He recognized that decline curve analysis was applicable only during the time period when production was in boundary dominated flow, i.e, during the depletion period. This means that the early production life of a well is not analyzable by the conventional decline curve methods. Fetkovich used analytical flow equations to generate type curves for transient flow, and he combined them with the empirical decline curve equations of Arps. Accordingly, Fetkovich type curves are made up of two regions, which have been blended to be continuous, and thereby encompass the whole production life from early time (transient flow) to late time (boundary dominated flow).

In order to generate Fetkovich decline type curves, two different sets of equations are used, one for the transient stems and another for the boundary-dominated stems. The transition from one to the other occurs at $t_{Dd} = 0.3$ (Note that for the cumulative type curves, this transition occurs at $t_{Dd} = 0.6$)

Fetkovich generated the transient and boundary dominated data for $q_D$ vs. $t_D$, for a vertical well producing at constant pressure from the centre of a cylindrical reservoir. The dimensionless flow rate, $q_D$ and the dimensionless time, $t_D$ are defined as follows:

$$q_D = \frac{141.3 q \mu B}{kh(p_i - p_{wf})} \qquad (2.31)$$

and

$$t_D = \frac{0.00634 kt}{\phi \mu c_t r_w^{\,2}} \qquad (2.32)$$

The solution was first derived by Van Everdingen and Hurst[46], who provided the solution in Laplace space, as follows:

$$q_D = L^{-1}(\bar{q}) \qquad (2.33)$$

where

$$\bar{q} = \frac{I_1(\sqrt{S}R_D)K_1(\sqrt{S}) - K_1(\sqrt{S}R_D)I_1(\sqrt{S})}{K_1(\sqrt{S}R_D)I_o(\sqrt{S}) - I_1(\sqrt{S}R_D)K_o(\sqrt{S})} \qquad (2.34)$$

The transient portion of these flow rate equations can be represented by numerical curve fit equations, reported by Edwardson *et al*[29] (1962). These are given by:

$$q_D = \frac{26.7544 + 43.5537 t_D^{\,0.5} + 13.3813 t_D + 0.492949 t_D^{\,1.5}}{47.42 t_D^{\,0.5} + 35.5372 t_D + 2.60967 t_D^{\,1.5}} \; with \; t_D < 200 \quad (2.35)$$

$$q_D = \frac{3.90086 + 2.02623t_D(\ln t_D - 1)}{t_D(\ln t_D)^2} \; with \; t_D > 200 \tag{2.36}$$

These definitions of $t_D$ and $q_D$ are based on well test applications. For decline curve analysis, the following definitions are more useful:

$$q_{Dd} = q_D\left[\ln\left(\frac{r_e}{r_{wa}}\right) - \frac{1}{2}\right] \tag{2.37}$$

$$t_{Dd} = \frac{t_D}{\frac{1}{2}\left[\left(\frac{r_e}{r_{wa}}\right)^2 - 1\right]\left[\ln\left(\frac{r_e}{r_{wa}}\right) - \frac{1}{2}\right]} \tag{2.38}$$

The boundary-dominated equations, which are used for $t_{Dd} > 0.3$ are obtained from the Arps decline equations which were discussed in the previous section.

Combining the Fetkovich transient curves with the Arps decline curves and blending them where the two sets of curves meet, results in the Fetkovich Decline type curves shown in **Figure 2.17**.
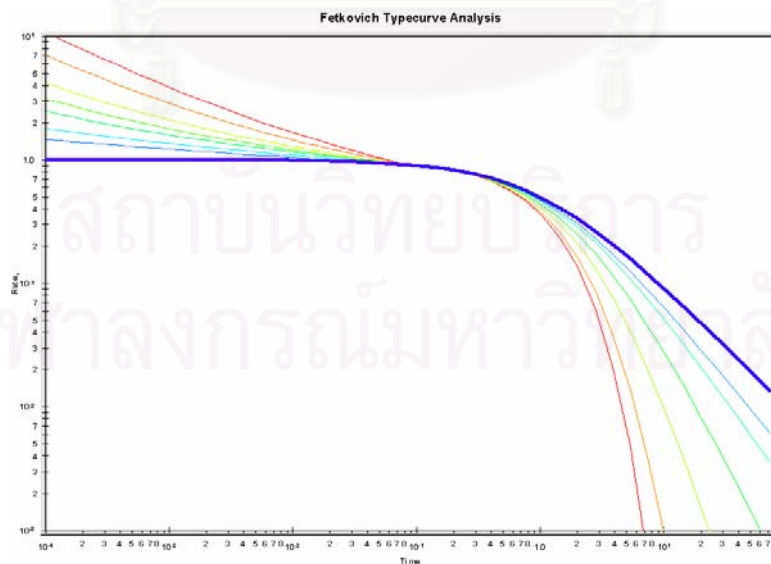


**Figure 2.17**:    Fetkovich rate type curves.

Production data are often quite noisy, and thus difficult to analyze. To reduce the effect of this noise, the cumulative production can be used. It is a much smoother curve than the production data, and can make the analysis more reliable. Fraim and Lee[32] developed cumulative type curves of $Q_{Dd}$ versus $t_{Dd}$, where $Q_{Dd}$ is the dimensionless cumulative production, defined as the ratio of cumulative production to the ultimate movable fluid, and $t_{Dd}$ is the dimensionless time defined in type curve-Arps.

For oil,

$$Q_{Dd} = \frac{BN_p 1.787}{c_t h \phi \left(r_e^2 - r_w^2\right)\left(p_i - p_{wf}\right)} = \frac{N_p}{N_{net}}$$ (2.39)

For gas,

$$Q_{Dd} = \frac{637.8 p_{sc} TG_p}{\overline{c_t \mu} h \phi T_{sc} \left(r_e^2 - r_w^2\right)\left(\psi_i - \psi_{wf}\right)} = \frac{G_p}{G_{net}} S$$ (2.40)

where (oil and gas)

$$Q_{Dd} = \int_0^{t_{Dd}} q_{Dd} dt_{Dd} = \frac{\int_0^{t_D} q_D dt_D}{\frac{1}{2}\left[\left(\frac{r_e}{r_w}\right)^2 - 1\right]} = \frac{Q_D}{\frac{1}{2}\left[\left(\frac{r_e}{r_w}\right)^2 - 1\right]}$$ (2.41)

$$t_{Dd} = \frac{t_D}{\frac{1}{2}\left[\left(\frac{r_e}{r_{wa}}\right)^2 - 1\right]\left[\ln\left(\frac{r_e}{r_{wa}}\right) - \frac{3}{4}\right]}$$ (2.42)

From the Fetkovich type curves, the rate can be integrated to give the cumulative production and plotted in type curve format.
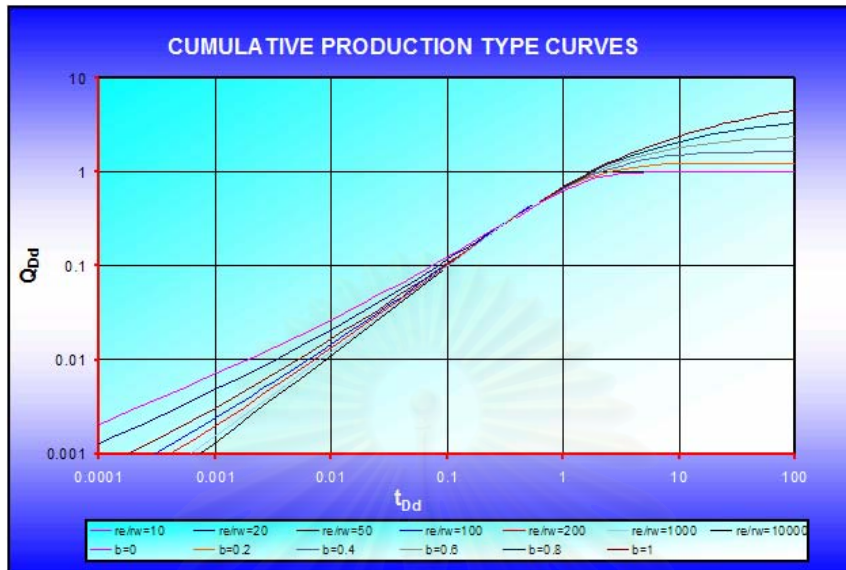
**Figure 2.18**:     Fetkovich cumulative production type curves.

Cumulative graphs (**Figure 2.18**) show that, at a $t_{Dd}$ of 100, harmonic decline leads to five times more cumulative production as compared to exponential decline.

The authors indicated that the dimensionless time-function, $t_{Dd}$, used for the cumulative plots above has ¾ in the denominator, whereas in the Fetkovich type curves the dimensionless time-function has ½ in the denominator.  The factor ¾ appears in the inflow equation when the drawdown is referenced to the average reservoir pressure, and the factor ½ appears when the reference is the initial pressure at $r_e$.  Fetkovich tried using ½, $^5/_8$, and ¾, and found that using ½ reduced the discontinuity between the transient stems and the hyperbolic stems.

## 2.3.2.2 Blasingame *et al*. Decline Type Curves

The production decline analysis techniques of Arps and Fetkovich are limited in that they do not account for variations in bottom hole flowing pressure in the transient regime and only account for such variations empirically during boundary dominated flow (by means of the empirical depletion stems).  In addition, changing PVT properties with reservoir pressure are not considered, for gas wells. Blasingame[30], [31]

and his students have developed a production decline method that accounts for these phenomena. The method uses a form of superposition time function that only requires one depletion stem for type curve matching, the harmonic stem. Blasingame's improvements on the Fetkovich style of production decline analysis are further enhanced by the introduction of two additional type curves, which are plotted concurrently with the normalized rate type curves. The 'rate integral' and 'rate integral derivative' type curves aid in obtaining a more unique match.

Recall that the Fetkovich type curves were based on combining the analytical solution to transient flow of a single-phase fluid at a constant wellbore flowing pressure, with the empirical Arps's equations for boundary dominated flow. Fetkovich was of the belief that the exponent $b$ could vary between zero and one and was correlated with fluid properties as well as recovery mechanism. For example, single-phase flow of oil would result in an exponent of zero, while single-phase gas flow would exhibit $b > 0$, because of changes in gas properties. Later, Fraim and Wattenberger[19] showed that if the changes in gas fluid properties were taken into account, i.e., with the use of pseudo time. Pseudo-time is a transformation applied to the timescale when plotting gas production data on type curves. Its purpose is to linearize the pressure equation for gas by accounting for variations in compressibility and viscosity with time (and reservoir pressure). Boundary-dominated gas flow against a constant back pressure exhibits the same behavior that an oil reservoir would do; the decline would follow the exponential curve, $b = 0$.

The above findings relate to flow at a constant wellbore pressure. A subsequent development by Blasingame $et\ al$[30] was to account for changing wellbore flowing pressures, by defining a superposition time function, which they called material-balance-time. They showed that if the material-balance-time were used instead of actual producing time, what was previously an exponential decline would follow the harmonic decline stem instead.
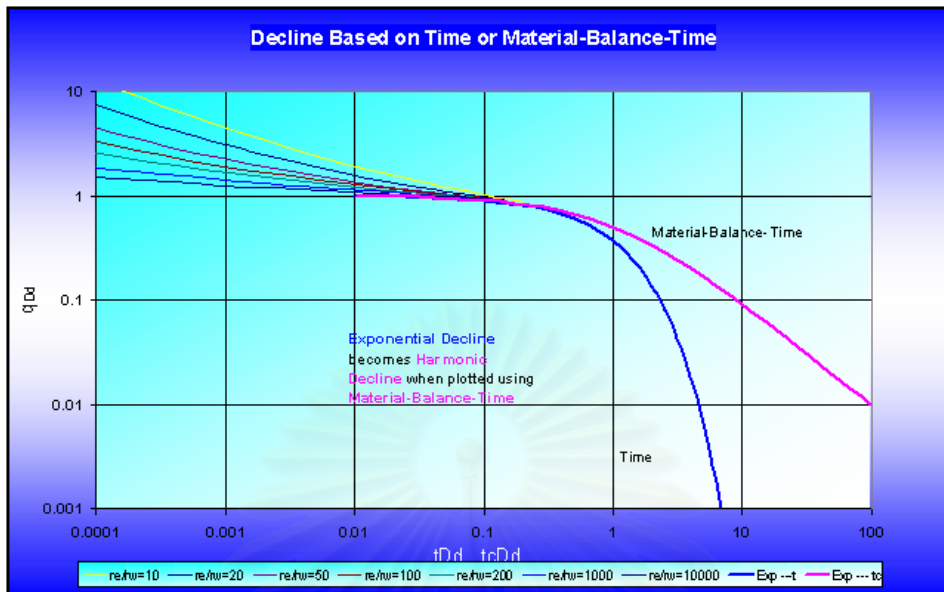
**Figure 2.19**: Decline curve plot on time and material balance time.

More importantly, data obtained when both the rate and the flowing pressure are varying, can now be analyzed if material-balance-time is used. For example, if the production rate from a well is monotonically declining, and at the same time, its flowing bottom hole pressure is on continuous decline, a plot of $q/\Delta p$ versus $Q(t)/q(t)$ would follow the harmonic curve. (For a gas well, the changing gas properties should also be accounted for by using pseudo-time).

Blasingame, McCray, and Palacio[31] developed type curves which show the analytical transient stems along with the analytical harmonic decline (but with the rest of the empirical hyperbolic stems absent). In addition, they introduced two other functions, the rate integral function and the rate integral derivative function. The rate integral is a type curve or family of type curves that is derived from the normalized rate type curves by taking a cumulative average of the normalized rate. Its purpose is to reduce the amount of noise in the production data, and to assist with type curve interpretation. The rate integral derivative is the semi-log derivative of the rate integral type curve. Its purpose is to provide a derivative type curve that has limited data scatter. As a secondary type curve, it helps reduce the non-uniqueness of a type

curve interpretation, which help in smoothing the often-noisy character of production data, and in obtaining a more unique match.

The Blasingame suite of type curves is very similar to the Fetkovich type curves for constant pressure production. The only real difference is the absence of the empirical depletion stems on the Blasingame type curves. These are not required because the usage of material balance time forces the boundary dominated data to fall only on the analytical harmonic stem. In Blasingame type curve analysis, three rate functions can be plotted against material balance time. Conceptually, the material-balance-time is defined as the ratio of cumulative production, $Q$, to instantaneous rate, $q$:

$$t_c = \frac{Q}{q} \qquad (2.43)$$

For gas wells,

$$t_{ca} = \frac{\mu_i c_{gi}}{q} \int_0^t \frac{qdt}{\mu c_g} = \frac{(\mu c)_i}{q} \frac{Z_i G_i}{2 p_i} \left[ p_{pi} - p_p \right] \qquad (2.44)$$

where $G_i$ is initial gas in place.

The symbol $t_c$ has been adopted as it represents a corrected time based on cumulative production. It is also similar to the corrected "Horner" time used in build-up analysis in well testing for correcting the effect of a varying flow rate. It is the value of time that a well would have to flow at the current rate in order to produce the same amount of fluid (and hence honor the material balance principle).
The three rate functions are as follows:

- **Normalized Rate**

For oil wells,

$$\frac{q}{\Delta p} = \frac{q}{p_i - p_{wf}}$$ (2.45)

For gas wells,

$$\frac{q}{\Delta p_p} = \frac{q}{p_i - p_{pwf}}$$ (2.46)

where $p_p$ is pseudo pressure.

- **Rate Integral**

The rate integral is defined at any point in the producing life of a well, as the average rate at which the well has produced until that moment in time. The normalized rate integral is defined as follows:

For oil wells,

$$\left(\frac{q}{\Delta p}\right)_i = \frac{\int_0^t \frac{q}{\Delta p} dt}{t}$$ (2.47)

For gas wells,

$$\left(\frac{q}{\Delta p_p}\right)_i = \frac{\int_0^{t_{ca}} \frac{q}{\Delta p} dt_{ca}}{t_{ca}}$$ (2.48)

- **Rate Integral Derivative**

The rate integral derivative is defined as the semi logarithmic derivative of the rate integral function, with respect to material balance time. It is defined as follows:

For oil wells,

$$\left(\frac{q}{\Delta p}\right)_{id} = -\frac{d\left(\frac{q}{\Delta p}\right)_i}{d\ln(t_c)} = -\frac{d\left(\frac{q}{\Delta p}\right)_i}{dt_c}t_c \qquad (2.49)$$

For gas wells,

$$\left(\frac{q}{\Delta p_p}\right)_{id} = -\frac{d\left(\frac{q}{\Delta p_p}\right)_i}{d\ln(t_{ca})} = -\frac{d\left(\frac{q}{\Delta p_p}\right)_i}{dt_{ca}}t_{ca} \qquad (2.50)$$
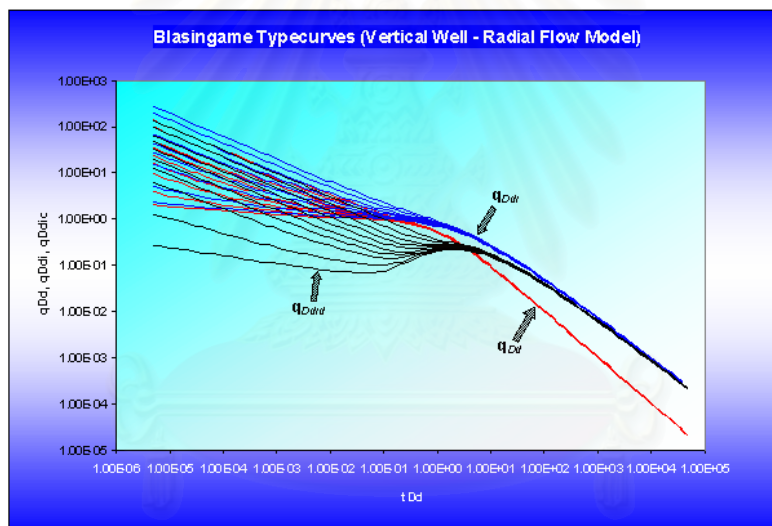


**Figure 2.20**:    Blasingame type curve for vertical well – radial flow model.

The Blasingame suite of type curves consists of a number of different models:

- Vertical well, radial flow model
- Vertical well, hydraulic fracture model
- Horizontal well model
- Water flood model
- Well interference model (declining reservoir pressure).

All models assume a circular outer boundary, with exception of horizontal, which assumes a square outer boundary.

**Figure 2.20** is Blasingame type curve for vertical well, with radial flow model. The actual normalized rate, rate integral, and rate integral derivative are plotted versus material balance time data on a log-log scale of the same size as the type curves. The data plot is moved over the type curve plot, while the axes of the two plots are kept parallel, until a good match is obtained. The rate, rate integral, and rate integral derivative data should all fit the same corresponding type curve. Several different type curves should be tried to obtain the best fit of all the data. The type curve that best fits the data is selected and its "$r_e/r_{wa}$" ($r_e/X_f$ for fractured case) value is noted. Type curve analysis is done by selecting a match point, and reading its co-ordinates off the data plot *(q/ΔP and $t_{ca}$)$_{match}$*, and off the type curve plot *($q_{Dd}$ and $t_{Dd}$)$_{match}$*. At the same time the stem value "$r_e/r_{wa}$" of the matching curve is noted. Given a curve match, the following reservoir parameters can be obtained, if, *β, μ, h, $c_t$, ϕ,* and $r_w$ are known: *k, s($X_f$),* area, GIP(OIP)

## 2.3.2.3 Agarwal-Gardner Decline Type Curve

Agarwal and Gardner[47] developed a new set of type-curves for analyzing production data that are similar to Fetkovich type curves but are fully analytical. The Agarwal-Gardner methodology is based on fundamental concepts of pressure transient analysis and the equivalence of the constant rate and constant pressure solutions.

A well produced at a constant rate exhibits a varying (declining) bottom hole flowing pressure, whereas a well produced at a constant bottom-hole pressure exhibits a varying decline rate. There is a strong symmetry between the two solutions, as both are obtained from the same equation, namely the equation that governs fluid flow in porous media. The symmetry is not exact, however, because the boundary conditions under which the two solutions are obtained are different.

The constant rate solution can be converted to a constant bottom hole pressure solution (and vice versa) using the principle of superposition. The constant bottom hole pressure solution would be obtained by superposing a large number of very short constant rate solutions in time. When plotted against superposition time, the superposed constant rate solution is very similar to the constant pressure solution, provided the discretization intervals are sufficiently small. It turns out that the two solutions are quite similar during transient flow anyway, and therefore superposition is not required to make one look like the other. However, they quickly diverge once boundary dominated flow begins. The constant rate solution behaves like the harmonic stem of the Arps type curves while the constant pressure solution declines exponentially.

A method for forcing one solution to look like the other during boundary dominated flow would be useful because the necessity of using superposition in time would be avoided completely. Because of pressure transient analysis, diagnostic tools for analyzing the constant rate solution are widely known and understood. Therefore, there is value in being able to analyze other types of solutions using the same diagnostic tools. The concept of material balance time provides the normalization necessary to make constant pressure and constant rate solutions equivalent. Material balance time converts the boundary dominated flow portion of the constant pressure solution into the pseudo steady-state portion of the equivalent constant rate solution. Plotting using material balance time also allows solutions with both declining rates and pressures to look like the equivalent constant rate solution.

In the Agarwal-Gardner method of parameter estimation, three separate analyses are performed:

- Rate versus modified cumulative production analysis
- Rate versus material balance time (pseudo time for gas) type curve analysis
- Normalize cumulative production versus material balance time (pseudo time)

**2.3.2.3.1 Rate versus Modified Cumulative Production Analysis**

The rate vs. cumulative production analysis is performed to estimate the hydrocarbons-in-place by plotting $q/\Delta p$ versus $Q_m$ (modified cumulative production) on Cartesian coordinates.

For oil wells,

$$Q_m = \frac{N_p}{c_t \left(p_i - p_{wf}\right)} \tag{2.51}$$

For gas wells,

$$Q_m = \frac{\left(p_{pi} - \overline{p}\right)G}{\left(p_{pi} - p_{wf}\right)} = \frac{2qt_{ca}p_i}{\left(c_t\mu Z\right)_i\left(p_{pi} - p_{pwf}\right)} \tag{2.52}$$

The right hand side of Equation 2.39 is only valid if $c_f$ is assumed to be negligible, in which case $c = c_g$ (on the left-hand side). Otherwise, the left-hand side definition must be used to calculate $Q_m$, and $c = c_t$, $t_{ca}$ is material balance pseudo time and is defined in Equation 2.42.

**2.3.2.3.2 Rate versus Material Balance Time Type Curve Analysis**

- Normalized rate versus material balance time type curve is the same as Blasingame's type curve. For oil wells, Equation 2.45 is applied, for gas wells, apply Equation 2.46 is used.

- Inverse of semi-log derivative versus material balance time

    For oil wells,

$$\frac{1}{DER} = \frac{1}{\left(\dfrac{\partial \dfrac{\Delta p}{q}}{\partial \ln(t_c)}\right)} \tag{2.53}$$

For gas wells,

$$\frac{1}{DER} = \frac{1}{\left(\dfrac{\partial \dfrac{\Delta p_p}{q}}{\partial \ln(t_{ca})}\right)} \tag{2.54}$$

where *DER* is pressure integral derivative.

### 2.3.2.3.3 Normalized Cumulative Production versus Material Balance Time

It is often useful to plot cumulative production versus time rather than rate versus time because cumulative production data tend to be smoother. Normalized cumulative production at time *"t"* for oil and gas wells is defined as follows:

For oil wells,

$$\frac{Q}{\Delta p} = \frac{N_p}{\Delta p} = \frac{\displaystyle\int_0^t q\,dt}{\Delta p} = \frac{q t_c}{\Delta p} \tag{2.55}$$

where material balance time $t_c$ is defined by Equation 2.41.

For gas wells,

$$\frac{Q}{\Delta p_p} = \frac{\mu_i c_{ti}}{\Delta p_p} \int_0^t \frac{q}{\mu(\bar{p}) c_t(\bar{p})}\,dt = \frac{q t_{ca}}{\Delta p_p} \tag{2.56}$$

where material balance time $t_{ca}$ is defined by Equation 2.42.

# CHAPTER 3

# THEORETICAL CONSIDERATIONS

This chapter discusses pressure drop in boundary-dominated liquid flow (pseudo steady state condition) under constant flow rate. Derivation of the solution is fully described. The section also introduces concept of rate normalization, gives an insight of bottom-hole pressure calculation algorithm in both gas and oil cases, as well as highlights input information requirement to run the model.

## 3.1 Closed Boundaries – Pseudo Steady State Condition

When a reservoir (or a well's own "drainage region") is closed on all sides, the pressure transient will be transmitted outwards until it reaches all sides, after which the reservoir depletion will enter a state known as pseudo steady state. In pseudo steady state flow or boundary dominated flow of a single-phase liquid system, pressure drop with time in every point of the reservoir would be equal. **Figure 3.1** illustrates pressure drop measured at different radial distances from the well while the well is flowing at a constant rate. Dropping on pressure at the wellbore is the same as the pressure drop that would be observed anywhere in the reservoir, including the location which represents average reservoir pressure.
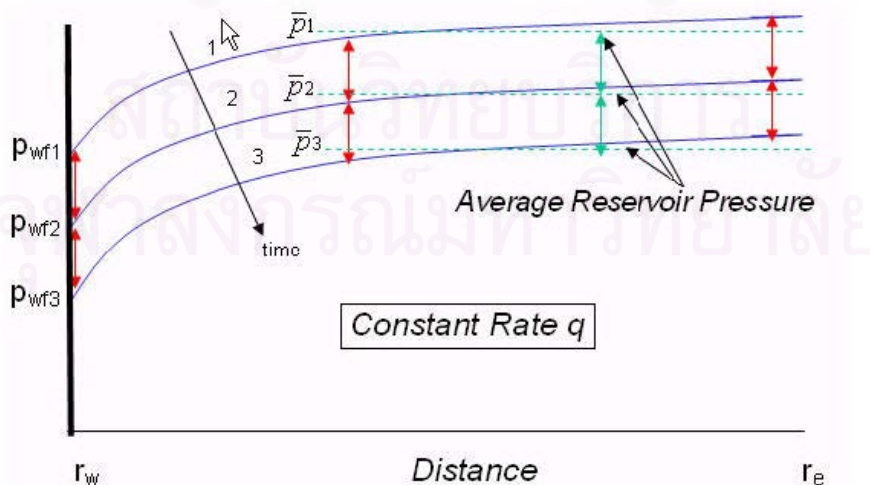


**Figure 3.1:**   Pressure drop in a reservoir as a function of radial distance and time.

Thus a pseudo steady state is not at all steady, and corresponds to the kind of pressure response that would be seen in a closed tank from which fluid is slowly being removed. The condition of the reservoir during pseudo steady state is that pressure drop (everywhere) is due to the decompression of the reservoir fluid as fluid is produced from the well. This volumetric pressure loss is given simply from the definition of compressibility:

$$c_t = -\frac{1}{V}\frac{\Delta V}{\Delta p} \tag{3.1}$$

or

$$\Delta V = -\frac{1}{V}\frac{q\Delta t}{c_t} \tag{3.2}$$

where $V$ is the total reservoir fluid volume, and the cumulative production $\Delta V$ is replaced by $q\,\Delta t$. From Equation 3.2, one can see that, during pseudo steady state, the pressure drop is:

- Directly proportional to time, hence is identifiable as a straight line on a $\Delta p$ versus $t$ or $log(\Delta p)$ versus $log(\Delta t)$.
- Dependent on reservoir volume, hence is extremely useful as a means of estimating reservoir size.

## 3.2 Pressure Response in Boundary-Dominated Liquid Flow

The original material balance approach for boundary-dominated flow (i.e., pseudo steady state) was developed by Blasingame and Lee[33], and the following derivation builds upon their development. In the following section, wellbore behavior of a single homogenous layer, filled with slightly compressible fluid of constant viscosity will be analyzed first, then followed with the discussion of behavior of reservoirs that contains two layers without crossflow and with distinct contrasts in properties across bedding planes.

### 3.2.1 Constant Liquid Flow Rate-Single Layer

From the definition of liquid compressibility, the following material balance can be derived

$$q_o = -\frac{A\phi h c_t}{5.615 B_o}\frac{d\bar{p}}{dt} \tag{3.3}$$

Since we are considering the single phase liquid case, the total compressibility, $c_t$ is assumed to be constant. Therefore, the integration of Equation 3.3 yields

$$\int_0^t q_o dt = -\frac{A\phi h c_t}{5.615 B_o}\int_{p_i}^{\bar{p}} d\bar{p} \tag{3.4}$$

Completing the integration, we have

$$N_p = \frac{A\phi h c_t}{5.615 B_o}\left(p_i - \bar{p}\right) \tag{3.5}$$

Solving this relation for the pressure difference, it follows that

$$\left(p_i - \bar{p}\right) = \frac{5.615 N_p B_o}{A\phi h c_t} = \frac{1}{N c_t}\frac{B_o}{B_{oi}}N_p \tag{3.6}$$

where Equation 3.6 can also be rearranged to yield

$$\left(p_i - \bar{p}\right)\frac{h}{B_o} = \frac{5.615 N_p}{A\phi c_t} \tag{3.7}$$

Multiply through by $\dfrac{k_o}{141.2 q_o \mu_o}$ gives

$$\left(p_i - \bar{p}\right)\frac{k_o h}{141.2 q_o B_o \mu_o} = \frac{5.615 k_o}{141.2 A\phi \mu_o c_t}\frac{N_p}{q_o} \tag{3.8}$$

As mentioned earlier, the system is producing under constant rate, $t = \dfrac{N_p}{q_o}$, it follows that

$$\left(p_i - \overline{p}\right)\frac{k_o h}{141.2 q_o B_o \mu_o} = \frac{2\pi(0.00633)k_o}{A\phi\mu_o c_t}t \qquad (3.9)$$

Redefining the dimensionless time based on drainage area, we have

$$t_{DA} = \frac{0.00633 k_o}{\phi\mu_o c_t A}t \qquad (3.10)$$

Combination of Equation 3.10 and Equation 3.9 will give us

$$\left(p_i - \overline{p}\right)\frac{k_o h}{141.2 q_o B_o \mu_o} = 2\pi t_{DA} \qquad (3.11)$$

It has been shown[34] that for a constant production rate of single phase liquid, the flow equation for pressure response under boundary-dominated flow can be written as

$$\left(\overline{p} - p_{wf}\right)\frac{k_o h}{141.2 q_o B_o \mu_o} = \frac{1}{2}\ln\left[\frac{4}{e^\gamma}\frac{A}{C_A r_w^{\,2}}\right] \qquad (3.12)$$

where $A$ is the drainage area assumed to be equal for all layers, $C_A$ is Dietz shape factor, $\gamma$ is Euler's constant (0.5772…).

The substitution of Equation 3.11 and Equation 3.12 yields

$$\left(p_i - p_{wf}\right)\frac{k_o h}{141.2 q_o B_o \mu_o} = 2\pi t_{DA} + \frac{1}{2}\ln\left[\frac{4}{e^\gamma}\frac{A}{C_A r_w^{\,2}}\right] \qquad (3.13)$$

Dimensionless pressure is defined as $p_{WD} = \dfrac{k_o h(p_i - p_{wf})}{141.2 q_o B_o \mu_o}$. Thus, in general form,

Equation 3.13 with addition of skin ($s$) can be written as follows:

$$p_{WD} = 2\pi t_{DA} + \frac{1}{2}\ln\left[\frac{4}{e^\gamma}\frac{A}{C_A r_w^2}\right] + s \qquad (3.14)$$

Examining the above equation, one recognizes that it combines both the material balance (first term on the right hand side) and the inflow performance (combining the second and third term on the right hand side); or

$$p_{wD} = \text{Material balance} + \text{Inflow Performance}$$

From the above, it is apparent that the pseudo steady state response is the sum of two distinct pressure change components:

- Pressure change due to depletion ($p_i - p_{average}$)
- Pressure change due to inflow ($p_{average} - p_{wf}$)

Also, expanding the left hand side term of Equation 3.14, one can write[35]

$$p_{wD} = \frac{k_o h(p_i - p_{wf})}{141.2 q_o B_o \mu_o} = \frac{k_o h\{(p_i - \bar{p}) + (\bar{p} - p_{wf})\}}{141.2 q_o B_o \mu_o} = 2\pi t_{AD} + \frac{1}{2}\ln(\frac{4A}{e^\gamma C_A r_w^2}) + s \qquad (3.15)$$

or

$$\text{Material balance} \equiv \frac{k_o h\{(p_i - \bar{p})\}}{141.2 q_o B_o \mu_o} = 2\pi t_{AD} \qquad (3.16)$$

$$\text{Inflow performance} \equiv \frac{k_o h\{(\bar{p} - p_{wf})\}}{141.2 q_o B_o \mu_o} = \frac{1}{2}\ln(\frac{4A}{e^\gamma C_A r_w^2}) + s \qquad (3.17)$$

**Figure 3.2** illustrates the relationship between initial pressure, average reservoir pressure and flowing pressure at the wellbore of a single layer system at a constant flowing rate.



$$(p_i - p_{ave}) = \frac{2\pi(141.2qB\mu)t_{AD}}{kh}$$

$$(p_{ave} - p_{wf}) = \left[\frac{1}{2}\ln\left(\frac{4A}{e^{\gamma}C_A r_{w2}}\right) + skin\right]\left(\frac{141.2qB\mu}{kh}\right)$$
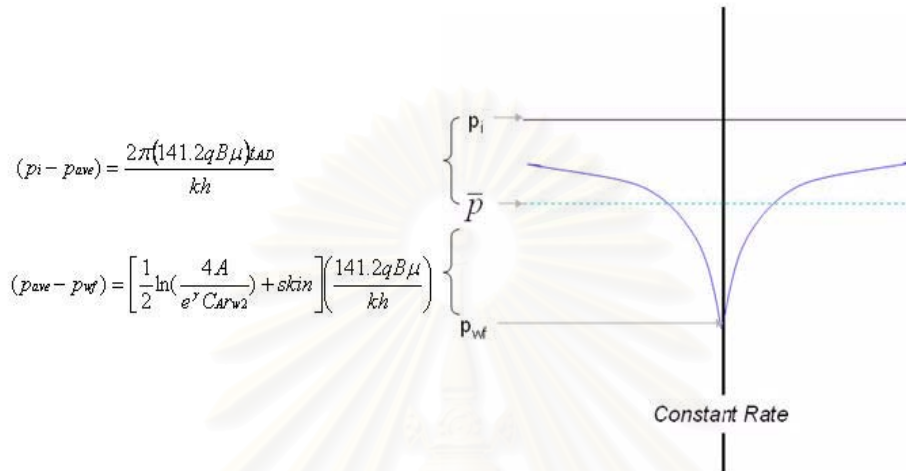
**Figure 3.2:** Fluid flows in reservoir –single layer

Equation 3.14 is the most fundamental expression to relate wellbore pressures and rates for transient analysis. It also serves as the basis for the rate forecast associated with decline curve analyses by its inversion or reciprocity. For compressible gas systems, the general form of Equation 3.14 or Equation 3.15 can still be used by replacing the pressure and time terms with appropriate pseudo-pressures and pseudo-times[35].

For rate decline analysis, simultaneous iteration solving for rate, bottom-hole well flowing, and average reservoir pressures is needed to fully define Equation 3.14 or Equation 3.15. Practically, in various forms of approximation, one can use the material balance (for example, *P/Z* method) to estimate average pressure with production (or time) for observing (or calibrating) the inflow performance relationship, or vice versa, use the inflow estimate to calibrate the material balance for average reservoir pressure estimate[35].

### 3.2.2 Variable Liquid Flow Rate – Single Layer

In practice, it is sometimes difficult to maintain the production rate of a well constant over a long period of time. Therefore, if we define a material balance time function as

$$\bar{t} = \frac{N_p}{q_o} \tag{3.18a}$$

then Equation 3.8 becomes

$$\left(p_i - \bar{p}\right)\frac{k_o h}{141.2 q_o B_o \mu_o} = \frac{2\pi(0.00633)k_o}{A\phi\mu_o c_t}\bar{t} \tag{3.18b}$$

Redefining the dimensionless time based on drainage area, we have

$$\bar{t}_{DA} = \frac{0.00633 k_o}{\phi\mu_o c_t A}\bar{t} \tag{3.19}$$

Substituting Equation 3.19 into pressure relation Equation 3.18 gives us

$$\left(p_i - \bar{p}\right)\frac{k_o h}{141.2 q_o B_o \mu_o} = 2\pi\bar{t}_{DA} \tag{3.20}$$

The most important characteristic of Equation 3.20 is that this relation is always valid, regardless of time, flow regime, or production scenario, when the well experiences constant or variable flowing bottom-hole pressure, or constant or variable flow rate. This is due to the fact that Equation 3.20 is derived directly from material balance and is exact.

For a constant production rate of a single-phase liquid, the flow equation for the pressure response under boundary-dominated flow can be written as per Equation 3.12. Although Equation 3.12 was derived from a constant rate case (variable $p_{wf}$), this relation has been shown[33] to yield a very good approximation for the case where flowing bottom hole pressure is constant.

The substitution of Equation 3.20 and Equation 3.12 yields

$$\left(p_i - p_{wf}\right)\frac{k_o h}{141.2 q_o B_o \mu_o} = 2\pi \bar{t}_{DA} + \frac{1}{2}\ln\left[\frac{4}{e^\gamma}\frac{A}{C_A r_w^2}\right] \qquad (3.21)$$

Substituting the definition of dimensionless pressure, $p_{WD} = \dfrac{k_o h(p_i - p_{wf})}{141.2 q_o B_o \mu_o}$ into Equation 3.21 gives the dimensionless form of pseudo steady state flow solution to the diffusivity equation,

$$p_{WD} = 2\pi \bar{t}_{DA} + \frac{1}{2}\ln\left[\frac{4}{e^\gamma}\frac{A}{C_A r_w^2}\right] + s \qquad (3.22)$$

This validates the use of the material balance time function $\bar{t}$ for pseudo steady state flow.

The previous considerations imply that Equation 3.22 is valid for the pseudo steady state flow regime, for any rate or pressure profile. Substituting Equation 3.19 into Equation 3.22 gives the following:

$$\frac{\left(p_i - p_{wf}\right)}{q_o} = m\bar{t} + b_{pss} \qquad (3.23)$$

where

$$m = \frac{2\pi(0.00633)k_o}{A\phi\mu_o c_t}\frac{141.2 B_o \mu_o}{k_o h} = \frac{5.615 B_o}{Ah\phi c_t} = \frac{1}{Nc_t}\frac{B_o}{B_{oi}} \qquad (3.24)$$

and

$$b_{pss} = 141.2\frac{B_o \mu_o}{k_o h}\left[\frac{1}{2}\ln\left[\frac{4}{e^\gamma}\frac{A}{C_A r_w^2}\right]\right] + s \qquad (3.25)$$

Rearranging Equation 3.23, we would obtain the final form for behavior of a well producing a variable rate profile during pseudo steady state (or boundary-dominated) flow conditions. This result is given by

$$\frac{q_o}{\left(p_i - p_{wf}\right)}b_{pss} = \frac{1}{1 + \left[\dfrac{m}{b_{pss}}\right]\bar{t}} \qquad (3.26)$$

### 3.2.3 Behavior of Two-Layer Reservoirs

Behavior of wells completed in multiple producing zones has been studied and researched by many authors [21], [36]. Their work indicated that many of the common techniques [38], [39] for analyzing pressure data in single-layer reservoir may be used to analyze data in commingled reservoirs. The principal difference between single- and multiple- layered system is that late-transient period in the multilayer case can be much longer (in some cases hundred of times longer) than the late transient period for an equivalent single layer system. Thus, the time for onset of pseudo steady stead can be extremely long – much longer than any of the system documented for single-layer system [37].

Although the total production rate, $q$, is constant, the rate of production from each layer, $q_j$, will be a function of time. If layer skin factors, $s_j$, are zero and the well is produced at a constant rate, then Lefkovits $et\ al$[21] show that $q_j$ during the early transient period is given by:

$$\frac{q_j}{q} \cong \frac{k_j h_j}{\bar{k}h} \quad \text{for } j = 1, 2\ldots\ldots n, \qquad (3.27)$$

where $k_j$ and $h_j$ refer to permeability and thickness of layer $j$ respectively, and $n$ is the total number of layers, (for two layers, $n=2$) and $\bar{k}$ is thickness average permeability,

$$\bar{k} = \frac{\sum_{j=1}^{n} k_j h_j}{\sum_{j=1}^{n} h_j} \tag{3.28}$$

Equation 3.27 is also valid if the layer skin factors are equal. During pseudo steady state flow period, the layer flow rates are given by

$$\frac{q_j}{q} \cong \frac{\phi_j c_{tj} h_j}{\overline{\phi c_t} h} \text{ for } j = 1, 2.\ldots\ldots n, \tag{3.29}$$

where $\phi_j$ is porosity of layer $j$, $c_{tj}$ compressibility of layer $j$, $n$ is the total number of layers (for two layer, $n = 2$) and $\overline{\phi c_t}$ is thickness average porosity-compressibility product,

$$\overline{\phi c_t} \cong \sum_{j=1}^{n} \frac{\phi_j c_{tj} h_j}{h} \tag{3.30}$$

The well response during boundary-dominated flow for constant rate production is given by [21], [40]

$$p_{wD}(t_{DA}) \cong 2\pi t_{DA} + \sum_{j=1}^{n} \left( \frac{\phi_j c_{tj} h_j}{\overline{\phi c_t} h} \right)^2 \left( \frac{\bar{k} h}{k_j h_j} \right) \left( \frac{1}{2} \ln \left( \frac{4A}{e^{\gamma} C_A r_w^2} \right) + s_j \right) \tag{3.31}$$

$t_{DA}$ is dimensionless time based on the drainage area, $A$:

$$t_{DA} = \frac{0.0002637 \overline{\eta} t}{A} = t_D \left( \frac{r_w^2}{A} \right) \tag{3.32}$$

where $\overline{\eta}$ is given by:

$$\overline{\eta} = \frac{\overline{k}}{\overline{\phi c_t}} \tag{3.33}$$

For layered systems, equivalent skin factor during pseudo steady state flow is given by $s_{pss}$

$$s_{pss} = \sum_{j=1}^{n} \frac{\phi_j c_{tj} h_j}{\left(\overline{\phi c_t} h\right)^2} \frac{\overline{k} h}{k_j h_j} s_j \tag{3.34}$$

From Equation 3.31, we can conclude that analogy used in Equation 3.15 to Equation 3.17 can be applied into the case of two or more layer reservoirs commingly produced.

## 3.3 Relationship Between Flow Rate and Cumulative Production

In this section, development of flow rate and cumulative production by Vo. D. T.[35] will be discussed in details. This is a fundamental mathematical equation which helps explain the usefulness of rate normalization technique.

For a slightly compressible fluid under pseudo steady state condition of a depletion-drive-reservoir, assuming a radial flow of a single phase system with constant bottom-hole pressure, rate is written by Fetkovich as:

$$q_D = \frac{1}{\ln(0.472 r_{eD})} \cdot \exp\left\{\frac{-2t_D}{r_{eD}^2 \ln(0.472 r_{eD})}\right\} \tag{3.35}$$

where

$$q_D = \frac{141.2 q B \mu}{kh(p_i - p_w)} \tag{3.36}$$

$$t_D = \frac{0.00633 kt}{\phi \mu C_t r_w^2} \tag{3.37}$$

$$r_{eD} = r_e \big/ r_w \tag{3.38}$$

Cumulative production is defined by

$$Q_D = \int_0^D q_D . dt_D \tag{3.39}$$

The ultimate equation that we are trying to derive is $\left( dQ_D \big/ dq_D \right)$

Using chain rule we can write

$$\frac{dQ_D}{dq_D} = \frac{dQ_D}{dt_D} \cdot \frac{dt_D}{dq_D} \tag{3.40}$$

Take derivative from Equation 3.39, regarding to $t_D$, one can write

$$\frac{dQ_D}{dt_D} = \frac{d}{dt_D}\left( \int_0^D q_D . dt_D \right) = q_D \tag{3.41}$$

Take the dimensionless time derivative of Equation 3.35, we obtain

$$
\begin{aligned}
\frac{dq_D}{dt_D} &= \frac{d}{dt_D}\left[ \frac{1}{\ln(0.472 r_{eD})} \exp\left\{ \frac{-2t_D}{r_{eD}^2 \ln(0.472 r_{eD})} \right\} \right] \\
&= \left( \frac{1}{\ln(0.472 r_{eD})} \right) \cdot \left( \frac{-2}{r_{eD}^2 \ln(0.472 r_{eD})} \right) \cdot \exp\left\{ \frac{-2t_D}{r_{eD}^2 \ln(0.472 r_{eD})} \right\} \\
&= \left( \frac{-2}{r_{eD}^2 \ln(0.472 r_{eD})} \right) \cdot q_D
\end{aligned}
\tag{3.42}
$$

Substitute Equations 3.41 and 3.42 into Equation 3.40 yields

$$\frac{dQ_D}{dq_D} = \left( \frac{q_D}{-2q_D} \right) r_{eD}^2 \ln(0.472 r_{eD}) = \frac{r_{eD}^2 \ln(0.472 r_{eD})}{-2} \tag{3.43}$$

or

$$\frac{dq_D}{dQ_D} = \frac{-2}{r_{eD}^2 \ln(0.472 r_{eD})}$$

(3.44)

Equation 3.44 suggests $q_D$ versus $Q_D$ on a Cartesian plot should be linear during pseudo steady state flow with a lope of $\dfrac{-2}{r_{eD}^2 \ln(0.472 r_{eD})}$, dependent on area but not time.

In field units, using Equations 3.36, 3.37, 3.38 and 3.39, Equation 3.44 becomes

$$\frac{dq}{dQ} = \frac{-2(0.00633)k}{(\phi\mu C_t)r_e^2 \ln(0.472\, r_e/r_w)}$$

(3.45)

For non-radial system, a similar expression can be derived as

$$\frac{dq}{dQ} = \frac{-4\pi(0.00633)k}{(\phi\mu C_t)A\left(\ln\dfrac{4A}{e^\gamma C_A r_w^2}\right)}$$

(3.46)

In summary, for a depletion-drive reservoir, a Cartesian plot of rate versus the cumulative production during pseudo steady state flow condition will give

- a straight line with slope given in Equation 3.45 (or Equation 3.46)
- extrapolation of the line resulting in ultimate reserve
- estimation of $(k, A, C_A)$ from the slope
- if $k$ is dependently determined by a transient test (e.g. a buildup or a rate test, i.e. *1/q vs. lnt*) and well is in the middle of the drainage area ($C_A = 31.62$) then $A$ can be uniquely determined.

The above explanation applied for a slightly compressible system (liquid). For highly compressible system (gas), some adjustment needs to be made to rigorously account

for change in $(\mu C_t)$. Nevertheless, the basic plotting technique is practically applicable.

**3.4 Rate Normalization and Its Application**

Material balance method, based on obtaining average reservoir pressure varying with cumulative production, is a fundamental calculation in reservoir engineering for determining oil and gas in place. In principle, it consists of producing a certain amount of fluids, measuring the average reservoir pressure before and after production, and with knowledge of the PVT properties of the system for mass balance:

***Remaining hydrocarbon in place = Initial hydrocarbon in place - Produced hydrocarbon.***

The above equation appears simple; but in practice, its implementation can be complex as one must account for many possible variables, for example, external influx (water drive), compressibility of all fluids and the rock, hydrocarbon phase change, etc.

The analysis and interpretation of production data, on the other hand, is one of the oldest approaches for the characterization of oil and gas reservoirs, but production data analysis is typically considered to be a "low resolution" technique because of the frequency and quality of the production data. However, recent innovations, in particular, the development of the decline type curve approach[31], have greatly improved the analysis of this "poor" data. Of these methods to interpret oil and gas production data (conventional decline curve analysis, decline type curve analysis, expected ultimate recovery analysis), ultimate recovery analysis has high operational practicality, especially on reservoirs with small reserve and high decline rate. Method to estimate hydrocarbon in place and recovery efficiency on gas wells in Chevron Thailand was developed and applied by Vo D. T.[35]. The technique combines the material balance equation and rate normalization Equation 3.35 to track, monitor, and forecast reserve of a gas well. This approach is grounded in theory and result was developed by making a simplifying assumption that yielded a simple straight line

trend. It has been proven with actual production data from many wells and tested against commercial software for consistency. Based on the concept that the method has been successfully applied on gas wells, Chapter 4 will investigate practicality and applicability of rate normalization plot to estimate the expected ultimate recovery of oil wells where production data are available. Production data will be the only data needed for surface to bottom-hole pressure conversion.

For a slightly compressible fluid, rate normalization is defined as:

$$Rate \ \ normalization = \frac{q_{sf}}{p_i - p_{wf}} \tag{3.47}$$

Well productivity can also be estimated from

$$J = \frac{q_{sf}}{p - p_{wf}} \tag{3.48}$$

For single layer reservoir, one can expect that the slope of rate normalization curve, when plotted against cumulative production, would be constant once boundary-dominated flow is established. For multilayer reservoirs in commingle production system, depending on the degree of contrast on properties of layers and on the perforation strategy, one could expect that more than one slopes will be seen on the rate normalization graph. This is due to the change in bottom-hole pressure either by influence of newly added layer pressure or late establishment of pseudo steady state of layers with low flow capacity.

## 3.5 Bottom-Hole Pressure Calculation Methods

Well testing and pressure surveillance method such as production logging and static pressure measurement are the most reliable techniques to provide accurate reservoir and wellbore pressure data. Operationally speaking, to determine the average reservoir pressure, it is required that the well be shut-in. This results in deferring or delaying of production. In high permeability reservoir, it is not a

significant issue, but in medium to low permeability reservoirs, the shut-in duration may have to last for days before a reliable reservoir pressure can be estimated. This delaying of production opportunity as well as the cost of monitoring the shut-in pressure is often unacceptable. If, indeed, an average reservoir pressure can be obtained from flowing conditions with routine well test data such as tubing head pressure (THP), rate, etc, this is of great practical value.

The following discussion focuses on methods utilized in this thesis to calculate flowing bottom-hole pressure on both oil and gas well.

### 3.5.1 Bottom-Hole Pressure Calculation on Gas Well

Several methods currently exist for calculating bottom-hole pressure in gas wells. The method of Cullender and Smith[41], developed for dry gas wells, is generally believed to be the most accurate method to calculate the bottom-hole pressure. Several modifications have been made to the method to take into account condensate and water production. These adjustments treat the gas-liquid system as a pseudo-homogeneous mixture. Method of Cullender and Smith involves numerical integration to calculate both static and flowing bottom-hole pressures with consideration of variations in both temperature and compressibility factor ($Z$) with depth. It is assumed that the flow is steady state, and kinetic energy effects are neglected. The mechanical energy balance equation can be expressed as follows: (Derivation and calculation procedure of the method are shown in Appendix B)

$$\int_{p_{tf}}^{p_{wf}} \frac{\left(\dfrac{p}{Tz}\right)dp}{\dfrac{667 f_m q^2}{d^5 \left(\dfrac{H}{L}\right)} + \left(\dfrac{p}{Tz}\right)^2} = \frac{\gamma_g H}{53.34} \tag{3.49}$$

Evaluation of the frictional component of pressure drop, called $F^2$ by Cullender and Smith, and defined as

$$F^2 = \frac{667 f_m q^2}{d^5 \left( \dfrac{H}{L} \right)} \tag{3.50}$$

requires a value for $f_m$, the Moody friction factor. To properly evaluate $f_m$ requires knowledge of gas viscosity, flow ate, gas gravity, as well as tubing diameter and roughness. In order to avoid having to determine these parameters, Cullender and Smith generated a correlation between internal pipe diameter (ID) and $f_m$. A correlation between $f_m$ and pipe internal diameters is established and divided into two groups.

For pipes which have diameter less than 4.227 in.,

$$f_m = \frac{4.327 x 10^{-3}}{d^{0.224}} \tag{3.51}$$

For pipes which have a diameter greater than 4.227 in.,

$$f_m = \frac{4.007 x 10^{-3}}{d^{0.164}} \tag{3.52}$$

Since Cullender and Smith method is not applicable on wet gas (gas associated with some degree of liquids), Razasa and Katz[48] developed a chart relating the ratio of well fluids gravity (as a vapor) to the surface gas gravity and the barrels of condensate per million standard cubic feet of surface gas. This chart may be expressed by the following relationship:

$$\gamma_{wg} = \frac{\gamma_g + \dfrac{4584 \gamma_o}{R_g}}{1 + \dfrac{132800 \gamma_o}{M_o R_g}} \tag{3.53}$$

where $\gamma_{wg}$ = well stream gas specific gravity

$R_g$ = surface producing gas oil ratio, SCF/STB

$M_o$ = molecular weight of condensate

$\gamma_o$ = specific gravity of condensate

$\gamma_g$ = specific gravity of surface gas

When the molecular weight of the condensate is not known, it may be estimated with Cragoe's correlation[49]:

$$M_o = \frac{6084}{API - 5.9} = \frac{44.29\gamma_o}{1.03 - \gamma_o} \qquad (3.54)$$

The gas flow rate is adjusted by an equation from Ikoku[42] and the total gas flow rate is given by

$$q_t = q_g + Gq_o \qquad (3.55)$$

where $G$ = the gas equivalent of condensate, SCF/STB

$q_o$ = condensate flow rate, STB/d

$$G = \frac{133037\gamma_o}{M_o} \qquad (3.56)$$

Water production can also be significant. Ikoku[42] suggested using Vitter's formula to adjust the surface gas gravity for total liquid production, as

$$\gamma_{mix} = \frac{\gamma_g + \dfrac{4591\gamma_L}{R_g}}{1 + \dfrac{1123}{R_L}} \qquad (3.57)$$

where $\gamma_L$ = average liquid (condensate plus water) specific gravity

$R_L$ = producing gas liquid ratio, SCF/STB

The value of $q_t$ calculated in Equation 3.55 is used in Equation 3.49. The last and most important adjustment made to the original Cullender and Smith method is

frictional factor. Nikuradse[65] proposed a frictional factor correlation for truly turbulent flow as

$$\frac{1}{\sqrt{f_m}} = 1.74 + 2\log\left(\frac{d}{2e}\right), \qquad (3.58)$$

where $e$ = absolute roughness, in.

This frictional factor is considered to be one of the best available frictional factor correlations for truly developed turbulent flow in rough pipes.

### 3.5.2 Bottom-Hole Pressure Calculation on Oil Well

For the simplicity of the calculation, Hagedorn and Brown method is selected as a model to convert the surface pressure to the bottom-hole pressure. The Hagedorn and Brown method accounts for slip and makes no consideration for which flow pattern exists. The procedure to calculate pressure gradients using Hagedorn and Brown is listed in Appendix C.

# CHAPTER 4

# RATE NORMALIZATION AND FIELD EXAMPLES

The previous chapters review literature and introduce the definition of rate normalization. The objective of this chapter is to show application of rate normalization on both gas and oil wells. The contrast of layers' flow capacities is investigated, and conclusions is drawn. Simulated and actual data are presented, comparison with type curves are made to verify the use of rate normalization.

## 4.1 Single Layer Reservoir

Single layer reservoirs are the first group of reservoirs used in the study. This section focuses on analyzing reservoirs based on simulated data and actual production data using the rate normalization technique and other methods such as *P/Z* plot on gas wells.

### 4.1.1 Simulated Single Layer Gas Reservoir

Simulation data were generated by using MBAL commercial package with the abandonment condition set at 0.1 MMSCFD on production rate. The well initially flows at 8 MMSCFD constant rate and it is produced under volumetric depletion drive mechanism without any water influx. **Table 4.1** below illustrates reservoir properties.

**Table 4.1:**  Single layer gas reservoir properties-used to simulate pressure and flow rate.

| | |
|---|---|
| Gas density | 0.8 (Air = 1) |
| $CO_2$ | 15% |
| $H_2S$ | 0% |
| $N_2$ | 15% |
| BHT | $370^o$ F |
| $P_i$ | 3990 psi |

| | |
|---|---|
| Condensate API | 45 |
| Water specific gravity | 1 |
| Tubing ID | 2.441 in |
| Condensate ratio | 10 STB/MMSCF |
| Water salinity | 12000 ppm |
| Porosity | 0.2 |
| $S_w$ | 0.18 |
| Gas in place | 6 BSCF |
| $C_t$ | 3.49998 E-06 psi$^{-1}$ |
| Darcy flow coefficient | 500 psi/(MMSCFD) |

**Figure 4.1** shows inflow performance relationship (IPR) of the interested gas reservoir using Forchheimer model.
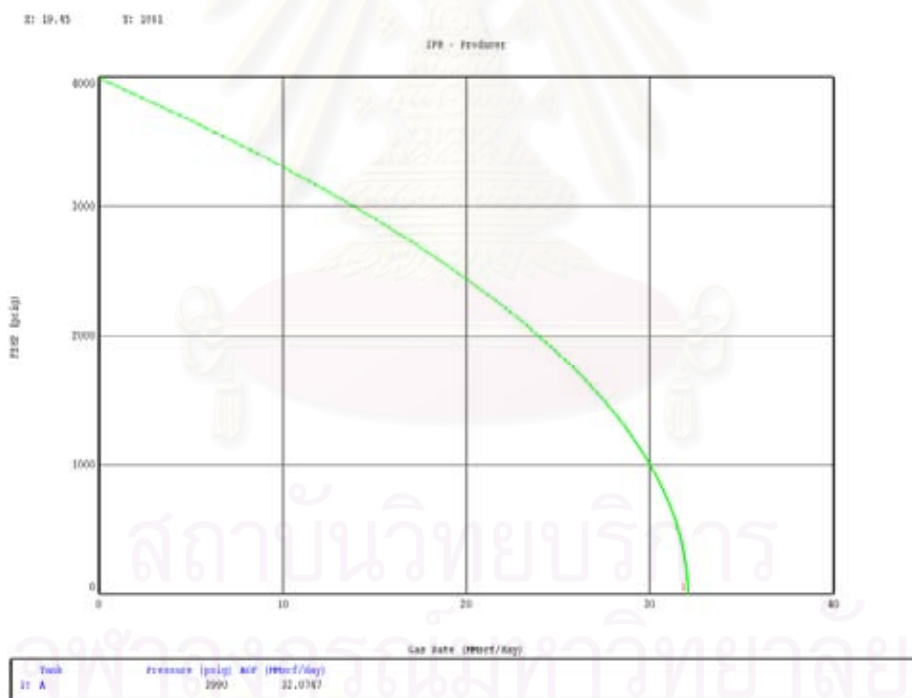


**Figure 4.1:**     Inflow performance relationship – Forchheimer

Simulated production data, generated by MBAL, are then used to convert to the bottom-hole pressure using Cullender and Smith method mentioned in Chapter 3.

Rate normalization is then plotted against cumulative production as shown in **Figure 4.2.** As one can see from rate normalization plot, there are two obvious parts on the graph illustrating conditions the reservoir has experienced throughout the whole production life. The first nonlinear part of the plot represents the state where the reservoir is in the transient period (wellbore storage and infinite acting). The later part of the graph where the slope of the curve is constant, or in another word, where a linear trend is established, is when boundaries have been felt and the reservoir is in pseudo steady state condition. At that point of time, pressure would be constantly dropped for the same amount at every point within the reservoir. Expected ultimate recovery is x-intercept of the linear trend line.

Simulation run of the case studied shows that at abandonment, the expected ultimate recovery of the producing well is at 5.02 BSCF. Rate normalization plot in **Figure 4.2** yields an expected ultimate recovery of 5.03 BSCF, which is about 0.16 % different from the simulated result. From the above comparison, one can recognize that there is a good agreement between expected ultimate recovery derived from rate normalization and result obtained from the simulation run. Now, take another look at the classical *P/Z* plot in **Figure 4.3**. The difference between actual gas in place (**Table 4.1**) and estimated gas in place derived from the calculated bottom-hole pressure is at 0.67%. This is another match that validates the application of rate normalization.
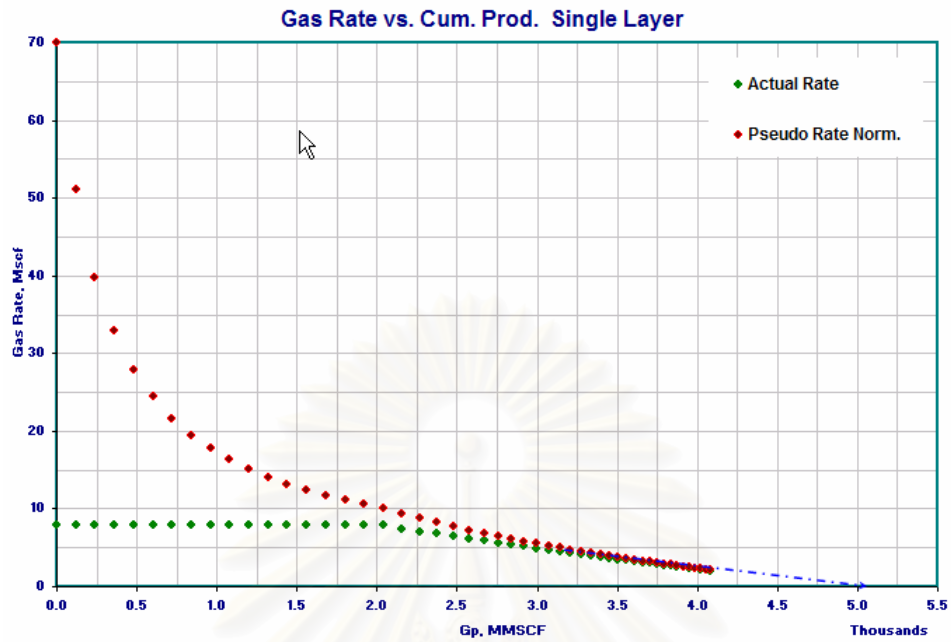
**Figure 4.2:** Normalized rate vs. cumulative production-(simulated single-layer gas reservoir).
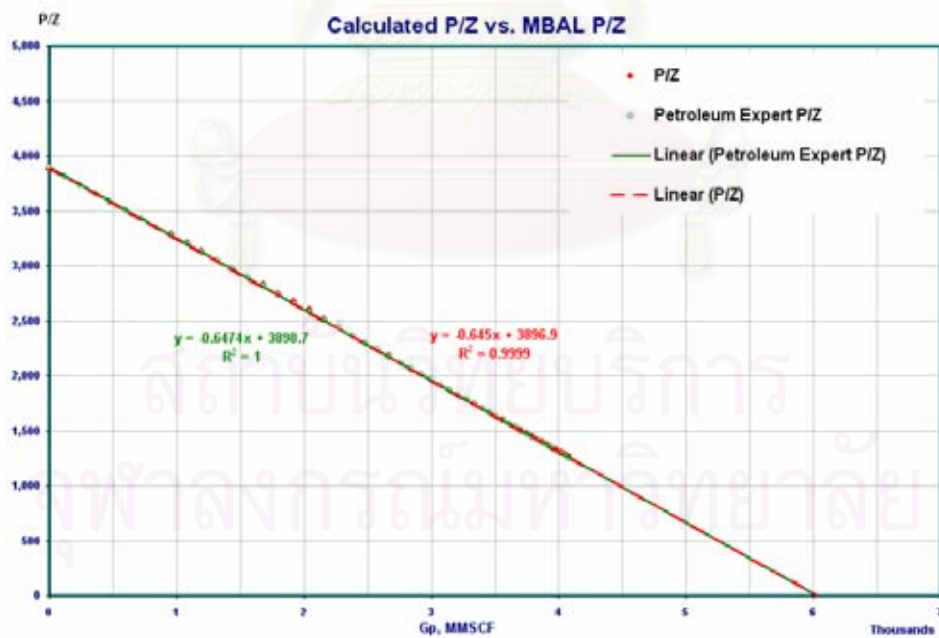


**Figure 4.3:** P/Z vs. cumulative production- (simulated single-layer gas reservoir).

As mentioned in Chapter 3, modified Cullender and Smith method is used to convert surface conditions to bottom-hole information. The method takes into account both condensate and water components provided that these two liquid elements are in the vapor form. **Figure 4.4** shows comparison on bottom-hole pressure from simulation and calculated bottom-hole pressure utilizing modified Cullender and Smith method. The chart shows that there is good alignment and match between simulated results from MBAL commercial software package and results derived from modified Cullender and Smith method. Average error between these two sources of calculations over a total of 50 data points is 8.1 psi, which is relatively small and can be considered as a good match.
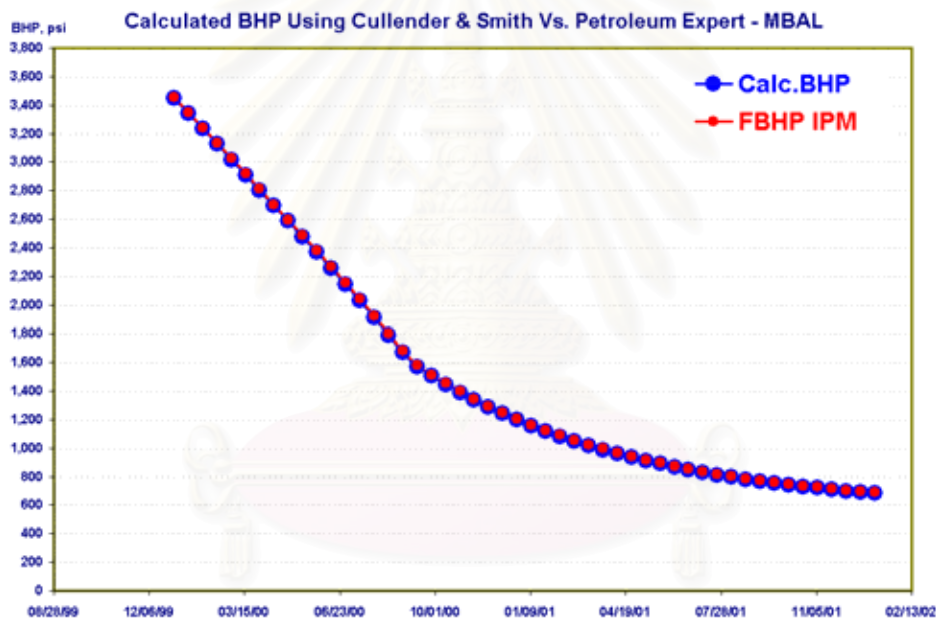


**Figure 4.4**:     Bottom-hole pressure comparison- (simulated single-layer gas reservoir).

## 4.1.2 Field Data – Single Layer Gas Reservoir

The following section discusses the application of rate normalization on field data. The well selected for study is located in a single sand reservoir and completed with 2-7/8" in. diameter tubing. The tubing is perforated with 2-1/8" hollow carried gun and high shot density (6 shot per foot) in 60 degree phasing. The well started producing for one month after initial perforation was completed. The well was shut in

for pressure build up and then opened back up for production. The slim-hole completion design was applied on the well and collection of production data was ceased before additional sands were perforated for commingled production. Well schematic is shown in Appendix D. The following table shows reservoir properties of the single sand producing well.

**Table 4.2** Single-layer gas reservoir properties-field data.

| | |
|---|---|
| Gas density | 0.81 (Air = 1) |
| $CO_2$ | 16% |
| $H_2S$ | 1% |
| $N_2$ | 2% |
| BHT | $280^o$ F |
| $P_i$ | 3000 psi |
| Condensate $^o$API | 43.8 |
| Water specific gravity | 1 |
| Tubing ID | 2.441 in |
| Porosity | 0.2 |
| $S_w$ | 0.18 |
| Gas in place | 6 BSCF |
| Measured depth (ft) | 10769 |
| TVD (ft) | 6543 |

Well production is shown in Appendix D. **Figure 4.5** is a plot of rate versus cumulative production. The transient ended, and pseudo steady state was established when the well produced for a total of 0.75 BSCF. As one can see in **Figure 4.5**, true production rate is steady around at 10 MSCFD. It would be very difficult to estimate the expected ultimate recovery (EUR) of the well by simply using this rate at this point in time. On the other hand, pseudo rate normalization has clearly shown the advantage of early prediction on EUR of the reservoir. In this case, extrapolation of linear trend line of the pseudo rate normalization yields a EUR value of 4.125 BSCF.
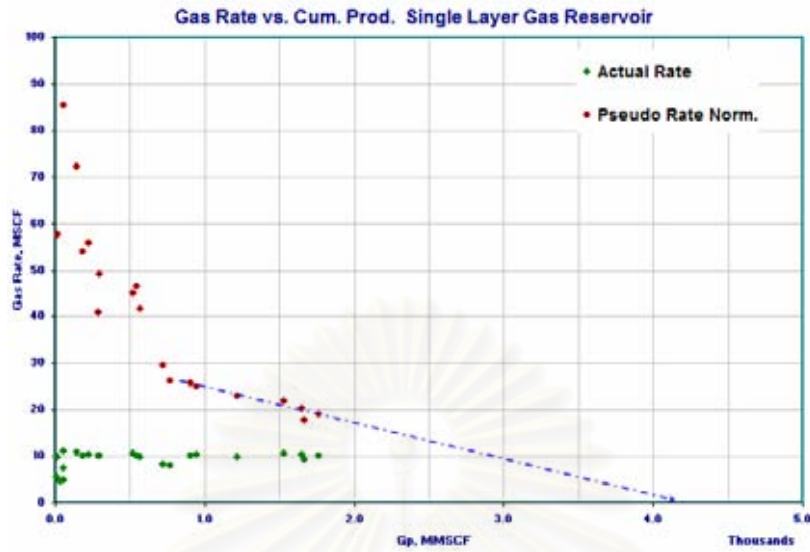
**Figure 4.5:** Normalized rate versus cumulative gas production-(single layer).

**Figure 4.6** is *P/Z* plot of the well. According to this graph, if the reservoir is opened for production until abandonment without any additional perforations, then recovery efficiency of the well is about 66%.
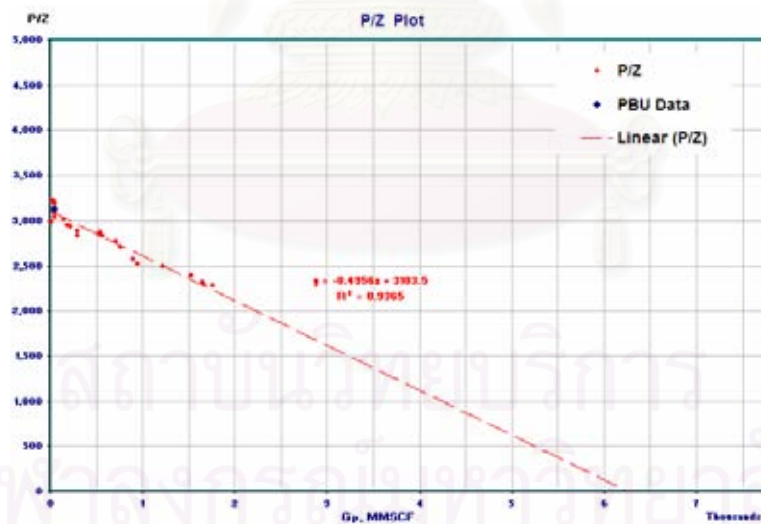


**Figure 4.6:** *P/Z* versus cumulative production plot-(single layer gas reservoir).

### 4.1.3 Simulated Single Layer Oil Reservoir

An oil reservoir selected for the study is a solution gas drive reservoir since a majority of oil wells are producing under this drive mechanism. **Table 4.3** illustrates well information and reservoir properties.

**Table 4.3**    Single layer oil reservoir-simulated data.

| | |
|---|---|
| Gas density | 0.8 (Air = 1) |
| $CO_2$ | 10% |
| $H_2S$ | 0% |
| $N_2$ | 0% |
| BHT | $350^o$ F |
| $P_i$ | 5000 psi |
| Oil $^o$API | 37.5 |
| Water specific gravity | 1 |
| Tubing ID | 2.441 in |
| Roughness | 0.0018 in |
| Porosity | 0.2 |
| $S_w$ | 0.18 |
| Original oil in place | 10 MMSTB |
| Measured depth (ft) | 9735 |
| TVD (ft) | 8108 |
| Geothermal gradient | 1.5 (deg/100 ft) |
| Solution gas ratio | 400 SCF/STB |
| Manifold pressure | 450 psi |
| Bubble point pressure | 2938 psi |

The well is produced with a maximum rate of 6000 STBD and with the abandonment flow rate of 10 STBD. **Figure 4.7** shows inflow performance relationship and tubing performance relationship with range of gas oil ratio (GOR) varied from 300 SCF/STB to 3,000 SCF/STB, liquid rate (both oil and water) in the range of 500 to 10,000 STBD. The reservoir is considered to be under normal

depletion mechanism, i.e., volumetric and without any water influx or encroachment during the production life of the well.
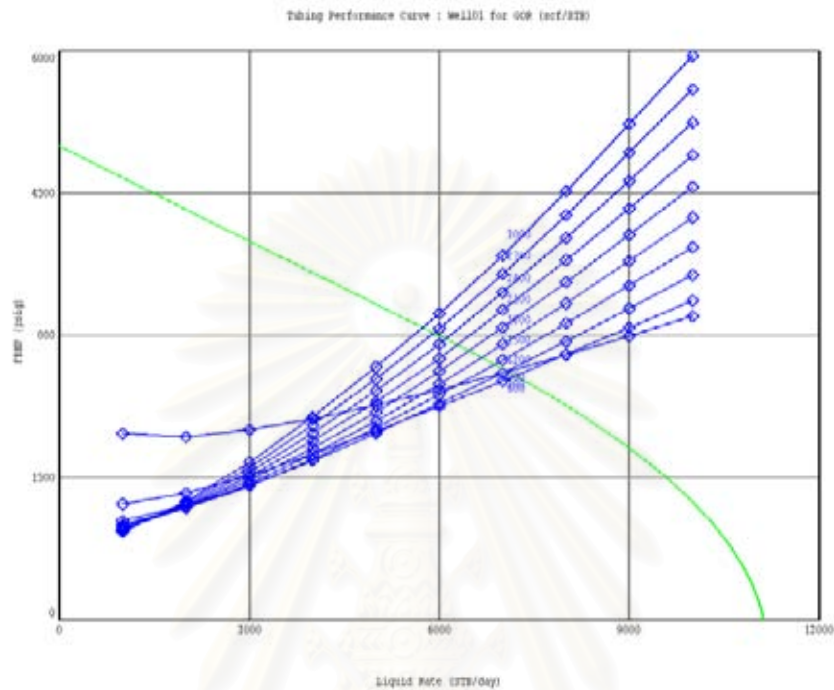


**Figure 4.7:**    IPR and TPR curves –single layer oil reservoir.

Simulated production data were obtained from using information given in **Table 4.3** and utilizing MBAL software module. The well production started on January 01, 2001 with initial production rate of 6000 STBD. The production rate is varied with an intension to generate a set of production data, which is similar to field production data, for the analysis. **Table 4.4** shows production schedule applied to the case.

**Table 4.4**    Schedule for production rate-single oil reservoir-simulated case.

| Date | Minimum oil rate, STBD | Maximum oil rate, STBD | Maximum water rate, SBTD | Maximum liquid rate, STBD |
|---|---|---|---|---|
| 01/01/2001 | 10 | 6000 | 1000 | 10000 |
| 04/01/2001 | 10 | 4000 | 2000 | 6000 |
| 07/01/2001 | 10 | 1000 | 1500 | 3000 |

| Date | Minimum oil rate, STBD | Maximum oil rate, STBD | Maximum water rate, SBTD | Maximum liquid rate, STBD |
|------|------------------------|------------------------|--------------------------|---------------------------|
| 01/01/2002 | 10 | 500 | 1200 | 2000 |
| 06/01/2002 | 10 | 700 | 1500 | 2000 |
| 01/01/2003 | 10 | 300 | 1300 | 1800 |
| 06/01/2003 | 10 | 1000 | 1500 | 2500 |
| 01/01/2004 | 10 | 400 | 1600 | 2000 |
| 06/01/2004 | 10 | 500 | 1500 | 2000 |

MBAL Simulation ended on 16 February, 2009 when the production reached the abandoned rate (10 STBD). At the abandoned condition, reservoir pressure is 2,287 psi, and the cumulative production is 1.423 MMSTB. Recovery efficiency of the well is 14.2%. Simulated production data were used to calculate normalized rate. It is then plotted against the cumulative production.
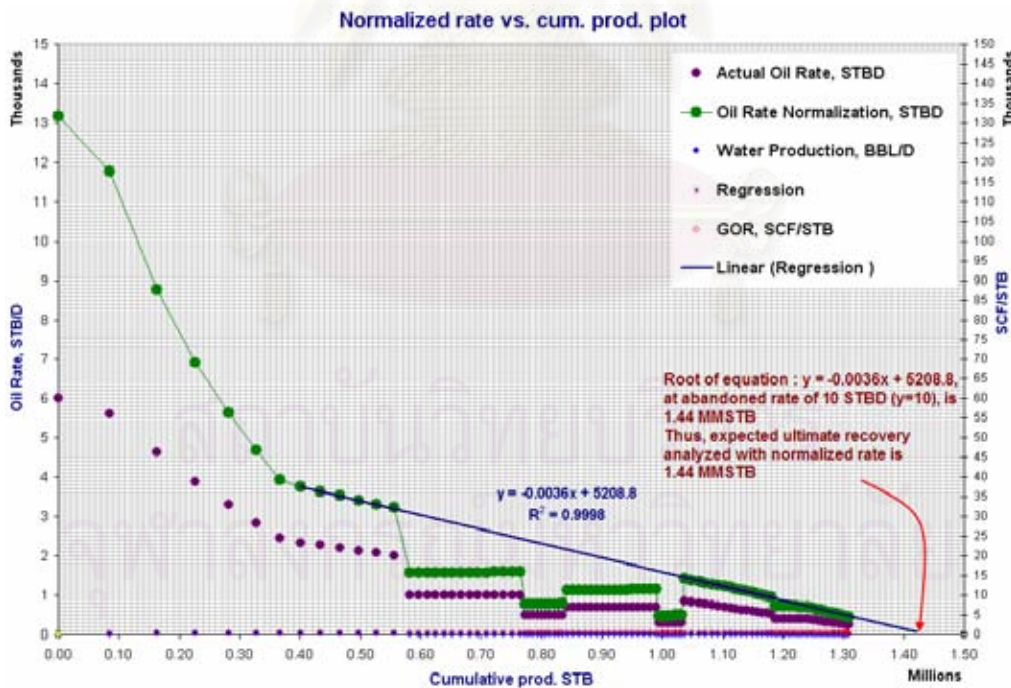


**Figure 4.8:** Normalized rate vs. cumulative oil production-(single layer oil reservoir).

As one can see from **Figure 4.8**, the well passed transient period and moved to pseudo steady state condition when the cumulative production reached 0.4 MMSTB. When the production is controlled to lower than the deliverability of the reservoir over the certain period of time, normalized rate also dropped off from the linear trend line. The adjustment on oil rate in June 2003 to 1000 STBD helped bring normalized rate data points to its straight line. A product of linear regression of uncontrolled rate data points is a single slope straight line represented by equation "*y = -0.0036x + 5208.8*". A calculation to find out root (*x*) of the above equation with *y* (abandoned rate) equals to 10 STBD gives *x* value of 1.44 MMSTB. This is the expected ultimate recovery of the well analyzed by normalized rate plot. The difference in EUR between MBAL simulation run and normalized rate plot is around 0.2 MMSTB or equivalent to 1.5 %.

Let us examine production data generated by MBAL by using Rate Transient Analysis (RTA) package from Fekete Associate Inc[43]. The software package offers several methods of analyzing production data, such as, traditional decline curve analysis, Fetkovich type curves, Blasingame decline type curve, Agarwal and Gardner rate-time analysis, flowing material balance, normalized pressure integral, model analysis and forecast analysis. However, for the purpose of comparing result of EUR derived from normalized rate plot, Fetkovich and Blasingame type are used. **Figure 4.9** plots the actual rates generated using the data in **Table 4.3** on Fetkovich type curve. At the abandonment conditions, flow rate of 10 STBD and 2,256 psi bottom-hole pressure (this pressure is MBAL bottom-hole pressure at the abandonment condition), the ultimate recovery of the reservoir is 1.460 MMSTB and the original oil in place is 11.519 MMSTB. Production data matches Fetkovich type curves on the lines where $r_{eD} = 10$ and $b = 0$. **Table 4.5** summarizes results of Fetkovich analysis on production data generated by MBAL for a single layer oil reservoir.

**Table 4.5**     Results of Fetkovich type curve analysis-(simulated single oil
reservoirs).

| | |
|---|---|
| Dimensionless drainage radius ($r_{eD}$) | 10 |
| Permeability ($k$), md | 18 |
| Skin | -9.3 |
| Decline exponent ($b$) | 0.0 |
| Nominal annual decline rate ($D_e$), % | 44.51 |
| Decline rate at start of forecast, $D$ | 0.589 |
| Rate at start of forecast $q_f$, STBD | 252.9 |
| Abandonment rate $q_{AB}$, STBD | 10 |
| Remaining recoverable reserves $RR$, MSTB | 150.5 |
| Expected ultimate recovery at abandonment pressure $EUR$, MSTB | 1,460.5 |
| Wellbore pressure at abandonment $p_{wf}$, psi | 2256 |
| Drainage area, acres | 126,988 |
| Original oil in place, MSTB | 11,519 |

From **Table 4.5**, recovery efficiency of the reservoir is around 12.68%.
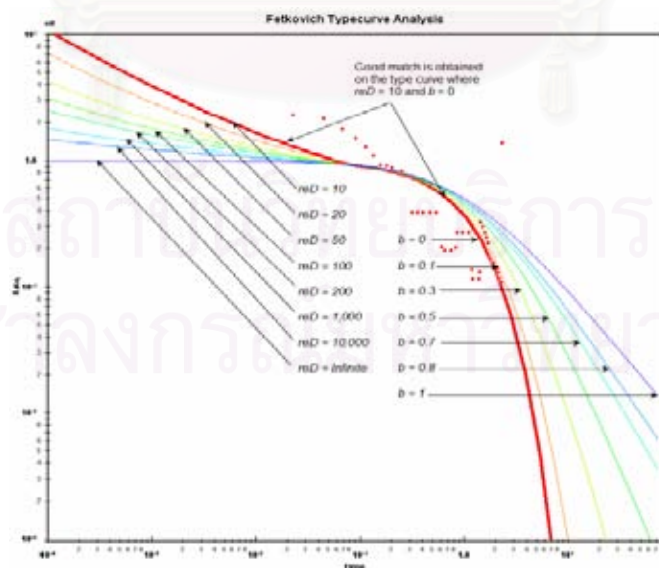


**Figure 4.9:**     Fetkovich type curve-(single layer oil reservoir).

When analyzing the actual rate using Blasingame type curves, with an input 14% recovery factor, EUR of the reservoir is 1.139 MSTB with estimated OOIP of 8.97 MMSTB. **Figure 4.10** presents result of Blasingame type curve analysis. A good match is obtained when value of dimensionless drainage radius is seven ($r_{eD} = 7$).
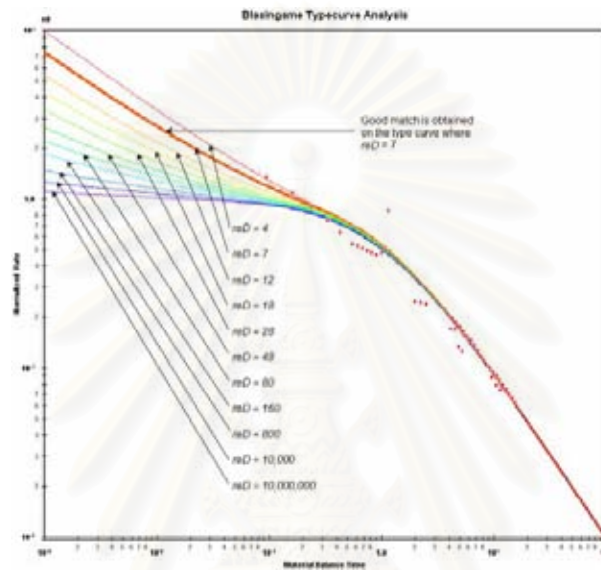


**Figure 4.10:** Blasingame type curves-(single layer oil reservoir).

**Table 4.6** presents results of actual production data analyzed by Blasingame type curves.

**Table 4.6**    Results of Blasingame type curve analysis-(simulated single oil reservoirs).

| | |
|---|---|
| Dimensionless drainage radius ($r_{eD}$) | 7 |
| Permeability ($k$), md | 27 |
| Skin | -9.6 |
| Drainage area, acres | 89,710 |
| Expected ultimate recovery at abandonment pressure *EUR*, MSTB | 1,139 |
| Original oil in place, MMSTB | 8,137 |

**Table 4.7** is a summary of results analyzed by different methods (MBAL, normalized rate, Fetkovich and Blasingame type curves).

**Table 4.7**        Summary of analysis result for single-layer oil reservoir.

|  | MBAL | Fetkovich | Blasingame | Normalized rate |
|---|---|---|---|---|
| OOIP, MMSTB | 10 | 11.519 | 8.137 | 10 |
| EUR, MMSTB | 1.42 | 1.46 | 1.139 | 1.44 |
| Recovery % | 14.2 | 12.7 | 14 | 14.4 |

As one can see from **Table 4.7**, if consider EUR result from MBAL simulation run as a reference point then results of EUR analyzed by both normalized rate and Fetkovich type curve have the least difference while Blasingame type curve shows bigger magnitude of separation- 20% off from the MBAL EUR prediction.

### 4.1.4 Field Data – Single Layer Oil Reservoir

As discussed in the previous section, rate normalization works well with a simulated one layer oil reservoir, where tubing pressure on surface is kept constant with production rate constrains from 10 to 8,000 STBD. To further consolidate the conclusion, an actual well producing out of one sand is selected. The sand was perforated in April 2002 with 27' of perforation. For the first month, the well produced on 25/64" choke. The well was shut-in for a pressure build up (PBU) test, and production started back up after four days of testing. At the end of August 2003, due to decline on production, the well was put through booster compressor (booster compressor is a device which allows the well to produce with its wellhead pressure to be few hundreds pressure per square inch lower than the line pressure of a producing field) to help improve vertical lift performance (VLP).   Additional layers were perforated on May 2004. Data collection for normalized rate analysis on this one single oil producing sand was stopped when booster compressor introduced.  **Table 4.8** describes the well information and reservoir properties.

**Table 4.8**     Single layer oil reservoir-field data.

| | |
|---|---|
| Gas density | 0.70 (Air = 1) |
| $CO_2$ | 6.68% |
| $H_2S$ | 0% |
| $N_2$ | 0.25% |
| BHT | $264^o$ F |
| $P_i$ | 2438 psi |
| Oil $^o$API | 40 |
| Perforation interval | 27 ft |
| Tubing ID | 2.441 in. |
| Roughness | 0.0018 in. |
| Porosity | 0.22 |
| $S_w$ | 0.4 |
| Measured depth (ft) | 7000 |
| TVD (ft) | 5890 |
| Geothermal gradient | 1.5 (deg/100 ft) |

The production data was used to construct normalized rate plot. **Figure 4.11** presents a plot between normalized rate and the cumulative production of a single-layer oil reservoir. As one can notice on the plot, the earlier part of the graph where the cumulative production is less than 60 MSTB is when the well produced under controlled choke size. The well underwent transient period and this condition was ended when the cumulative production reached 120 MSTB. When the well moved to pseudo steady state condition, normalized rate data started to fall into a single slope straight line. A linear regression was performed on a set of normalized rate data within boundary dominated flow condition. The straight line can be represented by an equation *y = -0.0195x + 7166.1*. To be consistence with the previous analysis on the simulated case of a single oil reservoir, we defined the abandonment condition is when the production rate is at 10 STBD. This value will be used throughout the study. Replacing the value of normalized rate at the abandonment condition (*y = 10*) into the equation *y = -0.0195x + 7166.1* to find the root of the linear regression. The cumulative oil production at the abandonment condition (root of the linear regression equation) is 366,979 STB, this is the expected ultimate recovery of the reservoir.
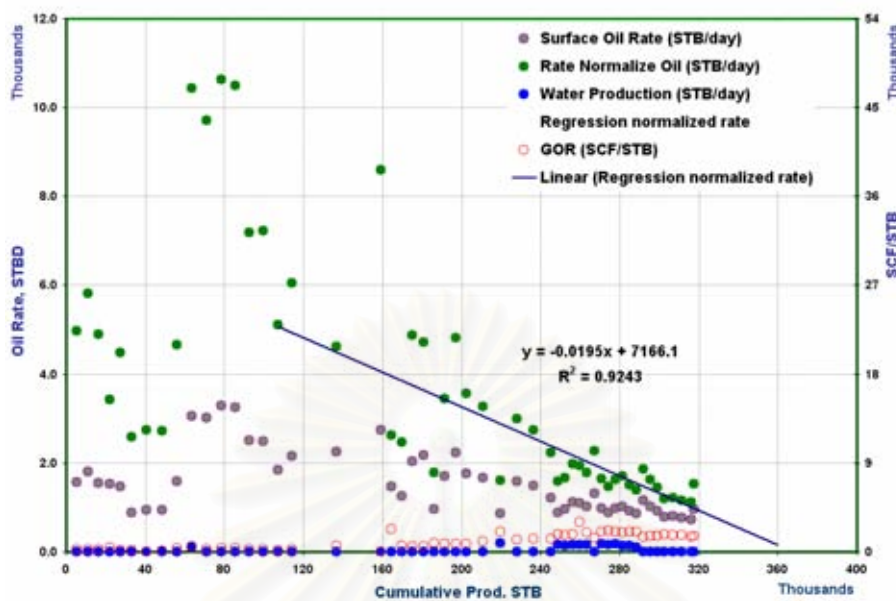
**Figure 4.11***:* Normalized rate vs. cumulative production –(single layer oil reservoir).

The production data were analyzed by Fekete rate transient analysis package on two type curves, Fetkovich and Blasingame. Production rate and cumulative production were plotted on Fetkovich type curves, shown on **Figure 4.12. Table 4.9** summarizes results of Fetkovich type curves analysis.

**Table 4.9** Results of Fetkovich type curve analysis-(field data single layer oil reservoirs).

| | |
|---|---|
| Decline exponent ($b$) | 0.5 |
| Decline rate at start of forecast, $D$ | 0.702 |
| Rate at start of forecast $q_f$, STBD | 80.7 |
| Abandonment rate $q_{AB}$, STBD | 10 |
| Remaining recoverable reserves $RR$, MSTB | 63 |
| Expected ultimate recovery at abandonment pressure $EUR$, MSTB | 399 |
| Wellbore pressure at abandonment $p_{wf}$, psi | 1000 |
| Drainage area, acres | 130.3 |
| Original oil in place, MSTB | 3586.3 |

Pressure value of 1000 psi was selected to be the abandonment pressure, this takes into account measured bottom-hole pressure from recent reservoir surveillance runs. Production data were scattered on the Fetkovich type curves in **Figure 4.12**, however, the best fit type curve was obtained with decline exponent *b=0.5* and $r_{eD}$ = infinite.
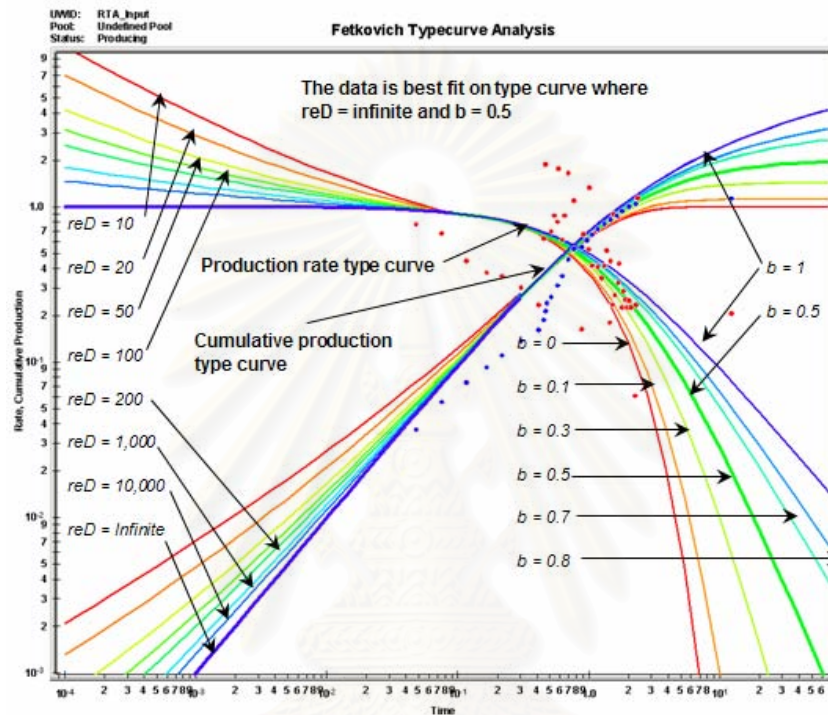


**Figure 4.12**: Fetkovich type curve analysis-(single layer oil reservoir).

The production data were analyzed by using Blasingame type curves with the input recovery factor 14 %. Normalized rate and rate integral were plotted against material balance time, shown in **Figure 4.13**. The best fit type curve was obtained with dimensionless drainage radius $r_{eD}$ = 10,000,000. **Table 4.10** summarizes Blasingame type curve analysis.

**Table 4.10**    Results of Blasingame type curve analysis-(field data single layer oil reservoirs).

| Dimensionless drainage radius ($r_{eD}$) | $10^7$ |
|---|---|
| Permeability ($k$), md | 180 |
| Skin | 8.3 |
| Expected ultimate recovery at abandonment pressure *EUR*, MSTB | 416.4 |
| Recovery factor, % | 14 |
| Drainage area, acres | 108.1 |
| Original oil in place, MSTB | 2974.4 |
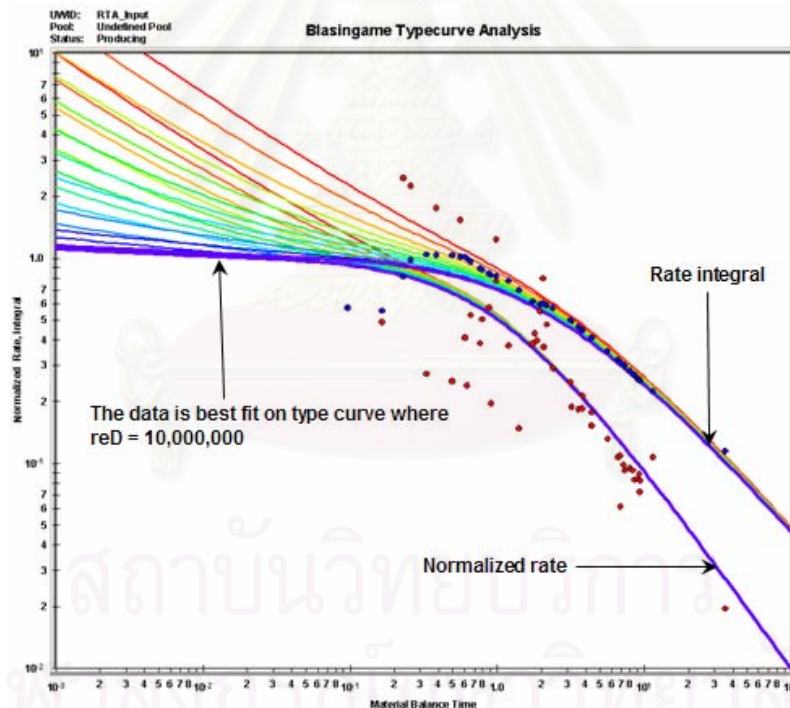


**Figure 4.13***:*    Blasingame type curve analysis-(single layer oil reservoir).

A series of other decline type curves within Fekete package were run to compare the results obtained from normalized rate plot. Additional type curve runs are Agarwal –Gardner, exponential decline, normalized pressure integral and transient type curve.

**Table 4.11** shows comparison between reserve estimation from the plot in **Figure 4.11** and different type curve models using Fekete rate transient analysis. The bottom-hole pressure and flow rate at the abandonment condition are at 1000 psi and 10 STBD accordingly on all cases.

**Table 4.11**: OOIP & EUR between Fekete rate transient analysis (RTA) and normalized rate plot –single oil reservoir.

| Estimation Methods | OOIP, MSTB | EUR, MSTB |
|---|---|---|
| Exponential Decline Curve (RTA) | 3,407 | 398.5 |
| Fetkovich (RTA) | 3,586 | 399.1 |
| Blasingame (RTA) | 2,974 | 416 |
| Agarwal – Gardner (RTA) | 2,982 | 417.5 |
| Normalized Pressure Integral (RTA) | 2,845 | 398.2 |
| Normalized rate (Thesis Model) | 2,352 | 367 |
| Transient Type Curve (RTA) | 2,892 | 404.9 |

According to **Table 4.11**, Blasingame, Agarwal-Garder, normalized pressure integral and transient type curve give similar results on both original oil in place and expected ultimate recovery. These approaches are based on the rigorous mathematic solutions with the absent of empirical depletion stems on the type curves. These are not required because the usage of material balance time forces the boundary dominated data to fall only on the analytical harmonic stem. On the other hand, similarity observed on analysis results from the exponential decline curves and the Fetkovich type curves.

Even thought all the decline curves and type curves are graphically easy to use and visually benefit when perform the data fitting, these approaches have their limitations. For a situation where operating conditions on surface changes very fast (adjusting choke, shut in the tubing for a period of time and then open the well for production, set or remove standing valve to control gas rate from the gas sand) production data when plot on the type curves will be scattered and it is very difficult to make the best fit on the curves, results of the analysis will bear some amount of

uncertainty. With normalized rate approach, it is visually easy to recognize the single slope straight line once all reservoir boundaries are felt. When pseudo steady state condition is on set, simple linear regression can be done on a set of data (normalized rates and cumulative production). With a known abandonment condition (we used 10 STBD as the abandonment on both simulated and field data cases), an EUR of the reservoir can be found by simply solve a linear regression equation. For this particular case, the analysis on single-layer producing sand yields a satisfactory result. Normalized rate method appears to be very comparable to commercial software package.

## 4.2 Two-Layer Reservoir

It has been proven in the previous section that rate normalization can be applied for both single oil and gas reservoirs. This section will investigate the application of rate normalization on two-layered systems with contrast on flow capacity between reservoirs. Before moving further, let us define some concepts that will be used throughout this section.

Transmissibility is a product of permeability and thickness of the reservoir. Reservoir contrast, defined by Vo. D. T.[35], is the ratio between transmissibility over pore volume of one layer to that of the other layer.

$$T_1 = k_1 * h_1 \tag{4.1}$$

$$T_2 = k_2 * h_2 \tag{4.2}$$

$$Contrast = \frac{T_1/V_1}{T_2/V_2} \tag{4.3}$$

$$V = A * h * \phi \tag{4.4}$$

We are going to study the effect of contrast between two reservoirs to establish a general correlation of contribution from sands in the commingled system. The study used porosity and permeability transform correlation from Chevron field in the Gulf of Thailand, which can be generalized by Equation. 4.5 and is shown in **Figure 4.14**

$$k = 0.0048*Exp(44.483*\phi) \tag{4.5}$$
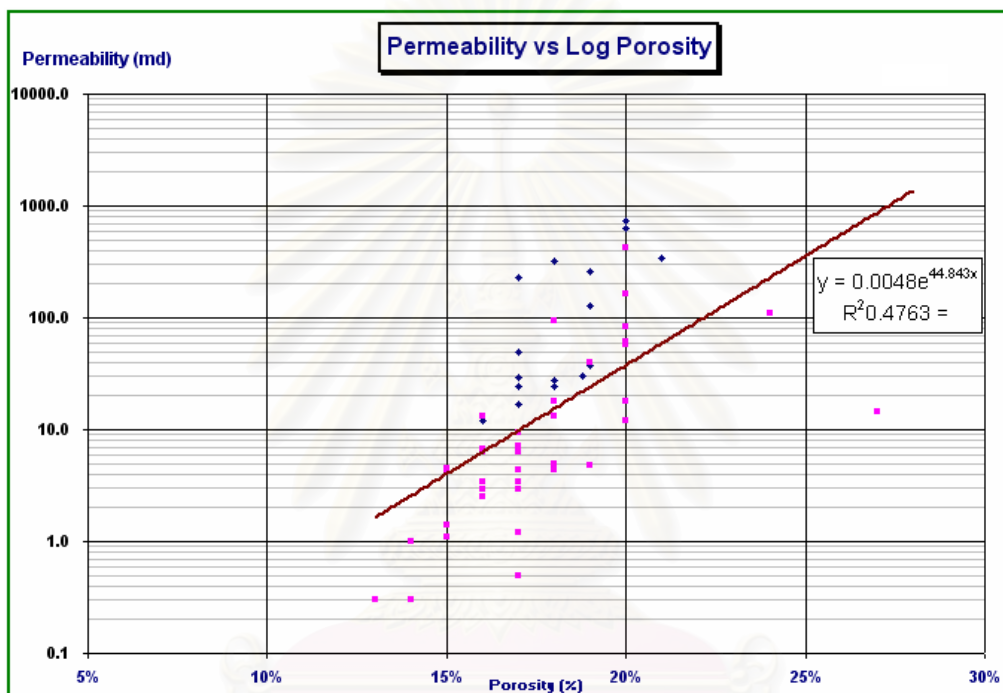


**Figure 4.14:**  Porosity-permeability correlation.

### 4.2.1 Contrast Study of Two-Layer Gas Reservoirs

A series of combinations of permeability, thickness, and reservoir pore volume were selected to make up a wide range of distribution of contrast, from as low as 1.48 to as high as 88. The simulation was scheduled so that during production of a well, there are times the well is shut in to measure static bottom-hole pressures. These pressure points are considered to be average reservoir pressure at the time of shut in and are used to make the *P/Z* plot. **Table 4.12** illustrates the contrast between sands in commingled two layered gas reservoir system, where reservoir volumes of each sands are not the same. According to results show in **Figure 4.15** to **Figure 4.22**, if the value

of contrast is greater than six, there are two distinct slopes exist on the *PZ* plot. The higher the value of contrast between the two layers, the more difference of the slopes observed on the plot. This indicates a large difference in contribution from each reservoir in the system. When the contrasts of the two layers are in the range of three to six, the difference in slopes on the *P/Z* gets smaller, as the value of the contrast gets closer to the lower side of the range. Difference in slopes on the *P/Z* plot tends to collapse to zero. This means the contribution of each layers in the system is very much on the same order of magnitude. If the contrast of the layers is less than three, the *P/Z* plot on shut in condition displayed as a straight line. This means each layer in the two-layered sand system almost equally contributes to the total well production. High transmissibility sand will drain out with a higher rate first and, the point of changing on slope is when low transmissibility sand is a main, or other word, only contributor of the system. As contrast values are higher, the differences between slopes on the *P/Z* curve on sands in shut in condition are getting higher.

**Figure 4.23** to **Figure 4.26** are plots between simulated production rates from individual sand and time. Since the two layers have different initial pressure, in our case study, big reservoir is deeper and has 200 psi higher pressure than smaller reservoir at shallower depth. As the result, during the shut in time, fluid will tend to move from higher pressure layer into lower pressure layer through production tubing. This cross flow event often happens at the earlier date of production. The degrees of cross flow as well as the duration that cross flow will exist are depending on layers characteristics. However, cross flow can also be observed from the lower reservoir pressure to higher reservoir pressure. This situation occurs when the high volume reservoir depletes fast, as cumulative production increases, reservoir pressure from the high pressure layer decreases to below reservoir pressure of the other layer. **Figure 4.25** illustrates the cross flow from lower initial pressure reservoir to higher initial pressure reservoirs during shut in condition.

In **Table 4.12**, data from Case I to Case VII were set up in such a way that reservoirs with lower porosity (lower permeability) will have higher pore volume and lower pressure than the layer which has higher porosity. Case VIII was set up in a different manner. Layer with low porosity has lower pressure and lower pore volume, layer with high porosity has high pore volume. The difference in pressure between

layers is 200 psi, ratio and the total of pore volumes is 4.7 and 8 BSCF respectively. The objective is to study the influence of volumes on contribution of each layer. According to **Figure 4.25**, majority of production contributed by high pore volume layer, obviously, the other layer has minimum affluent on the cumulative hydrocarbon produced. This reflects really well on the *P/Z* plot in **Figure 4.20**, there are no distinct slopes appears on the plot.

**Table 4.12**:    Contrast between reservoirs-different volumes.

| Case No. | Porosity | Thickness ft | Permeability md | Area, ft2 | Pore Volume (ft3), V | kh (T) | kh/V | Contrast |
|----------|----------|--------------|-----------------|-----------|---------------------|--------|------|----------|
| Case I | 20 | 5 | 37.7 | 500,000,000 | 500,000,000 | 188.46 | 3.769E-07 | 88.61 |
| | 10 | 30 | 0.4 | 1,000,000,000 | 3,000,000,000 | 12.76 | 4.254E-09 | |
| Case II | 20 | 5 | 37.7 | 500,000,000 | 500,000,000 | 188.46 | 3.769E-07 | 7.06 |
| | 15 | 15 | 4.0 | 500,000,000 | 1,125,000,000 | 60.06 | 5.339E-08 | |
| Case III | 15 | 15 | 4.0 | 500,000,000 | 1,125,000,000 | 60.06 | 5.339E-08 | 12.55 |
| | 10 | 30 | 0.4 | 1,000,000,000 | 3,000,000,000 | 12.76 | 4.254E-09 | |
| Case IV | 20 | 10 | 37.7 | 500,000,000 | 1,000,000,000 | 376.92 | 3.769E-07 | 6.53 |
| | 17 | 30 | 9.8 | 1,000,000,000 | 5,100,000,000 | 294.53 | 5.775E-08 | |
| Case V | 19 | 15 | 24.1 | 500,000,000 | 1,425,000,000 | 361.07 | 2.534E-07 | 4.39 |
| | 17 | 30 | 9.8 | 1,000,000,000 | 5,100,000,000 | 294.53 | 5.775E-08 | |
| Case VI | 20 | 10 | 37.7 | 500,000,000 | 1,000,000,000 | 376.92 | 3.769E-07 | 1.49 |
| | 19 | 15 | 24.1 | 500,000,000 | 1,425,000,000 | 361.07 | 2.534E-07 | |
| Case VII | 20 | 10 | 37.7 | 500,000,000 | 1,000,000,000 | 376.92 | 3.769E-07 | 2.98 |
| | 19 | 30 | 24.1 | 1,000,000,000 | 5,700,000,000 | 722.15 | 1.267E-07 | |
| Case VIII | 22 | 10 | 92.4 | 3,000,000,000 | 6,600,000,000 | 924.18 | 1.400E-07 | 3.83 |
| | 14 | 20 | 2.6 | 500,000,000 | 1,400,000,000 | 51.14 | 3.653E-08 | |
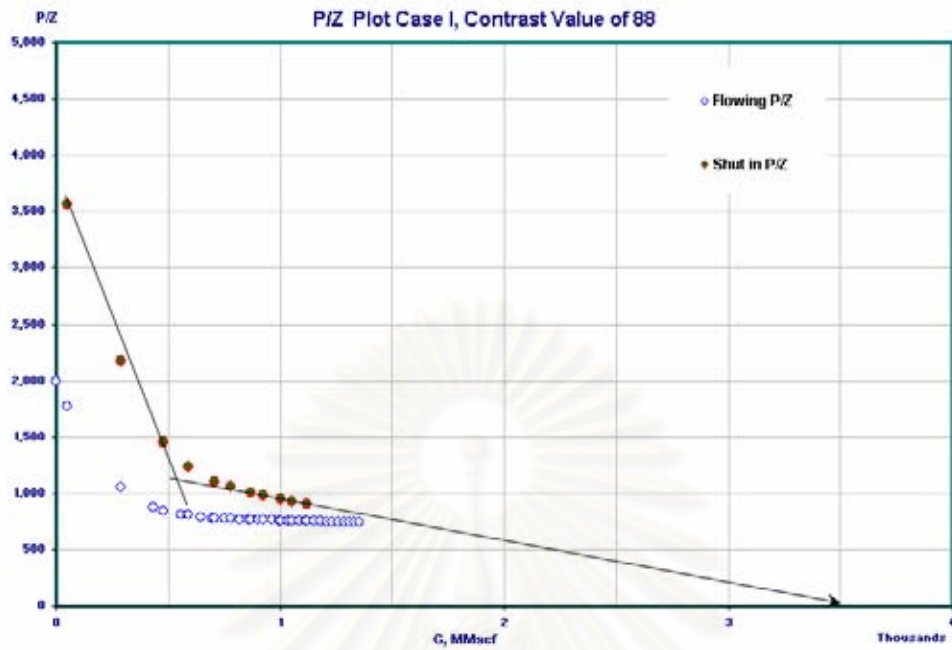
**Figure 4.15**:   P/Z plot – Case I. Contrast between reservoirs is 88.
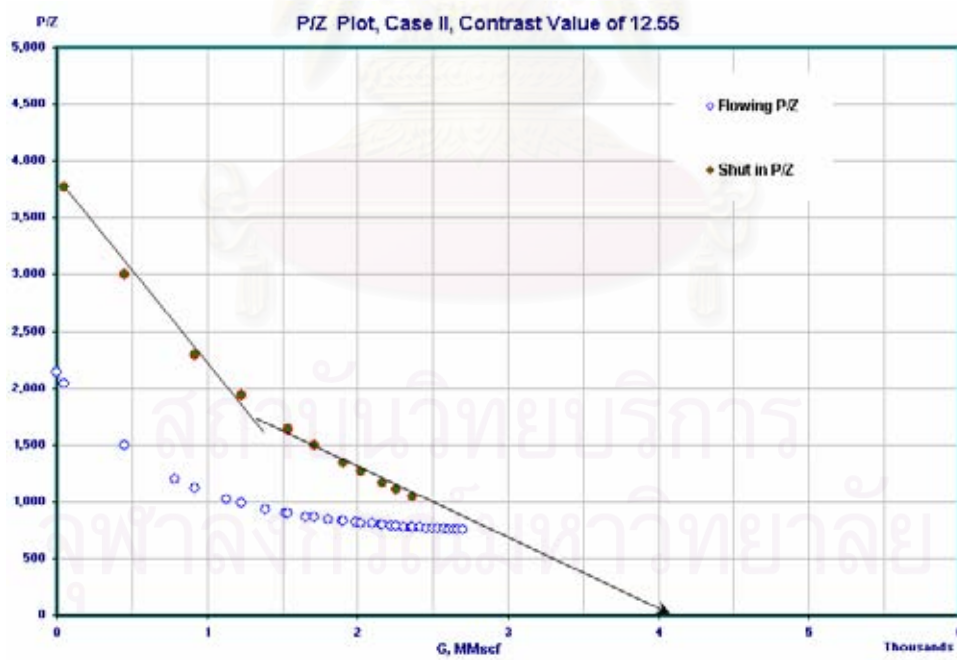


**Figure 4.16**:   P/Z plot – Case II. Contrast between reservoirs is 12.
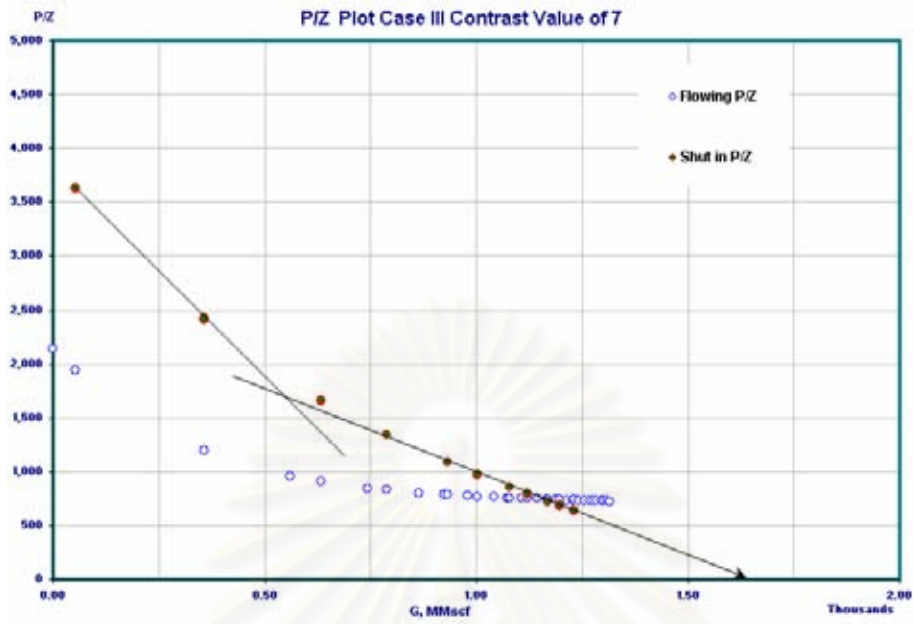
**Figure 4.17**: P/Z plot – Case III. Contrast between reservoirs is 7.
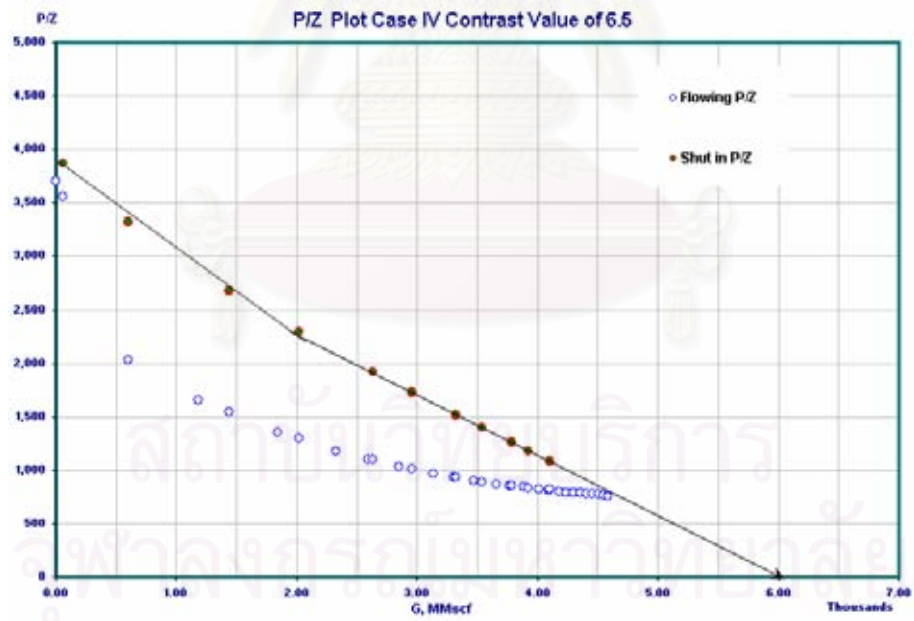


**Figure 4.18**: P/Z plot – Case IV. Contrast between reservoirs is 6.5.
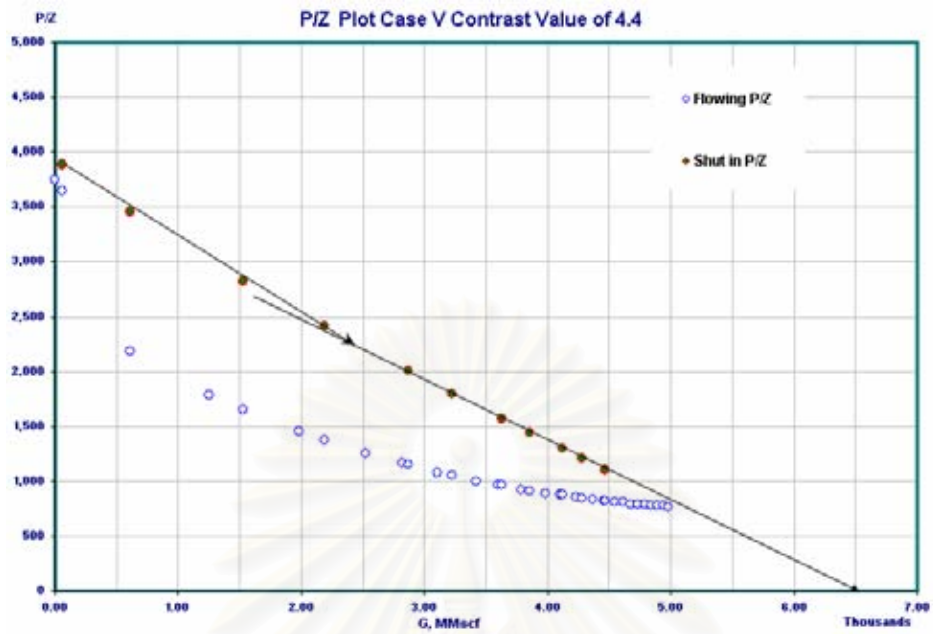
**Figure 4.19**:   P/Z plot – Case V. Contrast between reservoirs is 4.4
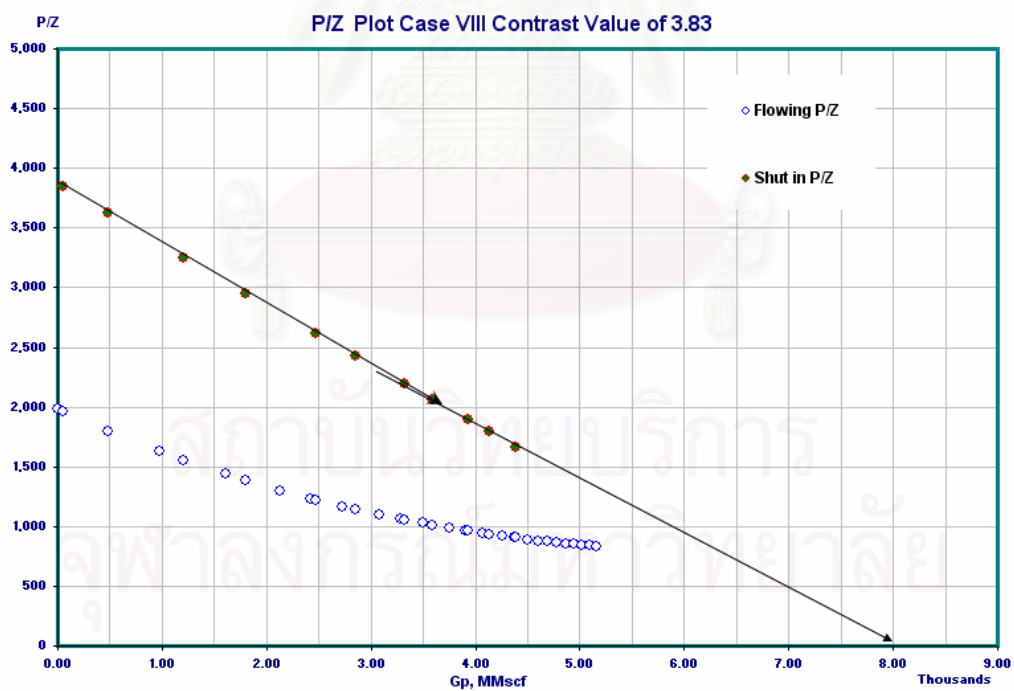


**Figure 4.20**:   P/Z plot – Case VIII. Contrast between reservoirs is 3.38.
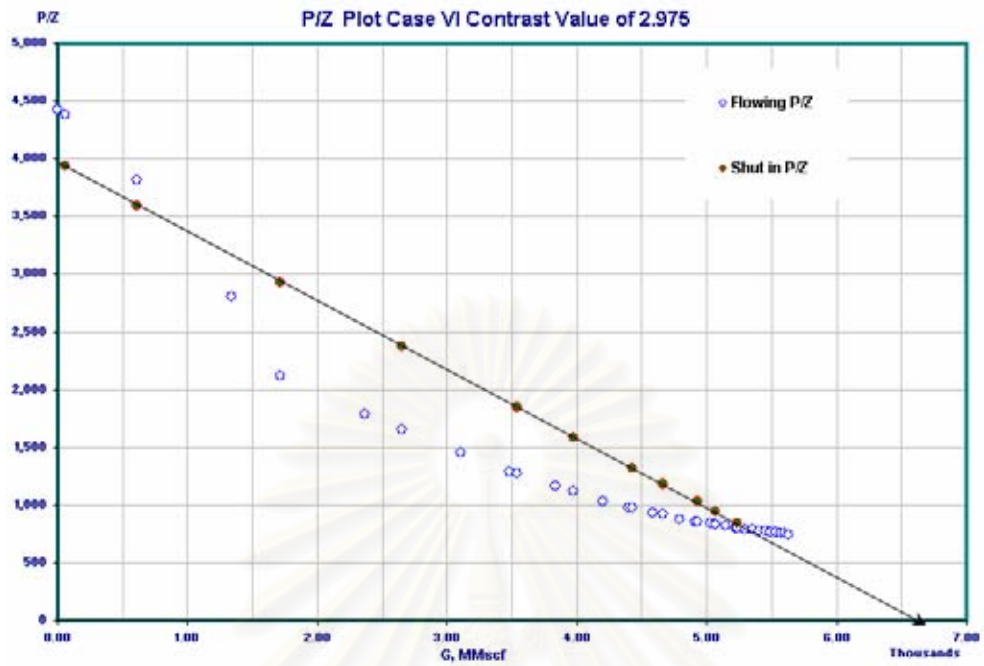
**Figure 4.21**:   P/Z plot – Case VI. Contrast between reservoirs is 2.98.
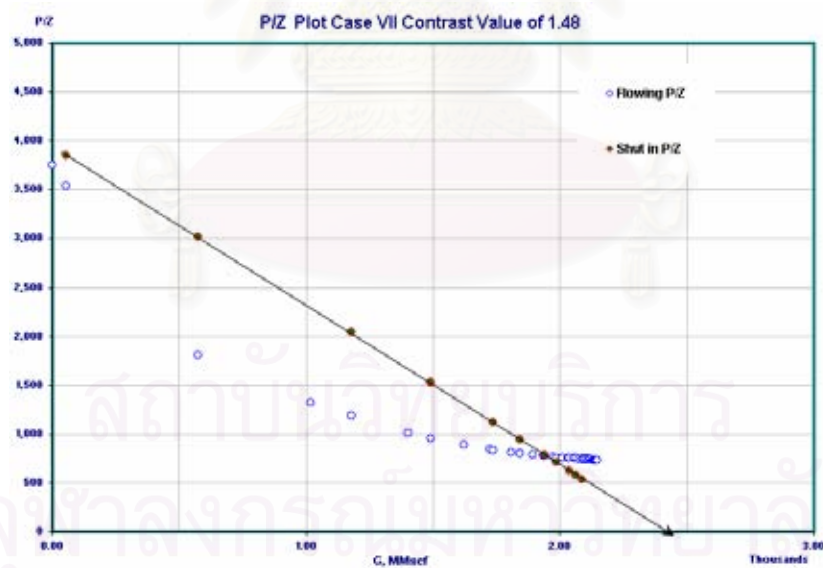


**Figure 4.22**:   P/Z plot – Case VII. Contrast between reservoirs is 1.48.
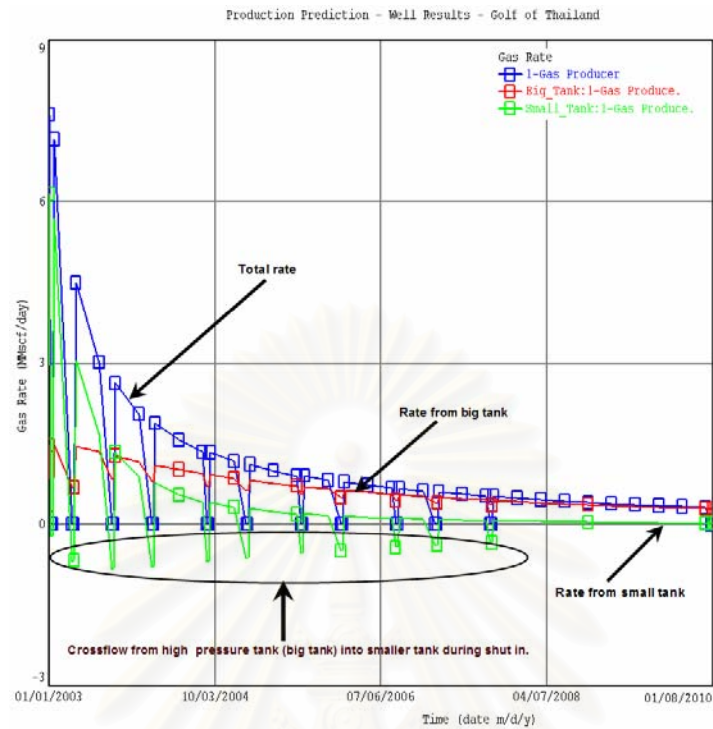
**Figure 4.23**: Rate versus production time. Contrast between reservoirs is 12.
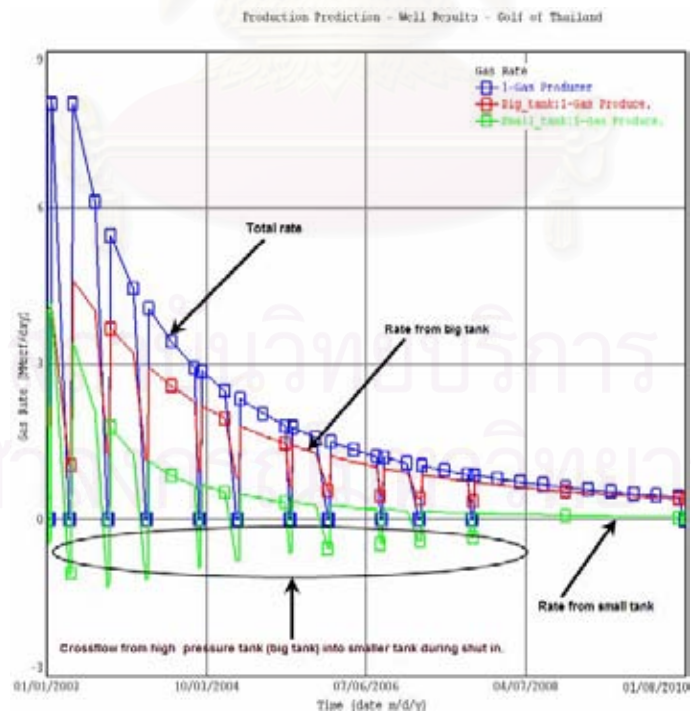


**Figure 4.24** Rate versus production time. Contrast between reservoirs is 4.4.
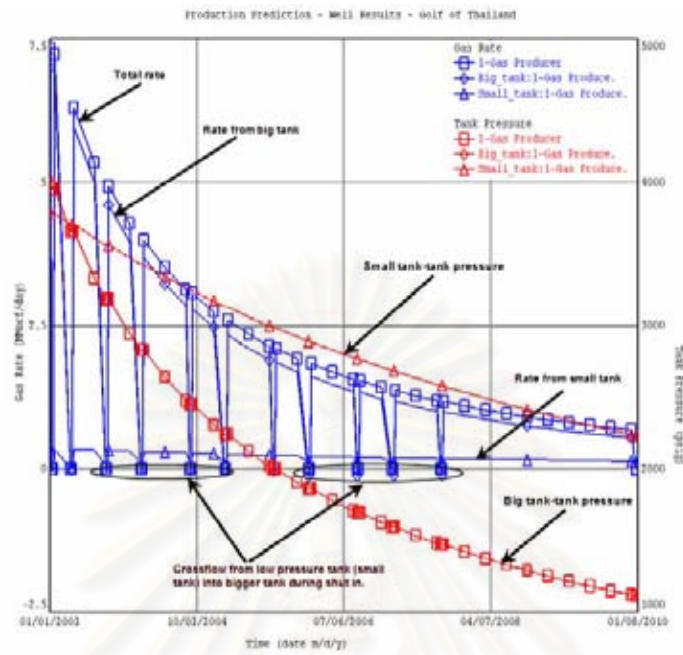
**Figure 4.25**: Rate versus production time. Contrast between reservoirs is 3.83.
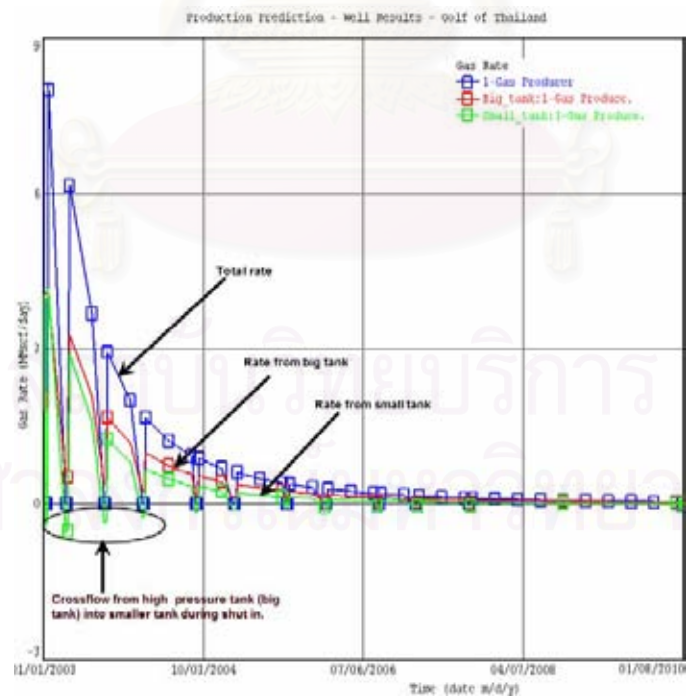


**Figure 4.26**: Rate versus production time. Contrast between reservoirs is 1.48.

To be more conclusive on study of contribution of each layer in the two layers system, simulations were run on another set of data. This time, reservoir area and pore volume are kept constant at 35,000 square feet and 2 BSCF accordingly. One layer in the two layer system was kept the same over eight cases we studied. We varied porosity on other layer from as low as ten to as high as twenty two and combine with the referenced layer to come up with eight different cases. **Table 4.13** shows reservoirs properties of layers. Reservoir contrasts showed in **Table 4.13** are distributed over the range that we mentioned in the previous discussion. Simulation runs were performed on each case with the production rate scheduled such that the well was shut in a few times throughout its life for average bottom-hole pressures measurement.

**Table 4.13**:     Contrast between reservoirs-the same volumes.

| Case No. | Porosity | Thickness ft | Permeability md | Area, ft2 | Pore Volume (ft3), V | kh (T) | kh/V | Contrast |
|---|---|---|---|---|---|---|---|---|
| Case IX | 18 | 9.07 | 15.4 | 35,000 | 2,000,000,000 | 139.44 | 6.972E-08 | 20.08 |
|  | 10 | 16.33 | 0.4 | 35,000 | 2,000,000,000 | 6.94 | 3.472E-09 |  |
| Case X | 18 | 9.07 | 15.4 | 35,000 | 2,000,000,000 | 139.44 | 6.972E-08 | 14.11 |
|  | 11 | 14.84 | 0.7 | 35,000 | 2,000,000,000 | 9.89 | 4.943E-09 |  |
| Case XI | 18 | 9.07 | 15.4 | 35,000 | 2,000,000,000 | 139.44 | 6.972E-08 | 9.83 |
|  | 12 | 13.61 | 1.0 | 35,000 | 2,000,000,000 | 14.19 | 7.095E-09 |  |
| Case XII | 18 | 9.07 | 15.4 | 35,000 | 2,000,000,000 | 139.44 | 6.972E-08 | 4.68 |
|  | 14 | 11.66 | 2.6 | 35,000 | 2,000,000,000 | 29.82 | 1.491E-08 |  |
| Case XIII | 18 | 9.07 | 15.4 | 35,000 | 2,000,000,000 | 139.44 | 6.972E-08 | 3.20 |
|  | 15 | 10.88 | 4.0 | 35,000 | 2,000,000,000 | 43.58 | 2.179E-08 |  |
| Case XIV | 18 | 9.07 | 15.4 | 35,000 | 2,000,000,000 | 139.44 | 6.972E-08 | 2.18 |
|  | 16 | 10.20 | 6.3 | 35,000 | 2,000,000,000 | 63.98 | 3.199E-08 |  |
| Case XV | 18 | 9.07 | 15.4 | 35,000 | 2,000,000,000 | 139.44 | 6.972E-08 | 0.67 |
|  | 19 | 8.59 | 24.1 | 35,000 | 2,000,000,000 | 206.84 | 1.034E-07 |  |
| Case XVI | 18 | 9.07 | 15.4 | 35,000 | 2,000,000,000 | 139.44 | 6.972E-08 | 0.45 |
|  | 20 | 8.16 | 37.7 | 35,000 | 2,000,000,000 | 307.69 | 1.538E-07 |  |

**Figures 4.27 to 4.34** show *P/Z* plots versus cumulative production of the eight cases with different values of contrast.
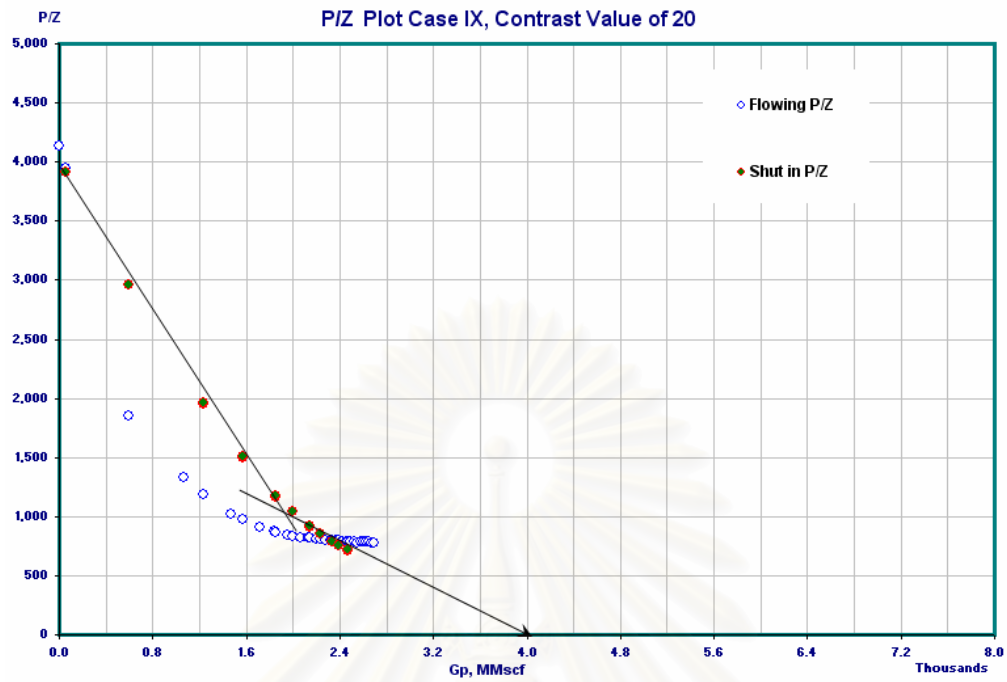
**Figure 4.27**:   P/Z plot – Case IX. Contrast between reservoirs is 20
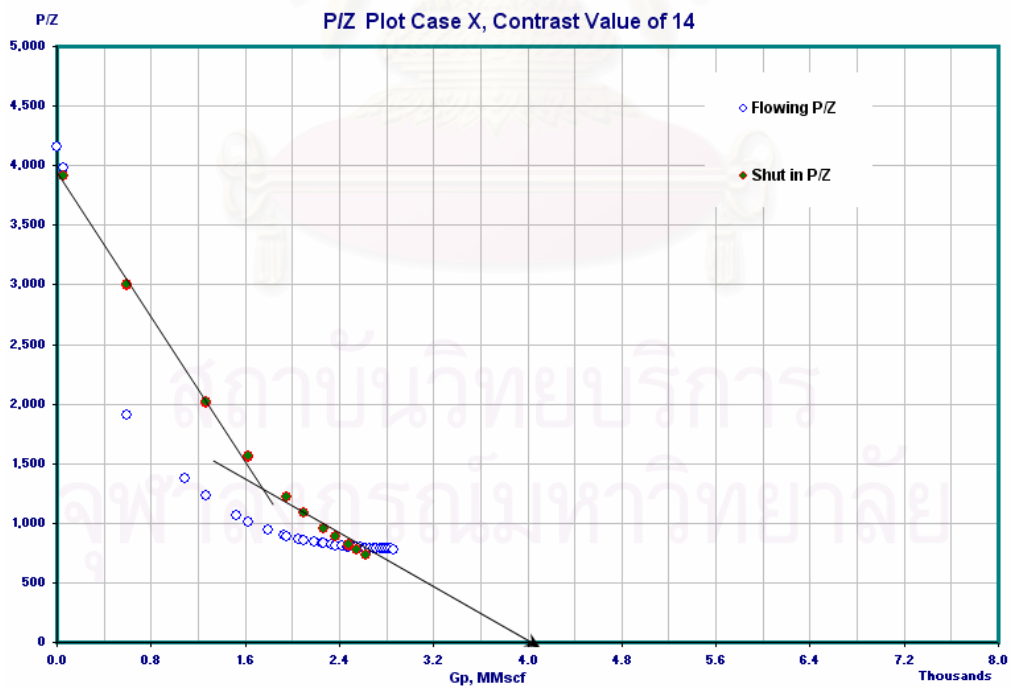


**Figure 4.28**:   P/Z plot – Case X. Contrast between reservoirs is 14
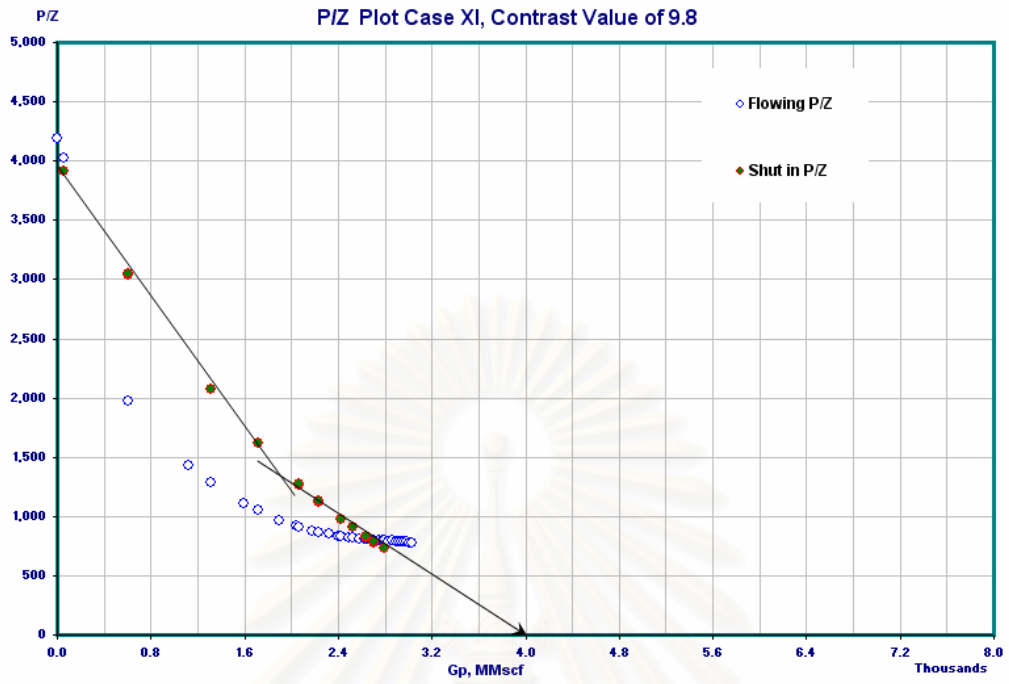
**Figure 4.29**:   P/Z plot – Case XI. Contrast between reservoirs is 9.8
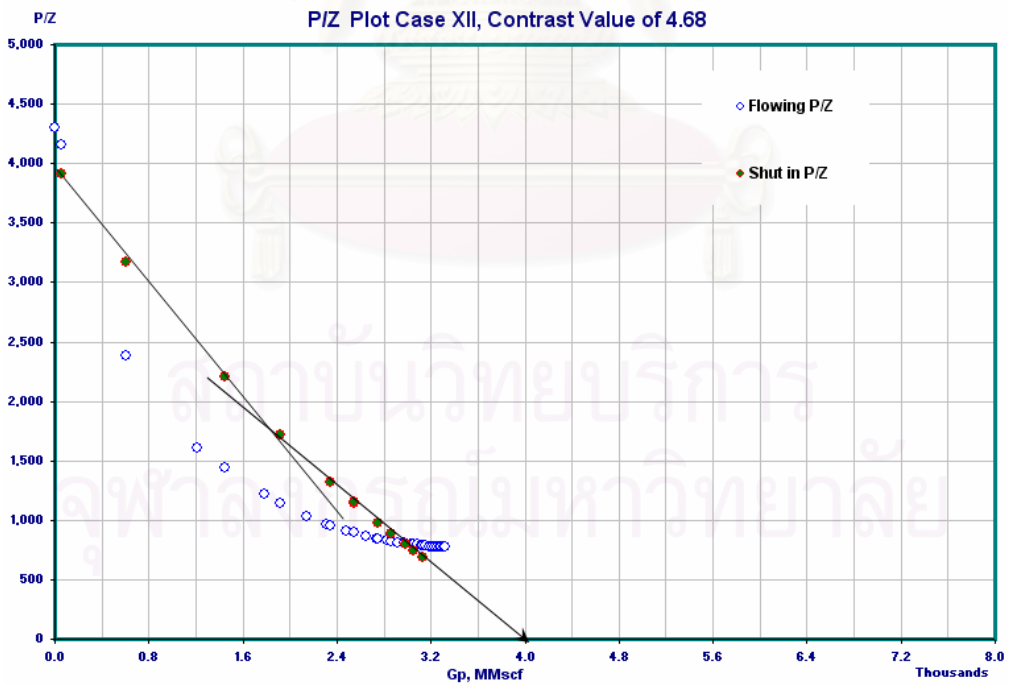


**Figure 4.30**:   P/Z plot – Case XII. Contrast between reservoirs is 4.68
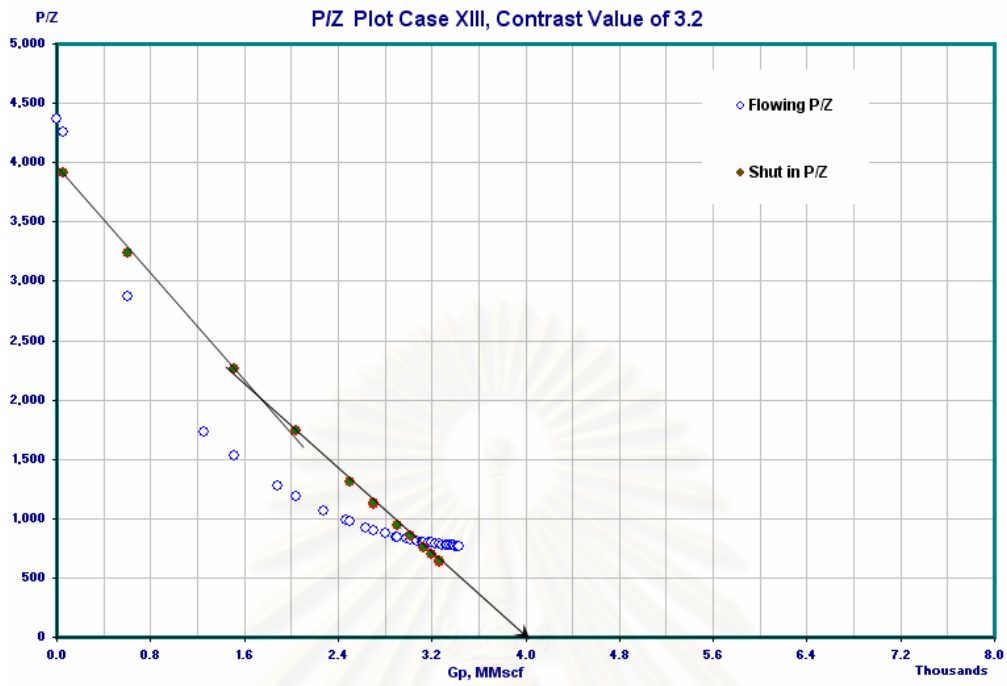
**Figure 4.31**:   P/Z plot – Case XIII. Contrast between reservoirs is 3.2
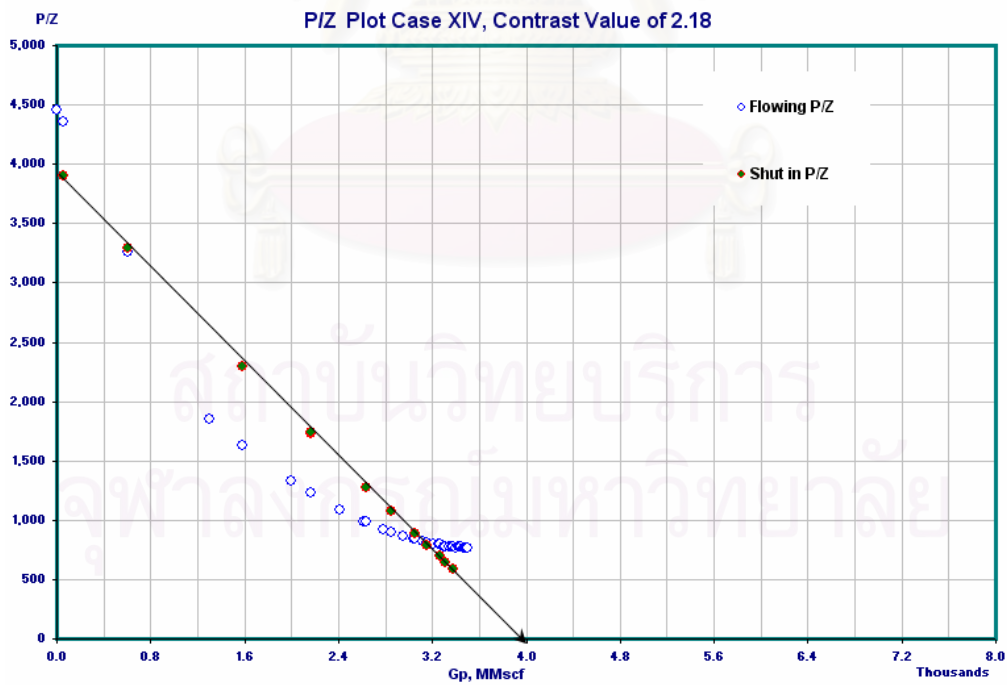


**Figure 4.32**:   P/Z plot – Case XIV. Contrast between reservoirs is 2.18
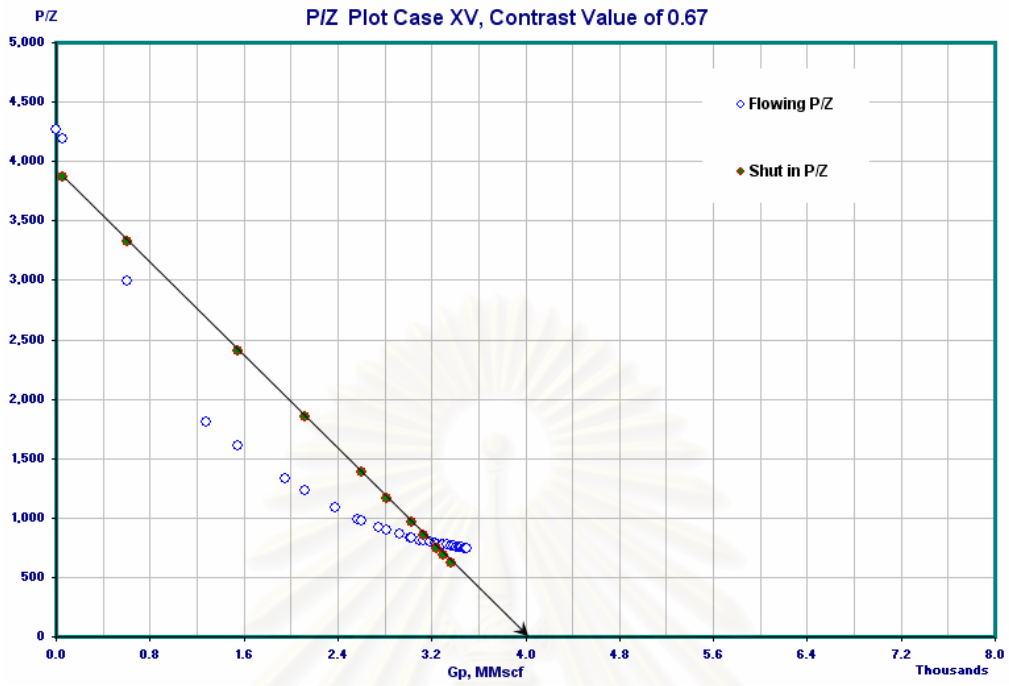
**Figure 4.33**:   P/Z plot – Case XV. Contrast between reservoirs is 0.67
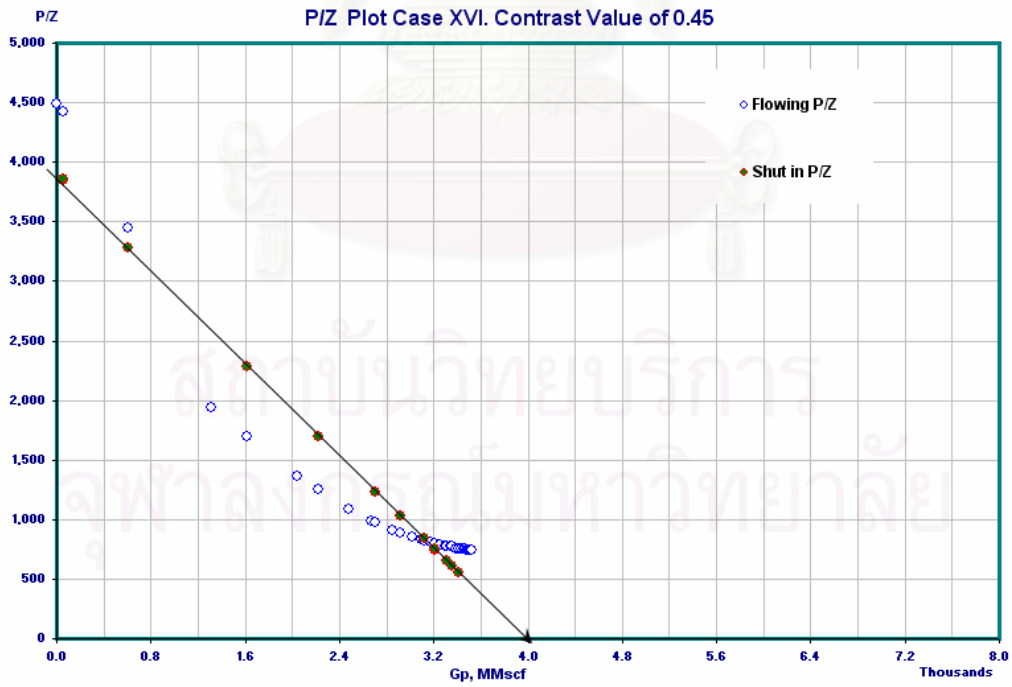


**Figure 4.34**:   P/Z plot – Case XV. Contrast between reservoirs is 0.45

There is similarity between the second eight cases and the first one. The higher the contrast between layers, the higher the differences in slope of the straight lines on the *P/Z* plot. In another word, contribution of layer will be easier to recognize in the higher contrast cases than in the cases of low contrast.

It appears on the *P/Z* plot that, the analysis performed on the fist straight line region in the case where the contrast of the layers greater than three, yields a underestimation of the total gas in place.

**Table 4.14** summarizes relationship between contrast of reservoir properties and slope of *P/Z* curve.

<p align="center">**Table 4.14:**  Two-Slope on P/Z Plot Indicator.</p>

| Reservoir Contrast | 2-Slope |
|---|---|
| Less than 3 | None |
| 3-6 | Low |
| 6-8 | Medium |
| Above 8 | High |

### 4.2.2 Simulated Two-Layer Gas Reservoirs

The previous section has investigated the contrast of reservoirs in commingled system and classified the two-slope behavior based on the degree of contrast. We now look at the application of rate normalization to a two-layer gas reservoir system that commingly produced. We selected the case where contrast of the two-layer is high (contrast = 89) to study. **Table 4.15** presents reservoir properties of the two layers.

**Table 4.15**    Two-layer gas reservoirs-(simulated data.)

|  | Layer 1 | Layer 2 |
|---|---|---|
| Gas density(Air = 1) | 1.04 | 1.04 |
| $CO_2$, % | 20 | 40 |
| $H_2S$, % | 0 | 0 |
| $N_2$, % | 5 | 5 |
| BHT, $^o$F | 370 | 370 |
| $P_i$, psi | 3790 | 3990 |
| Condensate, API | 42 | 45 |
| Water specific gravity | 1 | 1 |
| Tubing ID, in | 2.441 | 2.441 |
| Condensate ratio,  STB/MMSCF | 50 | 30 |
| Water salinity, ppm | 7000 | 7000 |
| Porosity | 0.1 | 0.2 |
| $S_w$ | 0.4 | 0.4 |
| Gas in place, BSCF | 3 | 1.5 |
| $C_t$, psi$^{-1}$ | 3.5 E-06 | 3.5 E-06 |

The well was scheduled to shut in regularly for average bottom-hole measurement. Production was started with well on 8 MMSCFD constant flow rate. This rate was maintained for about three months before it stated to drop. **Figure 4.35** shows a plot between *P/Z* and cumulative production. As one can easily see on this graph, if the prediction of OGIP of the reservoir had carried out at the third data point, the prediction of the total of gas in place of the two-layer reservoir could have been underestimated.
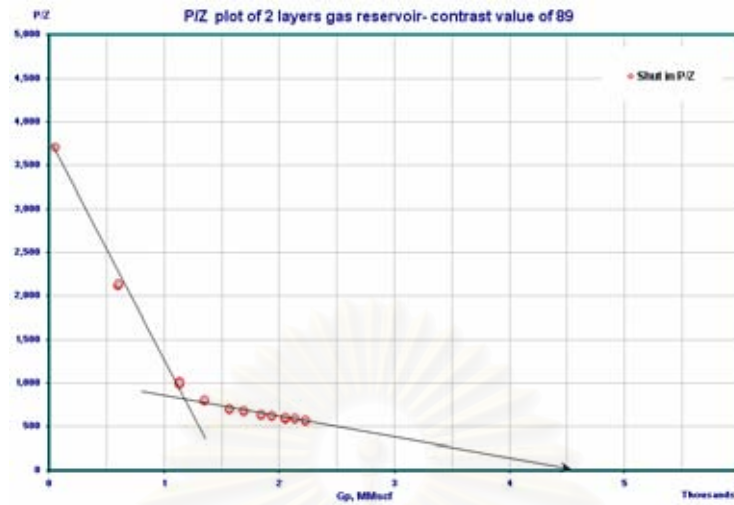
**Figure 4.35**:    P/Z plot – two layers gas reservoir with contrast value of 89.

**Figure 4.36** illustrates the graph between normalized rate and cumulative production of the simulated two-layer reservoir system. The same conclusion can be made when analyze the graph. If estimation of EUR carried out when the first straight line on the normalized rate was established, prediction on ultimate recovery of the reservoirs could well be under estimated (1.15 BSCF).
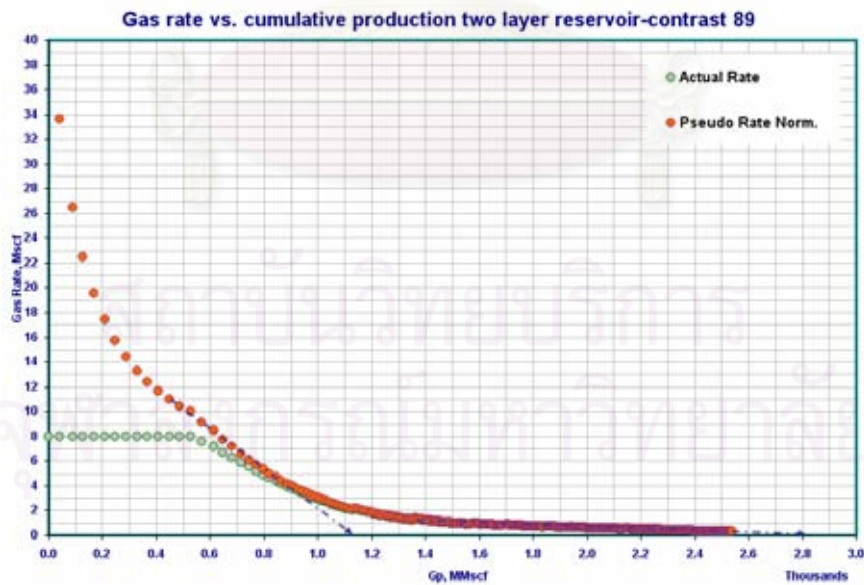


**Figure 4.36**:    Normalized rate vs. cum. prod.-(simulated two-layer gas reservoirs).

**4.2.2 Simulated Two-Layer Oil Reservoirs**

To study application of rate normalization and effect of layer property contrast on commingled oil reservoir, a model with a single well drilled through two layers was built. To examine behavior of the well production, transmissibility of each layer is varied. MBAL prediction run is carried out to generate simulated production data. **Table 4.16** shows reservoir properties of each layer (no water influx).

**Table 4.16**: Reservoir properties of simulated two-layer oil system-low contrast.

| Item | Unit | Layer 1 | Layer 2 |
|---|---|---|---|
| Initial pressure | Psia | 5000 | 4800 |
| BHT | Deg F | 350 | 330 |
| Porosity | Fraction | 0.2 | 0.2 |
| Swc | Fraction | 0.19 | 0.2 |
| OOIP | MMSTB | 10 | 60 |
| Rock compressibility | 1/psi | 3.49998E-6 | 3.49998E-6 |
| Gas specific gravity | sp (Air =1) | 0.8 | 0.8 |
| Condensate gravity | API | 37.5 | 40 |
| Bubble point pressure | psi | 2938 | 2244 |
| Reservoir thickness | ft | 10 | 30 |
| Permeability (*used permeability corr.*) | md | 37.7 | 37.7 |
| Reservoir area | ft$^2$ | 5,000,000 | 10,000,000 |
| Production tubing | in. | 2.875 | 2.875 |
| Mole % $H_2S$ | (%) | 0 | 0 |
| Mole % $CO_2$ | (%) | 10 | 10 |
| Mole % $H_2S$ | (%) | 0 | 0 |

The same method is applied, simulation runs are divided into two cases, one with a small contrast between the two reservoirs and other with a high contrast. **Figure 4.37** presents normalized rate curve on less contrast scenario (contrast value is equal to two in this case). During the simulation run, the flow rate was changed to obtain a set of data similar to field production data. The adjustment of the production

rate was carried out when the reservoir was in pseudo steady state condition. The production is scheduled such that regular shut-ins are performed during the production period in order to measure the average reservoir pressures. Linear regression was performed on the onset data points (data points when reservoir is in pseudo steady state condition) and that yields an equation showed in **Figure 4.37**. MBAL EUR prediction at 10 STBD abandoned rate is 25.08 MMSTB, apply this rate into the linear regression equation gives EUR of 26.64. Compare with MBAL result, normalized rate estimation is different around 6.2%.
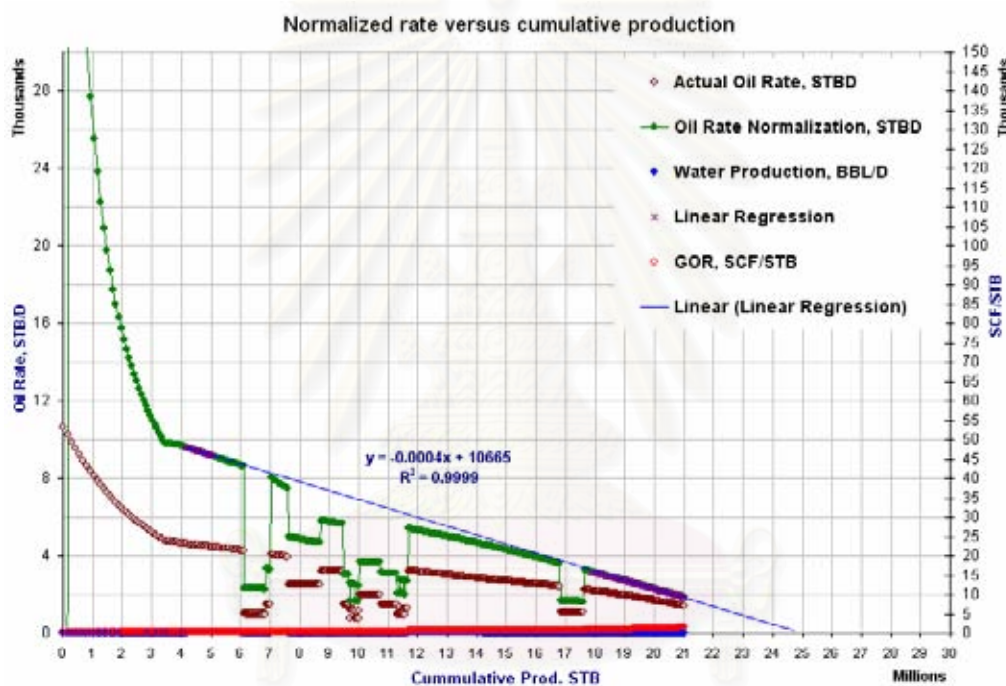


**Figure 4.37**: Rate normalization vs. cum. oil production – (two layer oil system).

**Figure 4.38** shows the plot of production rate versus time on data generated by MBAL. Based on the plot, it is obvious that production of the well was mainly contributed by the high volume and transmissibility layer. This matches very well with the results from cases we studied on two-layer gas reservoirs. The observation means that, reservoir contrast can be used as an indicator to determine contribution of each layer on production of the two-layer system.
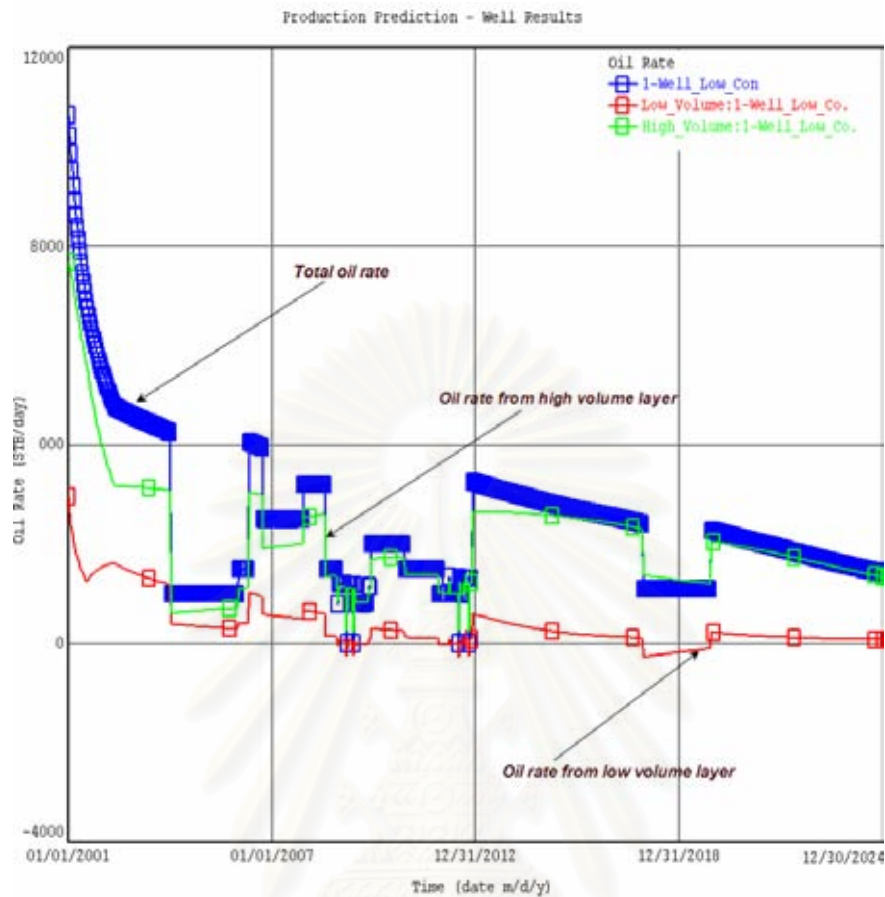
**Figure 4.38**:   Production rate versus production time – (two layer oil system).

The flowing bottom-hole pressures are plotted against cumulative production in **Figure 4.39.** The changes on flow rate during the production of the well can be recognized on the graph. Bottom-hole pressures are high when the well controlled to flow with low rates. **Figure 4.40** shows a plot between pseudo time (days) and *(pi-pwf)/q$_{normalized}$* from which the value of *bpss* (constant in the pseudo steady state equation for liquid flow, as defined by Equation 3.25) can be determined. This value of *bpss* can be used in Equation 3.12 to calculate average reservoir pressure. The start of straight line in **Figure 4.40** indicates reservoirs are in pseudo steady state flowing condition.
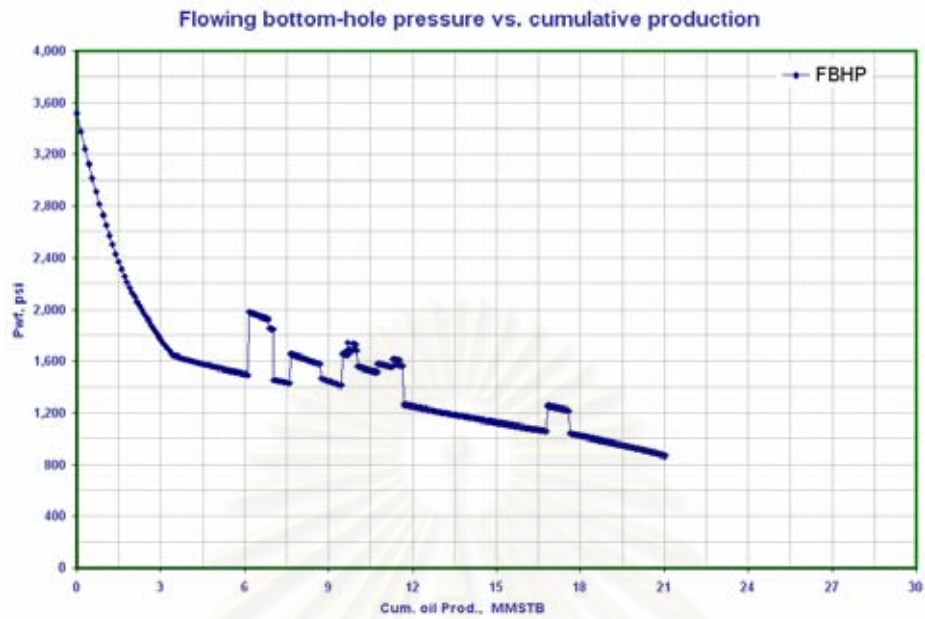
**Figure 4.39**:  Flowing bottom-hole pressure vs. cum. oil prod. (two-layer oil system
with low contrast).
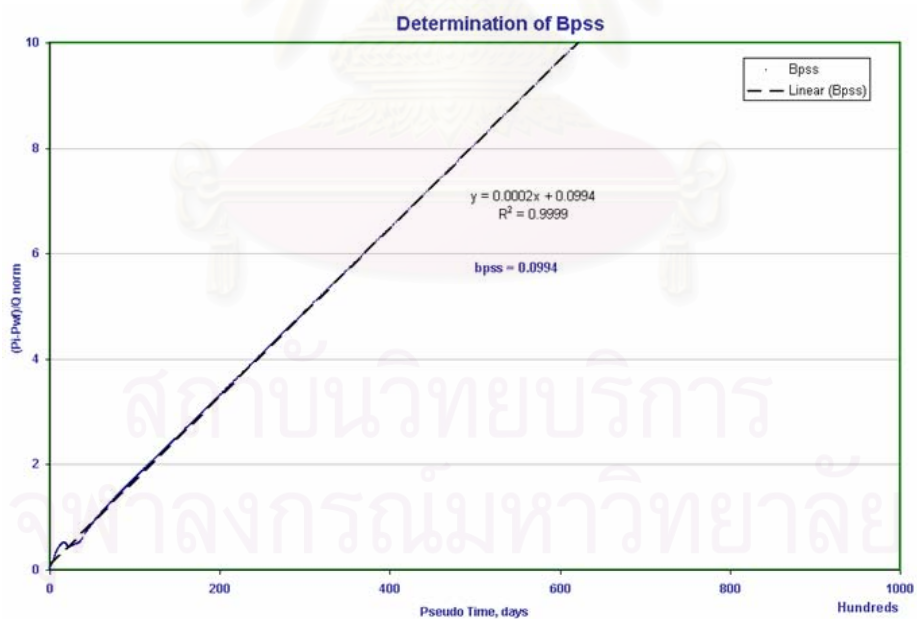


**Figure 4.40:**  Plot to determine *bpss* in a low reservoir contrast case – (two layer oil
system).

Case two is built where the contrast between layers is ninety three. **Table 4.17** illustrates simulated reservoir parameters of the two-layer system.

**Table 4.17**:    Reservoir properties of simulated two-layer oil system-high contrast.

| Item | Unit | Layer 1 | Layer 2 |
|------|------|---------|---------|
| Initial pressure | Psia | 5000 | 4800 |
| BHT | Deg F | 350 | 330 |
| Porosity | Fraction | 0.22 | 0.12 |
| $S_{wc}$ | Fraction | 0.1 | 0.1 |
| OOIP | MMSTB | 10 | 60 |
| Rock compressibility | 1/psi | 3.49998E-6 | 3.49998E-6 |
| Gas specific gravity | sp (Air =1) | 0.8 | 0.8 |
| Condensate gravity | API | 37.5 | 40 |
| Bubble point pressure | psi | 2938 | 2244 |
| Reservoir thickness | ft | 10 | 30 |
| Permeability (*used permeability corr.*) | md | 85.4 | 1.0 |
| Reservoir area | $ft^2$ | 5,000,000 | 10,000,000 |
| Production tubing | in. | 2.875 | 2.875 |
| Mole % $H_2S$ | (%) | 0 | 0 |
| Mole % $CO_2$ | (%) | 10 | 10 |
| Mole % $H_2S$ | (%) | 0 | 0 |

The well was shut in regularly after certain periods of production to determine average reservoir pressure. In this case, the well flows with full reservoir capacities with out any manipulation on surface flow rates.
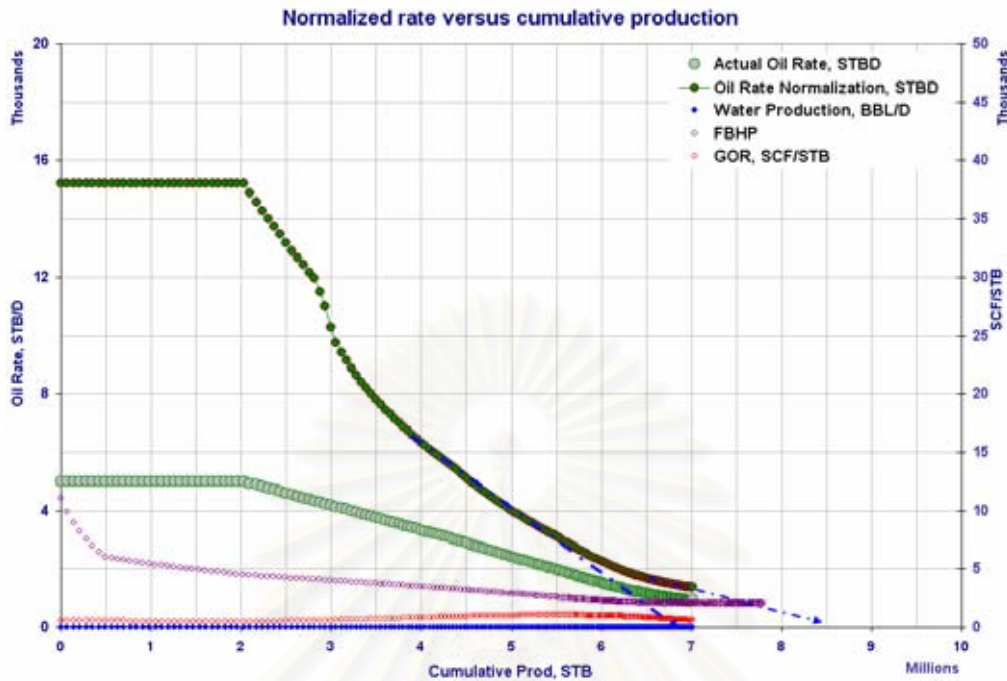
**Figure 4.41**:   Normalized rate plot of the high contrast case (two layer oil system).

**Figure 4.41** shows a plot between normalized rate of the two-layer oil reservoirs and the cumulative oil production. As it appears in **Figure 4.41**, there are two slopes on the graph, the earlier slope is when high flow capacity layer (layer one) is on set or reaching pseudo steady state condition. The later slope is contribution of layer two when its pseudo steady state is established. The same observation can be seen on the *bpss* plot in **Figure 4.42.** According to **Figure 4.41**, if prediction of movable oil in place had carried out on the first single slope straight line, the ultimate recovery of the two-layer reservoir system could have been underestimated. **Figure 4.43** presents a plot between total flow rate, flow rate of individual sand and production time. As one can see from the plot, production rate of the well is mainly contributed by the high flow capacity layer (layer one) in the earlier time of the production. As layer one is depleted, the well production mainly comes from layer two. Its domination becomes obvious when the well production reached 6.5 MMSTB or when production time passed year 2007. Estimation of recoverable oil in place made on the second single slope straight line from **Figure 4.41** yields 8.45 MMSTB. MBAL simulation run, at

the abandonment condition of 10 STBD, gives the total cumulative production of 8.25 MMSTB. The two calculated results considered to be in good agreement.

Based on the above analysis on both gas and oil cases, it is obvious that rate normalization from daily production data can be used as another reservoir tool to estimate ultimate recovery of reservoirs.
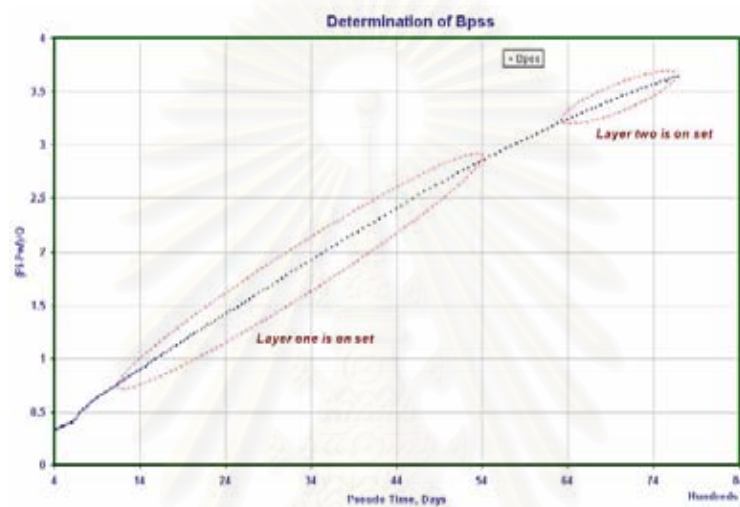


**Figure 4.42**: Plot determining *bpss* in high reservoir contrast (two layer oil system).
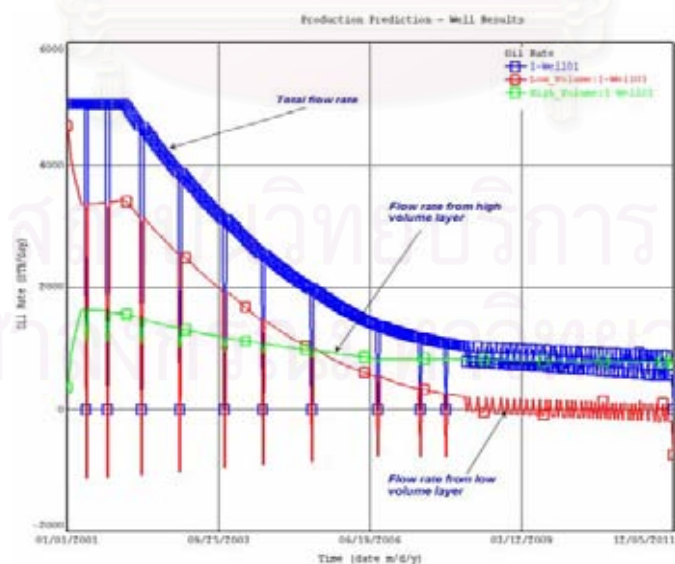


**Figure 4.43:** Oil flow rates versus time (two layer oil system).

The following sections will discuss on application of rate normalization on commingled reservoirs through field examples on both gas and oil wells.

### 4.2.3 Field Data – Commingled Gas Reservoirs

#### Case I – Two layers gas reservoirs

This section shows the application of rate normalization on a gas well where reservoirs are commingly produced. The first case is a well where production is from two sands with similar reservoir characteristics. The well was drilled and completed with a slim-hole design. Completion tubing is 2-7/8 in. diameter with R-nipples at certain depths to give control on well management especially with water production. Sands properties are listed on **Table 4.18**

**Table 4.18**:    Producing Sands properties – field data of two-layer gas system.

| Sands | 63-4 | 64-5 |
|---|---|---|
| Depth MD, ft | 7,930 | 8,060 |
| Depth TVD, ft | 6,343 | 6,453 |
| Porosity, % | 22 | 24 |
| Permeability, md | 519* | 1,987** |
| Sand Thickness MD, ft | 51 | 41 |
| Sand Thickness TVD, ft | 41 | 32 |
| Perforation length, ft | 18 | 10 |
| Reservoir area, acre | 102 | 102 |
| Water Saturation, % | 28 | 38 |

* Permeability derived from BPU, ** Permeability calculated from correlation $k=0.0002e^{67.13*\phi}$
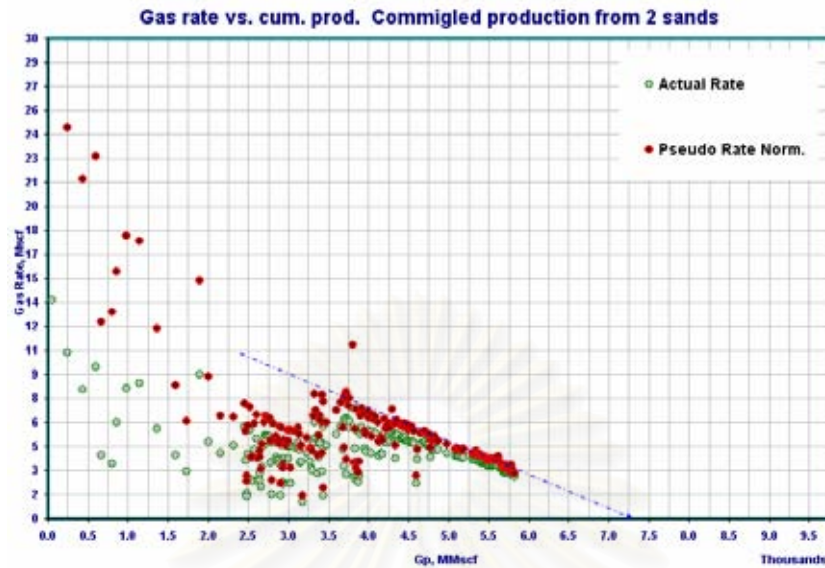
**Figure 4.44**: Normalized rate vs. cumulative production-(two-layer gas reservoirs).

Sand (sand 63-4) was selected to be the first sand to perforate and perform a pressure-build-up (PBU) test. The reservoir was partially opened to wellbore condition with 9 feet of perforation located at the top of the sand on March 2002. The PBU was carried out to determine the reservoir size, characteristics, and initial pressure. Upon completion of the PBU program, perforation was resumed on sand (sand 63-4) with another additional 9 feet right below the first perforation interval. Sand (sand 64-5) was also exposed to wellbore with 10 feet of perforation at the same time. Both reservoirs have been commingly produced since May 2002. During the production period, the well was shut in for bottom-hole pressure measurement. Those pressure points help establish the total gas in place from the two reservoirs. Based on the given information in **Table 4.18**, reservoir contrast of the two layers is three point five. As one can see in **Figure 4.44**, there is a small degree of difference on slopes on the *P/Z* curve. From **Figure 4.44**, estimated ultimate recovery from the two sands is 7.25 BSCF. The linear trend started after the well has produced 3.25 BSCF of gas.
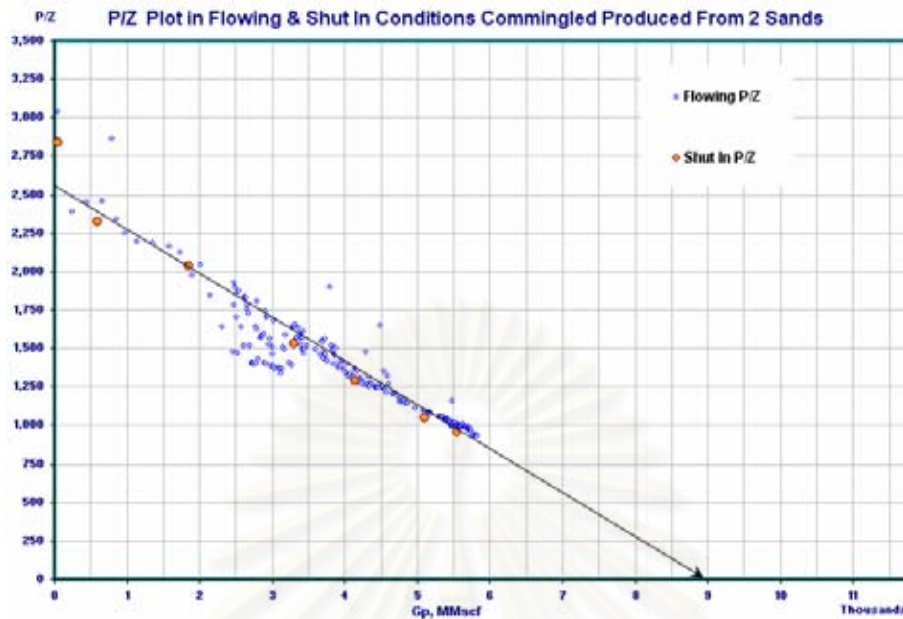
**Figure 4.45**:   P/Z plot of well commingled produced from two-(layer gas reservoirs).

As one can see in **Figure 4.45**, the horizontal intercept gives the total gas in place of the two-sand system. In this case, the intersection yields 9 BSCF original gas in place, placing the recovery efficiency of the well to 80%.

**Case II – Multi layers gas reservoirs**

Now, let us look at the second scenario where more than two sands with various reservoir characteristics contribute to the performance of the well.

The well of interest was drilled and completed in June 1998. A total of twenty three sands were perforated and the well has been produced since August 1999. The sands have various porosities, ranging from 8% to 22%. During the production period, several well surveillance programs were carried out to measure static bottom-hole pressures. The purpose of those pressure surveys is to estimate the original gas in place from all individual reservoirs by utilizing the *P/Z* plot. The well has been flowing via a booster compressor since November 2004 and two more sands were added in November 2005 to increase the production rate.

**Figure 4.46** presents the rate normalization plot of the well. From this plot, one can easily recognize the advantage of the rate normalization graph. It gives an early estimation of the ultimate recovery of the well when compared with the actual gas rate. Without the booster compressor, estimated ultimate recovery of the well is 5.5 BSCF. However, when the well flows via the booster compressor, which lowers the wellhead flowing pressure from 500-700 psi (production system pressure) to 200-300 psi, an additional reserve of 1.6 BSCF is gained.
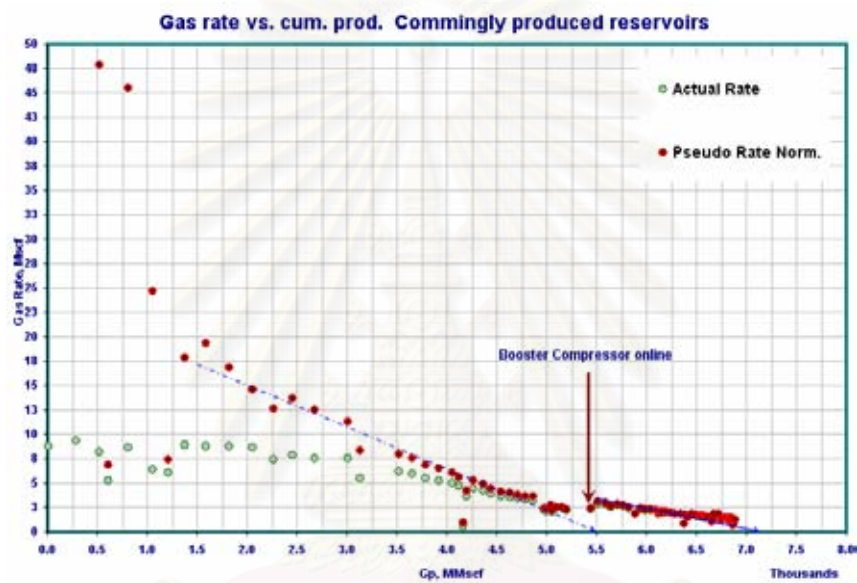


**Figure 4.46**:   Normalized rate vs. cumulative prod. – (multi-layer gas reservoirs).

It appears that there are two slopes on the normalized rate curve in **Figure 4.46**. The first slope is when the multilayer system is in the pseudo steady state condition. The last slope incurred when the booster compressor was introduced to help improve reserve recovery.
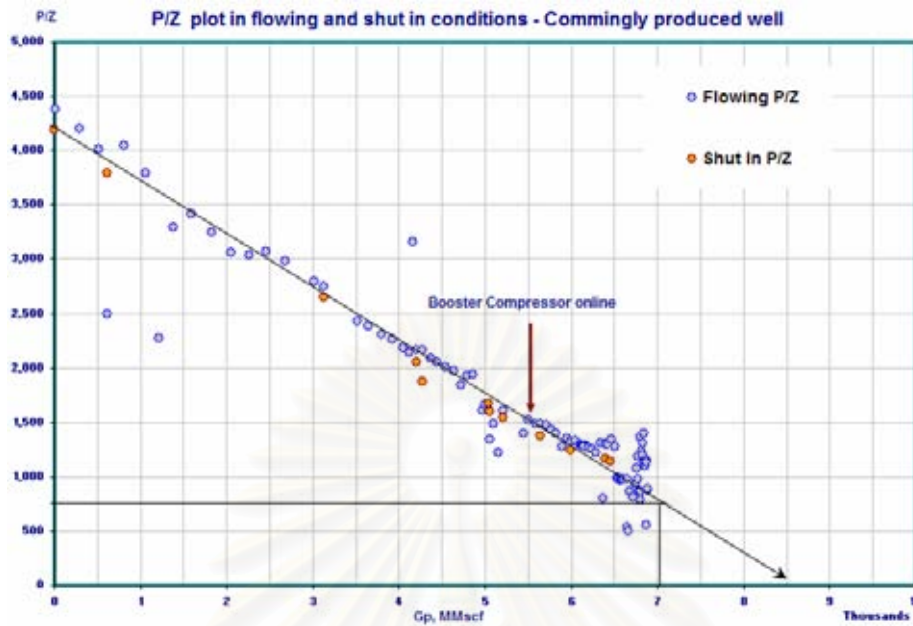
**Figure 4.47**:   P/Z plot of well commingly produced from multi-layer gas reservoirs.

According to **Figure 4.47**, original gas in place of the reservoir is 8.5 BSCF. The booster compressor helps gain an additional $(7.1-5.5)/8.5 = 18\%$ gas production from reservoirs, which improves recovery efficiency from 64.7 % to 83.5%.

### 4.2.3 Field Data– Commingled Oil Reservoirs

This section shows the practicality of the rate normalization method to an oil well where more than one sands are exposed to the wellbore and commingly produced to surface.

**Case I – Two layers oil reservoirs**

First, a well where the production is contributed by two reservoirs is considered. The well of interest was drilled and completed in July 2001 with a mono-bore design. A 2-7/8" in. diameter tubing was used as completion string with optional gas lift mandrels set up to allow artificial lift if needed. The well schematic can be found in Appendix D. The bottom most sand (sand 90-0) and the sand with oil water contact (sand 71-0) were perforated in April and June 2002 respectively. Then, the well was put into production on June 2002, and the production was diverted through a booster

compressor to increase hydrocarbon recovery in January 2004. By November 2004, the well performance was very poor, and it was decided to perforate more oil sands to increase the well productivity. Data collection for the analysis was ceased when the third sand (sand 85-4) was perforated. The following table illustrates reservoir properties of the two sands (sands 90-0 and 70-1).

**Table 4.19**:    Producing sands properties – (field data of two-layer oil reservoirs).

| Sands | 90-0 | 70-1 |
|---|---|---|
| Depth MD, ft | 11,570 | 8,246 |
| Depth TVD, ft | 9,100 | 7,200 |
| Porosity, % | 15 | 17 |
| Permeability, md | 5** | 18** |
| Sand thickness MD, ft | 28 | 81 |
| Sand thickness TVD, ft | 24 | 66 |
| Perforation length, ft | 28 | 26 |
| Oil water contact | | 8,299 |
| Water saturation, % | 46 | 43 |

** Permeability calculated from correlation $k=0.0002e^{67.13*\phi}$

**Figure 4.48** displays normalized rate plotted against the cumulative oil production. According to the graph, the transient period completed when the well production reached 280 MMSTB or after the well had been producing for about one year. The single slope straight line was established and the intersection of this line with the horizontal axis gives an estimated ultimate recovery of the two sands of 490 MSTB of oil.
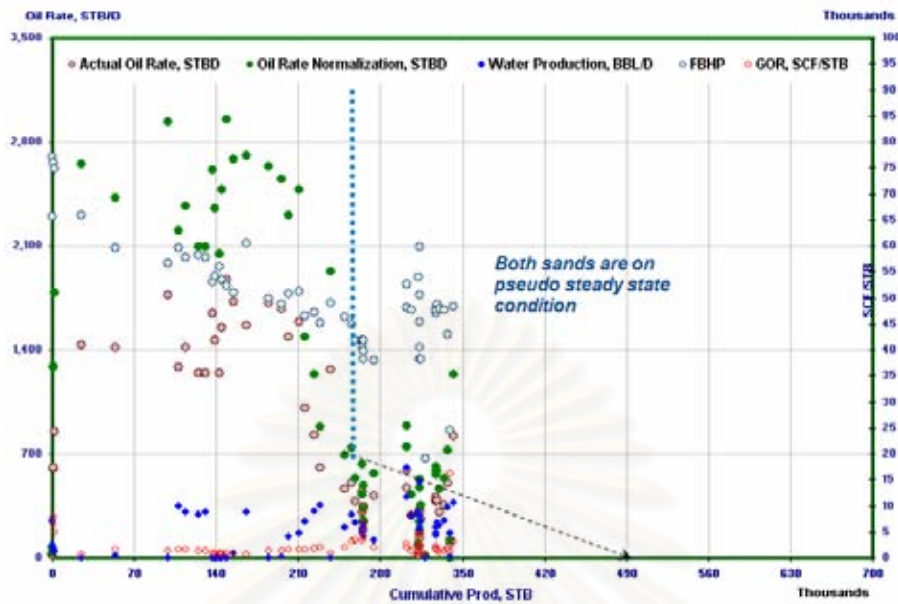
**Figure 4.48**:   Normalized rate vs. cumulative production (field two-layer oil reservoirs).

Production data of the well was also analyzed by using rate transient analysis (RTA) software package from Fekete Associates Inc. to verify the applicability of rate normalization on cases where the production is from multi-layer reservoirs.

**Figure 4.51** to **Figure 4.55** represent analysis results of production data by using various type curve models from Fekete rate transient analysis software package. For consistency with other analyses performed earlier, the abandoned rate of 10 STBD was used on the decline curve and type curves analyses. In the Gulf of Thailand where Chevron is operating, the abandonment pressure of an oil platform (twelve to sixteen wells) and the total oil recovery factor are varied from field to field. For the simplicity of the subsequent decline curves and type curves analyses, we selected Platong field as a reference point for abandonment pressure (1500 psi) and recovery efficiency (10-14 %). The Fetkovich type curve analysis gives the expected ultimate recovery of 559.7 MSTB of oil. On the other hand, Blasingame type curve analysis with recovery factor 10% gives an estimation of EUR of 475.9 MSTB. At 14% recovery efficiency, Blasingame type curve gives the EUR of 666.6 MSTB.

The field production data, representative sand properties and PVT information of the well were used to build a material balance model. The model is a single tank with consideration of water support. Hurst-Van Everdingen-Dake[66] is a selected model for water influx, the water support is radial aquifer system. Tables **4.20** and **4.21** represent tank properties and properties of an aquifer.

**Table 4.20**: Reservoir properties of a tank used in material balance calculation.

| | |
|---|---|
| Temperature, deg F: | 290 |
| Initial pressure, psig: | 3084 |
| Porosity, fraction: | 0.16 |
| $S_w$, fraction: | 0.45 |
| Formation GOR, SCF/STB: | 600 |
| Oil gravity, $^o$ API: | 39.5 |
| Gas gravity (air = 1): | 0.75 |
| Mole percent $CO_2$, % | 10 |
| Mole percent $N_2$, % | 0 |
| Mole percent $H_2S$, % | 0 |
| Reservoir thickness, ft | 90 |
| Reservoir radius, ft | 3000 |
| Outer / inner radius ratio: | 2.592 |
| Rock compressibility, $psi^{-1}$ | 3.876 E-6 |

**Table 4.21**: Water influx input parameter.

| | |
|---|---|
| Aquifer model: | Hurst-van Everdingen-Dake |
| System: | Radial Aquifer |
| Encroachment angle, degrees: | 227.5 |
| Aquifer permeability, md: | 5.17 |

During production time, the well was shut in twice for measuring average reservoir pressure. The first pressure measurement was carried out on 13 August, 2002 and the average reservoir pressure across sand (sand 70-1) was at 2661 psi. The second pressure survey was done on 30 June, 2003 and the average reservoir pressure was at

2494 psi. These two pressure points were incorporated into a regression calculation of the analytical method in the material balance model. The analytical method provides a non-linear regression to assist practitioner in estimating the unknown reservoir and aquifer parameters. The plot show the response of the model plotted against historical data. The result of the regression will then be used to re-plot the model response against the match data. **Figure 4.49** shows a result of the analytical method.
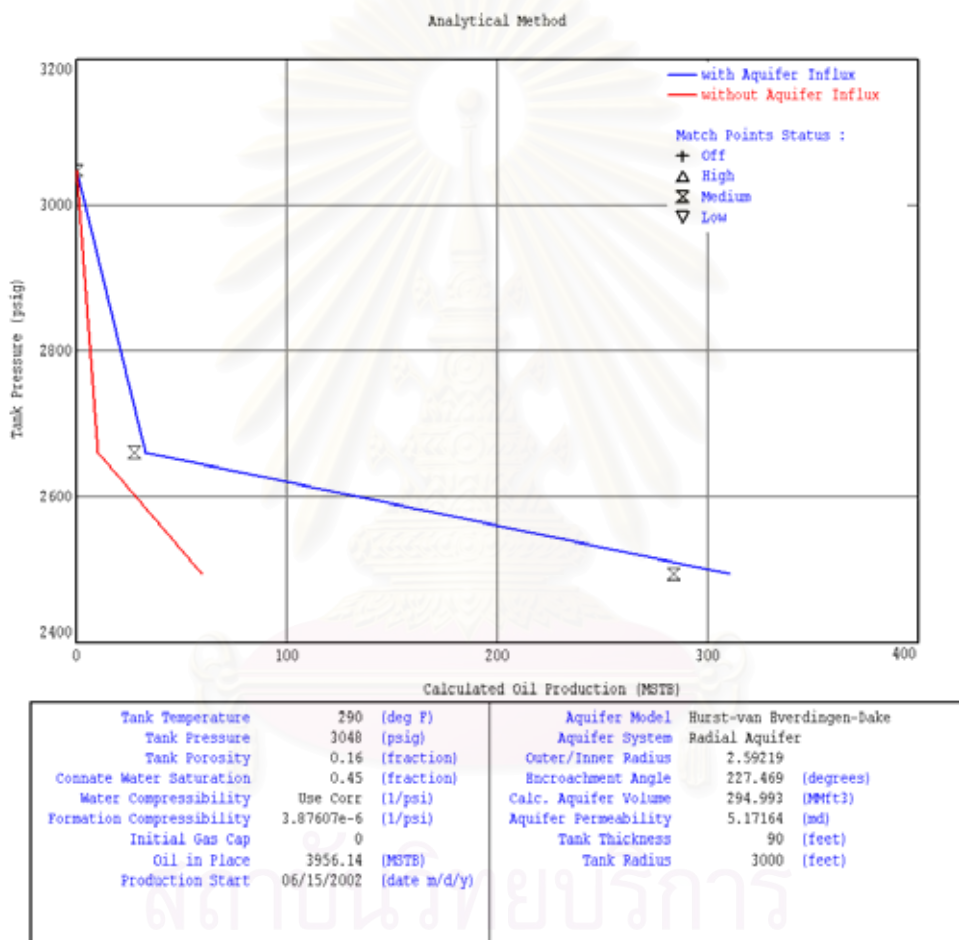


**Figure 4.49**:   Results of the analytical method

Results of the analytical method show that original oil in place of the system is 3956.1 MSTB with a calculated aquifer volume of 294.99 millions cubic feet. With the above original oil in place and using estimated ultimate recovery from the rate normalization technique, recovery efficiency of the well is equal to 12.39%.

**Figure 4.50** presents result of the analysis using graphical method. The graphical method is used to visually determine the different reservoir and aquifer parameters. The aim of most graphical methods is to align all the data points on a straight line. The intersection of this line with one of the axes (and, in some cases the slope of the straight line) gives some information about the hydrocarbons in place. The method that best fits with given data is the *(F-We)/(Eo+Efw) vs Eg/(Eo+Efw)* approach.
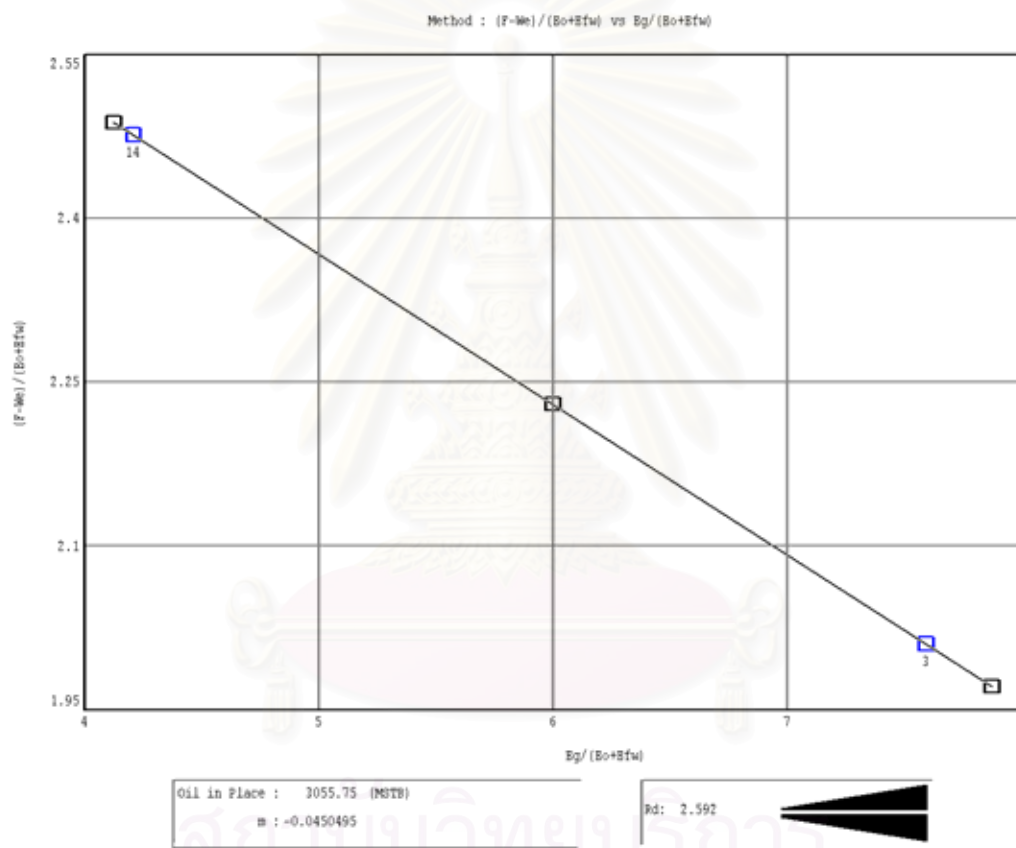


**Figure 4.50**: Graphical method using in material balance calculation.

According to **Figure 4.50**, the straight line connects the two points on the graph yields the original oil in place of the system of 3055.8 MSTB. The recovery efficiency of the well with regard to estimated ultimate recovery from the rate normalization approach stands at 16.04%.

**Table 4.22** presents results of different type curve analyses using Fekete software package with different recovery factors:

**Table 4.22**: OOIP and EUR between Fekete rate transient analysis and normalized rate plot – (field data of two-layer oil reservoirs).

| Estimation Methods | OOIP, MSTB | EUR, MSTB 10% recovery factor | EUR, MSTB 14% recovery factor |
|---|---|---|---|
| Fetkovich (RTA) | 5597 | 559.7 | 783.6 |
| Blasingame (RTA) | 4759 | 476 | 666.3 |
| Agarwal – Gardner (RTA) | 4,568 | 456.8 | 639.5 |
| Flowing Material Balance (RTA) | 6,520 | 652 | 913.6 |
| Normalized Pressure Integral (RTA) | 4574.5 | 457.4 | 640 |
| Rate Normalization  Thesis Model | 3956*/3056** | 490 | 490 |
| Transient Type Curve (RTA) | 4297 | 429.7 | 601 |

* Value derived from material balance calculation using analytical method

** Value derived from material balance calculation using *(F-We)/(Eo+Efw) vs Eg/(Eo+Efw)* approach.

<u>*Note:*</u> If value in column three equals to value in column four, then these values are independent on the estimated ultimate recovery.

As one can see from **Table 4.22**, ultimate recovery estimation using rate normalization method is very comparable with results from other type curve analyses with recovery factor of 10% (except for flowing material balance and Fetkovich type curve).
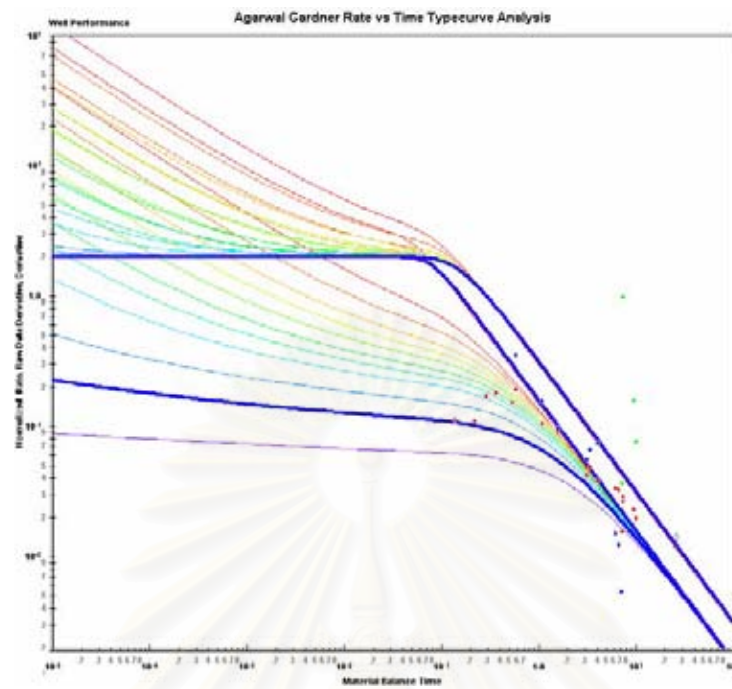
**Figure 4.51**:   Agarwal Gardner rate versus time type curve –(field data of two-layer oil reservoirs).
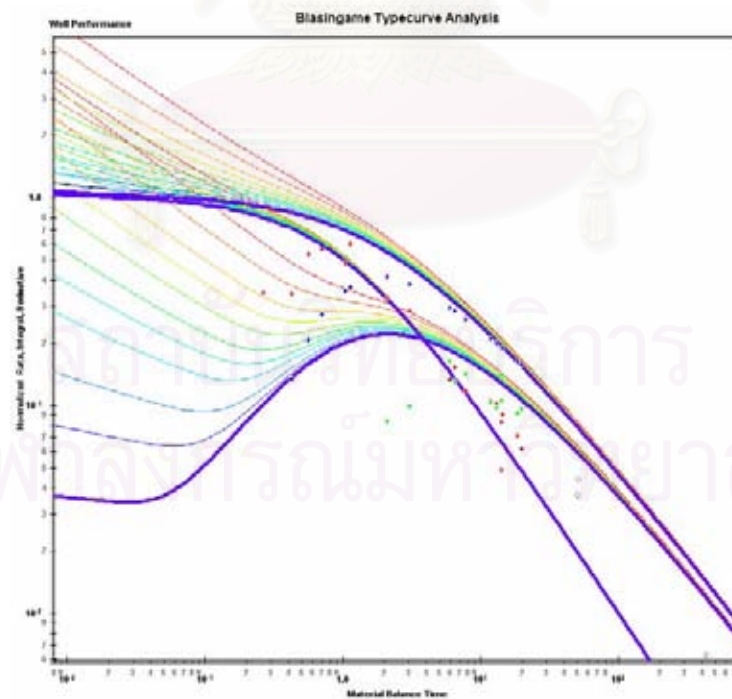


**Figure 4.52**:   Blasingame type curve analysis–(field data of two-layer oil reservoirs).
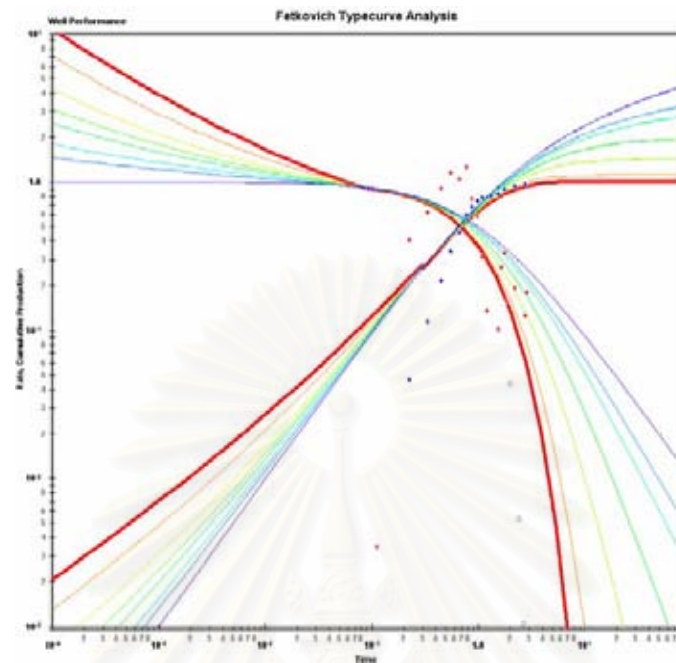
**Figure 4.53**: Fetkovich type curve analysis– (field data of two-layer oil reservoirs).
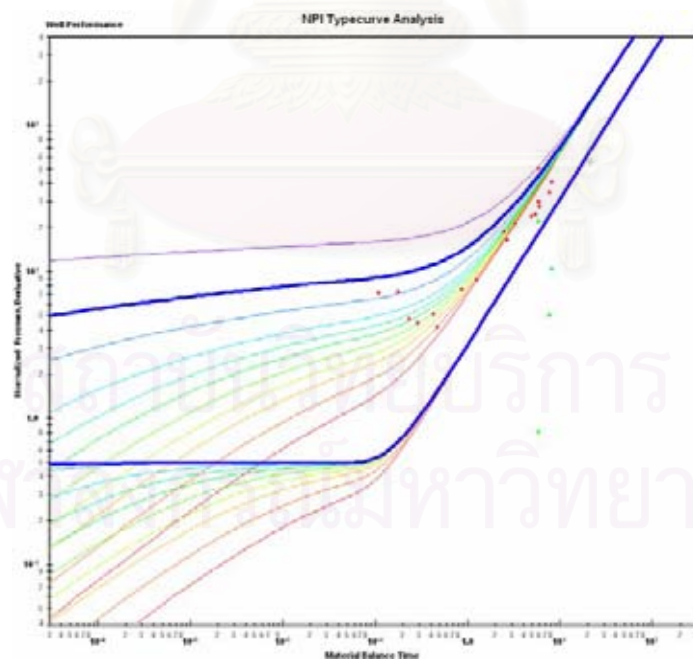


**Figure 4.54**: Normalized pressure integral type curve analysis–(field data of two-layer oil reservoirs).
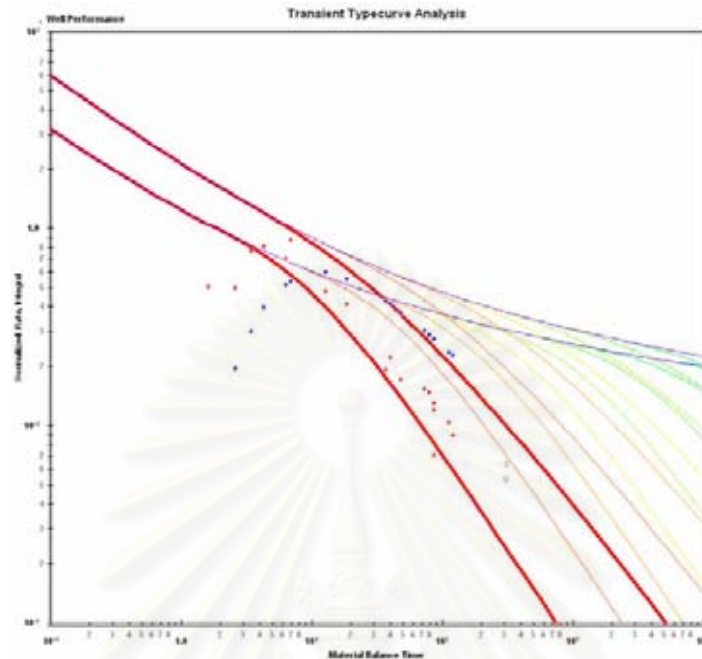
**Figure 4.55**: Transient type curve analysis–(field data of two-layer oil reservoirs).

To further evaluate the rate normalization methodology in determining expected ultimate recovery (EUR) of an oil well, a well with multi-layers of oil sands is selected to perform such analysis.

### Case II – Multi layers oil reservoirs

The well of interest was drilled and completed in Jan 2004. A slim hole 2-7/8" in. diameter tubing completion design with capability to lift gas was selected. Ten sands were perforated and put to production in May 2004. Oil water contact, sands with gas oil contact, and additional zones of interest (AZI) were included in this batch of perforation. The well has been commingly producing since June 2004. The production gas oil ratio is controlled by a down-hole choke, which is set in R-nipple at 8,872 feet. A reservoir surveillance run  using multi phases logging tools in November 2005 identified that the oil water contact sand (sand 48-7) produced a large amount of water with a very little amount of oil and gas and that sand (sand 64-0) produced most of the oil but little gas with evidence of water. The shut-in pass of the

surveillance run recorded 2393 psig the average reservoir pressure from the sand (sand 64-0). A booster compressor has been utilized to help improve recovery efficiency since December 30, 2005. The Water producing sand (sand 48-7) was temporarily patched by a retrievable straddle packer. The well schematic can be found in Appendix D. Recent bottom-hole pressure survey run on 16 July, 2006 showed that average reservoir pressure of the major oil producing sand (sand 64-0) was at 2059 psi. **Figure 4.56** is rate normalization plot of multi-layer reservoirs. As seen in the figure, the water rate started to increase when the cumulative production was at 450 MSTB or after thirteen months of production. The drop off of water rate when the cumulative production reached 550 MSTB was the result of successfully setting a temporary patch across sand (sand 48-7). According to the graph, expected ultimate recovery (EUR) of the well is 1,230 MSTB.
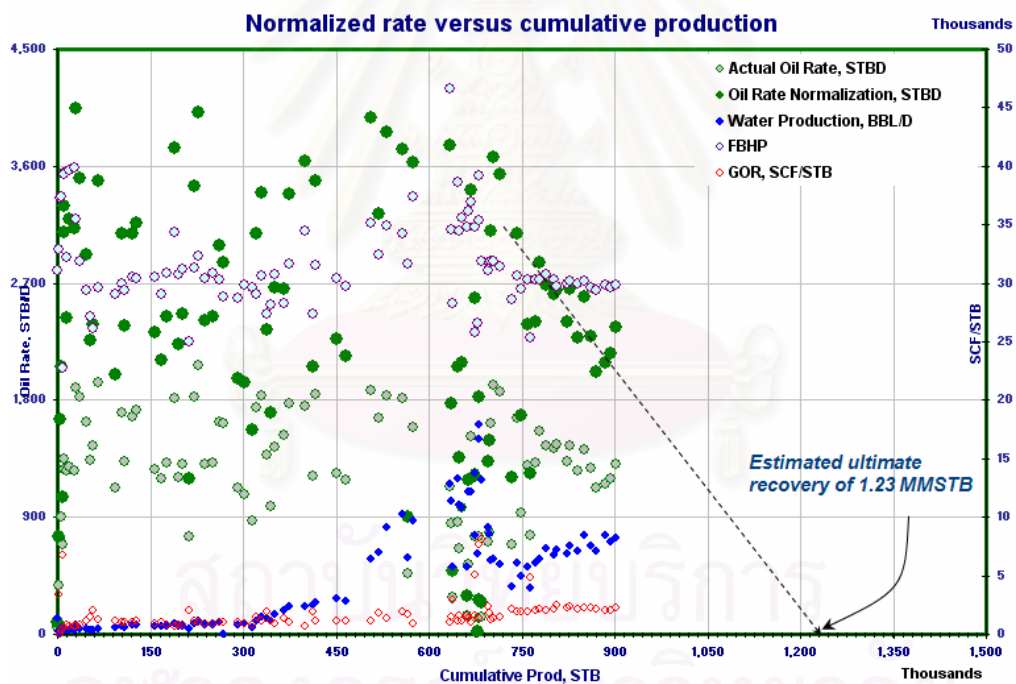


**Figure 4.56**:   Normalized rate vs. cumulative production– (field data of multi-layer oil reservoirs).

Similar to the case of two-layer oil reservoir, a single tank model was built to perform the material balance calculation on field production data and. Reservoir properties and water influx assumed model are shown in **Table 4.23 and Table 4.24** accordingly.

**Table 4.23**: Reservoir properties of a tank used in material balance calculation.

| | |
|---|---|
| Temperature, deg F: | 310 |
| Initial pressure, psig: | 4574 |
| Porosity, fraction: | 0.25 |
| $S_w$, fraction: | 0.43 |
| Formation GOR, scf/STB: | 600 |
| Oil gravity, $^o$ API: | 39.5 |
| Gas gravity (air = 1): | 0.75 |
| Mole percent $CO_2$, % | 10 |
| Mole percent $N_2$, % | 0 |
| Mole percent $H_2S$, % | 0 |
| Reservoir thickness, ft | 238 |
| Reservoir radius, ft | 2785 |
| Outer / inner radius ratio: | 1.242 |
| Rock compressibility, $psi^{-1}$ | 3.26 E-6 |

**Table 4.24**: Water influx input parameter.

| | |
|---|---|
| Aquifer model: | Hurst-van Everdingen-Dake |
| System: | Radial Aquifer |
| Encroachment angle, degrees: | 180 |
| Aquifer permeability, md: | 2.1 |

**Figure 4.57** and **Figure 4.58** show results of material balance calculations performed on analytical and graphical methods. The analytical approach gives estimates of aquifer volume of 66.8 millions cubic feet and the original oil in place (OOIP) of 9495.96 MSTB. Graphical model between *F-We* and *Et* was selected to estimate the original oil in place of the system. The best fit straight line on the graph yields OOIP of 9496.51 MSTB.
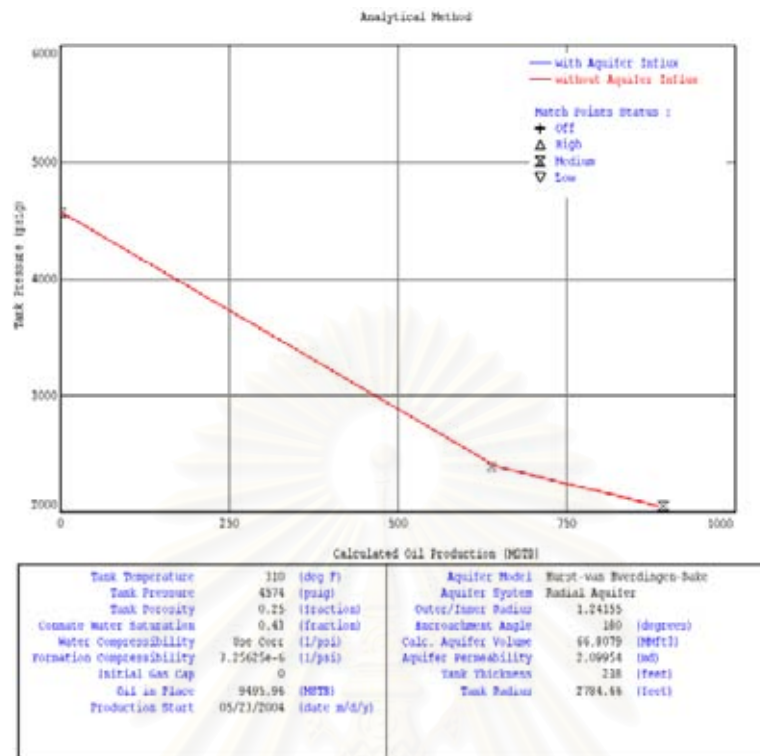
**Figure 4.57**: Results of the analytical method
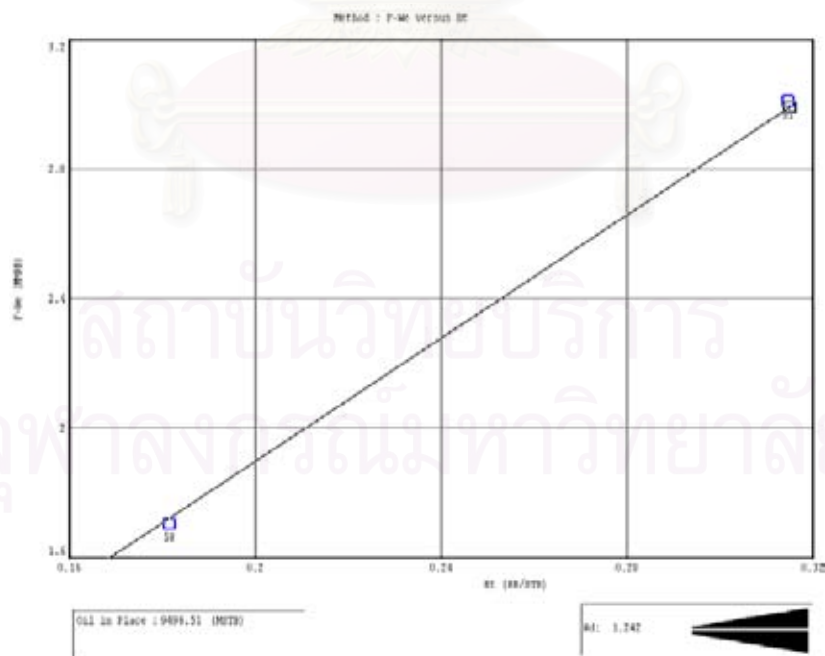


**Figure 4.58**: Graphical method using in material balance calculation.

Recovery factor of the well with EUR derived from the rate normalization technique and OOIPs obtained from the above material balance calculations is 12.95%. This is a typical oil recovery figure on oil wells in the Gulf of Thailand.

**Figures 4.59 to 4.63** show type curve analyses using Fekete software module. The analysis of well production data using rate transient analysis software package was summarized in **Table 4.25.** The abandoned conditions are the same as the case of two-layer reservoir, 10 STBD oil rate and 1500 psi bottom-hole pressure. Recovery factor used in the analysis is in the range of 10 to 14%. According to results shown in **Table 4.25**, Fetkovich type curves and exponential decline curve appear to match very well with normalized rate analysis. Even with higher recovery factor, 14%, other type curve approaches showed big difference from the normalized rate method. This infers that the recovery factor used in type curve analyses need to be adjusted to give a reasonable agreement with the normalized rate technique.

**Table 4.25**:    OOIP and EUR between Fekete rate transient analysis (RTA) and normalized rate plot – (field data of multi-layer oil reservoirs).

| Estimation Methods | OOIP, MSTB | EUR, MSTB 10% recovery factor | EUR, MSTB 14% recovery factor |
|---|---|---|---|
| Fetkovich (RTA) | 10,570 | 1,057.9 | 1,479.8 |
| Blasingame (RTA) | 6,307 | 630.7 | 883 |
| Agarwal – Gardner (RTA) | 5,961.5 | 596.2 | 834.6 |
| Flowing Material Balance (RTA) | 7,703.4 | 770.3 | 1,078.5 |
| Normalized Pressure Integral (RTA) | 5,995.9 | 599.6 | 839.4 |
| Rate Normalization  Thesis Model | 9495.96* 9496.51** | 1,230 | 1,230 |
| Transient Type Curve (RTA) | 4297 | 630.2 | 882.3 |

* Value derived from material balance calculation using analytical method

** Value derived from material balance calculation using *F-We* versus *Et* approach.

*Note:* If value in column three equals to value in column four, then these values are independent on the estimated ultimate recovery.
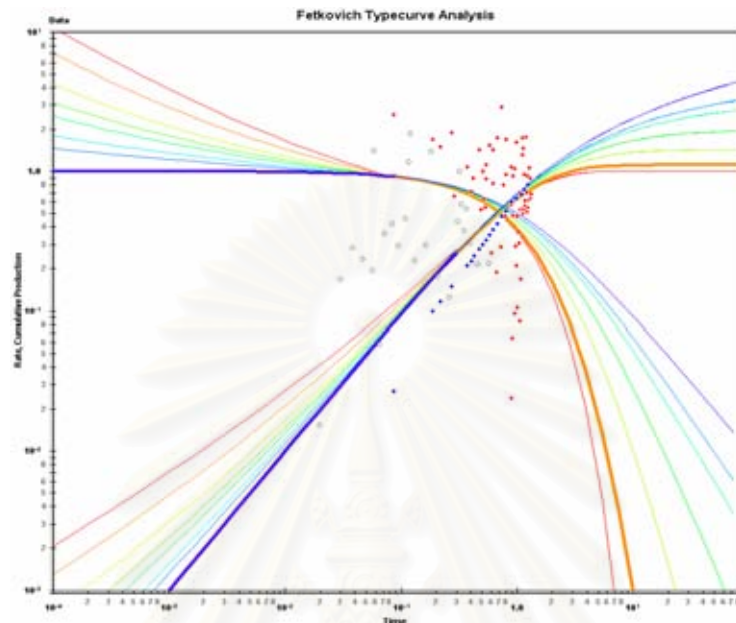


**Figure 4.59**:   Fetkovich type curve analysis– (field data of multi-layer oil reservoirs).
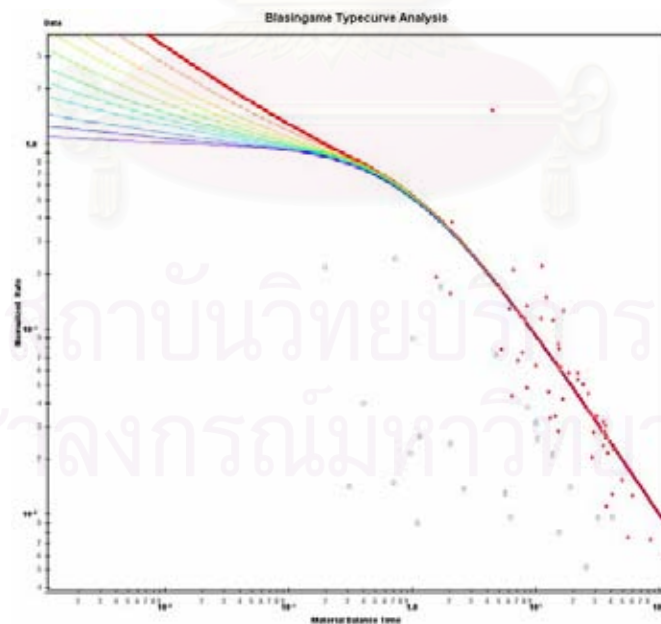


**Figure 4.60**:   Blasingame type curve analysis– (field data of multi-layer oil reservoirs).
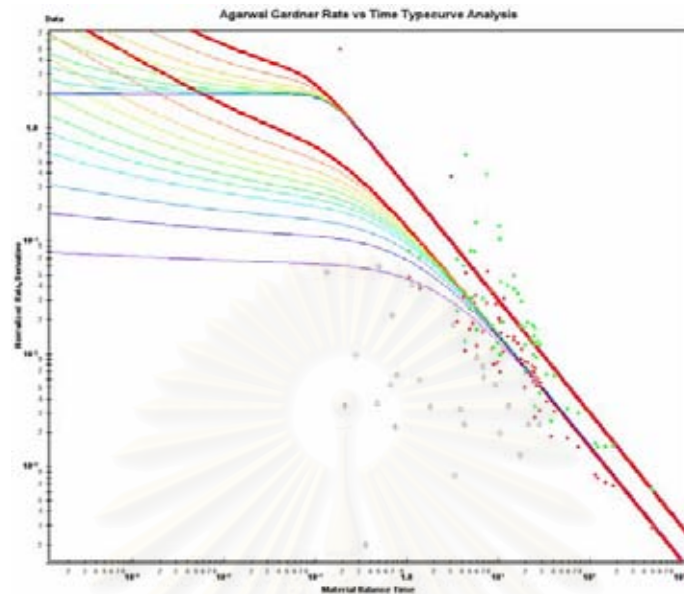
**Figure 4.61**: Agarwal Gardner rate versus time type curve –(field data of multi-layer oil reservoirs).
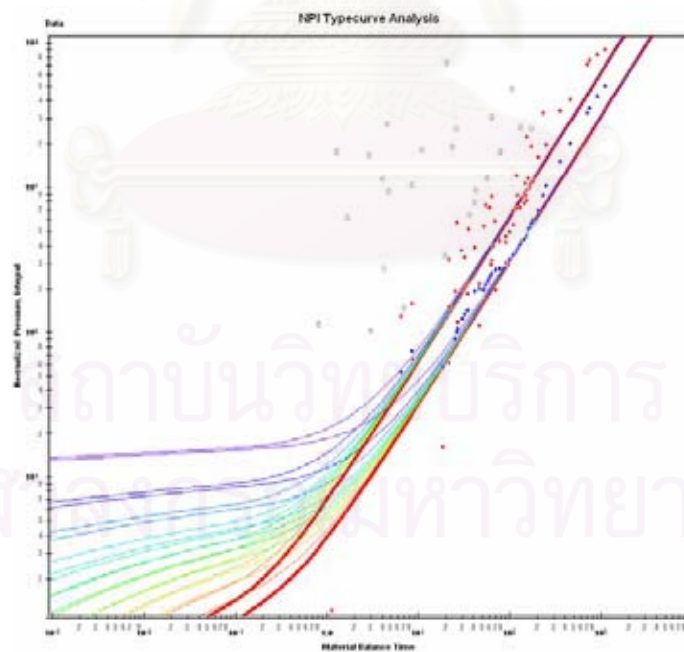


**Figure 4.62**: Normalized pressure integral type curve analysis–(field data of multi-layer oil reservoirs).
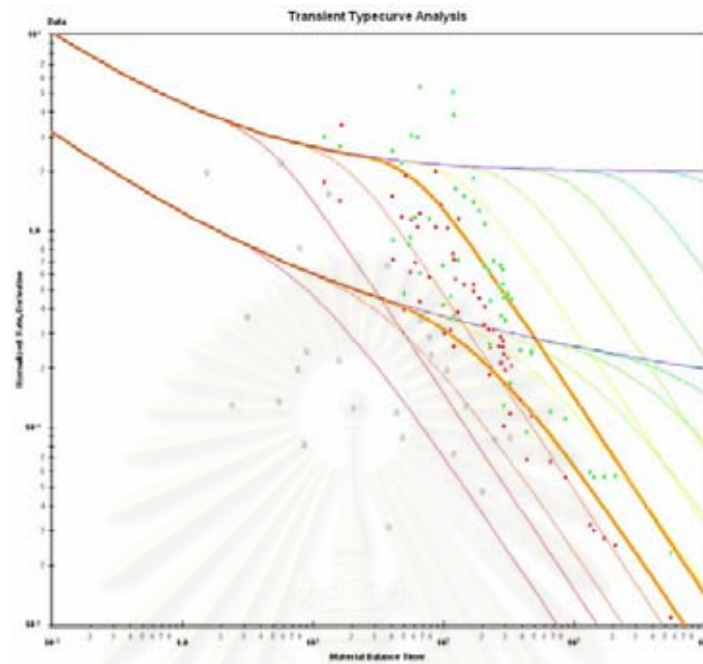
**Figure 4.63**:   Transient type curve analysis–(field data of multi-layer oil reservoirs).

The above two cases illustrate that rate normalization has an application in predicting the amount of oil that can be produced from reservoirs where more than one sands are commingled produced through the same tubing string.

# CHAPTER 5

# SUMMARY, CONCLUSIONS

# AND RECOMMENDATIONS FOR FUTURE WORK

## 5.1 Summary

In this study, we have reviewed pressure responses of a closed boundary system where production comes from either single layer or two-layer reservoirs. First of all, we have investigated applicability to estimate ultimate oil recovery of rate normalization solution developed by Vo. D. T[35] for a single-layer oil reservoir. Then, the study further examined on two-layer reservoir system with different contrasts between layers. Input for rate normalization techniques is surface production data such as cumulative production, flowing tubing pressure, temperature and oil and gas compositions. The bottom-hole pressure is estimated by using Cullender and Smith algorithm for a gas well and a multi-phase flow correlation for an oil well. The Expected Ultimate Recovery of a well is derived when plotting rate normalization against cumulative production. Series of cases with different contrast properties between reservoirs were analyzed to understand affluent of reservoir parameters to the contribution of individual sand to production of a well. Several simulation runs were performed on production data from both oil and gas wells covering both single and multiple layers to validate the practicality and applicability of rate normalization. The results obtained from rate normalization technique were compared with results from other type curve analysis from Fekete Association, Inc. commercial software package to confirm the capability and efficiency of rate normalization solution.

## 5.2 Conclusions

From the application examples, the following conclusions can be made:

1.  Rate normalization method is an approximate estimate of the de-convolution technique. The technique is simple and practical to support large amount of commingled producing wells in the Gulf of Thailand. It is also useful as a diagnostic tool to identify well problem for improvement.

2.  Rate normalization method can be used as another additional reservoir engineering tool to give an estimation on expected ultimate recovery of not only gas wells but also oil wells. Small water influx or water drive mechanism can be tolerated in the oil case. Its applicability is not only suitable to single layer oil and gas reservoir, but also extended to two-layer and multi layer system, where sands are commingly produced from the same tubing string. However, the rate normalization itself is not sufficient to validate the estimated recovery. This needs to be coupled with material balance approach to validate the estimated results for both recovery estimate and efficiency.

3.  From reservoir-contrast study, it is obvious that, in the situation where the property contrast between reservoirs in a two-layer system is high, production will first mainly come from layer with high transmissibility ($kh$), this is normally taken place during the first few months or few years of production, depending on size and characteristic of high transmissibility reservoir. Low transmissibility layer will take control of well production when the other reservoir within the two-layer system depletes. For certain range of property contrast, this can be easily seen by a distinctive two-slope from a plot of bottom-hole pressure or $P/Z$ (for a gas well) versus cumulative hydrocarbon production. Having a good understanding of the two-slope characteristics will help obtain a more accurate estimate on reserve recovery from wells producing commingling.

4.  When a well production is established in pseudo steady state condition, a single slope line will develop on rate normalization graph. If the condition of the wellbore is changed, for example, adding more perforation to the well, putting the well through booster compressor, setting plug inside the tubing to provide temporary or permanent isolation or straddling tubing

patch to shut off water producing zone, a second straight line with a different slope from the first line will be established as the whole system re-establishing a new pseudo steady state condition due to either bottom-hole flowing condition and or volumes have changed. The Estimated Ultimate Recovery of the well will be derived from intersection of the second straight line with horizontal axis – cumulative production. Pseudo steady state condition can also be identified from the $b_{pss}$ plot by a single slope line.

5. Using rate normalization method coupling with flowing material balance to analyze and interpret production data is relatively straightforward and can provide excellent estimates of reservoir movable volume without the associated cost of data acquisition or loss of production.

6. Rate normalization also serves as one of reservoir management tools with regard to early detection of poor reservoir or well performance, normally associated with increased in water production. Abnormal data points which are deviated from a straight line on a rate normalization plot triggers deployment of additional reservoir surveillance tools such as downhole fluid gradient or production logs. Better pictures of individual sand production will be known, and subsequent optimization work can be carried out to improve well productivity and maximize reservoir performance.

## 5.3 Recommendations for Future Work

We believe that investigation of the following topics will assist in the development the proposed approach into a reliable and robust tool for use in production data analysis, and for monitoring and managing the performance of oil and gas reservoirs:

1. Integration with Decline Type Curve Analysis: In the study, we have used Rate Transient Analysis software module from Fekete Associate, Inc. to

validate results from rate normalization plot. Having in the Arps empirical rate decline functions or the Fetkovich McCray type curves added on to the rate normalization spreadsheet would be very useful.

2. Single application for both oil and gas well: Excel is selected to be the main domain to build rate normalization application for both oil and gas wells. Application for both oil and gas wells on a more robust computer language program with a single data base is recommended to improve computational time and capture well information in one single source.

# REFERENCES

[1.]    Aprs, J.J., Analysis of Decline Curves, *Trans*. AIME (1945) 160, 228-274.

[2.]    Agbi, B. and Ng, M.C, A Numerical Solution to Two Parameter Representation of Production Decline Curve Analysis, SPE 16505, resented at SPE Petroleum Industry Applications of Microcomputers, Montgomery, Texas, June 23-26, 1987.

[3.]    Camacho, V. and Raghavan, R., Boundary Dominated Flow in Solution Gas Drive reservoir, SPERE (November 1989), 503-512.

[4.]    Fetkovich, M. J., Decline Curve Analysis Using Type Curves, JPT (June 1980) 1065-1077.

[5.]    Fetkovich , M. J., The Isochronal Testing of Oil Wells, SPE 4529, presented at the SPE 48th Annual Fall Meeting, Las Vegas, September 30-October 3, 1973.

[6.]    Fetkovich, M. J., A Simple Approach to Water Influx Calculations-Finite Aquifer System, JPT (July 1971) 814-823.

[7.]    Da Prat, G Cinco-Ley, H., and Ramey, H.J. Jr., Decline Curve Analysis Using Type Curve for Two Porosity System, SPEJ (June 1981), 354-362.

[8.]    Ehilg-Economides, C.A. and Ramey, H.J. Jr., Transient Rate Decline Analysis for well Produce at Constant Pressure, SPEJ (February 1981), 94-104.

[9.]    Lefkovits, H.C and Matthrews C.S., Application of Decline Curve to Gravity Drainage Reservoirs in the Stripper Stage, *Trans*., AIME 213 (1958) 275-280.

[10.] Fetkovich, M.D., Guerrero, E.D., Fetkovich, M.J., and Thomas, L.K., Oil and Gas Relative Permeability Determined from Rate-Time Performance Data, SPE 15431, presented at the 61th SPE Annual Technical Conference and Exhibition, New Orleans, LA, USA, October 5-8, 1986.

[11.] El-Banbi, Ahmed H. and Wattenbager, Robert A., Analysis of Commingled Tight Gas Reservoirs, Paper SPE 36736 presented at the 1996 SPE Annual Technical Conference and Exhibition, Denver, CO. 6-9 Oct., 1996.

[12.] El-Banbi, Ahmed H. and Wattenbager, Robert A., Analysis of Commingled Gas Reservoirs with variable bottom-hole flowing pressure and non-Darcy flow, Paper SPE 38866 presented at the 1997 SPE Annual Technical Conference and Exhibition, San Antonio, Texas. 5-8 Oct..

[13.] Jorge A. Arevalo-Villagran, Wattenbager, Robert A, El-Banbi, Ahmed H., Production Analysis of Commingled Gas Reservoirs – Case Histories Paper SPE 58958 presented at the 2000 SPE International Petroleum Conference and Exhibition, Villahermosa, Mexico, 1-3 February, 2000.

[14.] Amanat U. Chaudhry, Oil Well Testing Handbook, – Advanced TWPSOM Petroleum System, Inc. Houston Texas. 505-510.

[15.] Russell, D. G., Goodrich, J. H., Perry, G. E., and Brushkotter, J. F., Methods for predicting Gas Well Performance, /. *Petroleum Technol. J*an. 1966), 99-108.

[16.] Cobb, W. M., Ramey, H. J., Jr., and Miller, F. G., Well Test Analysis for Wells Producing Commingled Zones, J. Petroleum Technol. (Jan. 1972), 27-37: Trans AIME 253.

[17.] Al-Hussainy, R., Ramey, H. Jr., and Crawford, P. B., <u>The Flow of Real Gas Through Porous Media</u>, JPT (May 1966) 624-636.

[18.] Agawal, R. B., <u>Real Gas Pseudo-time, A New Fuction for Pressure Buildup Analysis of MHF Gas Well</u>, paper SPE 10325 presented at the 1979 SPE Annual Technical conference and exhibition, Las Vegas, Sept. 23-26.

[19.] Fraim, M. L. Wattenbarger, R. A., <u>Gas Reservoir Decline Curve Analysis Using Type Curve with Real Gas Pressure and Normalized Time</u>, SPEFE (Dec. 1987) 671-682

[20.] Ding, W., Mustafa, O. and Reynolds, A. C., <u>Analysis of Gas Well Late-Time Pressure Rate Data</u>, JPSE 4 (1990) 293-370.

[21.] Leftkovits, H. C., Hazebroek, P. Allen, E.E., and Matthew, C. S., <u>A study of Behavior of Bounded Reservoir Composed of Stratified Layers</u>, Soc. Per. Eng. J. (March 1961) 43-58, Trans. AIME, 222.

[22.] Tariq, S.M. and Ramey, H.J. Jr., <u>Drawdown Behavior of a Well With Storage and Skin Effect Communicating with Layers of Different Radii and Other Characteristics</u>, paper SPE 7453 presented at the 1978 SPE Annual Fall Technical Conference and Exhibition, Houston, 1-3 October.

[23.] Spath, J.B., Ozkan, E., and Raghavan, R., <u>An Efficient Algorithm for Computation of Well Responses in Commingled Reservoirs</u>, paper CIM/SPE 90-1 presented at the 1990 International Technical Meeting, Calgary, 10-13 June.

[24.] Blasingame, T.A., Johnston, J.L., Lee, W.J., and Raghavan, R., <u>Advances in the Use of Convolution Methods in Well Test Analysis</u>, paper SPE 21826 presented at the 1991 SPE Rocky Mountain Regional Symposium, Denver, CO, 15-17 April.

[25.]   Stehfest, H., <u>Numerical Inversion of Laplace Transforms</u>, *Communications of ACM* (January 1970) 13, No. 1, 47-49.

[26.]   Spath, J.B., <u>Solutions for Vertically Fractured Injection Wells in Heterogeneous Reservoirs</u>, MS Thesis, Texas A&M U., College Station, TX (May 1990).

[27.]   Wolfram, S., <u>The Mathematica Book</u>, fourth edition, Wolfram Research, Inc., Champaign, IL, 1999.

[28.]   Johnston, J.L. and Lee, W.J., <u>Identification of Productive Layers in Low Permeability Gas Wells</u>, paper SPE 21270 presented at the 1990 Eastern Regional Meeting, Columbus, OH, 31 October – 1 November.

[29.]   Edwardson, M.J; Girner, H.M; Parkison, H.R; Williams, C.D; Matthews, C.S, <u>Calculation of Formation Temperature Disturbances Caused by Mud Circulation</u>, paper SPE 124 presented at the 36th Annual Fall Meeting of SPE, Dallas, 8-11 October.

[30.]   Blasingame, T.A; McCray, T.L; Lee, W.J, <u>Decline Curve Analysis for Variable Pressure Drop/Variable Flowrate Systems</u>, paper SPE 21513 presented at the SPE Gas Technology Symposium , 23-24 January, 1991.

[31.]   Palacio, J.C; and Blasingame, T.A., <u>Decline Curve Analysis Using Type Curves Analysis of Gas Well Production Data</u>, paper SPE 25909 presented at the 1993 Joint Rocky Mountain Regional and Low Permeability Reservoirs Symposium, Denver, 26-28 April.

[32.]   Fraim, M.L; Lee, W.J, <u>Determination of Formation Properties From Long-Term Gas Well Production Affected By Non-Darcy Flow</u>, paper SPE 16934 presented at the 1985 Annual Technical Conference and Exhibition, Dallas, 27-30 September.

[33.]    Blasingame, T.A. and Lee, W.J, <u>The Variable-Rate Reservoir Limits Testing</u>, paper SPE 15028 presented at the SPE Permian basin Oil & Gas Recovery Conference, Midland, March 13-14, 1986.

[34.]    Dake, L. P., <u>Fundamental of Reservoir Engineering</u>, Elsevier Scientific Publishing Company, 1978, 145-150.

[35.]    Vo, D. T. – <u>Chevron Thailand Exploration and Production, Ltd (CTEP) Internal Reports, 2002</u>

[36.]    Rajogopal Raghavan U. of Tulsa, <u>Behavior of Well Completed in Multiple Producing Zones</u>, paper SPE 14111 June 1989.

[37.]    Dietz, D. N., <u>Determine of Average Reseroir Pressure From Buildup Survey</u>, JPT (Aug, 1965) 955-959; Trans, AIME, 234.

[38.]    Muskat, M.., <u>Use of Data on the Buildup of Bottom Hole Pressure</u>, Trans, AIME(1973) 123, 44-48.

[39.]    Horner, D. R., <u>Pressure Buildup in Wells, Proc.</u>, Third World Pet. Cong., E.J. Brill (ed), Leiden (1951) II, 502-503.

[40.]    Larsen, L., <u>Wells Producing Commingled Zones with Unequal Initial Pressure and Reservoir Properties</u>, paper SPE 10325, presented at the 1981 SPE Annual Techinical Conference and Exhibition, San Antonio, Oct 5-7.

[41.]    Cullender, M. H. and Smith, R. V., <u>Practical Solutions of Gas-Flow Equations for Wells and Pipelines with Large Temperature Gradients</u>, Trans., AIME, 207 (1956) 281-287.

[42.]    Ikoku, C. U., <u>Natural Gas Production Engineering</u>, John Wiley & Son, New York, (1984).

[43.]   Rate Transient Analysis software package – <u>Fekete Associate Inc</u>.

[44.]   Horner, D. R., <u>Pressure Behavior in a Well Producing From a Number of Different Horizons</u>, Shell Oil Co. Report.

[45.]   Papadopulos, I. S., <u>Nonsteady Flow to Multiaquifer Wells</u>, J. Geophys. Research (1966) 71, No. 20, 4791-4797.

[46.]   Van Everdingen, A.F and Hurst, W, <u>The Application of the Laplace Transformation to Flow Problems in Reservoirs</u>, *Trans.*AIME (1949), 186, 305-324.

[47.]   Agarwal, R.G; Gardner, D.C; Kleinsteiber, S.W. and Fussell, D.D., <u>Analyzing Well Production Data Using Combined Type Curve and Decline Curve Analysis Concepts</u>, paper SPE 57916 presented at the 1998 SPE Annual Technical Conference and Exhibition, New Orleans, 27-30 September.

[48.]   Razasa, M. J and Katz, D. L., <u>Calculation of Static Pressure Gradients in Gas Wells</u>, Trans AIME, 160 (1945) 100.

[49.]   Cragoe, C. S., <u>Thermodynamic Properties of Petroleum Products</u>, Bureau of Standards, U. S. Department of Commerce, (1929), Miscellaneous Publication No. 97, 22.

[50.]   McCain, W. D. Jr., 1973, <u>The Properties of Petroleum Fluids,</u> Publishing Co., Tulsa.

[51.]   Tarek Ahmed. <u>Hydrocarbon Phase Behavior</u>, Contribution in Petroleum Geology & Engineering, Gulf Publishing Company, Houston, Texas, 1989.

[52.]   Sutton, R. P., <u>Compressibility Factor for High-Molecular-Weight Reservoir Gases</u>, Paper SPE 14265, Presented at the 60th Annual Technical

conference and Exhibition of the Society of Petroleum Engineering, Las Vegas, September 22-25, 1985.

[53.]   Wichert, E. and Aziz, K., Calculation of Z's for Sour Gases, Hydrocarbon Processing, Vol. 51, No. 5, 1972, pp. 119-122.

[54.]   Dranchuk, P. M., Purvis, R. A., and Robinson, D. B, Computer Calculation of Natural Gas Compressibility Factor Using the Standing and Katz Correlation, Inst. Of Petroleum Technical Series, N. IP 74-008, 1974.

[55.]   Lee, A. L., Gonzalez, M. H. and Eakin, B. E., The Viscosity of Natural Gases, Journal of Petroleum Technology, August 1966, pp. 977-1000.

[56.]   Standing, M. B. and Katz, D. L., Density of Crude Oils Saturated with Natural Gas, Trans. AIME (1942), Vol. 146, pp 159-165.

[57.]   Vasquez, M. and Beggs, H. D., Correlation for Fluid Physical Properties Prediction, JPT, June 1980, pp. 968-970.

[58.]   J.T.H. Ng and E.O. Egbogah., An Improved Temperature-Viscosity Correlation for Crude Oil Systems, Petroleum Society of CIM 83-34-32, 1983.

[59.]   Beggs, H. D. and Robinson, J. R., Estimating the Viscosity of Crude Oil Systems, JPT September 1975, pp 1140-1141.

[60.]   Baker, O. and Swerdloff, W., Calculations of Surface Tension-3: Calculations of Surface Tension Parachor Values, OGJ, December 5, 1995, Vol. 43, p. 141.

[61.]   Kermit E. Brown, H. Dale Beggs, The Technology of Artificial Lift Methods Volume 1 – Inflow Performance, Multiphase Flow in Pipes, PennWell Books, 1997, pp 113-129.

[62.]   Patterson, <u>Viscosity of Liquid – Correlation.</u>

[63.]   Ramey. H. J. Jr., <u>Wellbore Heat Transmission</u>. *JPT* (April 1962) 14, 427-435.

[64.]   Shiu, K.C. and Beggs, H.D., <u>Predicting Res. Tech</u>. (March 1980) 102, 2.

[65.]   Nikuradse, J., <u>VDI-Forschungsheft</u>, No. 361, 1932, No. 361, 1938, Petr. Eng. 11(6), (1940) 1964.

[66.]   L.P. Dake, <u>Fundamental of Reservoir Engineering</u>, Developments in Petroleum Science.

[67.]   Hagedorn, A.R. and Brown, K.E., <u>Experimental Study of Pressure Gradients Occurring During Continuous Two-Phase Flow in Small-Diameter Vertical Conduits</u>, JPT (April 1965) 475.

[68.]   Osif, T. L., <u>The Effect of Salt, Gas, Temperature, and Pressure on the Compressibility of Water</u>, SPE *Res. Eng.* (Feb. 1988) 3, No. 1, 175 - 181

**APPENDICIES**

# APPENDIX A

## FLUID PROPERTIES

This appendix provides thermodynamic definitions for all PVT properties used in the equations and charts of RP 11S4. For a more comprehensive discussion of PVT properties the reader is referred to the text by McCain[50] or Ahmed[51].

## A.1 Basic Definitions

$T$ = System temperature (F) [C]
$P$ = System pressure (psig) [kPag]

Standard Conditions:

$T_{sc}$ = Standard Temperature (F) [C]
$P_{sc}$ = Standard Pressure (psia) [kPa]
Typically most PVT correlations and all those described in this Appendix assume that Standard Conditions are 14.65 psia and 60 F [15.6 C and 101 kPa]
Use the following formula to convert *SCF* (Standard Cubic Feet) at 14.65 psia and 60 F to *SCF* at any user defined $T_{sc}$ and $P_{sc}$.

$$SCF\ (@T_{sc}\ and\ P_{sc}) = SCF\ (@\ 14.65\ psia\ and\ 60\ F) * Xbase \qquad (A.1.0)$$

where:

$$Xbase = 14.65\ /\ P_{sc} * (T_{sc} + 459.67)\ /\ 51967 \qquad (A.1.1)$$

Atmospheric Pressure Corrections:

For simplicity, the correlations presented in this Appendix use pressure in (psig) and assume that atmospheric pressure is 14.65 psia. If more precise calculations are desired you can correct the input pressure $P$(psig) terms to actual atmospheric pressure $P_{atm}$ as follows:

$$P\ (psig)_{corrected} = P + 14.65 - P_{atm} \qquad (A.1.2)$$

## A.2 Gas Properties

$\gamma_g$ = Gas gravity (air = 1.000)

This is the ratio of the density of a gas sample to the density of pure dry air where both gas and air densities are measured at the same temperature and pressure. (Typically standard conditions)

$T_{pc}$ = Pseudo-critical temperature (R) [K]
$P_{pc}$ = Pseudo-critical pressure (psia) [kPa]

Since it is often difficult to measure the critical properties for mixtures these pseudo-critical properties are calculated either as a mole fraction weighted average of the critical properties for the pure components (see McCain[50]  p. 111) or using a correlation as described by Sutton[52] as given below. Correction factors described by Wichert and Aziz[53] are used to adjust these values for $N_2$, $CO_2$, and $H_2S$ content.

$$T_{pc} = 169.2 + 349.5 * \gamma_g - 74.0 * \gamma_g^2 \qquad (A.2.0)$$

$$P_{pc} = 759.8 - 131.0 * \gamma_g - 3.6 * \gamma_g^2 \qquad (A.2.1)$$

$Z$ = Z-factor also know as real gas deviation factor or super-compressibility.

The $Z$-factor is the ratio of the volume occupied by real gas molecules to the volume these same molecules would occupy if they behaved as an ideal gas. Calculation method is described by Dranchuk[54].
$B_g$ = Gas formation volume factor (bbl/SCF) [$m^3/m^3$]
This value is ratio of the volume occupied by gas molecules at a given temperature and pressure to the volume occupied by these same molecules at standard conditions.

$$B_g = Z*T*Psc/(Z_{sc}*T_{sc}*P) = 0.00502 * Z * (T + 459.67) / (P+14.65) \qquad (A.2.2)$$

Convert to user defined Standard Conditions as using "Xbase" from Equation A.1.1 as follows:

$$B_g \text{ (bbl/SCF@}T_{sc} \text{ and } P_{sc}) = B_g / \text{Xbase} \qquad \text{(A.2.3)}$$

$C_g$ = Gas isothermal compressibility (1/psi) [1/kPa]

This parameter is defined as the fractional change in volume that occurs as pressure changes and temperature is held constant. Note: This value is not the same as the $Z$ factor but is related to $Z$ by the following expression

$$C_g = 1/(P + 14.65) - 1/Z * (\partial Z / \partial P)_T \qquad \text{(A.2.4)}$$

Assuming ideal behavior, a good approximation can be estimated as using the following equation:

$$C_g = 1/(P + 14.65) \qquad \text{(A.2.5)}$$

$\rho_g$ = Gas density (lbm/ft$^3$) [kg/m$^3$]

Calculate gas density using an expression derived from the real gas equation.

$$\rho_g = 28.9625 * \gamma_g * (P + 14.65) / (10.732 * (T+459.67)) \qquad \text{(A.2.6)}$$

$\mu_g$ = Gas viscosity (cp)

Calculate gas viscosity using the correlation developed by Lee, Gonzales, and Eakins[55]

$$\mu_g = (A/B) * EXP(D * \rho_g{}^C ) / 10000. \qquad \text{(A.2.7)}$$

where:

$$A = (9.4 + 0.02 * G * 29.0) * (459.67 + T)^{1.5} \qquad \text{(A.2.8)}$$

$$B = (209.0 + 19.0 * G * 29.0 + (459.67 + T)) \qquad \text{(A.2.9)}$$

$$C = 3.5 + (986.0 / (459.67 + T)) + 0.01 * G * 29.0 \qquad \text{(A.2.10)}$$

$$D = 2.4 - 0.2 * (3.5 + (986.0 / (459.67 + T)) + 0.01 * G * 29.0 \qquad \text{(A.2.11)}$$

## A.3 Oil Properties:

$\gamma_{API}$ = Oil gravity term commonly used in the petroleum industry (API)

$\gamma_o$ = Specific gravity of oil (measured relative to water = 1.000)

This parameter is defined as the ratio of the density of an oil sample to the density of water both at 60 *F* and 14.65 psia [15.6 *C* and 101 kPa]. To convert between *API* gravity and specific gravity use the following conversions:

$$\gamma_o = 141.5 / (131.5 + \gamma_{API}) \qquad (A.3.0)$$

$$\gamma_{API} = (141.5 / \gamma_o) - 131.5 \qquad (A.3.1)$$

$R_s$ = Instantaneous solution gas oil ratio (SCF/STB) [$m^3/m^3$]

This parameter is the volume of gas that evolves from an oil sample as temperature and pressure are changed from a given temperature and pressure to the stock tank. Typically the stock tank is considered to be at standard conditions. Standing's[56] correlation given below can be used to calculate $R_s$ for pressures equal to or be below the oil bubble point. At pressures above the bubble point $R_s$ remains constant.

$$R_s = \gamma_g * (C1 * C2)^{1.2048} \qquad (A.3.2)$$

Where:

$$C1 = (P + 14.65) / 18.2 + 1.4 \qquad (A.3.3)$$

$$C2 = 10.0^{(0.0125 * \gamma_{API} - 0.00091 * T)} \qquad (A.3.4)$$

Convert to user defined Standard Conditions as using "Xbase" from Equation. A.1.1 as follows:

$$R_s (\text{SCF@}T_{sc} \text{ and } P_{sc} / \text{STB}) = R_s * \text{Xbase} \qquad (A.3.5)$$

$P_{bo}$ = Oil bubble point pressure (psig) [kPag]

You can re-arrange Equations A.3.2 and A.3.3 along with "*C2*" from Equation A.3.4 to calculate as follows:

$$P_{bo} = 18.2 * (C1 - 1.4) - 14.65 \qquad (A.3.6)$$

$$C1 = (1/C2) * (R_{sb} / \gamma_g)^{(1 / 1.2048)} \qquad (A.3.7)$$

$C_o$ = Oil isothermal compressibility (1/psi)

Compressibility of oil is defined as the fractional change in volume that occurs as pressure changes and temperature is held constant.

$$C_o = -1/V * (\partial V / \partial P)_T \qquad (A.3.8)$$

It is calculated using the following equation by Vasquez and Beggs[57] that was derived for under-saturated crude oil:

$$C_o = X1 / X2 \qquad (A.3.9)$$

where:

$$X1 = -1433.0 + 5.0 * R_s + 17.2 * T - 1180.0 * \gamma_{sep} + 12.61 * \gamma_{API} \qquad (A.3.10)$$

$$X2 = 100,000.0 * (P + 14.65) \qquad (A.3.11)$$

If separator conditions are unknown use $\gamma_g$ in place of $\gamma_{sep}$. However, Vasquez and Beggs[57] found that gas gravity resulting from a flash separation can change depending on separator temperature and pressure. To correct gas gravity for separator conditions they propose the following correlation.

$$\gamma_{sep} = \gamma_g * (1.0 + 5.912E\text{-}5 * \gamma_{API} * T_{sep} * Log_{10} ((P_{sep} + 14.65) / 114.7) ) \qquad (A.3.12)$$

$T_{sep}$ = Separator temperature (*F*)

$P_{sep}$ = Separator pressure (psig)

NOTE: In some reference books such as McCain[50], the total compressibility of the oil and its associated gas are referred to as "Oil Compressibility". This formulation will give you extremely large values of $C_o$ at pressures below the bubble point compared to those calculated by Equation A.3.9.

$B_o$ = Oil formation volume factor (bbl/STB)

This value is defined as the ratio of the volume occupied by an oil sample and its dissolved gas at a given temperature and pressure, to the volume occupied by the same oil in the stock tank. Typically the stock tank is assumed to be at standard conditions. Standings[55] correlation given below can be used to calculate $B_o$ for pressures below the bubble point.

$$B_o = 0.9759 + 0.00012 * C^{1.2} \qquad \text{(A.3.13)}$$

where:

$$C = R_s * ( \gamma_g / \gamma_o )^{0.5} + 1.25 * T \qquad \text{(A.3.14)}$$

For pressures above the bubble point, $B_o$ decreases with pressure as the liquid phase is compressed. To calculate $B_o$ use the following equation from McCain[50]

$$B_o = B_{ob} * EXP(C_o * ( P_{bo} - P )) \qquad \text{(A.3.15)}$$

where:

$B_{ob}$ = Oil formation volume factor at the bubble point (bbl/STB)

$C_o$ = Oil isothermal compressibility evaluated at $(P_{bo} - P)/2$ (psi)

$P_{bo}$ = Oil bubble point pressure (psig)

$\mu_o$ = Oil viscosity (*cp*)

This term is referred to as the "dynamic viscosity" of the oil and is a measure the oil's resistance to flow. Another term $\nu_o$ called the "kinematic viscosity" is often found in the literature. Both $\mu_o$ and $\nu_o$ are related as follows:

$$\nu_o \text{ (centistokes)} = \mu_o \text{ (cp)} / \text{oil density (g/cc)} \tag{A.3.16}$$

Correlations for viscosity calculations are given below:

The viscosity of the oil at one atmosphere pressure and a given temperature is referred to as the dead oil viscosity $\mu_{od}$ and is calculated using the Ng and Egbogah[58] correlation:

$$\mu_{od} = 10.0^X - 1.0 \tag{A.3.17}$$

where:

$$X = 10.0^{[1.8653 - 0.025086 * \gamma o - 0.5644 * Log10 (T)]} \tag{A.3.18}$$

For gas saturated conditions at or below the bubble point use the correlation by Beggs and Robinson[59].

$$\mu_o = A * \mu_{od}^{\,B} \tag{A.3.19}$$

where:

$$A = 10.715 * (R_s + 100.0)^{-0.515} \tag{A.3.20}$$

$$B = 5.44 * (R_s + 100.0)^{-0.388} \tag{A.3.21}$$

And for under-saturated oil at pressures above the bubble point the Vasquez and Beggs[57] correlation can be used.

$$\mu_o = \mu_{ob} * [(P + 14.65) / (P_{bo} + 14.65)]^X \tag{A.3.22}$$

where:
$\mu_{ob}$ = Oil viscosity at bubble point (cp)
$P_{bo}$ = Bubble point pressure (psig)

$$X = 2.6 * (P + 14.65)^{1.187} * EXP[-11.513 + (-8.98E-5)*( P + 14.65)] \qquad (A.3.23)$$

$\rho_o$ = Oil density (lbm/ft$^3$) [kg/m$^3$]

For gas saturated conditions (i.e. $P$ at or below $P_{bo}$) :

$$\rho_o = ( \gamma_o * 62.37 + G * 0.076079 * R_s / 5.615 ) / B_o \qquad (A.3.24)$$

For under-saturated conditions (i.e. $P > P_{bo}$)

$$\rho_o = \rho_{ob} * EXP( C_o * ( P - P_{bo}) ) \qquad (A.3.25)$$

where:

$\rho_{ob}$ = Oil density at bubble point as calculated from eq. A.3.24)

$C_o$ = Oil isothermal compressibility evaluated at $(P_{bo} - P)/2$ (psi)

$\sigma_o$ = Gas-oil surface tension (dynes/cm)

Calculate gas-oil surface tension using the correlation developed by Baker and Swerdloff.[60]

$$\sigma_o = A - ((T - 68.0) * (A - B) / 32.0 \qquad (A.3.26)$$

where:

$$A = 39.0 - 0.2571 * \gamma_{API} \qquad (A.3.27)$$

$$B = 37.5 - 0.2571 * \gamma_{API} \qquad (A.3.28)$$

Also if $T < 68$ then $\sigma_o = A$ or $T > 100$ then $\sigma_o = B$

## A.4 Water Properties

$R_{sw}$ = Instantaneous solution gas water ratio (SCF/STB) [$m^3/m^3$]

This property is defined as the volume of gas that evolves from a water sample as the temperature and pressure are changed to the stock tank. Typically the stock tank is considered to be at standard conditions. The correlation given by McCain[50](pp. 525-526) can be used to calculate $R_{sw}$.

$$R_{swp} = A + B*(P + 14.65) + C*(P +14.65)^2 \qquad (A.4.0)$$

where:

$R_{swp}$ = Instantaneous solution gas water ratio with no dissolved solids (SCF/STB)

$$A= 8.15839 - 6.12265E\text{-}2*T + 1.91663E\text{-}4*T^2 - 2.1654E\text{-}7*T^3 \qquad (A.4.1)$$

$$B = 1.01021E\text{-}02 - 7.44241E\text{-}5*T + 3.05553E\text{-}7*T^2 -2.94883E\text{-}10*T^3 \qquad (A.4.2)$$

$$C = [-9.02505 + 0.130237*T -8.53425E\text{-}4*T^2 + 2.34122E\text{-}6*T^3 -2.37049E\text{-}9*T^4] * 1.0E\text{-}7$$

. $\qquad (A.4.3)$

To account for salinity use the following correction factor:

$$R_{sw} = R_{swp} * 10.0^X \qquad (A.4.4)$$

where:

$$X = -0.0840655* (0.0001* C_{ppm}) * T^{-0.285854} \qquad (A.4.5)$$

$C_{ppm}$ = Salinity or total dissolved solids (ppm)

Convert to user defined Standard Conditions as using "Xbase" from Equation A.1.1 as follows:

$$R_{sw} \text{ (SCF@T}_{sc} \text{ and P}_{sc} \text{ / STB)} = R_{sw} * Xbase \qquad \text{(A.4.6)}$$

$P_{bw}$ = Water bubble point pressure (psig)

As the pressure on a water sample is decreased under isothermal conditions, the bubble point is defined as the pressure where the first bubble of gas is evolves. For cases where a liquid hydrocarbon phase is in equilibrium with the water phase, both phases will have the same bubble point. In most cases the liquid hydrocarbon phase dominates the system so that

$P_{bw} = P_{bo}$.

$\rho_w$ = Water density (lbm/ft$^3$) [kg/m$^3$]

The following correlation from McCain[50] (p. 525) can be used to calculate the density of brine at standard conditions:

$$\rho_w = 62.368 + 4.38603\text{E-5}* C_{ppm} + 1.60074\text{E-11}*(C_{ppm})^2 \qquad \text{(A.4.7)}$$

$\gamma_w$ = Specific gravity of brine (measured relative to pure water = 1.000)

This parameter is defined as the ratio of the density of a water sample to the density of pure water both at 60F and 14.65psia [15.6 C and 101 kPa].

$C_w$ = Water isothermal compressibility (1/psi)

Compressibility of water is defined as the fractional change in volume that occurs as pressure changes and temperature is held constant.

$$C_w = -1/V * (\partial V / \partial P)_T \qquad \text{(A.4.8)}$$

It is calculated using the following equation by Oisf[68]:

$$C_w = 1.0 / [7.033*(P + 14.65) + 0.5415*C_{sd} - 537.0*T + 403,300] \qquad (A.4.9)$$

where:

$$C_{sd} = \rho_{w1} / 62.368 * C_{ppm} \qquad (A.4.10)$$

$\rho_{w1}$ = Brine density at one atmosphere (14.65 psia) pressure.

$B_w$ = Water formation volume factor (bbl/STB) [m$^3$/m$^3$]

This property is the volume occupied by a brine sample and its dissolved gas at a given temperature and pressure to the volume occupied by the same brine at stock tank conditions. Typically the stock tank is considered to be at standard conditions. At pressures below or equal to $P_{bw}$ the following correlation from McCain[50] can be used:

$$B_w = (1.0 + dV_{WP}) * (1.0 + dV_{WT}) \qquad (A.4.11)$$

where:

$$dV_{WP} = -1.95301E\text{-}9*(P + 14.65)*T - 1.72834E\text{-}13*(P + 14.65)^2 * T$$
$$- 3.58922E\text{-}7*(P + 14.65) - 2.25341E\text{-}10*(P + 14.65)^2 \qquad (A.4.12)$$

$$dV_{WT} = -1.0001E\text{-}9 + 1.33391E\text{-}4*T + 5.50654E\text{-}7*T^2 \qquad (A.4\text{-}13)$$

$\mu_w$ = Water viscosity (cp)

This term is referred to as the "dynamic viscosity" of the brine and is a measure the fluids resistance to flow. The correlation presented by McCain[50] can be used to calculate this term.

$$\mu_w = \mu_{w1} * 0.9994 + 4.0295E\text{-}5*(P+14.65) + 3.1062E\text{-}9*(P+14.65)^2 \qquad (A.4.14)$$

where:

$\mu_{w1}$ = Brine viscosity at atmospheric pressure (cp)

$$\mu_{w1} = A*T^B \qquad (A\text{-}4.15)$$

$$A = 109.574 - 8.40564E\text{-}4* C_{ppm} + 3.13314E\text{-}9* (C_{ppm})^2$$
$$+ 8.72213E\text{-}15*(C_{ppm})^3 \qquad (A\text{-}4.16)$$

$$B = -1.12166 + 2.63951E\text{-}6* C_{ppm} - 6.79461E\text{-}12*(C_{ppm})^2$$
$$- 5.47119E\text{-}17*(C_{ppm})^3 + 1.55586E\text{-}22*(C_{ppm})^4 \qquad (A\text{-}4.17)$$

$\sigma_w$ = Gas-water surface tension (dynes/cm)

Calculate gas-water surface tension using the correlation found in the reference by Beggs.[64]

$$\sigma_w = A - (T - 74.0) * (A - B) / 280.0 \qquad (A\text{-}4.18)$$

where:

$$A = 75.0 - 1.108 * P^{0.349} \qquad (A\text{-}4.19)$$

$$B = 53.0 - 0.1048 * P^{0.637} \qquad (A\text{-}4.20)$$

Also if $T < 74.0$ then T = A or if $T > 100.0$ then $T = B$

# APPENDIX B

# CULLENDER AND SMITH DERIVATION
# AND
# ALGORITHM FOR CALCULATING
# FLOWING BOTTOM-HOLE PRESSURE

## 1- DERIVATION OF CULLENDER AND SMITH EQUATION:

Start with the general form of the energy balance:

$$\frac{144}{\rho_g}dP + \frac{g}{g_c}dz + \frac{fV^2}{2g_c\left(\frac{d}{12}\right)}dL = 0 \qquad (B.1)$$

where:
$d$ = Pipe internal diameter (in)

$\rho_g$ = Gas density (lbm/ft3)

$P$ = Pressure (psia)

$g$ = Gravitational acceleration (32.2 ft/s2)

$g_c$ = Mass-to-force conversion factor (32.2 lb f/lb m)

$f$ = Moody friction factor

$L$ = Pipe length (ft)

$z$ = Elevation (ft)

The gas density can be evaluated by

$$\rho_g = \frac{0.01875\gamma_g p}{TZ} \qquad (B.2)$$

where $p$ (lower case) is the pressure (lbf/ft$^2$). For a real gas in a constant area pipe, the average gas velocity at any point in the flow is

$$V = \frac{q}{A} = \frac{1000Q_{sc}}{86400} \frac{TP_{sc}Z}{T_{sc}PZ_{sc}} \frac{4}{\pi\left(d/12\right)^2} = \frac{4.152x10^{-4}Q_{sc}TZ}{P\left(d/12\right)^2} \tag{B.3}$$

where:     $Q_{sc}$ = Gas flow rate (MSCFD)

$T_{sc}$ = 520 ºR

$P_{sc}$ = 14.65 psia

$Z_{sc}$ = 1.0 (**Z** factor evaluated at $P_{sc}$ and $T_{sc}$ )

Substituting Equations (B.2) and (B.3) into Equation (B.1) yields

$$\frac{53.33TZ}{\gamma}\frac{dP}{P} + \frac{g}{g_c}dz + \frac{f}{2g_c\left(\frac{d}{12}\right)}\left(\frac{4.152x10^{-4}TZQ_{sc}}{P\left(\frac{d}{12}\right)^2}\right)^2 dL = 0 \tag{B.4}$$

Finally, we have the following (note that $dz$ has been replaced with $cos\theta \, dL$ and also assumed that $g = g_c$)

$$\frac{53.33TZ}{\gamma}\frac{dP}{P} + \cos\theta \, dL + \frac{6.67x10^{-4}f}{d^5}\left(\frac{TZ}{P}\right)^2 Q_{sc}^{\ 2}dL = 0 \tag{B.5}$$

Equation (B.5) is the basis for all prediction methods. It can be integrated using a variety of techniques.

For pipes which have diameter less than 4.227 in.

$$f = \frac{4.327x10^{-3}}{d^{0.224}} \tag{B.6}$$

For pipes which have diameter greater than 4.227 in.

$$f = \frac{4.007x10^{-3}}{d^{0.164}} \tag{B.7}$$

Unlike other methods, the Cullender and Smith makes no simplifying assumptions for the variations of temperature and compressibility factor in the wellbore. To achieve accuracy, the wellbore is divided into two or more segments.

Starting with Equation B.5 and separating variables we can write

$$\frac{\dfrac{TZ}{P}}{\cos\theta + \dfrac{6.67x10^{-4}Q_{sc}{}^2 f}{d^5}\left(\dfrac{TZ}{P}\right)^2}\,dP = -\frac{\gamma}{53.33}\,dL \tag{B.8}$$

Rearrange Equation B.6 we get

$$\frac{\dfrac{P}{TZ}}{\left(\dfrac{P}{TZ}\right)^2 \cos\theta + \dfrac{6.67x10^{-4}Q_{sc}{}^2 f}{d^5}}\,dP = -\frac{\gamma}{53.33}\,dL \tag{B.9}$$

Integrate Equation B.7 yields

$$\int_{P_{tf}}^{P_{wf}} \frac{\dfrac{P}{TZ}}{\left(\dfrac{P}{TZ}\right)^2 \cos\theta + \dfrac{6.67x10^{-4}Q_{sc}{}^2 f}{d^5}}\,dP = \int_0^L \frac{\gamma}{53.33}\,dL \tag{B.10}$$

or

$$\int_{P_{tf}}^{P_{wf}} \frac{\dfrac{P}{TZ}}{\left(\dfrac{P}{TZ}\right)^2 \cos\theta + \dfrac{6.67x10^{-4}Q_{sc}{}^2 f}{d^5}}\,dP = \frac{\gamma L}{53.33} \tag{B.11}$$

Assuming a two-step calculation procedure that consider an intermediate value of pressure (at the mid point of the production string), the integral is approximated by

$$\int_{P_{tf}}^{P_{wf}} \frac{\dfrac{P}{TZ}}{\left(\dfrac{P}{TZ}\right)^2 \cos\theta + \dfrac{6.67x10^{-4}Q_{sc}{}^2 f}{d^5}}\,dP \approx \frac{\left(I_{mp}+I_{tf}\right)\left(P_{mp}-P_{tf}\right)}{2} + \frac{\left(I_{wf}+I_{tmp}\right)\left(P_{wf}-P_{mp}\right)}{2} = \frac{\gamma L}{53.33}$$

(B.12)

where I is the integrand defined by

$$I = \frac{\dfrac{P}{TZ}}{\left(\dfrac{P}{TZ}\right)^2 \cos\theta + F^2} \qquad (B.13)$$

$F^2$ is defined as

$$F^2 = \frac{6.67x10^{-4} fQ_{sc}^{\;2}}{d^5} \qquad (B.14)$$

The subscripts mp, *tf* and *wf* indicate midpoint, tubing flowing and wellbore flowing respectively.

Eq. B.12 can be separated into two expressions, one for each half of the flow string. For the upper half

$$\frac{\left(I_{mp} + I_{tf}\right)\left(P_{mp} - P_{tf}\right)}{2} = \frac{\gamma L}{53.33} \qquad (B.15)$$

For the lower half

$$\frac{\left(I_{mp} + I_{wf}\right)\left(P_{wf} - P_{mp}\right)}{2} = \frac{\gamma L}{53.33} \qquad (B.16)$$

Simpson's rule gives

$$\frac{\gamma L}{53.33} = \frac{\left(P_{wf} - P_{tf}\right)}{3}\left(I_{tf} + 4I_{mp} + I_{wf}\right) \qquad (B.17)$$

## 2- CALCULATION PROCEDURE.

The following procedure is recommended for solving Equation B.14

1. Calculate the left hand side of Equation B.15 for the upper half of the flow string..
2. Calculate friction factor as per Equations B.6 or B.7.
3. Calculate $I_{tf}$ from Equation B.13 and wellhead condition.
4. Assume $I_{mp} = I_{tf}$ for the condition at the average well depth or at the mid point of the flow string.
5. Calculate $p_{mp}$ from Equation B.15.

6. Using the value of calculated in step 5 and the average arithmetic average temperature $T_{mp}$ determine value Imp from Equation B.13.

7. Recalculate $p_{mp}$ from Equation B.15 if this calculated value is not in within 1 psi of the $p_{mp}$ calculated in step 5, repeat step 6 and 7 until the above criterions are satisfied.

8. Assume $I_{wf} = I_{mp}$ for the condition at the bottom of the flow string.

9. Repeat step 5 to 7, using Equation B.16 for the lower half of the flow string and obtain a value of bottom hole pressure, $p_{wf}$

10. Apply Simpson's rule as expressed by Equation B.17 to obtain more accurate value of flowing bottom-hole pressure.
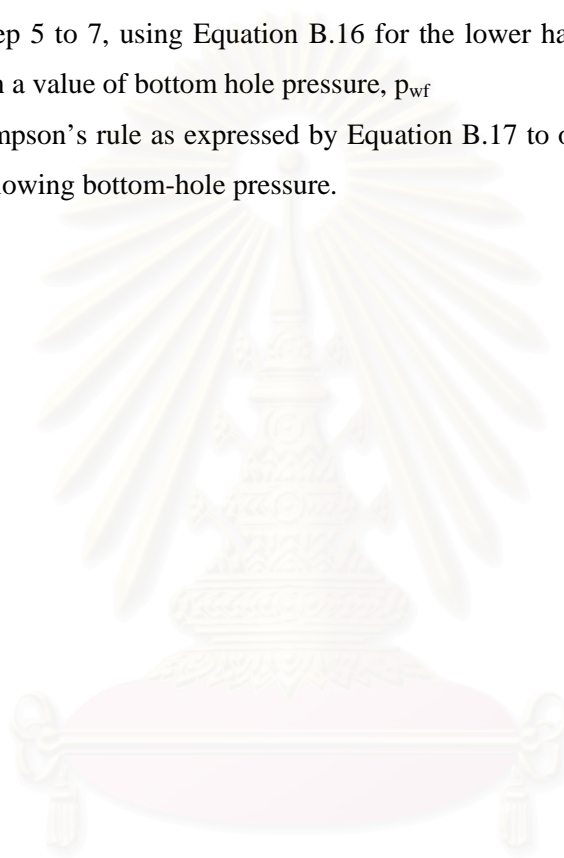
# APPENDIX C

# FLUID FLOW CALCULATIONS

This appendix discusses a few common methods that can be used to predict the pressure drop at a given flow rate in a pipe. Calculations for mixture properties and common terminology used in multiphase flow calculations are also discussed. For more information about specific multiphase flow calculations see references by Hagedorn, Beggs and Duns[67].

## C.1 General

Starting from a point of known pressure ($P_1$), the total pressure gradient, *(dP/dL)* is calculated for an incremental length (*ΔL*) of pipe. The pressure at the opposite end of the pipe ($P_2$) can then be calculated as follows:

$$P_2 = P_1 + (dP/dL) * \Delta L \qquad (C.1.0)$$



$\Delta L$

For this example *dP/dL ≈ (P₂ - P₁) / (ΔL)* and fluid flows from point 2 to point 1. The surface flowline and downhole production tubing can also be broken up into a series of increments and Equation C.1.0 can be solved for each increment in order to determine the pressure gradient and pressure profile of the system. In a typically application the downhole flowing pressure *(P_wf)* is calculated from a known tubing wellhead pressure *(P_wh)*.

Numerous calculation methods are available for determining the pressure gradients in single phase and multiphase flow system. From a fundamental view all the calculation methods are designed to solve the basic pressure gradient equation

given below in Equation C.1.1. This equation shows that the total pressure gradient is the sum of individual gradients for elevation, friction, and acceleration.

$$\frac{dP}{dL} = \left(\frac{dP}{dL}\right)_{el} + \left(\frac{dP}{dL}\right)_f + \left(\frac{dP}{dL}\right)_{acc} \tag{C.1.1}$$

where:

$\dfrac{dP}{dL} =$ Total pressure gradient (psi/ft)

The individual pressure gradient terms of this equation are as follows:

*Pressure gradient due to elevation (psi/ft):*

Typically this term account for 70 to 90% of the total pressure drop.

$$\left(\frac{dP}{dL}\right)_{el} = \frac{g}{g_c} * \rho \sin\theta \tag{C.1.2}$$
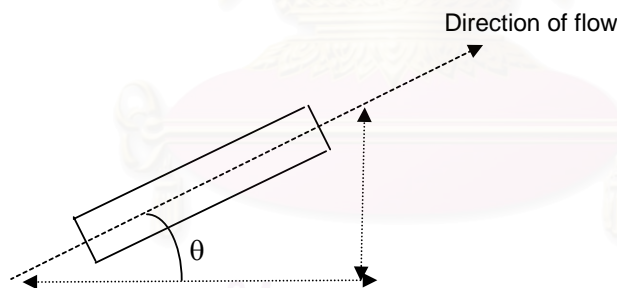


where:

$\rho =$ fluid density (lbm/ft$^3$)

$g =$ gravity acceleration $= 32$ (ft/sec$^2$)

$g_c =$ constant $= 32$ (lbm ft/sec$^2$ / lbf)

$\theta =$ inclination angle from horizontal (deg)

*Pressure gradient due to friction (psi/ft):*

Typically this term accounts for 10 to 30% of the total pressure drop.

Single phase flow

$$\left(\frac{dP}{dL}\right)_f = 2f\rho v^2 / (g_c\, d)$$ (C.1.3)

Where:

$\rho$ = fluid density (lbm/ft$^3$)

$v$ = velocity (ft/sec)

$g_c$ = constant = 32 (lbm ft/sec$^2$ / lbf)

$d$ = diameter of flow area (ft)

$f$ = Fanning friction factor

*Simplified Method for Single Phase Flow*

Calculation of head loss (ft) due to friction per 1000 ft of tubing is made using the Hazen-Williams formula:

$$F = 2.083 * (100 / C)^{1.85} * (q / 34.3)^{1.85} / (D_T)^{4.8655}$$ (C.1.4)

$$\left(\frac{dP}{dL}\right)_f = (F * \gamma_f) / (2.31 \text{ ft/psi} * 1000 \text{ ft})$$ (C.1.5)

where:

$F$ = Head loss due to friction (ft / 1000 ft of tubing)

$C$ = 120 for new tubing and C = 94 for old tubing (> 10yrs.)

q = Flow rate (BPD)

$D_T$ = Tubing ID (in)

$\gamma_f$ = Specific gravity of fluid (measured relative to pure water = 1.000)

*Pressure gradient due to acceleration (psi/ft):*

This term typically accounts for less than 10% of the total pressure drop and is often ignored. At high velocities this term becomes more significant. From reference by Duns and Ros.

$$\left(\frac{dP}{dL}\right)_{acc} = E_k * \left(\frac{dP}{dz}\right) \qquad (C.1.6)$$

$$\frac{dP}{dz} = \frac{\left[\left(\frac{dP}{dL}\right)_{el} + \left(\frac{dP}{dL}\right)_f\right]}{1 - E_k} \qquad (C.1.7)$$

$$E_k = (\rho_s\, \nu_m\, \nu_{sg})\, /\, (144\, g_c\, P) \qquad (C.1.8)$$

where:

$\rho_s$ = Two phase density (lbm /ft$^3$)

$\nu_m$ = Superficial mixture velocity (ft /sec)

$\nu_{sg}$ = Superficial gas velocity (ft /sec)

$g_c$ = constant = 32 (lbm ft/sec$^2$ / lbf)

$P$ = pressure (psi)

### C.2 Mixture Properties

Calculations such as the multiphase flow correlations require us to estimate the physical properties of a fluid mixture (e.g. oil, brine, and gas). This section defines some methods and assumptions that are typically made.

$f_w$ = Water cut (fraction range 0 to 1)

This term is fraction of the liquid phase that is water and can be calculated as:

$$f_w = (\% \text{Water} / 100). \text{ The range of } f_w \text{ is from 0 to 1.} \qquad (C.2.0)$$

$S_g$ = Free gas saturation (fraction range 0 to 1)

$$S_g = \text{Free gas volume / total fluid volume (fraction range 0 to 1)} \qquad (C.2.1)$$

$\gamma_f$ = Specific gravity of fluid (measured relative to pure water = 1.000)

Estimate this term as a weighted average of the oil and water specific gravities. In cases where the fluid is single phase liquid $S_g = 0$.

$$\gamma_f = [\gamma_o * (1.0 - f_w) + \gamma_w * f_w \quad] * (1 - S_g) \qquad (C.2.2)$$

$\mu_f$ = Fluid viscosity (cp)

Estimate this term as a volume weighted average of the oil and water viscosities. This viscosity formula is often used by the multiphase flow correlations.

$$\mu_f = \mu_o * (1.0 - f_w) + \mu_w * f_w \qquad (C.2.3)$$

An alternate method has been proposed by Patterson. This method assumes that at high oil cuts, the pipe will be oil wet; hence the friction calculations need to use oil viscosity rather than the volume average fluid viscosity as given by equation C.2.3. Also, this method assumes that at high water cuts, the pipe is water wet and friction depends on water viscosity.

$$\mu_f = \mu_o \qquad \text{for} \qquad f_w <= f_{inversion} \qquad (C.2.4)$$

$$\mu_f = \mu_w \qquad \text{for} \qquad f_w > f_{inversion} \qquad (C.2.5)$$

Where: $f_{inversion}$ = highest water cut where the pipe remains oil wet. At higher water cuts the system switches to being water wet. The value of $f_{inversion}$ is determined by experiments. Typical values range from 0.4 to 0.78 (i.e. 40% to 78% water)

$SSU$ = Saybolt Seconds Universal viscosity.

Engineering charts, monographs, and formulas use $SSU$ as a correlating parameter.

$$SSU = 2.273 * [\, (\mu_o / \gamma_f) + ((\mu_o / \gamma_f)^2 + 158.4)^{1/2}\,] \qquad (C.2.6)$$

If emulsions are present the value of SSU needs to be corrected as follows:

$$SSU_{Corrected} = SSU * C \qquad (C.2.7)$$

Where:

$$\text{Tight emulsions:} \qquad C = 0.8520 * EXP(\,0.0470 * \%Water) \qquad (C.2.8)$$

$$\text{Medium emulsions:} \qquad C = 0.8762 * EXP(\,0.0428 * \%Water) \qquad (C.2.9)$$

$$\text{Loose emulsions:} \qquad C = 0.8990 * EXP(\,0.0397 * \%Water) \qquad (C.2.10)$$

%Water = Percent water (i.e. %Water $= f_w * 100\%$)

(NOTE: Correlation is valid for %Water ranging from 2.5% to 60.0%. For %Water below 2.5% use C = 1.0)

### C.3 Multiphase Flow Terminology

This section defines some of the common terms used in the most multiphase flow calculations. Note: Individual multiphase flow calculation methods often define their own set of terms.

$$H_L = \text{Liquid hold-up} = (\text{Volume of liquid in pipe}) / (\text{Volume of pipe}) \qquad (C.3.0)$$

$$H_G = \text{Gas hold-up} = 1 - H_L \qquad (C.3.1)$$

$q_g$ = In-situ gas volumetric flow rate ( $ft^3$ / day)
$q_L$ = In-situ liquid (oil + water) volumetric flow rate ( $ft^3$ / day)
$A_{XS}$ = Cross sectional area for flow ($ft^2$)

$$\lambda_L = \text{No-slip liquid hold-up} = q_L / ( q_L + q_g ) \qquad (C.3.2)$$

$$\lambda_g = \text{No-slip gas hold-up} = 1 - \lambda_L \qquad (C.3.3)$$

Under no-slip conditions the gas and liquid phases move at the same velocity

$$v_{sg} = \text{Superficial gas velocity (ft /sec)} = q_g / ( 86400 \text{ sec/day} * A_{XS} ) \qquad (C.3.4)$$

$$v_{sL} = \text{Superficial liquid velocity (ft /sec)} = q_L / ( 86400 \text{ sec/day} * A_{XS} ) \qquad (C.3.5)$$

$$v_m = \text{Superficial mixture velocity (ft /sec)} = v_{sL} + v_{sg} \qquad (C.3.6)$$

$$v_g = \text{Actual gas velocity (ft /sec)} = v_{sg} / H_G \qquad (C.3.7)$$

$$v_L = \text{Actual liquid velocity (ft /sec)} = v_{sL} / H_L \qquad (C.3.8)$$

where:

$\rho_L$ = Liquid density (lbm /$ft^3$)
$\rho_g$ = Gas density (lbm /$ft^3$)

$$\rho_s = \text{Two phase density (lbm /ft}^3) = \rho_L * H_L + \rho_g * H_G \qquad (C.3.9)$$

$$\rho_\lambda = \text{Mixture density based on no-slip hold-up (lbm/ft}^3) = \rho_L * \lambda_L + \rho_g * \lambda_g \qquad (C.3.10)$$

(Note: specific multiphase flow calculations may use different formulas for density)

### C.4 Flowing Temperature Profile

The calculation of a flowing pressure profile requires that PVT data for the fluid be evaluated at changing temperatures as the fluid flows from the bottom-hole to the surface. The equation developed by Ramey[63] can be used to estimate the flowing temperature profile.

$$T_2 = T_1 - g_T * (\Delta L - A_{rel} * (1.0 - EXP( - \Delta L / A_{rel} ) ) ) \qquad (C.4.0)$$

Using a correlation developed by Shiu[15] a value of $A_{rel}$ can be estimated.

$$A_{rel} = 0.0149 * w^{0.5253} * \rho_L^{2.9303} * d^{0.2904} * \gamma_{API}^{0.2608} * \gamma_g^{4.4146} \qquad (C.4.1)$$

Where:

$T_2$ = Outlet temperature (F)

$T_1$ = Inlet temperature (F)

$g_T$ = Geothermal gradient (deg F / 100 ft)

$\Delta L$ = Length of flow conduit between points 1 and 2. (ft)

$A_{rel}$ = Relaxation distance (ft)

$w$ = total mass flow rate (lbm/sec)

$\rho_L$ = Liquid density (lbm /ft$^3$)

$d$ = Inside diameter of flow conduit (in)

$\gamma_{API}$ = Oil gravity (API)

$\gamma_g$ = Gas gravity (air = 1.000)

### C.5 Erosion Velocity

When producing at high rates it is often beneficial to calculate the erosion velocity as the minimum velocity where pipe may erode. The following equation can be used to make this estimate.

$$\nu_e = C_{er} / \rho_\lambda^{0.5} \tag{C.5.0}$$

where:

$\nu_e$ = Erosion velocity (ft/sec)

$C_{er}$ = Erosion constant, typically equal to 100

$\rho_\lambda$ = Mixture density based on no-slip hold-up (lbm/ft$^3$)

### C.6 Calculating Procedure

The following are procedures to calculate bottom-hole pressure give surface conditions such as wellhead pressure, liquid rate, water cut, tubing *GOR*, directional survey, production string and heat transfer information. Start from known surface pressure *Pwh = P₁*

1. Calculate mixed-fluid density by equation C.2.2
2. Guess total pressure gradient   by using $Grad_{total}$ = 0.433 * Mixed-Fluid Density
3. For the first survey station with length of Δ*L*, calculate
   a. Temperature using  Equation C.4.0 and C-4.1
   b. Initial guess for pressure $P = P_1 + Grad_{total} * \Delta L * Cos(Angle)$
4. With the initial guess for pressure
   a. Recalculate PVT of gas, oil, water and mixture based on new pressure and temperature from step 3.a
   b. Calculate gas rate $q_g$ = $(q_o*(R_{GOR}-R_{Smix})-q_w*R_{Swmix})*B_{gmix}*5.615/86400$
   c. Calculate superficial velocities of gas, oil, water, liquid and mixture.
      i. $V_{sg} = q_g/(Tbg\ Area)$
      ii. $V_{so} = 0.000065*q_o*B_{omix}/(Tbg\ Area)$
      iii. $V_{sw} = 0.000065*q_w*B_{wmix}/(Tbg\ Area)$
      iv. $V_{sL=}\ V_{sw}+ V_{so}$
      v. $V_{smix} =\ V_{sL} + V_{sg}$
   d. Calculate No slip Hold Up $NSHD = V_{sL} / V_{smix}$
   e. Calculate liquid properties
      i. Liquid viscosity, $Viscliq = ViscOil*(1-f_w) + ViscWater*f_w$
      ii. $STLiq = STOil * (1 - f_w) + STWater * f_w$
      iii. Liquid density, $Densliq = DensOil*(1-f_w) + DensWater*f_w$
      iv. No slip liquid Density, $DensNS = Densliq*NSHD + DensGas(1-NSDH)$
   f. Calculate SSU according to C-2.6 to C-2.10
   g. Calculate Liquid hold up (HL)
      i. $NLV = 1.938 * V_{sL} * (DensLiq / STLiq)^{0.25}$
      ii. $NGV = 1.938 * V_{sg} * (DensLiq / STLiq)^{0.25}$

    iii. Nd = 120.872*(Tbg Dia)/12 * (DensLiq / STLiq) $^{0.5}$

    iv. NL = 0.15726*Viscliq*(1/(Densliq*STLiq$^3$))$^{0.25}$

    v. Using Function in section C.7 to calculate Liquid Hold up

  h. Calculate mixture properties

    i. Densmix = DensLiq * HL + DensGas * (1- HL)

    ii. ViscMix = (ViscLiq$^{HL}$) * (ViscGas $^{(1 - HL)}$)

 i. Calculate friction related properties

    i. DensFric = DensNS $^2$ / DensMix

    ii. Relative Pipe roughness ED = (Pipe Roughness) / (Tbg Dia)

    iii. Reynolds Number, Nrem = 1488 * DensNS * $V_{mix}$ * ((Tbg Dia) / 12) / ViscMix

    iv. Using function in section C.7 to calculate Moody friction factor, $f_{TP}$

  j. Calculate pressure gradient

    i. Elevation pressure gradient, gradEL = DensMix * Cos(Angle) / 144

    ii. Friction pressure gradient, gradFric= ($f_{TP}$ * DensFric * $V_{mix}^2$) / (2 * 144 * 32.2 * ((Tbg Diam) / 12))

    iii. Using Eq. C-16 to C-18 to calculate Acceleration pressure gradient ,GradAcc

    iv. Calculate Total pressure gradient gradTot = gradEL + gradFric + gradAcc

  k. Calculate Pressure *Pcalc = P1 + gradTot * ΔL*

5. If the difference between *Pcalc* and *P* (from step 3.b) is less than 5 psi, the initial guess value is acceptable and this value will be using as starting pressure for the next survey station. Calculation is carried on until the last survey station is reached.

6. If the difference between *Pcalc* and *P* (from step 3.b) is more than 5 psi, then calculation will be repeated from step 3.b with *P* equals to *Pcalc*.

**C.7 Hagedorn and Brown Holdup Correlation Functions**

| CNL1 | -1.61976 | HL1 | 30.6276 | PSI1 | 1.50205 |
|------|----------|-----|---------|------|---------|
| CNL2 | 1.71817 | HL2 | 55.3801 | PSI2 | -103.905 |
| CNL3 | 3.80699 | HL3 | 41.5344 | PSI3 | 6731.55 |
| CNL4 | 4.80062 | HL4 | 15.9345 | PSI4 | -154664 |
| CNL5 | 2.83744 | HL5 | 3.29416 | PSI5 | 1550040 |
| CNL6 | 0.781583 | HL6 | 0.349847 | PSI6 | -5723820 |
| CNL7 | 0.0816439 | HL7 | 0.0149951 | | |

**Table C.1**    Constants for Hagedorn-Brown hold-up correlation

```
Function Log10(x)

    Log10 = Log(x) / Log(10)

End Function


Function fnCNL(NL As Single) As Single

    Dim x As Single, A As Single, B As Single

    If NL < 0.002 Then

        B = 0.0019

    ElseIf NL > 0.4 Then

        B = 0.0115

    Else

        x = Log10(NL)

        A = CNL1 + CNL2 * x + CNL3 * x ^ 2# + CNL4 * x ^ 3# + CNL5 * x ^ 4# _
            + CNL6 * x ^ 5# + CNL7 * x ^ 6#

        B = 10# ^ A

    End If

    If B < 0.0019 Then B = 0.0019

    If B > 0.0115 Then B = 0.0115

    fnCNL = B

End Function

Function fnHL(A As Single) As Single

    Dim x As Single, B As Single

    If A < 0.000002 Then
```

```
      B = 0.04
    ElseIf A > 0.01 Then
      B = 1#
    Else
      x = Log10(A)
      B = HL1 + HL2 * x + HL3 * x ^ 2# + HL4 * x ^ 3# + HL5 * x ^ 4# _
          + HL6 * x ^ 5# + HL7 * x ^ 6#
    End If
    If B < 0.04 Then B = 0.04
    If B > 1# Then B = 1#
    fnHL = B
End Function


Function fnPSI(x As Single) As Single
    Dim B As Single
    If x < 0.01 Then
      B = 1#
    ElseIf x > 0.09 Then
      B = 1.83
    Else
      B = PSI1 + PSI2 * x + PSI3 * x ^ 2# + PSI4 * x ^ 3# + PSI5 * x ^ 4# _
          + PSI6 * x ^ 5#
    End If
    If B < 1# Then B = 1#
    If B > 1.83 Then B = 1.83
    fnPSI = B
End Function




Function FricFact(RE As Single, ED As Single) As Single
'----------------------------------------------------------------------------
'  This subroutine calculates Moody friction factor.
'----------------------------------------------------------------------------
```

```
    Dim I As Integer
    Dim FGuess As Single
    If RE < 2000# Then
'-- Calculate friction factor for laminar flow.
        FricFact = 64# / RE
    Else
'-- Calculate friction factor for turbulent flow.  Jain equation is used for
'   first guess (Jain, A.K.: "An Accurate Explicit Equation for Friction
' Factor, " J. HYDRAULICS DIV ASCE, VOL. 102, NO. HY5, MAY, 1976.)."
        FGuess = 1# / (1.14 - 2# * Log10(ED + 21.25 / RE ^ 0.9)) ^ 2#
        For I = 1 To 20
           FricFact = 1# / (1.74 - 2# * Log10(2# * ED + _
              18.7 / (RE * Sqr(FGuess)))) ^ 2#
           If (Abs(FricFact - FGuess) <= 0.0001) Then Exit Function
           FGuess = FricFact
        Next I
    End If
End Function
```

**APPENDIX D**

**WELLBORE SCHEMATIC AND PRODUCTION DATA**



**Figure D.1** Single layer gas reservoir – well schematic

**Table D.1** Single layer gas reservoir - well production data

| Date | TFP psi | Tubing Temp. (F) | Gas Rate (MMscfd) | Condy. Rate (bbld) | Water Rate (bbld) | Gas Cum. (MMscf) |
|---|---|---|---|---|---|---|
| 25-Jun-05 | 2,245.0 | 110.0 | 5.760 | 175.000 | 28.000 | 7.97 |
| 26-Jun-05 | 1,720.0 | 146.0 | 9.710 | 223.000 | 41.000 | 15.94 |
| 28-Jun-05 | 2,303.0 | 133.0 | 4.750 | 146.000 | 24.000 | 31.90 |
| 24-Jul-05 | 2,258.0 | 80.0 | 5.010 | 132.000 | 32.000 | 52.61 |
| 25-Jul-05 | 2,110.0 | 91.0 | 7.500 | 201.000 | 36.000 | 53.41 |
| 25-Jul-05 | 1,686.0 | 135.0 | 11.110 | 234.000 | 48.000 | 53.41 |
| 27-Jul-05 | 1,673.0 | 148.0 | 10.940 | 203.000 | 42.000 | 55.00 |
| 8-Aug-05 | 1,646.0 | 137.0 | 10.820 | 212.000 | 45.000 | 143.65 |
| 14-Aug-05 | 1,670.0 | 148.0 | 10.000 | 186.000 | 45.000 | 187.98 |
| 19-Aug-05 | 1,640.0 | 158.0 | 10.320 | 170.000 | 38.000 | 224.92 |
| 28-Aug-05 | 1,560.0 | 159.0 | 9.950 | 165.000 | 40.000 | 291.41 |
| 29-Aug-05 | 1,625.0 | 156.0 | 10.140 | 162.000 | 30.000 | 298.80 |
| 8-Nov-05 | 1,500.0 | 162.0 | 10.600 | 200.000 | 0.000 | 524.46 |
| 14-Nov-05 | 1,610.0 | 156.0 | 10.100 | 185.000 | 0.000 | 543.53 |
| 22-Nov-05 | 1,601.0 | 152.0 | 9.800 | 147.000 | 38.000 | 568.96 |
| 7-Dec-05 | 1,660.0 | 132.0 | 8.320 | 151.000 | 36.000 | 717.24 |
| 12-Dec-05 | 1,665.0 | 145.0 | 7.910 | 123.000 | 33.000 | 766.67 |
| 26-Dec-05 | 1,213.0 | 166.0 | 10.050 | 130.000 | 38.000 | 905.07 |
| 30-Dec-05 | 1,125.0 | 171.0 | 10.230 | 125.000 | 38.000 | 944.61 |
| 27-Jan-06 | 1,175.0 | 163.0 | 9.730 | 168.000 | 0.000 | 1,214.66 |
| 1-Mar-06 | 847.0 | 181.0 | 10.480 | 128.000 | 22.000 | 1,532.93 |
| 13-Mar-06 | 845.0 | 166.0 | 10.230 | 122.000 | 0.000 | 1,648.66 |
| 15-Mar-06 | 1,010.0 | 160.0 | 9.200 | 128.000 | 0.000 | 1,667.95 |
| 25-Mar-06 | 800.0 | 184.0 | 10.000 | 128.000 | 0.000 | 1,764.40 |
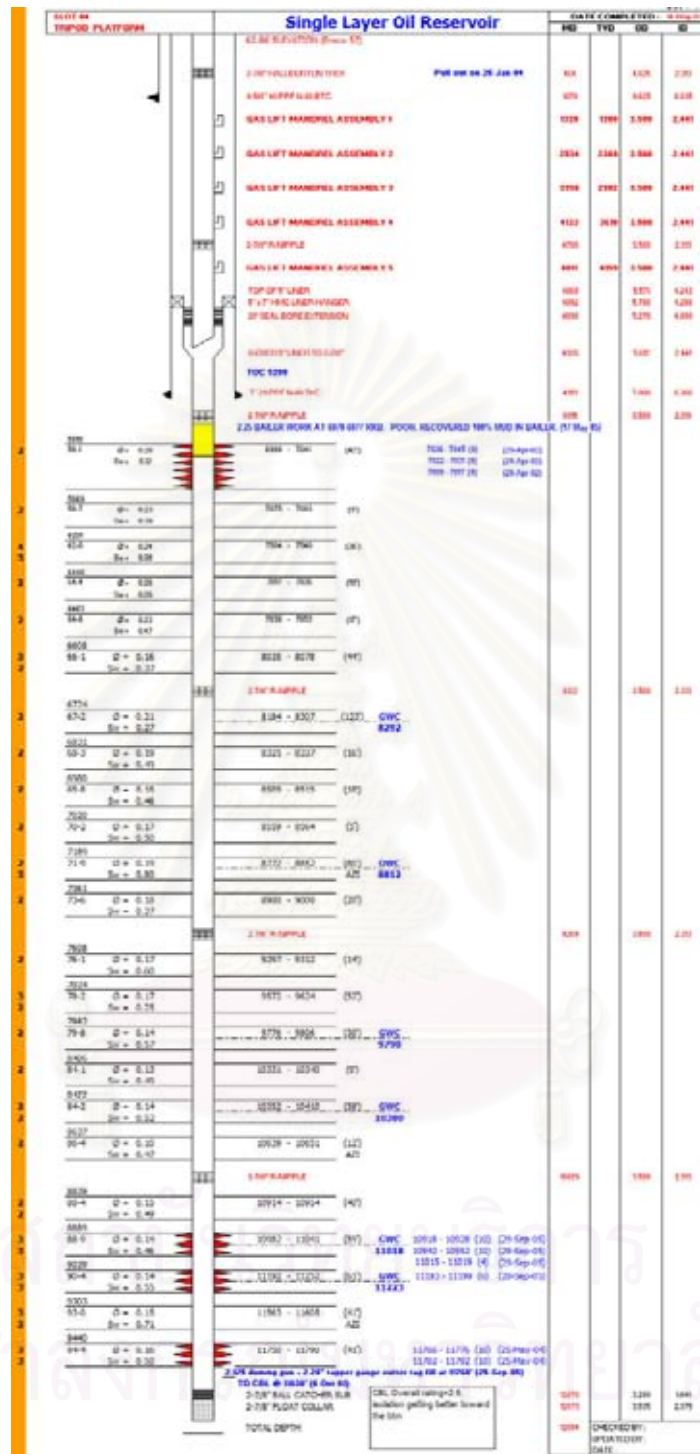
**Figure D.2** Single layer oil reservoir – well schematic

**Table D.2** Single layer oil reservoir - well production data

| Date | Wellhead Pressure (psig) | Fluid Rate (STB/day) | Water cut (fraction 0 to 1) | Tubing GOR (SCF/STB) |
|---|---|---|---|---|
| 6-May-02 | 810 | 1,578 | 0.00 | 224 |
| 11-May-02 | 819 | 1,801 | 0.00 | 228 |
| 13-May-02 | 810 | 1,554 | 0.00 | 251 |
| 16-May-02 | 786 | 1,533 | 0.00 | 470 |
| 21-May-02 | 781 | 1,465 | 0.00 | 212 |
| 30-May-02 | 737 | 892 | 0.00 | 157 |
| 6-Jun-02 | 728 | 949 | 0.00 | 11 |
| 16-Jun-02 | 714 | 950 | 0.00 | 116 |
| 19-Jun-02 | 715 | 1,579 | 0.00 | 329 |
| 20-Jun-02 | 640 | 3,187 | 0.04 | 411 |
| 21-Jun-02 | 641 | 3,015 | 0.00 | 279 |
| 3-Jul-02 | 589 | 3,296 | 0.00 | 352 |
| 5-Jul-02 | 596 | 3,256 | 0.00 | 369 |
| 10-Jul-02 | 556 | 2,502 | 0.00 | 268 |
| 11-Jul-02 | 572 | 2,493 | 0.00 | 261 |
| 23-Jul-02 | 581 | 1,850 | 0.00 | 162 |
| 25-Jul-02 | 565 | 2,158 | 0.00 | 283 |
| 15-Aug-02 | 585 | 2,264 | 0.00 | 658 |
| 20-Aug-02 | 645 | 2,748 | 0.00 | 4 |
| 2-Sep-02 | 592 | 1,478 | 0.00 | 2,253 |
| 4-Sep-02 | 800 | 1,251 | 0.00 | 655 |
| 6-Sep-02 | 785 | 2,033 | 0.00 | 492 |
| 8-Sep-02 | 669 | 2,175 | 0.00 | 561 |
| 11-Sep-02 | 825 | 953 | 0.00 | 913 |
| 12-Sep-02 | 755 | 1,710 | 0.00 | 836 |
| 16-Sep-02 | 725 | 2,229 | 0.00 | 812 |
| 16-Sep-02 | 756 | 1,756 | 0.00 | 797 |
| 5-Oct-02 | 735 | 1,675 | 0.00 | 1,081 |
| 12-Oct-02 | 770 | 1,060 | 0.19 | 2,058 |
| 18-Oct-02 | 699 | 1,591 | 0.00 | 1,194 |
| 23-Oct-02 | 688 | 1,487 | 0.00 | 1,311 |
| 27-Oct-02 | 760 | 1,216 | 0.00 | 1,316 |
| 1-Nov-02 | 720 | 1,041 | 0.15 | 1,805 |
| 3-Nov-02 | 635 | 1,094 | 0.12 | 1,707 |
| 8-Nov-02 | 615 | 1,280 | 0.12 | 1,775 |
| 9-Nov-02 | 615 | 1,254 | 0.12 | 3,000 |
| 14-Nov-02 | 611 | 1,182 | 0.14 | 1,961 |
| 23-Nov-02 | 594 | 1,323 | 0.00 | 1,413 |
| 30-Nov-02 | 536 | 1,153 | 0.15 | 2,055 |
| 30-Nov-02 | 580 | 1,029 | 0.15 | 2,094 |
| 1-Dec-02 | 530 | 1,149 | 0.15 | 2,072 |
| 3-Dec-02 | 540 | 1,165 | 0.12 | 1,928 |
| 5-Dec-02 | 540 | 1,056 | 0.13 | 2,054 |
| 11-Dec-02 | 521 | 969 | 0.11 | 2,025 |
| 14-Dec-02 | 514 | 1,154 | 0.00 | 1,508 |
| 17-Dec-02 | 520 | 1,026 | 0.00 | 1,550 |

**Table D.2** Single layer oil reservoir - well production
data (continued)

| Date | Wellhead Pressure (psig) | Fluid Rate (STB/day) | Water cut (fraction 0 to 1) | Tubing GOR (SCF/STB) |
|---|---|---|---|---|
| 23-Dec-02 | 531 | 919 | 0.00 | 1,567 |
| 27-Dec-02 | 510 | 780 | 0.00 | 1,799 |
| 27-Dec-02 | 510 | 780 | 0.00 | 1,799 |
| 1-Jan-03 | 505 | 796 | 0.00 | 1,709 |
| 6-Jan-03 | 501 | 756 | 0.00 | 1,640 |
| 11-Jan-03 | 504 | 725 | 0.00 | 1,531 |
| 10-Feb-03 | 560 | 954 | 0.00 | 1,583 |
| 27-Apr-03 | 525 | 298 | 0.00 | 4,161 |
| 18-Sep-03 | 507 | 57 | 0.61 | 8,182 |
| 8-Sep-05 | 1,120 | 716 | 0.93 | 27,500 |
| 9-Sep-05 | 904 | 1,038 | 0.76 | 15,857 |
| 10-Sep-05 | 1,093 | 636 | 0.21 | 9,444 |
| 13-Sep-05 | 1,150 | 438 | 0.17 | 11,315 |
| 14-Sep-05 | 1,132 | 450 | 0.04 | 10,694 |
| 15-Sep-05 | 1,113 | 442 | 0.00 | 10,814 |
| 20-Sep-05 | 1,019 | 390 | 0.18 | 13,594 |
| 30-Sep-05 | 1,942 | 865 | 0.18 | 4,727 |
| 1-Oct-05 | 2,001 | 1,016 | 0.12 | 3,973 |
| 2-Oct-05 | 2,360 | 819 | 0.22 | 3,969 |
| 6-Oct-05 | 2,304 | 610 | 0.32 | 6,553 |
| 8-Oct-05 | 2,001 | 495 | 0.52 | 21,218 |
| 10-Oct-05 | 2,374 | 487 | 0.40 | 9,172 |
| 13-Oct-05 | 2,273 | 503 | 0.43 | 9,066 |
| 19-Oct-05 | 1,577 | 750 | 0.68 | 16,074 |
| 26-Oct-05 | 1,601 | 615 | 0.60 | 14,696 |
| 29-Oct-05 | 1,622 | 572 | 0.55 | 13,813 |
| 1-Nov-05 | 1,515 | 580 | 0.56 | 14,553 |
| 2-Nov-05 | 1,569 | 547 | 0.65 | 18,860 |
| 15-Nov-05 | 1,799 | 600 | 0.47 | 11,906 |
| 16-Nov-05 | 883 | 967 | 0.76 | 24,163 |
| 23-Nov-05 | 1,905 | 470 | 0.49 | 11,176 |
| 3-Dec-05 | 1,761 | 443 | 0.76 | 26,981 |
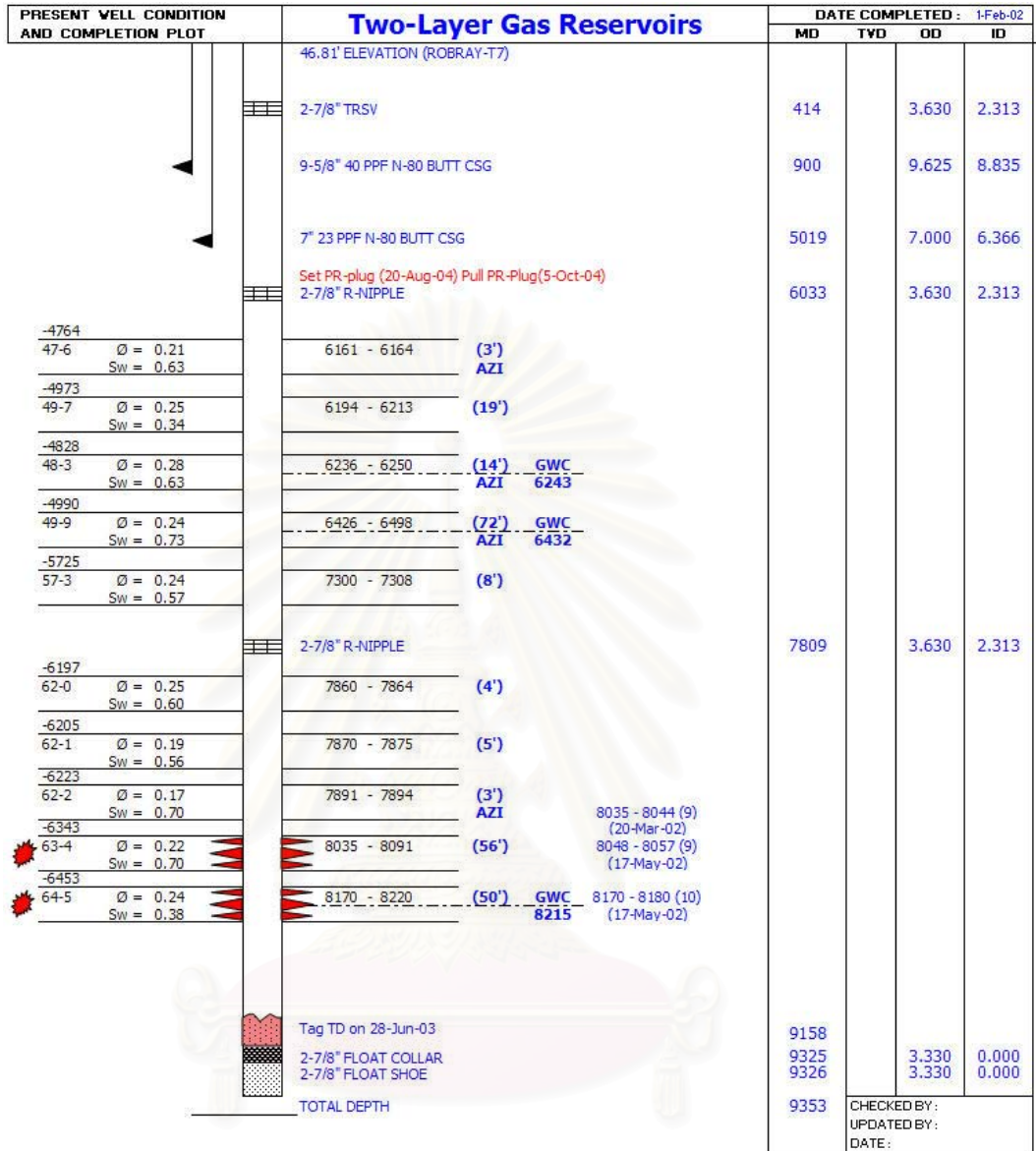
**Figure D.3** Two-layer gas reservoirs – well schematic

**Table D.3** Two-layer gas reservoirs - well production data

| Date | TFP (psi) | Tubing Temp. (F) | Gas Rate (MMscfd) | Condy Rate (bbld) | Water Rate (bbld) | Gas Cum (MMcf) |
|---|---|---|---|---|---|---|
| 19-Jun-02 | 1,720.0 | 171.0 | 13.640 | 28.000 | 40.000 | |
| 20-Jun-02 | 1,720.0 | 171.0 | 13.640 | 30.000 | 39.000 | 51.36 |
| 9-Jul-02 | 1,382.0 | 171.0 | 10.740 | 35.000 | 61.000 | |
| 19-Jul-02 | 1,161.0 | 171.0 | 10.370 | 33.794 | 105.206 | 250.88 |
| 30-Jul-02 | 1,985.0 | 119.0 | 5.760 | 18.771 | 21.229 | |
| 9-Aug-02 | 1,517.0 | 140.0 | 8.040 | 26.532 | 98.468 | 438.20 |
| 24-Aug-02 | 1,857.0 | 113.0 | 5.750 | 18.975 | 7.025 | |
| 5-Sep-02 | 1,743.0 | 119.0 | 6.550 | 21.615 | 77.385 | |
| 18-Sep-02 | 1,358.0 | 83.0 | 9.450 | 31.185 | 1.000 | 606.18 |
| 28-Sep-02 | 1,856.0 | 85.0 | 3.720 | 44.640 | 5.000 | |
| 7-Oct-02 | 1,850.0 | 84.0 | 3.760 | 45.120 | 1.000 | |
| 21-Oct-02 | 1,820.0 | 74.0 | 3.950 | 47.400 | 1.000 | 667.94 |
| 3-Nov-02 | 1,323.0 | 139.0 | 9.100 | 109.200 | 1.000 | |
| 15-Nov-02 | 1,812.0 | 101.0 | 3.390 | 22.374 | 188.626 | 798.09 |
| 26-Nov-02 | 1,652.0 | 118.0 | 6.010 | 19.000 | 16.000 | 859.08 |
| 28-Dec-02 | 1,375.0 | 137.0 | 7.730 | 24.438 | 149.562 | |
| 8-Jan-03 | 1,310.0 | 124.0 | 7.560 | 2.000 | 274.000 | |
| 19-Jan-03 | 1,375.0 | 144.0 | 8.110 | 2.146 | 47.854 | 978.81 |
| 31-Jan-03 | 1,615.0 | 119.0 | 5.760 | 19.000 | 31.000 | |
| 9-Feb-03 | 1,484.0 | 135.0 | 7.050 | 16.000 | 25.000 | |
| 14-Feb-03 | 1,754.0 | 108.0 | 3.370 | 8.000 | 13.000 | |
| 19-Feb-03 | 1,125.0 | 166.0 | 9.440 | 22.000 | 18.000 | |
| 25-Feb-03 | 1,274.0 | 157.0 | 8.460 | 19.000 | 30.000 | 1,141.42 |
| 3-Mar-03 | 1,115.0 | 163.0 | 9.280 | 20.000 | 29.000 | |
| 8-Mar-03 | 1,153.0 | 159.0 | 8.980 | 18.000 | 28.000 | |
| 13-Mar-03 | 1,664.0 | 111.0 | 4.050 | 12.150 | 1.000 | |
| 18-Mar-03 | 1,414.0 | 144.0 | 6.950 | 20.000 | 20.000 | |
| 19-Mar-03 | 1,417.0 | 144.0 | 6.900 | 19.000 | 22.000 | |
| 23-Mar-03 | 1,242.0 | 148.0 | 8.145 | 21.000 | 25.000 | |
| 28-Mar-03 | 1,524.0 | 131.0 | 5.590 | 14.000 | 23.000 | 1,361.44 |
| 1-Apr-03 | 878.0 | 171.0 | 9.883 | 21.000 | 26.000 | |
| 8-Apr-03 | 1,215.0 | 154.0 | 14.653 | 108.000 | 160.000 | |
| 15-Apr-03 | 967.0 | 168.0 | 9.332 | 10.000 | 34.000 | |
| 18-Apr-03 | 1,338.0 | 149.0 | 6.931 | 42.000 | 104.000 | |
| 25-Apr-03 | 1,591.0 | 113.0 | 3.943 | 10.000 | 18.000 | 1,591.18 |
| 1-May-03 | 1,617.0 | 118.0 | 3.238 | 5.000 | 13.000 | |
| 7-May-03 | 1,220.0 | 155.0 | 7.553 | 15.000 | 27.000 | |
| 12-May-03 | 1,506.0 | 131.0 | 4.854 | 8.000 | 22.000 | |
| 18-May-03 | 1,172.0 | 152.0 | 7.722 | 14.000 | 29.000 | |
| 24-May-03 | 1,604.0 | 112.0 | 2.938 | 5.000 | 11.000 | 1,726.67 |
| 30-May-03 | 1,183.0 | 155.0 | 7.587 | 16.000 | 25.000 | |
| 10-Jun-03 | 1,140.0 | 162.0 | 7.780 | 16.000 | 26.000 | |
| 14-Jun-03 | 912.0 | 169.0 | 8.981 | 12.000 | 30.000 | |
| 19-Jun-03 | 902.0 | 174.0 | 8.983 | 16.000 | 28.000 | 1,897.44 |
| 3-Jul-03 | 1,499.0 | 96.0 | 3.726 | 15.000 | 22.000 | |

**Table D.3** Two-layer gas reservoirs - well production data (continued)

| Date | TFP (psi) | Tubing Temp. (F) | Gas Rate (MMscfd) | Condy Rate (bbld) | Water Rate (bbld) | Gas Cum (MMcf) |
|---|---|---|---|---|---|---|
| 5-Jun-03 | 1,432.0 | 131.0 | 5.406 | 16.000 | 28.000 | |
| 10-Jul-03 | 1,523.0 | 109.0 | 3.666 | 8.000 | 18.000 | |
| 17-Jul-03 | 1,425.0 | 130.0 | 4.981 | 8.000 | 24.000 | |
| 23-Jul-03 | 1,440.0 | 125.0 | 4.757 | 5.000 | 24.000 | 2,009.47 |
| 28-Jul-03 | 1,509.0 | 121.0 | 3.724 | 6.000 | 19.000 | |
| 3-Aug-03 | 1,545.0 | 104.0 | 1.951 | 3.000 | 18.000 | |
| 9-Aug-03 | 981.0 | 163.0 | 5.526 | 10.000 | 33.000 | |
| 14-Aug-03 | 1,339.0 | 141.0 | 3.754 | 9.000 | 27.000 | |
| 20-Aug-03 | 928.0 | 161.0 | 5.612 | 11.000 | 36.000 | |
| 25-Aug-03 | 1,274.0 | 141.0 | 4.071 | 8.000 | 31.000 | 2,153.47 |
| 30-Aug-03 | 953.0 | 166.0 | 5.465 | 8.000 | 35.000 | |
| 5-Sep-03 | 1,325.0 | 135.0 | 3.616 | 11.000 | 26.000 | |
| 10-Sep-03 | 1,094.0 | 151.0 | 4.817 | 8.000 | 34.000 | |
| 15-Sep-03 | 1,093.0 | 155.0 | 4.775 | 9.000 | 32.000 | |
| 19-Sep-03 | 877.0 | 165.0 | 5.553 | 8.000 | 35.000 | |
| 24-Sep-03 | 1,047.0 | 151.0 | 4.587 | 5.000 | 31.000 | 2,314.81 |
| 29-Sep-03 | 891.0 | 164.0 | 5.420 | 9.000 | 36.000 | |
| 5-Oct-03 | 768.0 | 165.0 | 5.743 | 11.000 | 33.000 | |
| 7-Oct-03 | 828.0 | 164.0 | 5.548 | 9.000 | 35.000 | |
| 12-Oct-03 | 1,214.0 | 136.0 | 3.874 | 13.000 | 26.000 | |
| 16-Oct-03 | 695.0 | 169.0 | 5.845 | 10.000 | 34.000 | |
| 21-Oct-03 | 731.0 | 163.0 | 5.695 | 10.000 | 35.000 | 2,460.17 |
| 29-Oct-03 | 1,236.0 | 126.0 | 3.596 | 12.000 | 26.000 | 2,470.45 |
| 2-Nov-03 | 1,437.0 | 89.0 | 1.540 | 3.000 | 16.000 | 2,477.78 |
| 7-Nov-03 | 1,419.0 | 89.0 | 1.389 | 6.000 | 11.000 | 2,488.56 |
| 11-Nov-03 | 1,150.0 | 138.0 | 3.996 | 14.000 | 25.000 | 2,502.79 |
| 14-Nov-03 | 758.0 | 164.0 | 5.493 | 10.000 | 33.000 | 2,522.42 |
| 19-Nov-03 | 1,378.0 | 125.0 | 2.358 | 5.000 | 19.000 | 2,534.14 |
| 24-Nov-03 | 1,378.0 | 118.0 | 2.326 | 3.000 | 23.000 | 2,548.12 |
| 1-Dec-03 | 1,073.0 | 158.0 | 4.280 | 9.000 | 27.000 | 2,580.60 |
| 8-Dec-03 | 873.0 | 166.0 | 4.999 | 7.000 | 34.000 | 2,606.50 |
| 15-Dec-03 | 1,340.0 | 119.0 | 2.397 | 2.000 | 26.000 | 2,623.27 |
| 22-Dec-03 | 1,329.0 | 113.0 | 2.391 | 2.000 | 26.000 | 2,625.67 |
| 23-Dec-03 | 1,329.0 | 117.0 | 2.410 | 2.000 | 26.000 | 2,641.18 |
| 29-Dec-03 | 1,283.0 | 123.0 | 2.764 | 2.000 | 30.000 | 2,652.99 |
| 7-Jan-04 | 1,320.0 | 103.0 | 1.994 | 2.000 | 10.000 | 2,663.31 |
| 11-Jan-04 | 1,194.0 | 116.0 | 3.172 | 4.000 | 37.000 | 2,674.96 |
| 23-Jan-04 | 722.0 | 169.0 | 5.167 | 9.000 | 33.000 | 2,730.84 |
| 25-Jan-04 | 722.0 | 170.0 | 5.136 | 7.000 | 34.000 | 2,746.20 |
| 28-Jan-04 | 727.0 | 173.0 | 5.098 | 8.000 | 31.000 | 2,765.84 |
| 1-Feb-04 | 1,119.0 | 148.0 | 3.505 | 11.000 | 24.000 | 2,776.37 |
| 4-Feb-04 | 1,113.0 | 146.0 | 3.507 | 1.000 | 30.000 | 2,783.93 |
| 7-Feb-04 | 1,320.0 | 103.0 | 1.533 | 2.000 | 22.000 | 2,796.45 |
| 14-Jan-04 | 914.0 | 159.0 | 4.601 | 9.000 | 31.000 | 2,694.58 |

**Table D.3** Two-layer gas reservoirs - well production data (continued)

| Date | TFP (psi) | Tubing Temp. (F) | Gas Rate (MMscfd) | Condy Rate (bbld) | Water Rate (bbld) | Gas Cum (MMcf) |
|---|---|---|---|---|---|---|
| 18-Jan-04 | 720.0 | 170.0 | 5.211 | 8.000 | 33.000 | 2,720.53 |
| 11-Feb-04 | 809.0 | 165.0 | 4.731 | 7.000 | 32.000 | 2,813.53 |
| 15-Feb-04 | 1,034.0 | 151.0 | 3.806 | 7.000 | 29.000 | 2,846.79 |
| 24-Feb-04 | 1,065.0 | 152.0 | 3.582 | 9.000 | 27.000 | 2,857.53 |
| 27-Feb-04 | 1,059.0 | 146.0 | 3.582 | 13.000 | 26.000 | 2,873.99 |
| 4-Mar-04 | 1,089.0 | 139.0 | 3.386 | 10.000 | 26.000 | 2,886.00 |
| 7-Mar-04 | 794.0 | 157.0 | 4.616 | 8.000 | 35.000 | 2,895.11 |
| 10-Mar-04 | 1,288.0 | 98.0 | 1.454 | 2.000 | 16.000 | 2,910.16 |
| 15-Mar-04 | 791.0 | 158.0 | 4.574 | 11.000 | 37.000 | 2,917.00 |
| 17-Mar-04 | 1,228.0 | 121.0 | 2.270 | 3.000 | 25.000 | 2,928.00 |
| 22-Mar-04 | 1,236.0 | 111.0 | 2.126 | 3.000 | 24.000 | 2,936.80 |
| 25-Mar-04 | 988.0 | 145.0 | 3.743 | 7.000 | 33.000 | 2,947.60 |
| 28-Mar-04 | 1,043.0 | 143.0 | 3.461 | 8.000 | 34.000 | 2,972.11 |
| 31-Mar-04 | 1,052.0 | 142.0 | 3.395 | 7.000 | 30.000 | 2,980.04 |
| 2-Apr-04 | 778.0 | 162.0 | 4.527 | 11.000 | 32.000 | 2,992.45 |
| 5-Apr-04 | 977.0 | 148.0 | 3.735 | 7.000 | 33.000 | 2,999.92 |
| 7-Apr-04 | 977.0 | 156.0 | 3.730 | 7.000 | 3.000 | 3,004.04 |
| 8-Apr-04 | 777.0 | 164.0 | 4.505 | 10.000 | 36.000 | 3,014.06 |
| 11-Apr-04 | 1,211.0 | 117.0 | 2.165 | 3.000 | 23.000 | 3,024.08 |
| 14-Apr-04 | 764.0 | 162.0 | 4.510 | 14.000 | 30.000 | 3,042.04 |
| 18-Apr-04 | 773.0 | 164.0 | 4.465 | 8.000 | 36.000 | 3,082.27 |
| 27-Apr-04 | 756.0 | 161.0 | 4.466 | 14.000 | 33.000 | 3,105.75 |
| 1-May-04 | 705.0 | 160.0 | 4.682 | 10.000 | 33.000 | 3,128.20 |
| 6-May-04 | 784.0 | 157.0 | 4.301 | 12.000 | 31.000 | 3,143.72 |
| 10-May-04 | 987.0 | 139.0 | 3.458 | 14.000 | 28.000 | 3,157.76 |
| 14-May-04 | 965.0 | 149.0 | 3.558 | 12.000 | 35.000 | 3,169.16 |
| 19-May-04 | 1,189.0 | 83.0 | 0.997 | 9.000 | 1.000 | 3,179.28 |
| 23-May-04 | 856.0 | 144.0 | 4.057 | 9.000 | 30.000 | 3,236.03 |
| 30-May-04 | 891.0 | 144.0 | 3.516 | 9.000 | 27.000 | 3,275.81 |
| 11-Jun-04 | 1,151.0 | 106.0 | 3.113 | 6.000 | 19.000 | 3,291.03 |
| 16-Jun-04 | 1,161.0 | 113.0 | 2.975 | 7.000 | 17.000 | 3,306.61 |
| 20-Jun-04 | 942.0 | 136.0 | 4.811 | 5.000 | 72.000 |  |
| 23-Jun-04 | 992.0 | 140.0 | 4.698 | 3.000 | 75.000 | 3,313.65 |
| 30-Jun-04 | 770.0 | 155.0 | 6.026 | 4.000 | 33.000 | 3,330.26 |
| 3-Jul-04 | 938.0 | 148.0 | 5.042 | 10.000 | 27.000 | 3,338.11 |
| 5-Jul-04 | 1,160.0 | 122.0 | 2.805 | 6.000 | 16.000 | 3,364.51 |
| 13-Jul-04 | 1,064.0 | 119.0 | 3.791 | 8.000 | 22.000 | 3,377.41 |
| 16-Jul-04 | 955.0 | 146.0 | 4.815 | 7.000 | 26.000 | 3,395.97 |
| 20-Jul-04 | 999.0 | 143.0 | 4.462 | 9.000 | 22.000 | 3,418.12 |
| 26-Jul-04 | 1,135.0 | 113.0 | 2.923 | 6.000 | 17.000 | 3,426.86 |
| 30-Jul-04 | 1,099.0 | 98.0 | 1.445 | 8.000 | 0.000 | 3,436.04 |
| 2-Aug-04 | 924.0 | 127.0 | 4.677 | 11.000 | 26.000 | 3,399.55 |
| 5-Aug-04 | 713.0 | 159.0 | 6.056 | 10.000 | 28.000 | 3,423.06 |
| 9-Aug-04 | 772.0 | 156.0 | 5.702 | 11.000 | 29.000 | 3,438.49 |
| 12-Aug-04 | 928.0 | 143.0 | 4.585 | 9.000 | 23.000 | 3,482.15 |

**Table D.3** Two-layer gas reservoirs - well production data (continued)

| Date | TFP (psi) | Tubing Temp. (F) | Gas Rate (MMscfd) | Condy Rate (bbld) | Water Rate (bbld) | Gas Cum (MMcf) |
|---|---|---|---|---|---|---|
| 16-Aug-04 | 989.0 | 141.0 | 4.272 | 9.000 | 21.000 | 3,678.34 |
| 7-Oct-04 | 1,078.0 | 108.0 | 3.274 | 7.000 | 4.000 | 3,692.68 |
| 10-Oct-04 | 633.0 | 155.0 | 6.284 | 4.000 | 37.000 | 3,717.66 |
| 14-Oct-04 | 645.0 | 165.0 | 6.207 | 7.000 | 31.000 | 3,726.59 |
| 16-Oct-04 | 1,114.0 | 122.0 | 2.723 | 1.000 | 15.000 | 3,730.57 |
| 17-Oct-04 | 834.0 | 149.0 | 5.237 | 8.000 | 25.000 | 3,604.21 |
| 25-Oct-04 | 723.0 | 159.0 | 5.753 | 6.000 | 30.000 | 3,657.70 |
| 3-Nov-04 | 618.0 | 165.0 | 6.135 | 7.000 | 29.000 | 3,694.29 |
| 9-Nov-04 | 621.0 | 166.0 | 6.059 | 7.000 | 28.000 | 3,723.57 |
| 14-Nov-04 | 699.0 | 165.0 | 5.656 | 6.000 | 29.000 | 3,747.04 |
| 18-Nov-04 | 595.0 | 164.0 | 6.078 | 7.000 | 32.000 | 3,759.93 |
| 23-Nov-04 | 1,074.0 | 129.0 | 6.892 | 34.000 | 37.000 | 3,802.73 |
| 2-Dec-04 | 1,072.0 | 121.0 | 2.620 | 3.000 | 16.000 | 3,816.69 |
| 6-Dec-04 | 894.0 | 134.0 | 4.360 | 11.000 | 29.000 | 3,836.94 |
| 12-Dec-04 | 1,061.0 | 99.0 | 2.391 | 6.000 | 14.000 | 3,853.11 |
| 19-Dec-04 | 1,009.0 | 107.0 | 2.228 | 5.000 | 27.000 | 3,868.65 |
| 23-Dec-04 | 679.0 | 154.0 | 5.542 | 12.190 | 18.810 | 3,846.64 |
| 29-Dec-04 | 1,056.0 | 114.0 | 2.673 | 5.000 | 18.000 | 3,862.69 |
| 4-Jan-05 | 1,051.0 | 112.0 | 2.677 | 4.000 | 16.000 | 3,882.45 |
| 9-Jan-05 | 722.0 | 155.0 | 5.228 | 8.000 | 28.000 | 3,898.81 |
| 12-Jan-05 | 624.0 | 163.0 | 5.679 | 5.000 | 30.000 | 3,920.94 |
| 16-Jan-05 | 673.0 | 156.0 | 5.386 | 10.000 | 24.000 | 3,945.25 |
| 21-Jan-05 | 851.0 | 143.0 | 4.340 | 5.000 | 25.000 | 3,958.05 |
| 24-Jan-05 | 873.0 | 138.0 | 4.189 | 3.000 | 24.000 | 3,970.44 |
| 30-Jan-05 | 623.0 | 170.0 | 5.522 | 3.000 | 29.000 | 4,002.69 |
| 5-Feb-05 | 652.0 | 152.0 | 5.229 | 9.000 | 27.000 | 4,016.70 |
| 8-Feb-05 | 854.0 | 144.0 | 4.106 | 3.000 | 23.000 | 4,035.79 |
| 12-Feb-05 | 586.0 | 163.0 | 5.440 | 3.000 | 30.000 | 4,051.66 |
| 15-Feb-05 | 648.0 | 162.0 | 5.140 | 6.000 | 27.000 | 4,072.55 |
| 19-Feb-05 | 598.0 | 167.0 | 5.306 | 5.000 | 29.000 | 4,098.55 |
| 2-Mar-05 | 845.0 | 143.0 | 3.901 | 6.000 | 23.000 | 4,137.28 |
| 5-Mar-05 | 814.0 | 139.0 | 4.101 | 8.000 | 21.000 | 4,157.57 |
| 10-Mar-05 | 814.0 | 151.0 | 4.018 | 8.000 | 22.000 | 4,171.56 |
| 13-Mar-05 | 543.0 | 167.0 | 5.303 | 7.000 | 25.000 | 4,201.71 |
| 19-Mar-05 | 671.0 | 158.0 | 4.748 | 8.000 | 26.000 | 4,211.19 |
| 21-Mar-05 | 670.0 | 160.0 | 4.731 | 7.000 | 27.000 | 4,225.91 |
| 24-Mar-05 | 597.0 | 167.0 | 5.084 | 9.000 | 25.000 | 4,236.01 |
| 26-Mar-05 | 595.0 | 165.0 | 5.021 | 7.000 | 27.000 | |
| 29-Mar-05 | 598.0 | 169.0 | 4.989 | 7.000 | 27.000 | 4,243.52 |
| 31-Mar-05 | 604.0 | 168.0 | 4.822 | 7.000 | 26.000 | 4,274.12 |
| 6-Apr-05 | 802.0 | 142.0 | 5.377 | 7.000 | 22.000 | 4,300.21 |
| 11-Apr-05 | 572.0 | 163.0 | 5.060 | 6.000 | 26.000 | 4,315.56 |
| 24-Feb-05 | 660.0 | 166.0 | 5.008 | 5.000 | 28.000 | 4,125.27 |

**Table D.3** Two-layer gas reservoirs - well production data (continued)

| Date | TFP (psi) | Tubing Temp. (F) | Gas Rate (MMscfd) | Condy Rate (bbld) | Water Rate (bbld) | Gas Cum (MMcf) |
|---|---|---|---|---|---|---|
| 14-Apr-05 | 539.0 | 162.0 | 5.170 | 5.000 | 27.000 | 4,324.50 |
| 16-Apr-05 | 806.0 | 140.0 | 3.770 | 4.000 | 17.000 | 4,333.37 |
| 18-Apr-05 | 549.0 | 166.0 | 5.104 | 7.000 | 25.000 | 4,343.72 |
| 20-Apr-05 | 554.0 | 167.0 | 5.247 | 5.000 | 28.000 | 4,354.16 |
| 22-Apr-05 | 564.0 | 158.0 | 5.190 | 6.000 | 26.000 | 4,369.00 |
| 24-Apr-05 | 566.0 | 169.0 | 4.989 | 6.000 | 26.000 | 4,408.59 |
| 28-Apr-05 | 564.0 | 166.0 | 4.946 | 7.000 | 27.000 | 4,423.42 |
| 30-Apr-05 | 529.0 | 166.0 | 5.100 | 9.000 | 25.000 | 4,428.43 |
| 2-May-05 | 571.0 | 168.0 | 4.908 | 4.000 | 27.000 | 4,438.32 |
| 5-May-05 | 550.0 | 168.0 | 4.979 | 5.000 | 27.000 | 4,452.74 |
| 6-May-05 | 576.0 | 167.0 | 5.042 | 5.000 | 29.000 | 4,467.09 |
| 8-May-05 | 551.0 | 162.0 | 4.845 | 141.000 | 276.000 | 4,491.25 |
| 11-May-05 | 584.0 | 166.0 | 4.769 | 2.000 | 35.000 | 4,502.00 |
| 14-May-05 | 585.0 | 169.0 | 4.800 | 2.000 | 33.000 | 4,530.44 |
| 19-May-05 | 546.0 | 168.0 | 4.863 | 14.000 | 136.000 | 4,547.77 |
| 26-May-05 | 570.0 | 167.0 | 4.742 | 10.000 | 21.000 | 4,553.61 |
| 1-Jun-05 | 562.0 | 165.0 | 4.738 | 1.000 | 27.000 | 4,574.34 |
| 6-Jun-05 | 918.0 | 125.0 | 2.192 | 5.000 | 15.000 | 4,597.80 |
| 8-Jun-05 | 757.0 | 142.0 | 3.653 | 9.000 | 22.000 | 4,613.40 |
| 13-Jun-05 | 563.0 | 161.0 | 4.638 | 8.000 | 28.000 | 4,650.81 |
| 18-Jun-05 | 540.0 | 166.0 | 4.747 | 8.000 | 27.000 | 4,691.78 |
| 25-Jun-05 | 535.0 | 141.0 | 4.750 | 6.000 | 27.000 | 4,710.03 |
| 3-Jul-05 | 540.0 | 170.0 | 4.602 | 8.000 | 26.000 | 4,733.10 |
| 12-Jul-05 | 547.0 | 170.0 | 4.503 | 10.000 | 24.000 | |
| 16-Jul-05 | 545.0 | 166.0 | 4.621 | 8.000 | 27.000 | 4,737.50 |
| 21-Jul-05 | 506.0 | 166.0 | 4.606 | 9.000 | 25.000 | 4,759.12 |
| 26-Jul-05 | 652.0 | 151.0 | 3.842 | 7.000 | 26.000 | 4,772.30 |
| 30-Jul-05 | 536.0 | 155.0 | 4.331 | 8.000 | 28.000 | 4,789.79 |
| 4-Aug-05 | 539.0 | 162.0 | 4.317 | 8.000 | 27.000 | 4,806.90 |
| 7-Aug-05 | 538.0 | 165.0 | 4.468 | 9.000 | 26.000 | 4,824.00 |
| 11-Aug-05 | 536.0 | 158.0 | 4.280 | 7.000 | 26.000 | 4,836.79 |
| 15-Aug-05 | 534.0 | 162.0 | 4.273 | 5.000 | 28.000 | 4,864.00 |
| 19-Aug-05 | 531.0 | 166.0 | 4.276 | 3.000 | 28.000 | |
| 22-Aug-05 | 527.0 | 166.0 | 4.253 | 5.000 | 27.000 | |
| 26-Aug-05 | 533.0 | 166.0 | 4.221 | 5.000 | 26.000 | |
| 1-Sep-05 | 531.0 | 166.0 | 4.176 | 5.000 | 25.000 | |
| 5-Sep-05 | 530.0 | 164.0 | 4.173 | 5.000 | 25.000 | |
| 12-Sep-05 | 532.0 | 160.0 | 4.104 | 7.000 | 26.000 | |
| 14-Sep-05 | 531.0 | 161.0 | 4.098 | 5.000 | 23.000 | 4,975.00 |
| 22-Sep-05 | 528.0 | 160.0 | 4.089 | 5.000 | 24.000 | |
| 26-Sep-05 | 534.0 | 160.0 | 4.032 | 5.000 | 28.000 | |
| 30-Sep-05 | 528.0 | 164.0 | 4.008 | 5.000 | 23.000 | |
| 5-Oct-05 | 524.0 | 164.0 | 4.031 | 6.000 | 25.000 | |
| 9-Oct-05 | 530.0 | 164.0 | 3.983 | 4.000 | 26.000 | |
| 13-Oct-05 | 545.0 | 163.0 | 3.890 | 4.000 | 27.000 | |

**Table D.3** Two-layer gas reservoirs - well production data (continued)

| Date | TFP (psi) | Tubing Temp. (F) | Gas Rate (MMscfd) | Condy Rate (bbld) | Water Rate (bbld) | Gas Cum (MMcf) |
|---|---|---|---|---|---|---|
| 17-Oct-05 | 534.0 | 163.0 | 3.919 | 6.000 | 27.000 | 5,087.00 |
| 22-Oct-05 | 535.0 | 159.0 | 3.862 | 6.000 | 26.000 | 5,094.68 |
| 26-Oct-05 | 540.0 | 161.0 | 3.880 | 3.880 | 25.120 | 5,109.89 |
| 31-Oct-05 | 535.0 | 163.0 | 3.862 | 3.860 | 24.140 | 5,132.92 |
| 2-Nov-05 | 538.0 | 159.0 | 3.822 | 3.000 | 28.000 | 5,148.38 |
| 6-Nov-05 | 544.0 | 162.0 | 3.780 | 5.000 | 25.000 | 5,167.60 |
| 12-Nov-05 | 514.0 | 164.0 | 3.897 | 3.000 | 27.000 | 5,182.92 |
| 16-Nov-05 | 523.0 | 161.0 | 3.834 | 2.000 | 27.000 | 5,188.00 |
| 21-Nov-05 | 502.0 | 154.0 | 3.854 | 1.000 | 27.000 | |
| 25-Nov-05 | 522.0 | 153.0 | 3.807 | 4.000 | 28.000 | |
| 29-Nov-05 | 534.0 | 159.0 | 3.741 | 3.000 | 27.000 | |
| 2-Dec-05 | 526.0 | 161.0 | 3.769 | 5.000 | 25.000 | |
| 5-Dec-05 | 526.0 | 162.0 | 3.749 | 4.000 | 26.000 | |
| 8-Dec-05 | 528.0 | 155.0 | 3.756 | 3.000 | 28.000 | |
| 12-Dec-05 | 524.0 | 157.0 | 3.716 | 5.000 | 25.000 | |
| 15-Dec-05 | 526.0 | 150.0 | 3.678 | 5.000 | 27.000 | 5,293.00 |
| 18-Dec-05 | 524.0 | 153.0 | 3.675 | 5.000 | 26.000 | 5,315.34 |
| 24-Dec-05 | 522.0 | 155.0 | 3.657 | 5.000 | 25.000 | 5,326.59 |
| 28-Dec-05 | 525.0 | 161.0 | 3.635 | 3.000 | 24.000 | 5,337.65 |
| 3-Jan-06 | 510.0 | 161.0 | 3.811 | 4.000 | 26.000 | 5,348.55 |
| 6-Jan-06 | 499.0 | 156.0 | 3.693 | 4.000 | 26.000 | 5,359.26 |
| 9-Jan-06 | 500.0 | 154.0 | 3.680 | 1.000 | 27.000 | 5,369.85 |
| 12-Jan-06 | 520.0 | 157.0 | 3.583 | 2.000 | 26.000 | 5,380.45 |
| 15-Jan-06 | 520.0 | 160.0 | 3.557 | 3.000 | 24.000 | 5,391.05 |
| 18-Jan-06 | 521.0 | 159.0 | 3.505 | 3.000 | 24.000 | 5,397.48 |
| 21-Jan-06 | 520.0 | 158.0 | 3.560 | 5.000 | 22.000 | 5,411.39 |
| 24-Jan-06 | 519.0 | 152.0 | 3.508 | 5.000 | 26.000 | 5,425.20 |
| 28-Jan-06 | 520.0 | 158.0 | 3.497 | 3.000 | 26.000 | 5,438.92 |
| 1-Feb-06 | 518.0 | 152.0 | 3.462 | 4.000 | 27.000 | 5,438.92 |
| 5-Feb-06 | 520.0 | 153.0 | 3.443 | 2.000 | 31.000 | 5,452.39 |
| 9-Feb-06 | 521.0 | 157.0 | 3.414 | 3.000 | 4.000 | 5,468.87 |
| 9-Feb-06 | 521.0 | 157.0 | 3.414 | 3.410 | 0.590 | 5,478.71 |
| 13-Feb-06 | 530.0 | 148.0 | 3.324 | 7.000 | 125.000 | 5,488.55 |
| 18-Feb-06 | 533.0 | 153.0 | 3.267 | 30.000 | 0.000 | 5,477.48 |
| 21-Feb-06 | 533.0 | 150.0 | 3.289 | 4.000 | 30.000 | 5,484.02 |
| 24-Feb-06 | 533.0 | 150.0 | 3.272 | 6.000 | 24.000 | 5,494.09 |
| 27-Feb-06 | 534.0 | 154.0 | 3.257 | 2.000 | 27.000 | 5,507.50 |
| 1-Mar-06 | 527.0 | 153.0 | 3.290 | 6.000 | 25.000 | 5,540.82 |
| 4-Mar-06 | 498.0 | 154.0 | 3.423 | 6.000 | 24.000 | 5,544.19 |
| 8-Mar-06 | 522.0 | 153.0 | 3.279 | 6.000 | 26.000 | 5,557.57 |
| 18-Mar-06 | 494.0 | 137.0 | 3.386 | 3.000 | 39.000 | 5,571.13 |
| 19-Mar-06 | 507.0 | 145.0 | 3.349 | 3.000 | 27.000 | 5,558.54 |
| 23-Mar-06 | 507.0 | 144.0 | 3.343 | 2.000 | 28.000 | 5,568.64 |
| 27-Mar-06 | 485.0 | 150.0 | 3.436 | 3.000 | 26.000 | 5,578.60 |
| 31-Mar-06 | 496.0 | 158.0 | 3.375 | 5.000 | 25.000 | 5,588.80 |

**Table D.3** Two-layer gas reservoirs - well production data (continued)

| Date | TFP (psi) | Tubing Temp. (F) | Gas Rate (MMscfd) | Condy Rate (bbld) | Water Rate (bbld) | Gas Cum (MMcf) |
|---|---|---|---|---|---|---|
| 3-Apr-06 | 497.0 | 157.0 | 3.355 | 4.000 | 27.000 | 5,595.61 |
| 6-Apr-06 | 508.0 | 158.0 | 3.287 | 5.000 | 26.000 | 5,608.74 |
| 9-Apr-06 | 492.0 | 155.0 | 3.516 | 8.000 | 25.000 | 5,624.84 |
| 11-Apr-06 | 503.0 | 155.0 | 3.288 | 7.000 | 26.000 | 5,640.45 |
| 15-Apr-06 | 493.0 | 154.0 | 3.277 | 4.000 | 27.000 | 5,638.42 |
| 20-Apr-06 | 509.0 | 154.0 | 3.165 | 4.000 | 25.000 | 5,653.66 |
| 25-Apr-06 | 524.0 | 154.0 | 3.079 | 4.000 | 24.000 | 5,665.41 |
| 30-Apr-06 | 522.0 | 153.0 | 3.063 | 5.000 | 24.000 | 5,676.96 |
| 5-May-06 | 522.0 | 153.0 | 3.032 | 4.000 | 25.000 | 5,685.70 |
| 9-May-06 | 555.0 | 150.0 | 2.842 | 4.000 | 24.000 | 5,688.58 |
| 13-May-06 | 535.0 | 155.0 | 2.931 | 4.000 | 23.000 | 5,697.17 |
| 16-May-06 | 537.0 | 149.0 | 2.897 | 5.000 | 24.000 | 5,703.07 |
| 17-May-06 | 540.0 | 150.0 | 2.873 | 6.000 | 23.000 | 5,712.09 |
| 20-May-06 | 539.0 | 145.0 | 2.852 | 6.000 | 24.000 | 5,724.00 |
| 22-May-06 | 497.0 | 144.0 | 3.046 | 6.000 | 25.000 | 5,732.49 |
| 25-May-06 | 498.0 | 151.0 | 2.969 | 5.000 | 26.000 | 5,738.44 |
| 29-May-06 | 533.0 | 149.0 | 2.777 | 6.000 | 23.000 | 5,753.14 |
| 1-Jun-06 | 508.0 | 154.0 | 2.880 | 6.000 | 22.000 | 5,766.84 |
| 3-Jun-06 | 464.0 | 154.0 | 3.071 | 4.000 | 24.000 | 5,780.54 |
| 8-Jun-06 | 504.0 | 150.0 | 2.809 | 4.000 | 24.000 | 5,794.24 |
| 13-Jun-06 | 522.0 | 147.0 | 2.671 | 5.000 | 22.000 | 5,807.94 |
| 17-Jun-06 | 528.0 | 143.0 | 2.580 | 4.000 | 22.000 | 5,821.64 |

**Figure D.4** Multi-layer gas reservoirs – well schematic

**Table D.4** Multi-layer gas reservoirs - well production data

| Date | TFP | Tubing Temp. | Gas Rate | Condy Rate | Water Rate | Gas Cum |
|------|-----|--------------|----------|------------|------------|---------|
| | (psi) | (F) | (MMscfd) | (bbld) | (bbld) | (MMcf) |
| 1-Oct-99 | 2,530.0 | 115.0 | 8.761 | 620.000 | 96.000 | 9.00 |
| 10-Oct-99 | 2,530.0 | 130.0 | 8.760 | 620.000 | 96.000 | |
| 23-Oct-99 | 2,347.0 | 183.0 | 8.825 | 524.000 | 96.000 | |
| 24-Oct-99 | 2,347.0 | 186.0 | 9.326 | 535.000 | 96.000 | 289.00 |
| 7-Nov-99 | 2,420.0 | 198.0 | 9.714 | 534.000 | 22.000 | |
| 18-Nov-99 | 2,329.0 | 182.0 | 8.390 | 336.000 | 156.000 | |
| 19-Nov-99 | 2,329.0 | 182.0 | 8.390 | 336.000 | 156.000 | |
| 23-Nov-99 | 2,391.0 | 178.0 | 7.659 | 322.000 | 145.000 | |
| 29-Nov-99 | 2,324.0 | 181.0 | 8.140 | 328.000 | 151.000 | 518.00 |
| 1-Dec-99 | 2,032.0 | 182.0 | 8.141 | 328.000 | 151.000 | |
| 3-Dec-99 | 2,342.0 | 177.0 | 7.838 | 324.000 | 149.000 | |
| 8-Dec-99 | 2,345.0 | 179.0 | 7.731 | 407.000 | 57.000 | |
| 9-Dec-99 | 2,345.0 | 179.0 | 7.731 | 407.000 | 57.000 | |
| 28-Dec-99 | 919.0 | 119.0 | 5.195 | 341.000 | 82.000 | 616.00 |
| 10-Jan-00 | 618.0 | 181.0 | 8.040 | 344.000 | 122.000 | |
| 18-Jan-00 | 2,069.0 | 195.0 | 9.509 | 374.000 | 140.000 | |
| 24-Jan-00 | 2,151.0 | 190.0 | 8.663 | 532.000 | 140.000 | 813.00 |
| 4-Feb-00 | 1,938.0 | 200.0 | 11.690 | 463.000 | 39.000 | |
| 19-Feb-00 | 2,236.0 | 178.0 | 6.420 | 421.000 | 40.000 | 1,056.00 |
| 6-Apr-00 | 267.0 | 188.0 | 6.050 | 386.000 | 22.000 | 1,214.00 |
| 18-Apr-00 | 1,264.0 | 202.0 | 7.490 | 320.000 | 98.000 | |
| 23-Apr-00 | 1,350.0 | 222.0 | 8.843 | 378.000 | 18.000 | |
| 24-Apr-00 | 1,350.0 | 222.0 | 8.843 | 378.000 | 18.000 | 1,379.00 |
| 11-May-00 | 1,580.0 | 213.0 | 8.803 | 281.000 | 50.000 | |
| 18-May-00 | 1,684.0 | 208.0 | 8.928 | 285.000 | 86.000 | |
| 30-May-00 | 1,503.0 | 214.0 | 8.733 | 398.000 | 49.000 | 1,587.00 |
| 6-Jun-00 | 1,329.0 | 222.0 | 8.827 | 396.000 | 53.000 | |
| 24-Jun-00 | 1,275.0 | 223.0 | 8.726 | 402.000 | 23.000 | 1,823.00 |
| 5-Jul-00 | 1,597.0 | 206.0 | 7.652 | 384.000 | 11.000 | |
| 4-Aug-00 | 968.0 | 227.0 | 8.637 | 342.000 | 59.000 | 2,054.00 |
| 9-Aug-00 | 1,355.0 | 213.0 | 8.391 | 343.000 | 56.000 | |
| 22-Aug-00 | 1,272.0 | 214.0 | 7.387 | 331.000 | 62.000 | 2,268.00 |
| 15-Sep-00 | 1,294.0 | 216.0 | 6.920 | 220.000 | 147.000 | |
| 21-Sep-00 | 1,266.0 | 218.0 | 7.790 | 305.000 | 53.000 | 2,458.00 |
| 17-Oct-00 | 1,155.0 | 219.0 | 7.738 | 290.000 | 63.000 | |
| 25-Oct-00 | 1,195.0 | 215.0 | 7.530 | 245.000 | 105.000 | 2,680.00 |
| 6-Nov-00 | 1,161.0 | 217.0 | 7.250 | 293.000 | 50.000 | |
| 13-Nov-00 | 1,190.0 | 198.0 | 5.950 | 275.000 | 70.000 | |
| 20-Dec-00 | 909.0 | 224.0 | 7.536 | 265.000 | 69.000 | 3,016.00 |
| 11-Jan-01 | 1,287.0 | 199.0 | 5.495 | 223.000 | 90.000 | 3,131.00 |
| 11-Apr-01 | 793.0 | 227.0 | 6.230 | 222.000 | 93.000 | |
| 17-Apr-01 | 754.0 | 227.0 | 6.177 | 201.000 | 112.000 | |
| 21-Apr-01 | 755.0 | 227.0 | 6.137 | 209.000 | 105.000 | |
| 25-Apr-01 | 707.0 | 229.0 | 6.215 | 206.000 | 105.000 | |
| 29-Apr-01 | 713.0 | 226.0 | 6.110 | 204.000 | 108.000 | 3,522.00 |
| 6-May-01 | 684.0 | 227.0 | 6.130 | 204.000 | 107.000 | |

**Table D.4** Multi-layer gas reservoirs - well production data
(continued)

| Date | TFP | Tubing Temp. | Gas Rate | Condy Rate | Water Rate | Gas Cum |
|------|-----|--------------|----------|------------|------------|---------|
| | (psi) | (F) | (MMscfd) | (bbld) | (bbld) | (MMcf) |
| 15-May-01 | 678.0 | 228.0 | 6.111 | 163.000 | 146.000 | |
| 21-May-01 | 696.0 | 227.0 | 6.007 | 167.000 | 143.000 | |
| 24-May-01 | 684.0 | 227.0 | 5.929 | 167.000 | 148.000 | |
| 27-May-01 | 689.0 | 230.0 | 5.897 | 157.000 | 150.000 | 3,650.00 |
| 13-Jun-01 | 684.0 | 230.0 | 5.720 | 186.000 | 116.000 | |
| 19-Jun-01 | 709.0 | 222.0 | 5.550 | 195.000 | 122.000 | |
| 26-Jun-01 | 695.0 | 222.0 | 5.478 | 192.000 | 121.000 | 3,792.00 |
| 2-Jul-01 | 656.0 | 225.0 | 5.509 | 189.000 | 125.000 | |
| 14-Jul-01 | 627.0 | 226.0 | 5.469 | 178.000 | 132.000 | |
| 18-Jul-01 | 660.0 | 227.0 | 5.295 | 181.000 | 135.000 | |
| 25-Jul-01 | 660.0 | 228.0 | 5.274 | 197.000 | 121.000 | 3,922.00 |
| 23-Aug-01 | 621.0 | 224.0 | 4.959 | 175.000 | 151.000 | 4,051.00 |
| 2-Sep-01 | 578.0 | 221.0 | 4.703 | 167.000 | 182.000 | |
| 16-Sep-01 | 1,038.0 | 171.0 | 1.953 | 54.000 | 125.000 | |
| 21-Sep-01 | 1,035.0 | 173.0 | 2.136 | 91.000 | 106.000 | |
| 27-Sep-01 | 602.0 | 222.0 | 4.666 | 166.000 | 166.000 | 4,122.00 |
| 8-Oct-01 | 1,010.0 | 172.0 | 2.272 | 147.000 | 88.000 | |
| 11-Oct-01 | 1,036.0 | 163.0 | 1.858 | 72.000 | 93.000 | |
| 9-Nov-01 | 947.0 | 155.0 | 0.612 | 67.000 | 119.000 | 4,165.00 |
| 20-Nov-01 | 826.0 | 175.0 | 3.398 | 282.000 | 180.000 | |
| 26-Nov-01 | 597.0 | 205.0 | 3.630 | 173.000 | 309.000 | 4,200.00 |
| 4-Dec-01 | 588.0 | 216.0 | 3.840 | 159.000 | 278.000 | |
| 8-Dec-01 | 607.0 | 221.0 | 4.320 | 156.000 | 209.000 | |
| 11-Dec-01 | 605.0 | 222.0 | 4.520 | 164.000 | 200.000 | |
| 14-Dec-01 | 614.0 | 218.0 | 4.430 | 167.000 | 200.000 | |
| 17-Dec-01 | 610.0 | 217.0 | 4.463 | 167.000 | 197.000 | |
| 24-Dec-01 | 589.0 | 222.0 | 4.230 | 154.000 | 197.000 | |
| 31-Dec-01 | 573.0 | 216.0 | 4.470 | 174.000 | 226.000 | 4,271.00 |
| 5-Jan-02 | 597.0 | 216.0 | 4.256 | 150.000 | 197.000 | |
| 9-Jan-02 | 607.0 | 219.0 | 4.040 | 153.000 | 190.000 | |
| 17-Jan-02 | 698.0 | 216.0 | 3.908 | 163.000 | 171.000 | |
| 24-Jan-02 | 619.0 | 222.0 | 4.151 | 155.000 | 191.000 | 4,370.00 |
| 3-Feb-02 | 555.0 | 219.0 | 4.288 | 143.000 | 201.000 | |
| 11-Feb-02 | 565.0 | 220.0 | 4.146 | 138.000 | 205.000 | |
| 16-Feb-02 | 583.0 | 220.0 | 3.456 | 12.000 | 324.000 | |
| 1-Mar-02 | 589.0 | 223.0 | 3.880 | 21.000 | 314.000 | 4,446.00 |
| 5-Mar-02 | 600.0 | 223.0 | 4.533 | 32.000 | 313.000 | |
| 31-Mar-02 | 592.0 | 220.0 | 3.580 | 15.000 | 317.000 | 4,545.00 |
| 13-Apr-02 | 522.0 | 216.0 | 3.678 | 64.000 | 247.000 | |
| 28-Apr-02 | 558.0 | 221.0 | 3.549 | 19.000 | 315.000 | 4,631.00 |
| 2-May-02 | 571.0 | 218.0 | 3.449 | 13.000 | 323.000 | |
| 8-May-02 | 569.0 | 218.0 | 3.399 | 8.000 | 324.000 | |
| 19-May-02 | 548.0 | 221.0 | 3.423 | 16.000 | 318.000 | |
| 24-May-02 | 557.0 | 223.0 | 3.258 | 20.000 | 309.000 | |
| 26-May-02 | 550.0 | 220.0 | 3.383 | 6.000 | 251.000 | 4,714.00 |
| 2-Jun-02 | 564.0 | 222.0 | 3.267 | 19.000 | 307.000 | 4,786.00 |

**Table D.4** Multi-layer gas reservoirs - well production data
(continued)

| Date | TFP | Tubing Temp. | Gas Rate | Condy Rate | Water Rate | Gas Cum |
|---|---|---|---|---|---|---|
| | (psi) | (F) | (MMscfd) | (bbld) | (bbld) | (MMcf) |
| 2-Jul-02 | 567.0 | 208.0 | 3.230 | 6.000 | 330.000 | 4,862.60 |
| 9-Sep-02 | 530.0 | 216.0 | 2.188 | 1.000 | 223.000 | 4,973.81 |
| 15-Oct-02 | 549.0 | 197.0 | 1.900 | 2.000 | 318.000 | |
| 22-Oct-02 | 516.0 | 213.0 | 2.207 | 1.000 | 281.000 | |
| 25-Oct-02 | 545.0 | 213.0 | 2.106 | 1.000 | 251.000 | |
| 29-Oct-02 | 521.0 | 216.0 | 2.130 | 1.000 | 246.000 | |
| 30-Oct-02 | 521.0 | 213.0 | 2.095 | 6.000 | 259.000 | |
| 31-Oct-02 | 521.0 | 213.0 | 2.095 | 6.000 | 259.000 | 5,001.54 |
| 2-Nov-02 | 516.0 | 209.0 | 2.170 | 6.000 | 154.000 | |
| 20-Nov-02 | 519.0 | 207.0 | 2.566 | 7.000 | 200.000 | 5,045.36 |
| 21-Dec-02 | 525.0 | 204.0 | 2.087 | 6.000 | 87.000 | 5,058.23 |
| 11-Feb-03 | 330.0 | 198.0 | 2.330 | 6.000 | 238.000 | 5,098.80 |
| 18-Feb-03 | 329.0 | 200.0 | 2.298 | 6.000 | 266.000 | |
| 20-Feb-03 | 335.0 | 201.0 | 2.401 | 6.000 | 64.000 | 5,150.00 |
| 19-Mar-03 | 353.0 | 186.0 | 2.149 | 104.000 | 248.000 | 5,204.00 |
| 13-Aug-03 | 527.0 | 152.0 | 1.450 | 0.000 | 34.000 | |
| 21-Aug-03 | 500.0 | 190.0 | 2.330 | 0.000 | 738.000 | |
| 3-Sep-03 | 398.0 | 188.0 | 2.280 | 47.000 | 132.000 | 5,441.91 |
| 3-Sep-03 | 515.0 | 194.0 | 2.607 | 4.000 | 111.000 | |
| 7-Sep-03 | 364.0 | 199.0 | 2.874 | 51.000 | 179.000 | |
| 10-Sep-03 | 370.0 | 194.0 | 2.850 | 23.000 | 171.000 | |
| 18-Sep-03 | 330.0 | 213.0 | 2.892 | 45.000 | 173.000 | |
| 29-Sep-03 | 316.0 | 205.0 | 2.889 | 48.000 | 168.000 | 5,508.63 |
| 8-Oct-03 | 303.0 | 203.0 | 2.910 | 43.000 | 165.000 | |
| 9-Oct-03 | 303.0 | 203.0 | 2.909 | 43.000 | 165.000 | |
| 21-Oct-03 | 296.0 | 193.0 | 2.794 | 49.000 | 164.000 | |
| 28-Oct-03 | 280.0 | 201.0 | 2.870 | 32.000 | 182.000 | |
| 29-Oct-03 | 283.0 | 202.0 | 2.807 | 36.000 | 178.000 | |
| 30-Oct-03 | 283.0 | 187.0 | 2.810 | 36.000 | 175.000 | 5,585.31 |
| 3-Nov-03 | 286.0 | 190.0 | 2.770 | 34.000 | 184.000 | |
| 11-Nov-03 | 285.0 | 204.0 | 2.739 | 42.000 | 161.000 | |
| 14-Nov-03 | 285.0 | 190.0 | 2.710 | 42.000 | 162.000 | |
| 15-Nov-03 | 286.0 | 200.0 | 2.710 | 42.000 | 162.000 | |
| 19-Nov-03 | 285.0 | 190.0 | 2.080 | 39.000 | 172.000 | |
| 21-Nov-03 | 285.0 | 206.0 | 2.088 | 33.000 | 173.000 | |
| 23-Nov-03 | 278.0 | 183.0 | 2.310 | 40.000 | 165.000 | |
| 25-Nov-03 | 286.0 | 189.0 | 2.130 | 36.000 | 157.000 | |
| 2-Dec-03 | 339.0 | 190.0 | 2.495 | 34.000 | 199.000 | 5,644.37 |
| 14-Dec-03 | 313.0 | 198.0 | 2.660 | 33.000 | 178.000 | |
| 19-Dec-03 | 278.0 | 202.0 | 2.711 | 32.000 | 191.000 | |
| 23-Dec-03 | 288.0 | 189.0 | 2.746 | 38.000 | 176.000 | |
| 26-Dec-03 | 277.0 | 203.0 | 2.760 | 39.000 | 172.000 | |
| 29-Dec-03 | 278.0 | 199.0 | 2.732 | 42.000 | 173.000 | |
| 30-Dec-03 | 278.0 | 201.0 | 2.743 | 41.000 | 171.000 | 5,706.46 |
| 1-Jan-04 | 270.0 | 193.0 | 2.760 | 39.000 | 168.000 | |
| 4-Jan-04 | 424.0 | 194.0 | 2.820 | 56.000 | 125.000 | |

**Table D.4** Multi-layer gas reservoirs - well production data
(continued)

| Date | TFP | Tubing Temp. | Gas Rate | Condy Rate | Water Rate | Gas Cum |
|---|---|---|---|---|---|---|
| | (psi) | (F) | (MMscfd) | (bbld) | (bbld) | (MMcf) |
| 17-Jan-04 | 272.0 | 201.0 | 2.643 | 38.000 | 167.000 | |
| 20-Jan-04 | 274.0 | 202.0 | 2.662 | 24.000 | 177.000 | |
| 22-Jan-04 | 272.0 | 185.0 | 2.630 | 32.000 | 172.000 | 5,767.02 |
| 13-Feb-04 | 267.0 | 196.0 | 2.581 | 17.000 | 173.000 | |
| 16-Feb-04 | 428.0 | 197.0 | 1.909 | 43.000 | 114.000 | |
| 18-Feb-04 | 265.0 | 200.0 | 2.529 | 25.000 | 177.000 | |
| 20-Feb-04 | 265.0 | 200.0 | 2.529 | 25.000 | 177.000 | |
| 23-Feb-04 | 263.0 | 197.0 | 2.381 | 21.000 | 196.000 | |
| 24-Feb-04 | 263.0 | 191.0 | 2.440 | 23.000 | 185.000 | |
| 25-Feb-04 | 263.0 | 200.0 | 2.436 | 23.000 | 185.000 | 5,826.87 |
| 6-Mar-04 | 255.0 | 184.0 | 2.410 | 38.000 | 182.000 | |
| 11-Mar-04 | 263.0 | 200.0 | 2.473 | 29.000 | 174.000 | |
| 16-Mar-04 | 261.0 | 201.0 | 2.467 | 36.000 | 164.000 | |
| 18-Mar-04 | 261.0 | 190.0 | 2.464 | 37.000 | 165.000 | |
| 21-Mar-04 | 259.0 | 204.0 | 2.460 | 37.000 | 167.000 | |
| 1-Apr-04 | 401.0 | 195.0 | 1.796 | 39.000 | 113.000 | 5,892.64 |
| 3-Apr-04 | 265.0 | 192.0 | 2.382 | 83.000 | 124.000 | |
| 4-Apr-04 | 265.0 | 201.0 | 2.400 | 84.000 | 120.000 | |
| 9-Apr-04 | 269.0 | 194.0 | 2.402 | 84.000 | 114.000 | |
| 14-Apr-04 | 399.0 | 181.0 | 1.761 | 62.000 | 74.000 | |
| 23-Apr-04 | 382.0 | 173.0 | 1.266 | 22.000 | 76.000 | |
| 4-May-04 | 278.0 | 199.0 | 2.294 | 76.000 | 131.000 | 5,942.99 |
| 7-May-04 | 265.0 | 186.0 | 2.247 | 74.000 | 141.000 | |
| 13-May-04 | 262.0 | 203.0 | 2.257 | 74.000 | 122.000 | |
| 14-May-04 | 296.0 | 206.0 | 2.150 | 71.000 | 122.000 | 5,993.64 |
| 12-Jun-04 | 250.0 | 202.0 | 2.196 | 33.000 | 168.000 | 6,047.10 |
| 6-Jul-04 | 277.0 | 189.0 | 2.140 | 24.000 | 159.000 | |
| 13-Jul-04 | 245.0 | 201.0 | 2.120 | 34.000 | 155.000 | 6,100.00 |
| 25-Jul-04 | 380.0 | 137.0 | 0.613 | 6.000 | 22.000 | |
| 31-Jul-04 | 385.0 | 119.0 | 0.560 | 5.000 | 16.000 | |
| 1-Aug-04 | 385.0 | 106.0 | 0.540 | 3.000 | 10.000 | |
| 9-Aug-04 | 374.0 | 122.0 | 0.010 | 1.000 | 4.000 | |
| 10-Aug-04 | 370.0 | 123.0 | 0.010 | 4.000 | 10.000 | |
| 16-Aug-04 | 231.0 | 189.0 | 1.410 | 21.000 | 287.000 | |
| 18-Aug-04 | 225.0 | 188.0 | 1.550 | 14.000 | 307.000 | |
| 21-Aug-04 | 270.0 | 193.0 | 1.640 | 23.000 | 226.000 | |
| 29-Aug-04 | 247.0 | 193.0 | 1.868 | 34.000 | 184.000 | 6,121.35 |
| 2-Sep-04 | 254.0 | 188.0 | 1.897 | 26.000 | 184.000 | 6,128.88 |
| 3-Sep-04 | 253.0 | 192.0 | 1.898 | 33.000 | 176.000 | 6,130.77 |
| 7-Sep-04 | 247.0 | 188.0 | 1.953 | 33.000 | 175.000 | 6,138.48 |
| 11-Sep-04 | 255.0 | 201.0 | 1.942 | 33.000 | 170.000 | 6,146.27 |
| 15-Sep-04 | 250.0 | 196.0 | 1.936 | 33.000 | 168.000 | 6,154.02 |
| 19-Sep-04 | 233.0 | 199.0 | 2.000 | 33.000 | 168.000 | 6,161.89 |
| 22-Sep-04 | 240.0 | 197.0 | 2.000 | 31.000 | 167.000 | 6,167.89 |
| 25-Sep-04 | 244.0 | 197.0 | 1.961 | 24.000 | 182.000 | 6,173.84 |
| 27-Sep-04 | 240.0 | 198.0 | 1.979 | 23.000 | 177.000 | 6,177.78 |

**Table D.4** Multi-layer gas reservoirs - well production data
(continued)

| Date | TFP | Tubing Temp. | Gas Rate | Condy Rate | Water Rate | Gas Cum |
|---|---|---|---|---|---|---|
| | (psi) | (F) | (MMscfd) | (bbld) | (bbld) | (MMcf) |
| 30-Sep-04 | 238.0 | 199.0 | 1.985 | 31.000 | 166.000 | 6,150.63 |
| 3-Oct-04 | 239.0 | 196.0 | 1.990 | 19.000 | 169.000 | 6,203.61 |
| 11-Nov-04 | 225.0 | 196.0 | 1.800 | 34.000 | 153.000 | |
| 19-Nov-04 | 232.0 | 188.0 | 1.750 | 21.000 | 180.000 | |
| 28-Nov-04 | 225.0 | 194.0 | 1.900 | 14.000 | 179.000 | 6,244.01 |
| 1-Dec-04 | 233.0 | 197.0 | 1.869 | 11.000 | 207.000 | |
| 7-Dec-04 | 228.0 | 181.0 | 1.839 | 30.000 | 157.000 | |
| 13-Dec-04 | 227.0 | 191.0 | 1.852 | 31.000 | 152.000 | |
| 17-Dec-04 | 226.0 | 196.0 | 1.872 | 21.000 | 161.000 | |
| 20-Dec-04 | 218.0 | 194.0 | 1.810 | 20.000 | 168.000 | |
| 24-Dec-04 | 217.0 | 191.0 | 1.817 | 21.000 | 166.000 | |
| 29-Dec-04 | 217.0 | 193.0 | 1.815 | 25.000 | 165.000 | 6,291.58 |
| 2-Jan-05 | 217.0 | 192.0 | 1.815 | 18.000 | 168.000 | |
| 6-Jan-05 | 233.0 | 195.0 | 1.784 | 26.000 | 156.000 | |
| 11-Jan-05 | 217.0 | 191.0 | 1.804 | 21.000 | 160.000 | |
| 14-Jan-05 | 213.0 | 188.0 | 1.802 | 23.000 | 160.000 | |
| 16-Jan-05 | 213.0 | 188.0 | 1.810 | 20.000 | 162.000 | |
| 18-Jan-05 | 210.0 | 192.0 | 1.810 | 18.000 | 163.000 | |
| 22-Jan-05 | 210.0 | 187.0 | 1.802 | 28.000 | 153.000 | |
| 26-Jan-05 | 212.0 | 193.0 | 1.760 | 17.000 | 170.000 | |
| 31-Jan-05 | 223.0 | 196.0 | 1.764 | 2.000 | 235.000 | 6,339.04 |
| 4-Feb-05 | 223.0 | 193.0 | 1.742 | 31.000 | 213.000 | |
| 10-Feb-05 | 252.0 | 190.0 | 1.527 | 14.000 | 202.000 | |
| 13-Feb-05 | 243.0 | 190.0 | 1.549 | 19.000 | 186.000 | |
| 17-Feb-05 | 238.0 | 195.0 | 1.510 | 9.000 | 178.000 | |
| 23-Feb-05 | 251.0 | 156.0 | 0.755 | 8.000 | 95.000 | |
| 24-Feb-05 | 114.0 | 167.0 | 0.778 | 8.000 | 100.000 | 6,373.23 |
| 5-Mar-05 | 204.0 | 172.0 | 1.310 | 13.000 | 232.000 | |
| 21-Mar-05 | 176.0 | 179.0 | 1.410 | 10.000 | 267.000 | |
| 26-Mar-05 | 183.0 | 184.0 | 1.620 | 15.000 | 248.000 | |
| 29-Mar-05 | 186.0 | 188.0 | 1.686 | 5.000 | 242.000 | 6,393.59 |
| 1-Apr-05 | 194.0 | 191.0 | 1.660 | 12.000 | 243.000 | |
| 11-Apr-05 | 187.0 | 189.0 | 1.409 | 12.000 | 207.000 | |
| 17-Apr-05 | 186.0 | 189.0 | 1.642 | 25.000 | 225.000 | |
| 23-Apr-05 | 191.0 | 191.0 | 1.714 | 26.000 | 234.000 | |
| 26-Apr-05 | 188.0 | 191.0 | 1.743 | 26.000 | 236.000 | |
| 4-May-05 | 178.0 | 186.0 | 1.452 | 11.000 | 262.000 | 6,424.99 |
| 11-May-05 | 184.0 | 188.0 | 1.500 | 12.000 | 273.000 | |
| 17-May-05 | 196.0 | 186.0 | 1.642 | 13.000 | 252.000 | |
| 21-May-05 | 182.0 | 188.0 | 1.679 | 7.000 | 256.000 | |
| 27-May-05 | 192.0 | 191.0 | 1.733 | 14.000 | 248.000 | |
| 2-Jun-05 | 190.0 | 188.0 | 1.785 | 9.000 | 256.000 | 6,460.90 |
| 7-Jun-05 | 187.0 | 185.0 | 1.747 | 14.000 | 242.000 | |
| 13-Jun-05 | 184.0 | 186.0 | 1.738 | 14.000 | 237.000 | |
| 21-Jun-05 | 176.0 | 155.0 | 1.653 | 9.000 | 249.000 | |
| 28-Jun-05 | 191.0 | 184.0 | 1.646 | 13.000 | 227.000 | |

**Table D.4** Multi-layer gas reservoirs - well production data
(continued)

| Date | TFP | Tubing Temp. | Gas Rate | Condy Rate | Water Rate | Gas Cum |
|---|---|---|---|---|---|---|
| | (psi) | (F) | (MMscfd) | (bbld) | (bbld) | (MMcf) |
| 2-Jul-05 | 190.0 | 193.0 | 1.638 | 13.000 | 228.000 | 6,504.17 |
| 9-Jul-05 | 192.0 | 194.0 | 1.591 | 10.000 | 237.000 | |
| 12-Jul-05 | 334.0 | 188.0 | 0.053 | 2.000 | 28.000 | |
| 18-Jul-05 | 182.0 | 133.0 | 1.552 | 8.000 | 256.000 | |
| 28-Jul-05 | 192.0 | 187.0 | 1.576 | 13.000 | 231.000 | |
| 2-Aug-05 | 190.0 | 184.0 | 1.556 | 9.000 | 238.000 | 6,537.32 |
| 7-Aug-05 | 191.0 | 186.0 | 1.530 | 7.000 | 238.000 | 6,545.15 |
| 12-Aug-05 | 190.0 | 182.0 | 1.547 | 11.000 | 234.000 | 6,552.86 |
| 22-Aug-05 | 181.0 | 182.0 | 1.539 | 11.000 | 234.000 | 6,560.55 |
| 27-Aug-05 | 181.0 | 190.0 | 1.524 | 11.000 | 240.000 | 6,575.98 |
| 1-Sep-05 | 193.0 | 186.0 | 1.416 | 10.000 | 238.000 | 6,583.64 |
| 5-Sep-05 | 177.0 | 185.0 | 1.400 | 10.000 | 245.000 | 6,590.99 |
| 23-Sep-05 | 184.0 | 186.0 | 1.484 | 10.000 | 236.000 | 6,596.62 |
| 15-Oct-05 | 170.0 | 187.0 | 1.458 | 10.000 | 246.000 | 6,612.02 |
| 19-Oct-05 | 168.0 | 184.0 | 1.414 | 10.000 | 248.000 | 6,644.38 |
| 3-Nov-05 | 160.0 | 184.0 | 0.970 | 6.000 | 60.000 | 6,650.12 |
| 15-Nov-05 | 136.0 | 139.0 | 1.207 | 7.000 | 23.000 | 6,668.00 |
| 25-Jan-06 | 162.0 | 173.0 | 1.740 | 15.000 | 156.000 | 6,681.06 |
| 1-Feb-06 | 162.0 | 183.0 | 1.743 | 0.000 | 141.000 | |
| 1-Feb-06 | 162.0 | 182.0 | 1.743 | 15.000 | 126.000 | 6,716.75 |
| 22-Feb-06 | 161.0 | 181.0 | 1.248 | 19.000 | 233.000 | 6,748.15 |
| 4-Mar-06 | 166.0 | 179.0 | 1.248 | 48.000 | 278.000 | 6,760.63 |
| 11-Mar-06 | 159.0 | 185.0 | 1.272 | 80.000 | 318.000 | 6,769.45 |
| 16-Mar-06 | 170.0 | 183.0 | 1.309 | 42.000 | 229.000 | 6,775.90 |
| 21-Mar-06 | 163.0 | 180.0 | 1.309 | 4.000 | 205.000 | 6,782.45 |
| 2-Apr-06 | 192.0 | 186.0 | 1.320 | 1.000 | 193.000 | 6,798.22 |
| 2-Apr-06 | 192.0 | 186.0 | 1.320 | 132.000 | 62.000 | 6,798.22 |
| 10-Apr-06 | 166.0 | 184.0 | 1.282 | 147.000 | 357.000 | 6,808.63 |
| 16-Apr-06 | 174.0 | 183.0 | 1.278 | 117.000 | 304.000 | 6,816.31 |
| 25-Apr-06 | 162.0 | 184.0 | 1.289 | 124.000 | 292.000 | 6,827.86 |
| 1-May-06 | 161.0 | 164.0 | 1.218 | 167.000 | 320.000 | 6,835.38 |
| 7-May-06 | 164.0 | 182.0 | 1.227 | 130.000 | 381.000 | 6,842.72 |
| 13-May-06 | 162.0 | 186.0 | 1.284 | 77.000 | 289.000 | 6,850.25 |
| 13-May-06 | 162.0 | 186.0 | 1.284 | 128.000 | 238.000 | 6,857.94 |
| 21-May-06 | 151.0 | 184.0 | 0.639 | 64.000 | 275.000 | 6,865.64 |
| 21-May-06 | 151.0 | 183.0 | 0.639 | 86.000 | 253.000 | 6,865.64 |
| 1-Jun-06 | 150.0 | 184.0 | 1.138 | 0.000 | 64.000 | 6,875.41 |
| 7-Jun-06 | 159.0 | 182.5 | 1.206 | 5.000 | 219.000 | 6,882.44 |
| 12-Jun-06 | 151.0 | 181.8 | 1.175 | 7.000 | 219.000 | 6,888.39 |
| 15-Jun-06 | 151.0 | 181.1 | 1.244 | 22.000 | 212.000 | 6,892.02 |

**Figure D.5** Two-layer oil reservoirs – well schematic

**Table D.5** Two-layer oil reservoirs - well production data

| Date | Wellhead Pressure (psig) | Fluid Rate (STB/day) | Water cut (fraction 0 to 1) | Tubing GOR (SCF/STB) |
|---|---|---|---|---|
| 25-Jun-02 | 1,600 | 99 | 0.84 | 230,625 |
| 26-Jun-02 | 1,735 | 281 | 0.89 | 141,875 |
| 1-Jul-02 | 1,751 | 673 | 0.11 | 6,528 |
| 2-Jul-02 | 1,764 | 650 | 0.07 | 7,868 |
| 3-Jul-02 | 1,656 | 902 | 0.06 | 5,018 |
| 13-Aug-02 | 1,025 | 1,428 | 0.00 | 742 |
| 13-Sep-02 | 1,015 | 1,428 | 0.01 | 1,633 |
| 18-Oct-02 | 805 | 1,772 | 0.00 | 1,264 |
| 25-Oct-02 | 783 | 1,630 | 0.21 | 1,681 |
| 29-Oct-02 | 715 | 1,721 | 0.18 | 1,550 |
| 6-Nov-02 | 760 | 1,533 | 0.19 | 1,418 |
| 11-Nov-02 | 720 | 1,552 | 0.20 | 1,325 |
| 15-Nov-02 | 696 | 1,640 | 0.00 | 963 |
| 17-Nov-02 | 755 | 1,460 | 0.00 | 890 |
| 20-Nov-02 | 847 | 1,241 | 0.00 | 838 |
| 21-Nov-02 | 695 | 1,549 | 0.00 | 826 |
| 24-Nov-02 | 586 | 1,869 | 0.00 | 851 |
| 29-Nov-02 | 572 | 1,756 | 0.02 | 910 |
| 6-Dec-02 | 560 | 1,866 | 0.16 | 761 |
| 18-Dec-02 | 622 | 1,715 | 0.00 | 1,273 |
| 25-Dec-02 | 601 | 1,686 | 0.01 | 1,421 |
| 29-Dec-02 | 620 | 1,631 | 0.09 | 1,676 |
| 7-Jan-03 | 584 | 1,750 | 0.09 | 1,537 |
| 13-Jan-03 | 540 | 1,248 | 0.19 | 1,682 |
| 22-Jan-03 | 547 | 1,140 | 0.28 | 1,780 |
| 28-Jan-03 | 510 | 954 | 0.37 | 2,056 |
| 8-Feb-03 | 642 | 1,266 | 0.00 | 829 |
| 22-Feb-03 | 670 | 671 | 0.30 | 2,099 |
| 4-Mar-03 | 615 | 794 | 0.36 | 3,069 |
| 11-Mar-03 | 578 | 617 | 0.38 | 3,281 |
| 27-Mar-03 | 631 | 615 | 0.27 | 3,277 |
| 28-Mar-03 | 612 | 507 | 0.39 | 5,049 |
| 31-Mar-03 | 612 | 569 | 0.39 | 4,063 |
| 1-Apr-03 | 628 | 410 | 0.42 | 6,483 |
| 2-Apr-03 | 619 | 330 | 0.44 | 8,757 |
| 22-May-03 | 506 | 539 | 0.22 | 1,914 |
| 14-Oct-03 | 580 | 1,074 | 0.56 | 2,787 |
| 18-Oct-03 | 541 | 995 | 0.41 | 2,024 |
| 1-Nov-03 | 485 | 563 | 0.50 | 1,312 |
| 12-Jan-04 | 357 | 322 | 0.92 | 370 |
| 13-Jan-04 | 393 | 358 | 0.86 | 2,400 |
| 26-Jan-04 | 732 | 366 | 0.57 | 2,377 |
| 29-Jan-04 | 535 | 600 | 0.47 | 1,897 |
| 30-Jan-04 | 532 | 343 | 0.60 | 4,191 |

**Table D.5** Two-layer oil reservoirs - well production data
(continued)

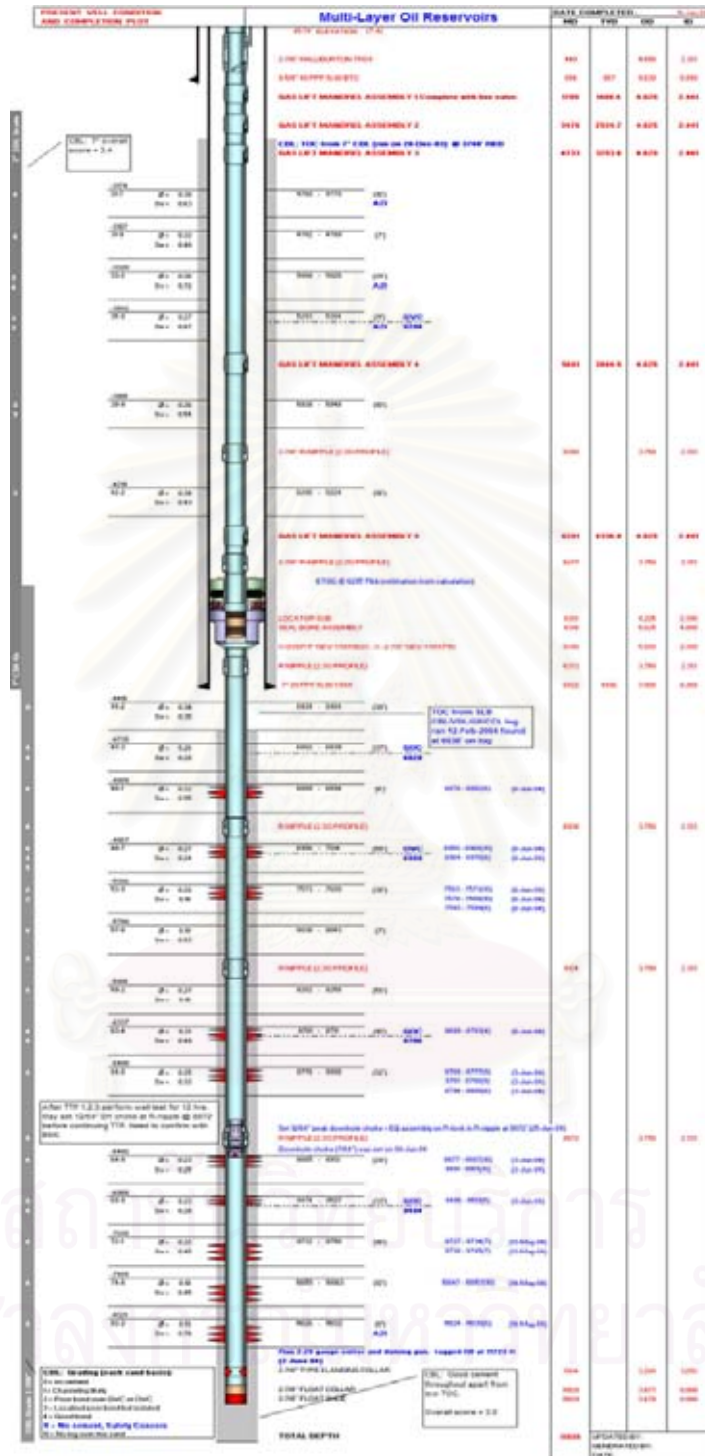| Date | Wellhead Pressure (psig) | Fluid Rate (STB/day) | Water cut (fraction 0 to 1) | Tubing GOR (SCF/STB) |
|---|---|---|---|---|
| 2-Feb-04 | 507 | 315 | 0.58 | 4,545 |
| 6-Feb-04 | 498 | 813 | 0.62 | 1,213 |
| 12-Feb-04 | 382 | 514 | 0.49 | 2,154 |
| 15-Mar-04 | 220 | 15 | 0.00 | 667 |
| 15-Jul-04 | 750 | 525 | 0.29 | 2,216 |
| 21-Jul-04 | 715 | 572 | 0.29 | 1,720 |
| 27-Jul-04 | 645 | 592 | 0.34 | 1,557 |
| 2-Aug-04 | 598 | 621 | 0.38 | 1,346 |
| 11-Aug-04 | 550 | 532 | 0.42 | 1,227 |
| 2-Sep-04 | 553 | 609 | 0.41 | 1,373 |
| 12-Sep-04 | 412 | 843 | 0.40 | 1,657 |
| 23-Sep-04 | 222 | 260 | 0.63 | 16,072 |
| 24-Sep-04 | 215 | 6 | 1.00 | 1,456 |
| 29-Nov-04 | 610 | 1,188 | 0.31 | 3,071 |

**Figure D.6** Multi-layer oil reservoirs – well schematic

**Table D.6** Multi-layer oil reservoirs - well production data

| Date | Wellhead Pressure (psig) | Fluid Rate (STB/day) | Water cut (fraction 0 to 1) | Tubing GOR (SCF/STB) |
|---|---|---|---|---|
| 23-May-04 | 1,814 | 169 | 0.73 | 94,826 |
| 4-Jun-04 | 1,997 | 398 | 0.05 | 3,386 |
| 10-Jun-04 | 1,045 | 737 | 0.01 | 14 |
| 15-Jun-04 | 1,046 | 916 | 0.02 | 386 |
| 20-Jun-04 | 1,015 | 745 | 0.07 | 6,773 |
| 26-Jun-04 | 1,175 | 1,389 | 0.03 | 564 |
| 27-Jun-04 | 1,190 | 1,299 | 0.02 | 540 |
| 1-Jul-04 | 1,228 | 1,285 | 0.02 | 734 |
| 5-Jul-04 | 1,222 | 1,323 | 0.02 | 681 |
| 12-Jul-04 | 1,245 | 1,286 | 0.02 | 646 |
| 14-Jul-04 | 1,074 | 1,967 | 0.04 | 699 |
| 19-Jul-04 | 1,090 | 1,869 | 0.02 | 773 |
| 27-Jul-04 | 1,137 | 1,668 | 0.02 | 1,097 |
| 1-Aug-04 | 1,133 | 1,369 | 0.02 | 1,444 |
| 3-Aug-04 | 1,045 | 1,476 | 0.02 | 1,988 |
| 10-Aug-04 | 1,073 | 1,975 | 0.02 | 1,207 |
| 29-Aug-04 | 1,245 | 1,172 | 0.04 | 1,107 |
| 9-Sep-04 | 1,110 | 1,758 | 0.03 | 1,035 |
| 13-Sep-04 | 1,184 | 1,374 | 0.04 | 1,020 |
| 26-Sep-04 | 1,137 | 1,735 | 0.04 | 991 |
| 1-Oct-04 | 1,150 | 1,794 | 0.04 | 1,140 |
| 25-Oct-04 | 1,190 | 1,326 | 0.05 | 887 |
| 3-Nov-04 | 1,178 | 1,255 | 0.05 | 1,047 |
| 12-Nov-04 | 1,175 | 1,371 | 0.04 | 830 |
| 24-Nov-04 | 1,120 | 1,888 | 0.04 | 729 |
| 1-Dec-04 | 1,177 | 1,262 | 0.05 | 815 |
| 8-Dec-04 | 1,191 | 1,373 | 0.05 | 833 |
| 18-Dec-04 | 1,186 | 781 | 0.05 | 2,013 |
| 28-Dec-04 | 1,170 | 1,907 | 0.04 | 1,108 |
| 2-Jan-05 | 1,125 | 2,165 | 0.04 | 1,031 |
| 12-Jan-05 | 1,174 | 1,382 | 0.05 | 912 |
| 22-Jan-05 | 1,182 | 1,384 | 0.05 | 868 |
| 30-Jan-05 | 1,116 | 1,720 | 0.05 | 1,024 |
| 5-Feb-05 | 1,129 | 1,623 | 0.00 | 1,031 |
| 24-Feb-05 | 1,128 | 1,196 | 0.06 | 990 |
| 5-Mar-05 | 1,158 | 1,148 | 0.07 | 879 |
| 16-Mar-05 | 1,204 | 920 | 0.05 | 824 |
| 23-Mar-05 | 1,059 | 1,844 | 0.06 | 1,465 |
| 30-Mar-05 | 1,069 | 1,971 | 0.07 | 1,177 |
| 7-Apr-05 | 1,069 | 1,500 | 0.08 | 1,942 |
| 12-Apr-05 | 1,126 | 1,089 | 0.10 | 1,129 |
| 16-Apr-05 | 1,079 | 1,587 | 0.09 | 939 |
| 29-Apr-05 | 973 | 1,707 | 0.10 | 1,348 |
| 5-May-05 | 1,037 | 1,990 | 0.11 | 1,040 |
| 23-May-05 | 930 | 1,970 | 0.11 | 719 |
| 2-Jun-05 | 1,018 | 1,437 | 0.15 | 1,942 |
| 4-Jun-05 | 995 | 2,086 | 0.12 | 1,098 |

**Table D.6** Multi-layer oil reservoirs - well
production data (continued)

| Date | Wellhead Pressure (psig) | Fluid Rate (STB/day) | Water cut (fraction 0 to 1) | Tubing GOR (SCF/STB) |
|---|---|---|---|---|
| 25-Jun-05 | 1,025 | 1,506 | 0.18 | 1,103 |
| 6-Jul-05 | 1,022 | 1,440 | 0.18 | 1,147 |
| 6-Aug-05 | 958 | 2,453 | 0.23 | 1,096 |
| 14-Aug-05 | 925 | 2,285 | 0.27 | 1,848 |
| 23-Aug-05 | 834 | 2,659 | 0.31 | 1,316 |
| 9-Sep-05 | 795 | 2,740 | 0.34 | 1,965 |
| 17-Sep-05 | 974 | 1,063 | 0.56 | 1,701 |
| 23-Sep-05 | 738 | 2,465 | 0.35 | 868 |
| 7-Nov-05 | 1,337 | 2,283 | 0.50 | 1,034 |
| 10-Nov-05 | 805 | 1,872 | 0.55 | 1,422 |
| 12-Nov-05 | 918 | 802 | 0.65 | 2,954 |
| 24-Nov-05 | 759 | 2,065 | 0.58 | 1,095 |
| 29-Nov-05 | 822 | 1,649 | 0.60 | 1,541 |
| 3-Dec-05 | 769 | 1,951 | 0.50 | 1,122 |
| 18-Dec-05 | 839 | 658 | 0.79 | 1,604 |
| 23-Dec-05 | 742 | 1,632 | 0.67 | 1,383 |
| 29-Dec-05 | 670 | 2,614 | 0.42 | 984 |
| 8-Jan-06 | 695 | 1,505 | 0.50 | 5,056 |
| 10-Jan-06 | 719 | 2,475 | 0.50 | 1,624 |
| 16-Jan-06 | 832 | 633 | 0.98 | 69,077 |
| 19-Jan-06 | 735 | 2,255 | 0.67 | 1,382 |
| 21-Jan-06 | 672 | 1,738 | 0.93 | 7,677 |
| 30-Jan-06 | 750 | 1,309 | 0.90 | 8,087 |
| 13-Feb-06 | 904 | 1,537 | 0.54 | 2,348 |
| 14-Feb-06 | 906 | 1,554 | 0.50 | 1,807 |
| 19-Feb-06 | 819 | 2,191 | 0.26 | 1,188 |
| 23-Feb-06 | 776 | 2,497 | 0.23 | 1,368 |
| 5-Mar-06 | 804 | 2,406 | 0.22 | 1,416 |
| 17-Mar-06 | 1,095 | 1,050 | 0.35 | 2,105 |
| 23-Mar-06 | 845 | 2,209 | 0.25 | 1,863 |
| 27-Mar-06 | 1,039 | 1,379 | 0.32 | 1,947 |
| 3-Apr-06 | 954 | 1,815 | 0.28 | 1,893 |
| 7-Apr-06 | 950 | 1,120 | 0.32 | 4,795 |
| 13-Apr-06 | 933 | 1,858 | 0.29 | 1,989 |
| 18-Apr-06 | 845 | 2,137 | 0.27 | 2,150 |
| 25-Apr-06 | 848 | 2,102 | 0.31 | 2,006 |
| 4-May-06 | 860 | 2,040 | 0.30 | 2,137 |
| 8-May-06 | 794 | 2,111 | 0.31 | 2,474 |
| 21-May-06 | 864 | 1,943 | 0.32 | 2,198 |
| 24-May-06 | 800 | 2,131 | 0.32 | 2,319 |
| 3-Jun-06 | 866 | 1,895 | 0.34 | 2,148 |
| 11-Jun-06 | 758 | 2,178 | 0.35 | 2,281 |
| 20-Jun-06 | 815 | 1,951 | 0.35 | 2,241 |
| 26-Jun-06 | 863 | 1,763 | 0.36 | 2,181 |
| 9-Jul-06 | 781 | 1,920 | 0.40 | 2,060 |
| 16-Jul-06 | 798 | 1,906 | 0.37 | 2,041 |

## **VITAE**

Tuan Anh Nguyen was born on 26 May, 1974 in Hanoi, Vietnam. He received the degree of Bachelor of Science in Petro-Chemical Engineering from the Hanoi University of Technology in 1996. He has been a graduate student in the Master's Degree Program in Petroleum Engineering, Chulalongkorn University since 2004. He currently works at Chevron Thailand E&P, Ltd. as a completion engineer.